

AD 659415

AD

USAAVLABS TECHNICAL REPORT 67-32

FLUIDIC SYSTEMS DESIGN MANUAL

By

Charles A. Belsterling

July 1967

U. S. ARMY AVIATION MATERIEL LABORATORIES

FORT EUSTIS, VIRGINIA

CONTRACT DA 44-177-AMC-390(T)

ASTROMECHANICS RESEARCH DIVISION

GIANNINI CONTROLS GROUP

CONRAC CORPORATION

MALVERN, PENNSYLVANIA

Distribution of this document is unlimited



D D C
RECEIVED
OCT 9 1967
REGISTERED
D

198

Disclaimers

When Government drawings, specifications, or other data are used for any purpose other than in connection with a definitely related Government procurement operation, the United States Government thereby incurs no responsibility nor any obligation whatsoever; and the fact that the Government may have formulated, furnished, or in any way supplied the said drawings, specifications, or other data is not to be regarded by implication or otherwise as in any manner licensing the holder or any other person or corporation, or conveying any rights or permission, to manufacture, use, or sell any patented invention that may in any way be related thereto.

Trade names cited in this report do not constitute an official endorsement or approval of the use of such commercial hardware or software.

Disposition Instructions

Destroy this report when no longer needed. Do not return it to originator.

REC DESIGN IN	
CFSTI	WRITE SECTION <input checked="" type="checkbox"/>
DOC	DIFF SECTION <input type="checkbox"/>
UNCLASSIFIED	<input type="checkbox"/>
BY	
DATE	APPROVAL
BY	APPROVAL



DEPARTMENT OF THE ARMY
U. S. ARMY AVIATION MATERIEL LABORATORIES
FORT EUSTIS, VIRGINIA 23604

This report has been reviewed by the U. S. Army Aviation Materiel Laboratories and is considered to be technically sound. The report is published for the exchange of information and the stimulation of ideas.

Task 1F121401A14186
Contract DA 44-177-AMC-390(T)
USAAVLABS Technical Report 67-32
July 1967

FLUIDIC SYSTEMS
DESIGN MANUAL

Report No. ARD-DM-052

by

Charles A. Belsterling

Prepared by

Astromechanics Research Division
Giannini Controls Group
Conrac Corporation
Malvern, Pennsylvania

for

U.S. ARMY AVIATION MATERIEL LABORATORIES
FORT EUSTIS, VIRGINIA

Distribution of this
document is unlimited

ABSTRACT

This document is a "how-to-do-it" guide to the design of control systems using analog fluidic devices. It includes reference information on definitions, symbols, and general principles; an integrated set of static and dynamic design methods; and a step-by-step design procedure illustrated with a practical sample problem.

The primary purpose of the Design Manual is to provide the control engineer with a unified set of analytical tools for the straightforward design of systems employing fluidic devices. Its secondary purpose is to provide a universally acceptable vocabulary so that the control engineer, the fluidic device manufacturer, and the user's project engineer can communicate in a common language.

The Fluidic Systems Design Manual contains the following major sections:

1. Introduction
2. Applicable Standards
3. Test Methods and Instrumentation
4. Graphical Characteristics of Typical Fluidic Devices
5. Large Signal Performance Analysis
6. Small Signal Performance Analysis
7. Detailed System Design Procedure
8. Illustrative Example of V/STOL Control System Design

PREFACE

The Fluidic Systems Design Manual was prepared by the Astromechanics Research Division of Giannini Controls Corporation at Malvern, Pennsylvania, during the period from February 15, 1966, to February 15, 1967. Charles A. Belsterling was Project Engineer and author of the manual. Norris G. Barr was a major contributor in the development of experimental data and in the calculation of the sample design problem. Steven Ciarochi contributed to the dynamic analysis of the illustrative system and cooperated with Rebecca Jacksteit in the preparation of the manuscript.

The manual was prepared under Contract DA 44-177-AMC-390(T) with the U.S. Army Aviation Materiel Laboratories at Fort Eustis, Virginia. George W. Fosdick was project monitor for the Government.

Related reports, books, and technical papers are contained in the Bibliography.

CONTENTS

	<u>Page</u>
ABSTRACT	iii
PREFACE	v
ILLUSTRATIONS	ix
SYMBOLS	xiv
1.0 INTRODUCTION	1
1.1 BACKGROUND	1
1.2 PURPOSE	1
1.3 APPLICABILITY	2
1.4 RECOMMENDED USE OF THE DESIGN MANUAL	2
2.0 APPLICABLE STANDARDS	4
2.1 TERMINOLOGY	4
2.2 NOMENCLATURE AND UNITS	11
2.3 SCHEMATICS	13
2.4 GRAPHICAL CHARACTERISTICS	16
2.5 EQUIVALENT ELECTRIC CIRCUITS	23
2.6 IMPORTANT PHYSICAL QUANTITIES	23
2.7 PERFORMANCE PARAMETERS	26
3.0 TEST METHODS AND INSTRUMENTATION	31
3.1 STATIC	31
3.2 DYNAMIC	37
3.3 SPECIAL TEST EQUIPMENT	50
4.0 GRAPHICAL CHARACTERISTICS OF TYPICAL FLUIDIC DEVICES	53
4.1 TURBULENT (NONLINEAR) RESTRICTORS	53

	<u>Page</u>
4.2 LAMINAR (LINEAR) RESTRICTORS	53
4.3 FLUIDIC AMPLIFIERS	53
4.4 SENSORS	57
4.5 ACTUATORS	57
5.0 LARGE SIGNAL PERFORMANCE ANALYSIS	66
5.1 THE LOAD LINE	66
5.2 CALCULATION OF THE TRANSFER (GAIN) CURVE	69
5.3 STATIC MATCHING OF CASCADED FLUIDIC COMPONENTS	72
6.0 SMALL SIGNAL PERFORMANCE ANALYSIS	81
6.1 DEVELOPMENT OF THE EQUIVALENT CIRCUITS FOR FLUIDIC COMPONENTS	81
6.2 CASCADING EQUIVALENT CIRCUITS	90
6.3 DERIVATION OF THE TRANSFER FUNCTION FOR CASCADED FLUIDIC COMPONENTS	90
6.4 CALCULATION OF EQUIVALENT CIRCUIT PARAMETERS	97
6.5 CALCULATION OF FREQUENCY RESPONSE	101
7.0 DETAILED SYSTEM DESIGN PROCEDURE	108
7.1 REQUIRED INFORMATION	108
7.2 STEP-BY-STEP DESIGN	108
7.3 DESIGN CHECKLIST	110
8.0 ILLUSTRATIVE EXAMPLE OF V/STOL CONTROL SYSTEM DESIGN	111
8.1 DESCRIPTION OF THE UH-1B YAW DAMPER SYSTEM	111
8.2 REQUIRED INFORMATION	111
8.3 STEP-BY-STEP DESIGN	120
BIBLIOGRAPHY	181
DISTRIBUTION	182

ILLUSTRATIONS

<u>Figure</u>		<u>Page</u>
1	Vented Jet-Interaction Amplifier	5
2	Closed Jet-Interaction Amplifier	6
3	Wall-Attachment Amplifier	7
4	Vortex Amplifier	7
5	Boundary-Layer-Control Amplifier (Vents Optional)	9
6	Turbulence Amplifier	9
7	Axisymmetric Focused-Jet Amplifier	10
8	Impact Modulator	10
9	Characteristics of Any Fluidic Component	18
10	Description of a Typical Vented Jet-Interaction Amplifier	19
11	Typical Static Input Characteristics (One Side Only)	20
12	Typical Transfer Curve (Differential Amplifier)	21
13	Typical Static Output Characteristics	22
14	Typical Electric Equivalent Circuit	24
15	Circuit for Measuring Differential Fluidic Amplifier	32
16	Typical Static Output Characteristics of a Jet-Interaction Amplifier	34
17	Circuit for Measuring Static Output Characteristics of a Vortex Rate Sensor	35
18	Typical Static Characteristics of a Vortex Rate Sensor	36
19	Circuit for Measuring Static Characteristics of a Passive Element	38
20	Typical Static Characteristics of a Fluidic Resistor	39
21	Circuit for Measuring Dynamic Characteristics of a Differential Amplifier	40

<u>Figure</u>		<u>Page</u>
22	Typical Oscilloscope Displays of Sinusoidal Response (XY mode).	42
23	Measuring Gain and Phase Angle from Oscilloscope Display	43
24	Typical Frequency Response of an Amplifier.	45
25	Typical Oscilloscope Display of Step Response (Common Time Base).	46
26	Circuit for Measuring Dynamic Characteristics of a Vortex Rate Sensor.	47
27	Circuit for Measuring Dynamic Characteristics of a Passive Element.	49
28	Pressure Transducer with Minimum-Volume Adapter	51
29	Static Characteristics of Typical Turbulent-Flow Restrictors	54
30	Static Characteristics of Typical Laminar-Flow Restrictors	55
31	Static Output Characteristics of Vented Jet-Interaction Amplifier.	56
32	Static Input Characteristics of Vented Jet-Interaction Amplifier.	58
33	Static Transfer Characteristics of Vented Jet-Interaction Amplifier.	59
34	Static Output Characteristics of Closed Jet-Interaction Amplifier.	60
35	Static Output Characteristics of Vented Elbow Amplifier	61
36	Static Output Characteristics of Vortex Rate Sensor.	62
37	Static Input Characteristics of Piston-Type Actuators	64
38	Static Input Characteristics of Piston-Type and Vane-Type Fluid Motors	65
39	Coupling a Differential Fluidic Amplifier to a Passive Load	67
40	Coupling Two Differential Fluidic Amplifiers	68

<u>Figure</u>		<u>Page</u>
41	Pressure Transfer Curve of Differential Amplifier Loaded with Second Differential Stage	71
42	Static Output Characteristics of Vortex Rate Sensor	73
43	Static Input Characteristics of Small Vented Jet-Interaction Amplifier	73
44	Superposition of Static Characteristics of Vortex Rate Sensor and Vented Jet-Interaction Amplifier	75
45	Impedance Matching for High Static Pressure Gain	76
46	Matching Operating Points by Raising Rate Sensor Output Bias	77
47	Matching Operating Points by Reducing Amplifier Supply Pressure	78
48	Matching Operating Points by Adding Restrictors in Each Side of the Circuit	79
49	Lumped Electrical Model of Vented Jet-Interaction Amplifier	82
50	Linearized Small-Signal Equivalent Circuit of Vented Jet-Interaction Amplifier	83
51	Equivalent Circuit of Vented Jet-Interaction Amplifier (Valid to 400 CPS)	85
52	Equivalent Circuit of Closed Jet-Interaction Amplifier (Valid to 400 CPS)	86
53	Equivalent Circuit of Vented Elbow Amplifier (Valid to 400 CPS).	88
54	Equivalent Circuit of Vortex Rate Sensor	89
55	Equivalent Circuit of Piston-Type Actuator	91
56	Equivalent Circuit of Piston-Type and Vane-Type Fluid Motors	92
57	Cascading Equivalent Circuits of Vortex Rate Sensor and Vented Jet-Interaction Amplifier.	93
58	Equivalent Circuit Parameters Defined from Static Output Characteristics of Vortex Rate Sensor	98

<u>Figure</u>		<u>Page</u>
59	Equivalent Circuit Parameters Defined from Static Input Characteristics of Jet-Interaction Amplifier.	100
60	Equivalent Circuit Parameters Defined from Static Output Characteristics of Amplifier	102
61	Effect of Dead Time on Sinusoidal Response	105
62	Frequency Response of Combined Rate Sensor and Vented Jet-Interaction Amplifier (Bode Diagram)	107
63	Block Diagram of UH-1B Yaw Damper System	112
64	Functional Requirements of Fluidic System.	113
65	Static Output Characteristics of Rate Sensor.	114
66	Normalized Output Characteristics of Amplifier A	115
67	Normalized Input Characteristics of Amplifier A.	116
68	Power Nozzle Characteristics of Amplifier A	117
69	Normalized Output Characteristics of Amplifier B	118
70	Normalized Input Characteristics of Amplifier B.	119
71	Power Nozzle Characteristics of Amplifier B	121
72	Input Characteristics of Servo Actuator	122
73	Characteristics of Typical Laminar-Flow Restrictor.	123
74	Dimensional Sketch of Amplifier A	124
75	Dimensional Sketch of Amplifier B	125
76	Preliminary Schematic Diagram of Fluidic Yaw Damper	126
77	Rate Sensor Output Characteristics with First Stage Input Bias Characteristics Superimposed	128
78	Rate Sensor Output Characteristics with First Stage Input Differential Characteristics Superimposed.	131
79	First Stage Amplifier Output Characteristics with Second Stage Input Characteristics Superimposed	133

<u>Figure</u>		<u>Page</u>
80	Matching the First Stage Amplifier with the Second Stage Amplifier	135
81	Matching the Second Stage Amplifier with the Third Stage Amplifier	137
82	Matching the Third Stage Amplifier with Parallel Fourth Stage Amplifiers.	139
83	Matching the Fifth Stage Amplifier with the Servo Actuator.	141
84	Matching the Fourth Stage Amplifier with the Fifth Stage Amplifier	143
85	Schematic Diagram of Complete Matched Fluidic Yaw Damper .	145
86	Static Transfer Curve of Fluidic Yaw Damper Without Highpass Characteristic	146
87	Equivalent Electrical Circuit for the Complete Fluidic Yaw Damper.	148
88	Detail of Network Between Stage 3 and Stage 4	149
89	Consolidation of the Network Between Stage 3 and Stage 4 .	150
90	Transfer Function Block Diagram for the Complete Fluidic Yaw Damper.	153
91	List of Transfer Functions for the Complete Fluidic Yaw Damper System.	154
92	Physical Layout of Circuit Associated with Stage 2	157
93	Tabulation of Equivalent Circuit Parameters.	166
94	Preliminary Values of the Transfer Functions at 10 CPS . .	173
95	Final Values of the Transfer Functions at 10 CPS	177
96	Frequency Response of Fluidic Yaw Damper.	178

SYMBOLS

a	acceleration, in./sec ²
A	area, in. ²
C	fluid capacitance, in. ⁵ /lb
db	decibels
e	base of natural logarithms
f	frequency, cps
F	force, lb
G _f	flow gain, incremental, dimensionless
G _p	pressure gain, incremental, dimensionless
G _w	power gain, incremental, dimensionless
j	imaginary factor ($\sqrt{-1}$)
K	proportional factor
K _p	pressure amplification factor, dimensionless
l	length, in.
L	fluid inductance, lb sec ² /in. ⁵
m	mass, lb sec ² /in.
M	magnitude, db
P	pressure, gage or drop, psi
P _{abs}	pressure, absolute, psia
Q	flow rate, in. ³ /sec
R	fluid resistance, lb sec/in. ⁵
s	Laplace operator, 1/sec
S/N	signal-to-noise ratio, dimensionless
t	time, sec

T	temperature static, degrees Rankine
v	velocity, in./sec
V	volume, in. ³
Z	fluid impedance, lb sec/in. ⁵
α	acceleration, angular, deg/sec
θ	angle, degrees
ρ	mass density, slugs/in. ³
ω	velocity, angular, deg/sec

SUBSCRIPTS

c	control
cd	control differential
co	control bias
d	delay
o	output
od	output differential
s	supply

1.0 INTRODUCTION

1.1 BACKGROUND

This document is a guide to the design of control systems using analog fluidic devices. It is intended to be a "how-to-do-it" manual describing a step-by-step design procedure and illustrating it with practical numerical examples. For completeness, it also includes textbook information on definitions, symbols, and general principles.

The design methods presented in this manual are the result of research programs supported by the Army Materiel Command since September 1963 (References 3,4,5). The long-range objective of the program is to develop the techniques for the design of systems using fluidic components. To date, the graphical and equivalent circuit analytical methods on which this manual is based have been developed and verified experimentally for wide classes of amplifiers and system components over the range of signal frequencies from zero to more than 400 cps (Reference 2). As a result, a unified analytical approach has been developed which in the future can be programmed for automatic design of complete control systems on a digital computer.

1.2 PURPOSE

The primary purpose of this manual is to provide the control engineer with a unified set of analytical tools for the straightforward design of systems employing fluidic devices. Its secondary purpose is to provide a universally acceptable vocabulary so that the control engineer, the fluidic device manufacturer, and the Government project officer can communicate in a common language.

To accomplish the first, the manual presents a complete and integrated set of design principles previously verified by experimental test results. It also includes the most up-to-date standards for the fluidic technology for ready reference. To accomplish the second, the first draft of this manual was circulated to a distinguished group of people active in the fluidic analog systems field for their review. Constructive comments and suggestions have been incorporated, wherever practical, in the final edition.

Finally, to communicate the contents of this manual to its readers with the least amount of excess material, the author has assumed a level of education equal to a Bachelor of Science in Mechanical or Electrical Engineering. In addition, we assume that the reader has a working knowledge of

1. Electrical circuit analysis (References 10 and 12)
2. Transform calculus (Reference 9)
3. Feedback control systems (Reference 8)

1.3 APPLICABILITY

This manual is limited to the design of control systems using analog fluidic components. The methods presented are applicable to all kinds of analog fluidic components: sensors, amplifiers, networks, and actuators. They are applicable to all kinds of fluids: gases, compressible liquids (like hydraulic fluids), and incompressible liquids (like water). They are applicable to all kinds of systems: aircraft, spacecraft, ships, land vehicles, and tracking devices. They are applicable to a broad spectrum of performance situations: static, large signal, dynamic, and small signal at frequencies up to those where the physical dimensions of the circuit approach the wavelength of the signal. They are applicable to practical situations where second-order effects of the behavior of fluids can be safely neglected; in other words, they cover most normal cases but must be modified for the extremes of temperature, pressure ratios, and jet velocity.

1.4 RECOMMENDED USE OF THE DESIGN MANUAL

The Fluidic Systems Design Manual can be divided into three major parts. Following the Introduction, there are three sections of background and reference material. Section 2.0, Applicable Standards, defines nomenclature symbols and performance criteria; Section 3.0, Test Methods, describes the procedures and instruments used to generate performance data. Section 4.0, Graphical Characteristics, covers a description of the static characteristic curves of typical components. The second major division covers system design procedures in sections titled Large Signal Analysis (5.0), Small Signal Analysis (6.0), and Detailed System Design Procedure (7.0). The third major division, Section 8.0, is devoted to the demonstration of the application of the design procedures to a practical system. It covers the step-by-step detailed design of a control system for V/STOL aircraft which employs fluidic components.

To learn the design procedures described in this manual in the most direct way, the author recommends the following.

First, become thoroughly familiar with the graphical characteristics (2.4 and 4.0), the performance parameters derived from them (2.7 and 6.4), and, with reference to test methods (3.0), what they represent in terms of the real fluidic device and its associated circuits.

Second, learn to apply these graphical characteristics to the analysis of the large signal behavior of a fluidic device in a particular circuit (5.0). This includes the problems of matching operating points (5.3) and defining the nonlinear response of the device at very low signal frequencies (5.2).

Third, learn the significance of the electrical equivalent circuit representation of fluidic devices and circuits (6.0). Even though in some cases the control engineer may not be concerned with linearized, high frequency performance of his fluidic system, the equivalent circuit approach provides tremendous insight into the behavior of the system, leading to a more

knowledgeable approach to solving circuit problems.

Finally, when the fundamentals have become almost second-nature, refer to the detailed design checklist (7.3) for procedural guidelines and to the illustrative design problem (8.0) to clarify any fine points of analysis and design procedure.

2.0 APPLICABLE STANDARDS (Reference 1)

2.1 TERMINOLOGY

2.1.1 General

FLUIDICS	The general field of fluid devices or systems performing sensing, logic, amplification, and control functions employing primarily no-moving-part (flueric) devices.
FLUERIC	An adjective applied in some quarters to fluidic devices and systems performing sensing, logic, amplification, and control functions using no moving mechanical elements.
ELEMENTS	The general class of devices in their simplest form used to make up fluidic components and circuits; for example, fluidic restrictors and capacitors. These are the "least common denominators" of the fluidics technology.
COMPONENTS	Fluidic devices which are interconnected with elements to form working circuits; for example, a proportional amplifier or an OR-NOR logic gate.
ANALOG	The general class of devices or circuits whose output is utilized as a continuous function of its input; for example, a proportional amplifier.
DIGITAL	The general class of devices or circuits whose output is utilized as a discontinuous function of its input; for example, a bistable amplifier.
ACTIVE	The general class of devices which control power from a separate supply.
PASSIVE	The general class of devices which operate on the signal power alone.
BIAS (QUIESCENT) POINT	The point on its static pressure-flow characteristics at which an element or component will be at equilibrium in a circuit with no signal applied.

OPERATING RANGE The maximum range of signal over which an element or component is recommended for operation in a circuit. In an amplifier it is normally limited to the range where the gain can be considered linear.

IMPEDANCE An effective restriction in the flow path.

LOADING Loading of a component is related to the output flow demanded from it in a circuit. For example, an amplifier is unloaded when it has an infinite impedance connected to its output port (blocked).

2.1.2 Amplifiers

AMPLIFIER An active fluidic component whose output signal is greater than its input signal.

PRESSURE AMPLIFIER A component designed specifically for amplifying pressure signals.

FLOW AMPLIFIER A component designed specifically for amplifying flow signals.

POWER AMPLIFIER A component designed specifically for amplifying power signals.

VENTED VS. CLOSED
AMPLIFIER A vented amplifier utilizes auxiliary ports to establish a reference pressure in a particular region of the amplifier geometry; a closed amplifier has no communication with an independent reference. Terminology for the geometry is defined in Figures 1 and 2.

JET-INTERACTION
AMPLIFIER An amplifier which utilizes control jets to deflect a power jet and to modulate the output. Usually employed as an analog amplifier. Terminology for the geometry is defined in Figure 1.

WALL-ATTACHMENT
AMPLIFIER An amplifier which utilizes control of the attachment of a free jet to a wall (Coanda effect) to modulate the output. Usually employed as a digital amplifier. Terminology for the geometry is defined in Figure 3.

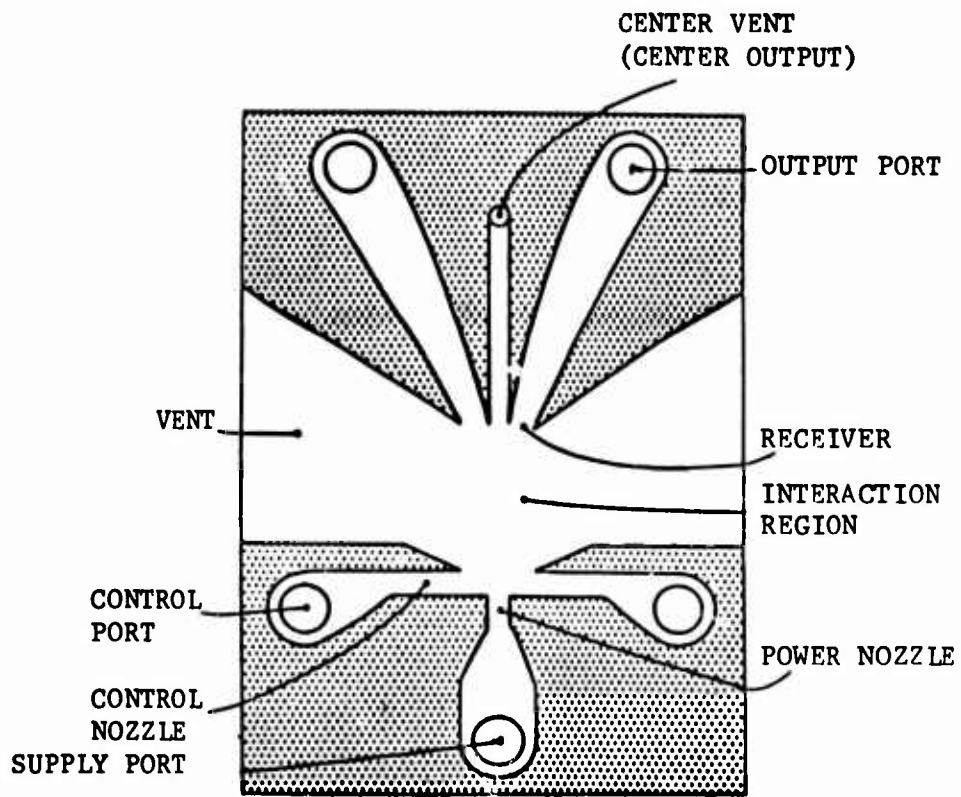


FIGURE 1 - VENTED JET-INTERACTION AMPLIFIER

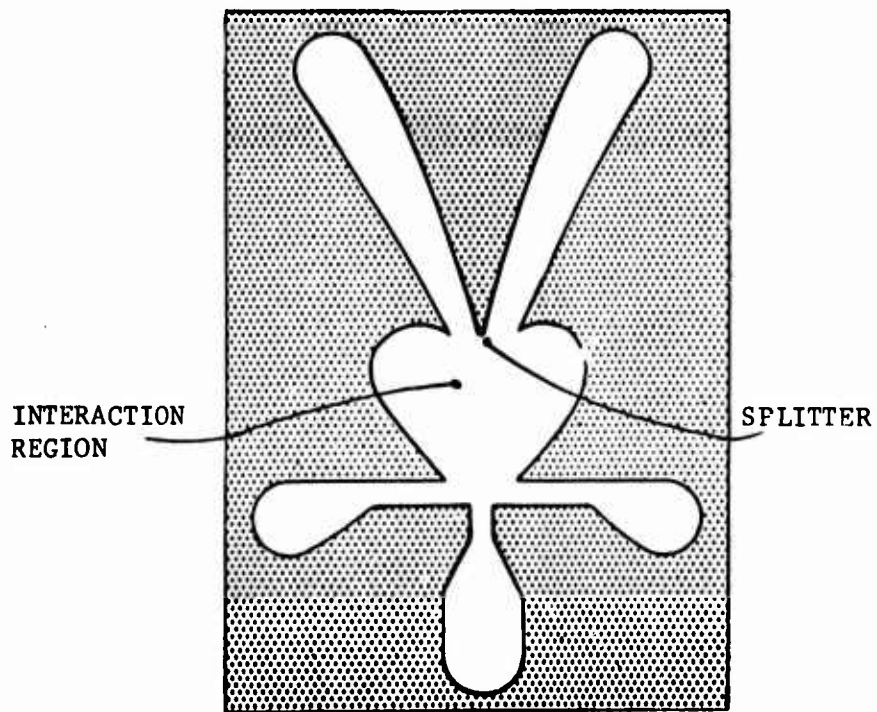


FIGURE 2 - CLOSED JET-INTERACTION AMPLIFIER

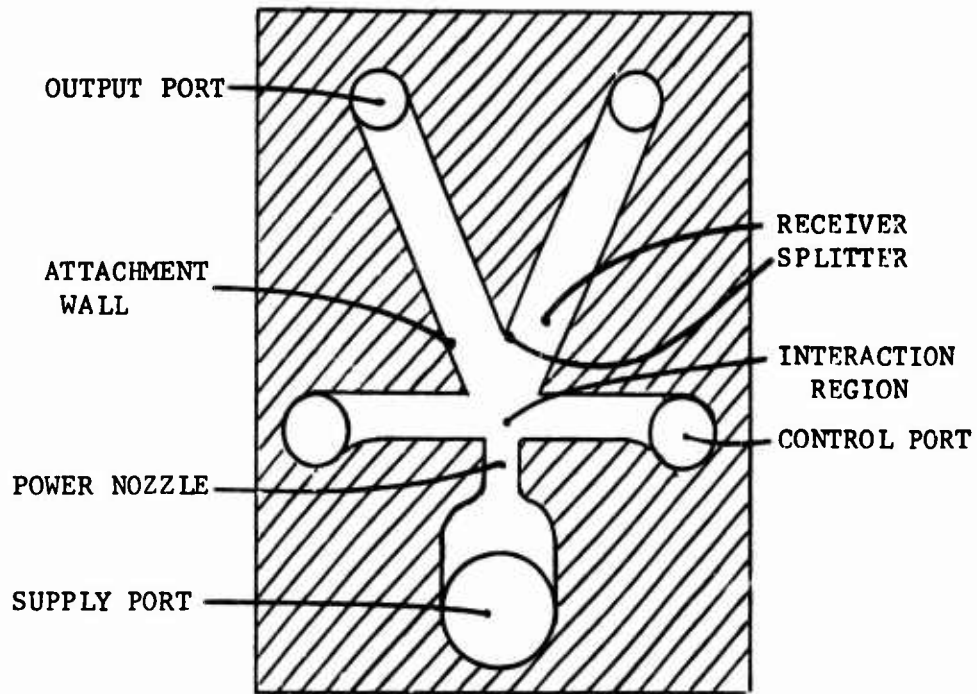


FIGURE 3- WALL-ATTACHMENT AMPLIFIER

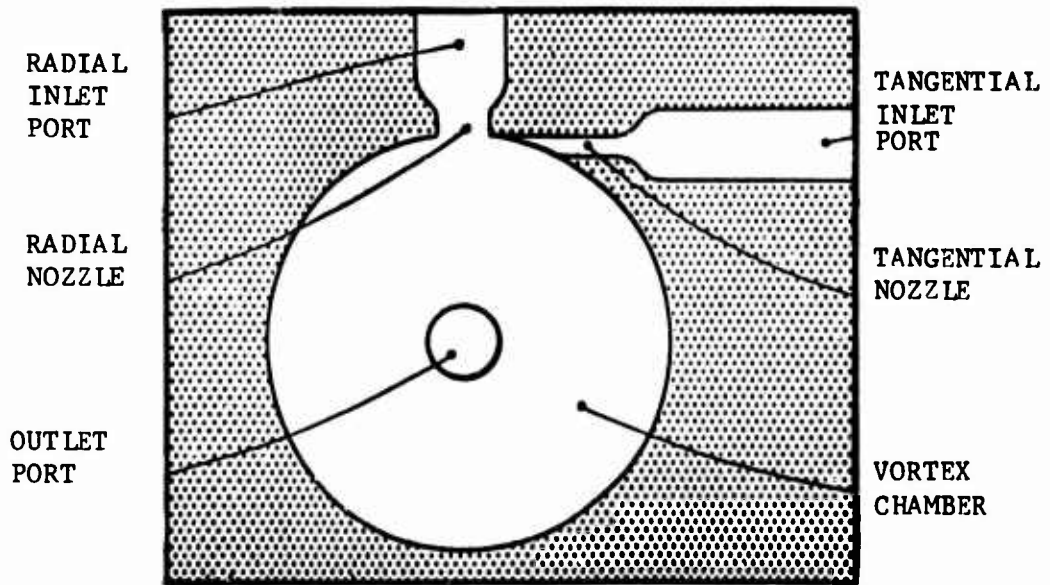


FIGURE 4 - VORTEX AMPLIFIER

VORTEX AMPLIFIER

An amplifier which utilizes the pressure drop across a controlled vortex for modulating the output. Terminology for the geometry is defined in Figure 4.

BOUNDARY-LAYER-CONTROL AMPLIFIER

An amplifier which utilizes the control of the separation point of a power stream from a curved or plane surface to modulate the output. Terminology for the geometry is defined in Figure 5.

TURBULENCE AMPLIFIER

An amplifier which utilizes control of the laminar-to-turbulent transition of a power jet to modulate the output. Terminology for the geometry is defined in Figure 6.

AXISYMMETRIC FOCUSED-JET AMPLIFIER

An amplifier which utilizes control of the attachment of an annular jet to an axisymmetric flow separator (that is, control of the focus of the jet) to modulate the output. Usually employed as a digital amplifier. Terminology is defined in Figure 7.

IMPACT MODULATOR

An amplifier which utilizes the control of the intensity of two directly opposed, impacting power jets, thereby controlling the position of the impact plane to modulate the output. Terminology is defined in Figure 8.

2.1.3 Sensors

SENSOR

A component which, in general, senses variables and produces a signal in a medium compatible with fluidic devices; for example, a temperature or angular rate sensor.

2.1.4 Transducers

TRANSDUCER

A component which, in general, converts a signal from one medium to an equivalent signal in a second medium, one of which is compatible with fluidic devices.

2.1.5 Actuators

ACTUATOR

A component which, in general, converts a fluidic signal into an equivalent mechanical output.

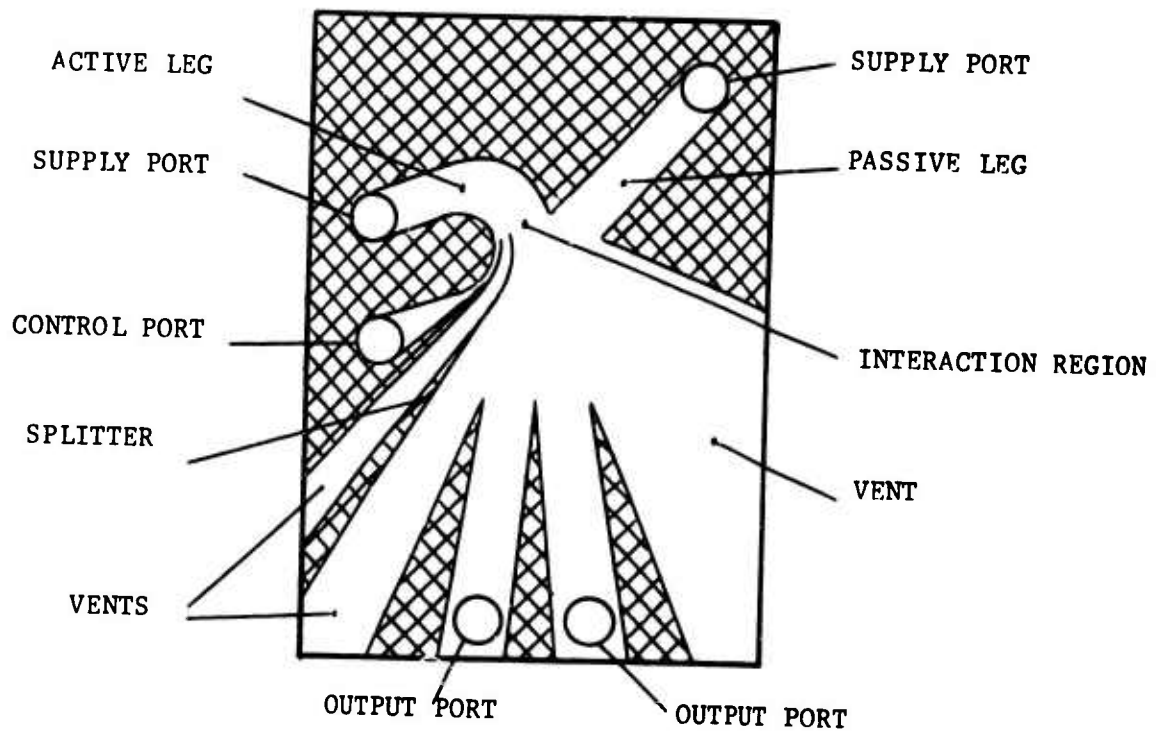


FIGURE 5 - BOUNDARY-LAYER-CONTROL AMPLIFIER (VENTS OPTIONAL)

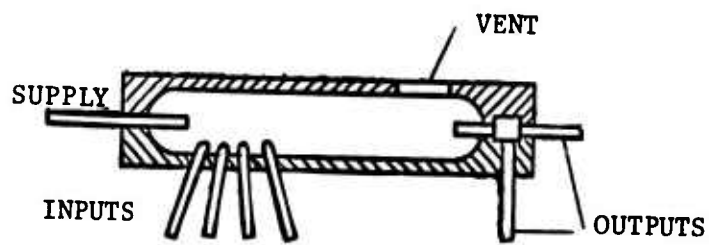


FIGURE 6 - TURBULENCE AMPLIFIER

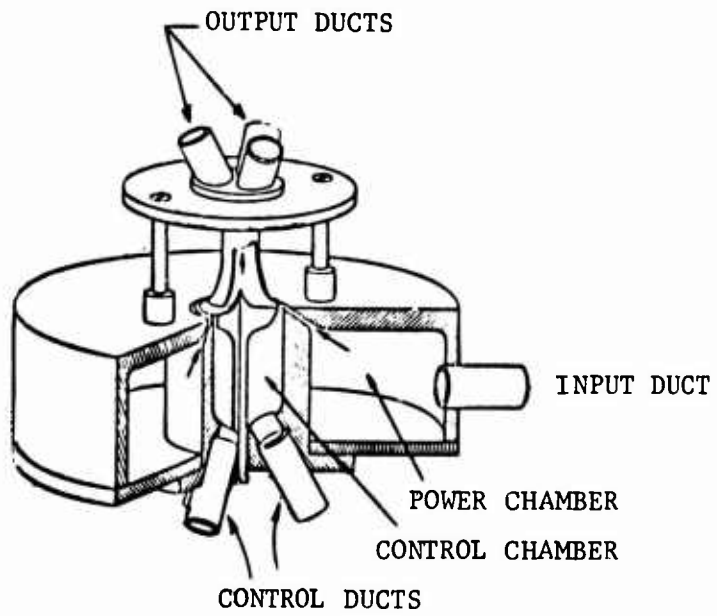


FIGURE 7 - AXISYMMETRIC FOCUSED-JET AMPLIFIER

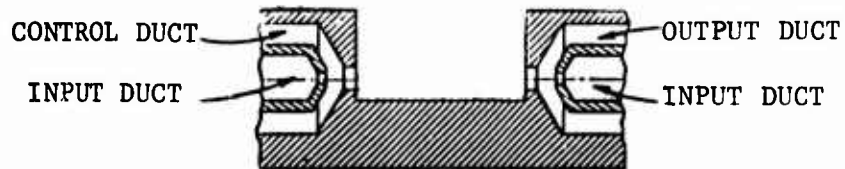


FIGURE 8 - IMPACT MODULATOR

2.1.6 Displays

DISPLAY

A component which, in general, converts a fluidic signal into an equivalent visual output.

2.1.7 Logic Devices

LOGIC DEVICE

The general category of digital fluidic components which perform logic functions; for example, AND, OR, NOR, and NAND. They can gate or inhibit signal transmission with the application, removal, or other combinations of input signals.

FLIP-FLOP

A digital component or circuit with two stable states and sufficient hysteresis so that it has "memory". Its state is changed with an input pulse; a continuous input signal is not necessary for it to remain in a given state.

2.1.8 Circuit Elements

IMPEDANCE

A passive fluidic element which requires a pressure drop to establish a flow through it. Transfer function may have real and imaginary parts.

RESISTOR

Passive fluidic element which, because of viscous losses, produces a pressure drop as a function of the flow through it and has a transfer function of essentially real components (i.e., negligible phase shift) over the frequency range of interest.

CAPACITOR

A passive fluidic element which, because of fluid compressibility, produces a pressure which lags flow into it by essentially 90°.

INDUCTOR

A passive fluidic element which, because of fluid inertance, has a pressure drop which leads flow by essentially 90°.

2.2 NOMENCLATURE AND UNITS

2.2.1 Basic Quantities

The quantities listed below are general; specific quantities should be identified by subscripts (e.g., P_{02} would be pressure at port 02).

<u>Quantity</u>	<u>Nomenclature</u>	<u>Units</u>	
		(Std)	(SI)
length	l	inch; in.	(meter, m)
force	F	pound; lb	(newton; N)
mass	m	lb-sec ² /in.	(kilogram; kg)
time	t	seconds; sec	(seconds; sec)
angle	--	degrees; °	(radians; rad)
frequency	f	cycles/sec;	(hertz; Hz)
area	A	in. ² cps	(m ²)
acceleration	a	in./sec ²	(m/sec ²)
temperature, static	T	degrees Rankine; °R	(degrees Kelvin; °K)
velocity, angular	ω	deg/sec	(rad/sec)
acceleration, angular	α	deg/sec ²	(rad/sec ²)
volume	V	in. ³	(m ³)
flow rate	Q	in. ³ /sec (std conditions); or scfm	(m ³ /sec) (std conditions)
velocity	v	in./sec	(m/sec)
pressure, general	P	lb/in. ² ; or psi	(N/m ²)
pressure, absolute	P _a	psia	(N/m ²)
pressure, gage or drop	P _g	psig	(N/m ²)
fluid impedance	Z	lb sec/in. ⁵	Nsec/m ⁵
fluid resistance	R	lb sec/in. ⁵	Nsec/m ⁵
fluid capacitance	C	in. ⁵ /lb	m ⁵ /N
fluid inductance	L	lb sec ² /in. ⁵	Nsec/m ⁵

<u>Quantity</u>	<u>Nomenclature</u>	(Std)	<u>Units</u>	(SI)
Laplace operator	s	1/sec		(/sec)
pressure gain, incremental	G_p		dimensionless	
flow gain, incremental	G_f		dimensionless	
power gain, incremental	G_w		dimensionless	
signal-to-noise ratio	S/N		dimensionless	

2.2.2 General Subscripts

control	c
output	o
supply	s
control bias	co
control differential	cd
output differential	od

2.3 SCHEMATICS

The function of the schematics is to enable the circuit designer to employ meaningful and specific symbols in drawings and schematics which will clearly define the type of device employed.

2.3.1 General

Output port -O

Control ports - C

Arrowhead on control line indicates continual flow required to maintain state, no memory (no hysteresis).

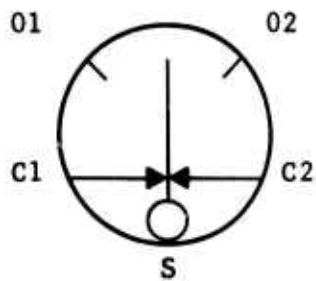
No arrowhead on control line indicates element has memory (has useful hysteresis).

Vent port -V

Supply port - S

2.3.2 Analog Amplifiers

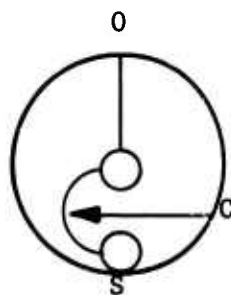
JET-INTERACTION AMPLIFIER



- S - supply
- C1 - left control
- C2 - right control
- O1 - left output
- O2 - right output

Operating Principle - Jet Interaction (Proportional)

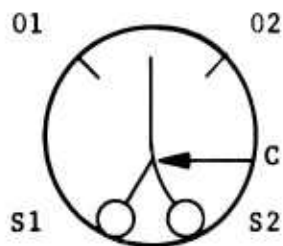
VORTEX AMPLIFIER



- S - supply
- C - control
- O - output

Operating Principle - Vortex

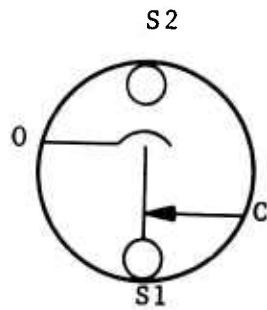
BOUNDARY-LAYER-CONTROL AMPLIFIER



- S1 - passive leg supply
- S2 - active leg supply
- C - control
- O1 - left output
- O2 - right output

Operating Principle - Separation Point Control

IMPACT MODULATOR

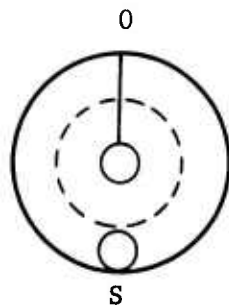


- S1 - controlled supply
- S2 - supply
- C - control
- O - output

Operating Principle - Jet Impact

2.3.3 Sensors and Transducers

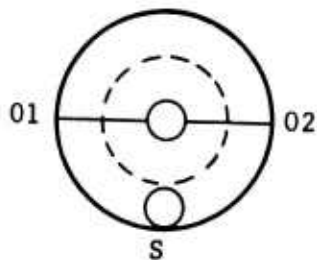
ANGULAR RATE SENSOR (series vortex type)



- O - output
- S - supply

Operating Principle - Vortex

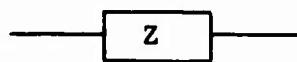
ANGULAR RATE SENSOR (vortex with ΔP pickoff)



- O1, O2 - outputs
- S - supply

Operating Principle - Vortex

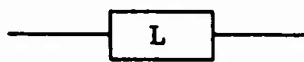
2.3.4 General Circuit Elements



GENERAL IMPEDANCE



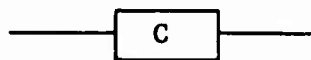
ORIFICE
(TURBULENT RESTRICTION)



INDUCTANCE



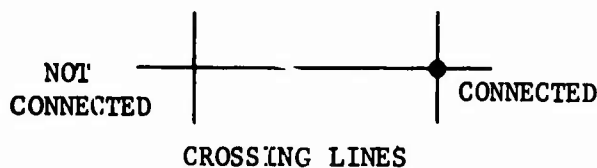
CAPILLARY
(LAMINAR RESTRICTION)



VOLUME CAPACITANCE



RETURN TO RESERVOIR



2.4 GRAPHICAL CHARACTERISTICS

In designing any system of interconnected components it is necessary to take into account the effect of one upon the other. This is true whether the components are electronic, mechanical, hydraulic, acoustic or fluidic.

The most practical systematic procedures used in control system design is the so-called "black box" method. This technique requires that each component be isolated from all other components in the system, then subjected to a few simple tests under typical operating conditions. This is normally done by the manufacturer before he ships a component to a user. For example, the vacuum tube manufacturer supplies a set of characteristic curves and dynamic parameters for each tube he markets.

The information is used in electronics for amplifier stage coupling (matching input and output impedances) and in hydraulics for matching servo valves pressure-flow characteristics with these loads.

By applying the same proven approach in fluidics, all the mathematical tools now used in electronics and hydraulics can be applied to fluidic systems analysis and design.

For most practical cases it is possible to describe the total behavior of any fluidic device with the three sets of data shown in Figure 9. Input characteristics define what load an input signal sees when it is applied to the input ports. Transfer characteristics define what happens to the output when an input signal is applied. Output characteristics define how the output signal is affected when an external load is connected at the output ports.

For static and large signal analysis these three characteristics are most conveniently described graphically, because the graphs take into account device nonlinearities without complex mathematics. For dynamic and small signal analysis these characteristics are more conveniently described in terms of equivalent electrical circuits, because well-developed linear circuit theory is directly applicable to the calculation of performance.

Typical fluidic component characteristics can be illustrated by those for one of the most common fluidic amplifiers, the vented jet-interaction amplifier (Figure 10).

Graphically, the input characteristic of a single input port is a plot of the control flow versus the pressure applied at the control port (Figure 11). In most vented amplifiers (which minimize internal feedback) the input characteristics are practically independent of output loading. Note that the locus of bias points is the curve generated when both control port pressures are always equal. The differential control curves result when one control port pressure is increased and the other decreased the same amount, keeping the average of the two always at a fixed bias pressure. These are the conditions under which the amplifier will normally be operated. The transfer characteristic defines the gain of the amplifier and is represented by a family of curves with output load as the parameter (Figure 12). Note that it is normal for the pressure gain to decrease as the load impedance is reduced (opened from blocked conditions), and that beyond saturation there can be a reversal in slope.

The output characteristics are a plot of the output flow versus output pressure as the load is varied from near zero impedance (relatively large flow) to near infinite impedance (blocked output port) (Figure 13). Because the output characteristics (which define the output impedance) are also a function of the control signal, a complete description of the output characteristics is a family of curves of output flow versus output pressure with control pressure or control flow as the parameter.

Now note that the transfer characteristic and the output characteristics contain the same information: output behavior, under load, in response to some input signal. Therefore, only one of these sets of curves is required. The output characteristics which are plotted in terms of flow and pressure are more convenient for analyzing the problems of cascading components; therefore, this form is preferred.

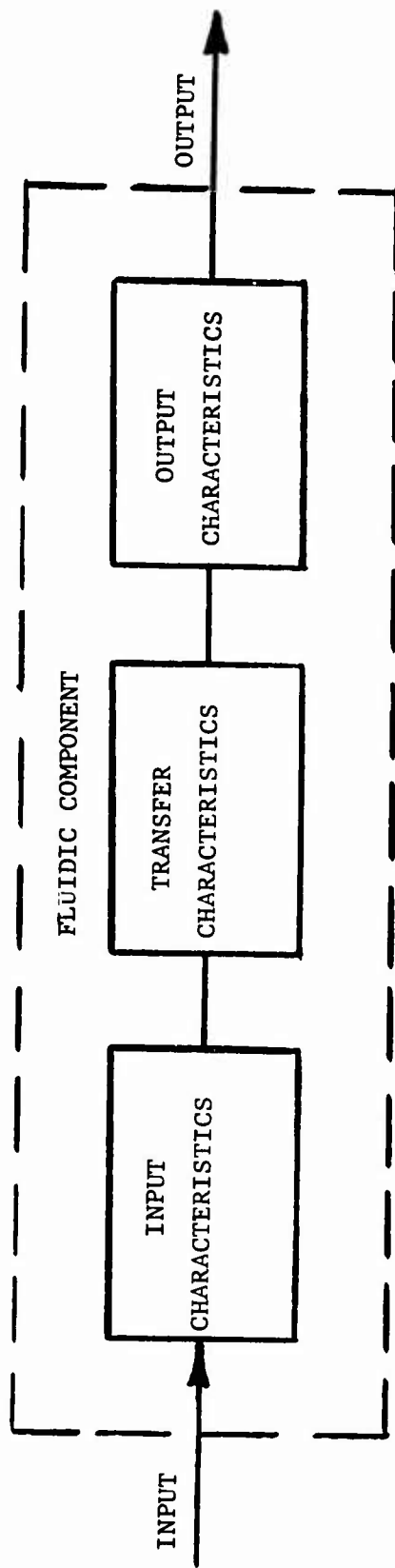


FIGURE 9 - CHARACTERISTICS OF ANY FLUIDIC COMPONENT

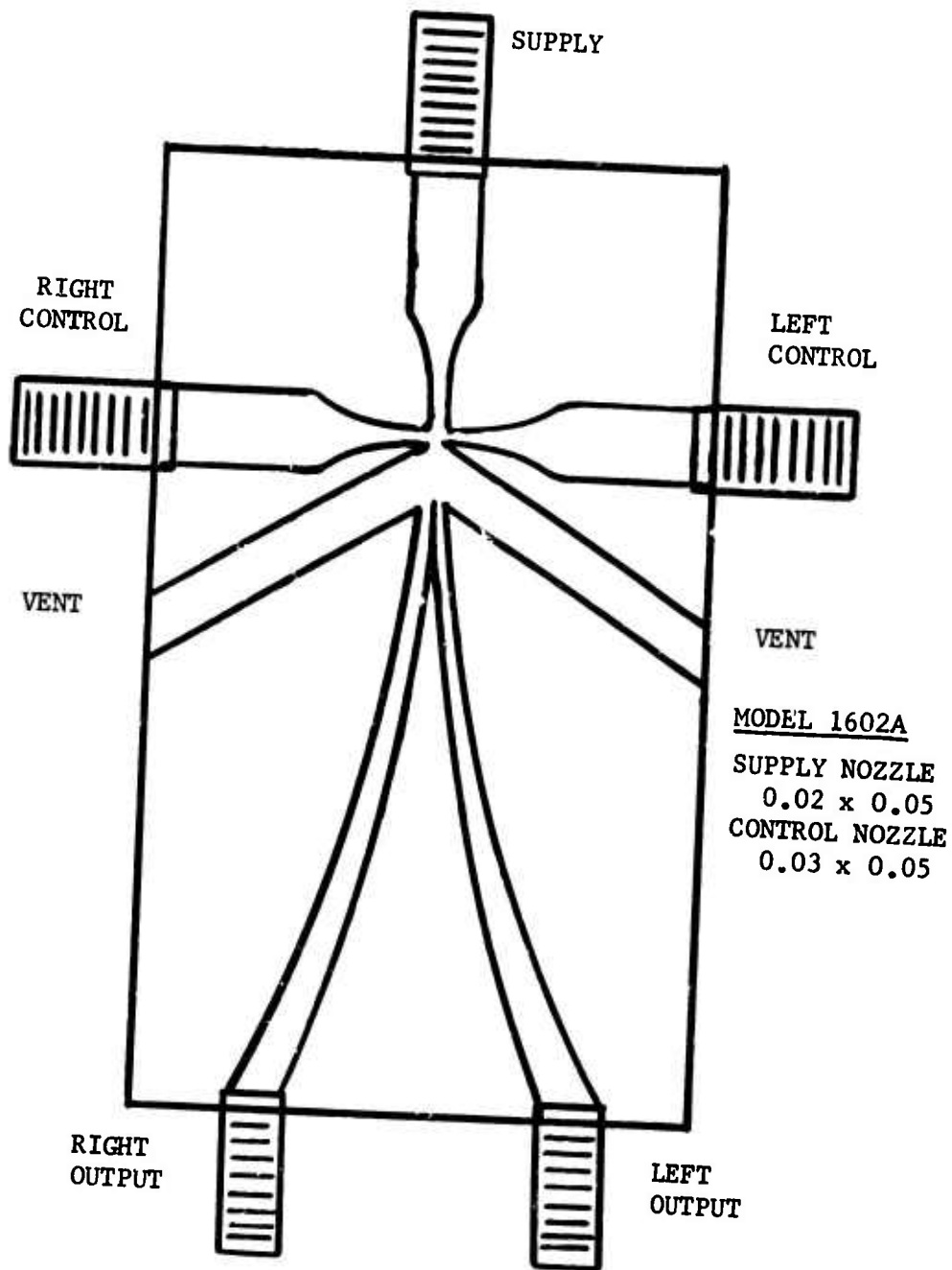


FIGURE 10 - DESCRIPTION OF A TYPICAL
 VENTED JFT-INTERACTION AMPLIFIER

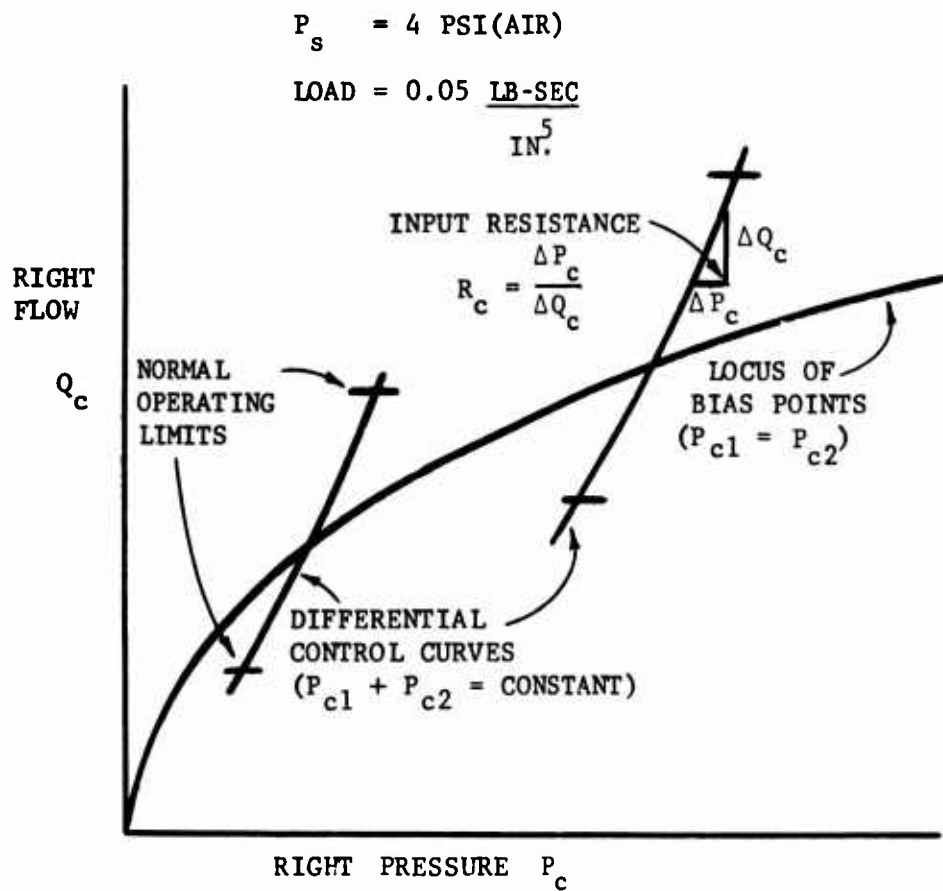


FIGURE 11 - TYPICAL STATIC INPUT CHARACTERISTICS (ONE SIDE ONLY)

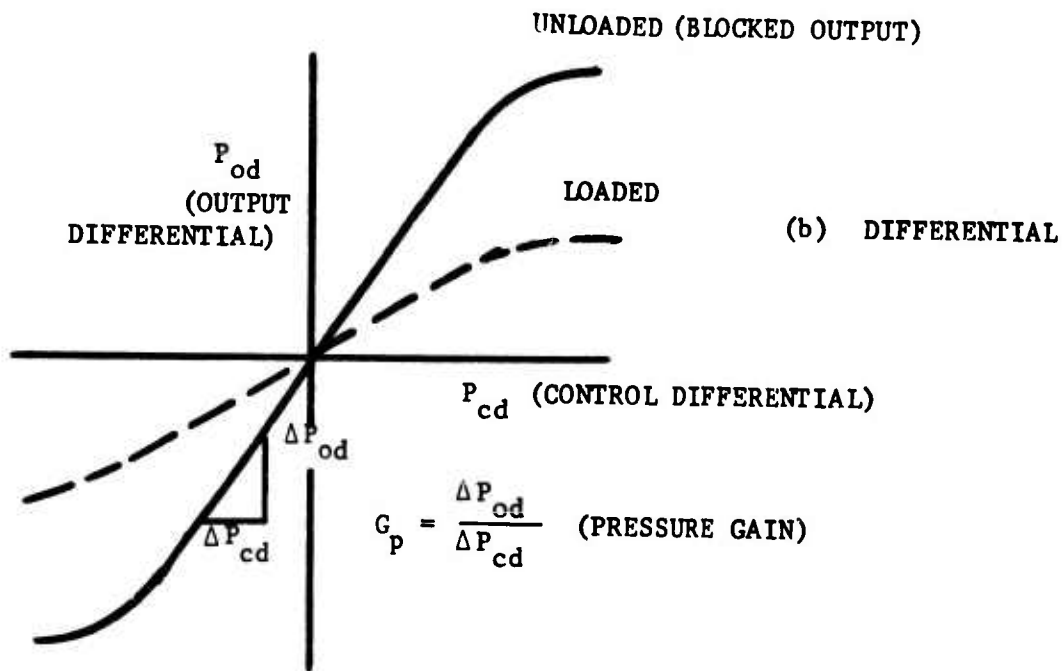
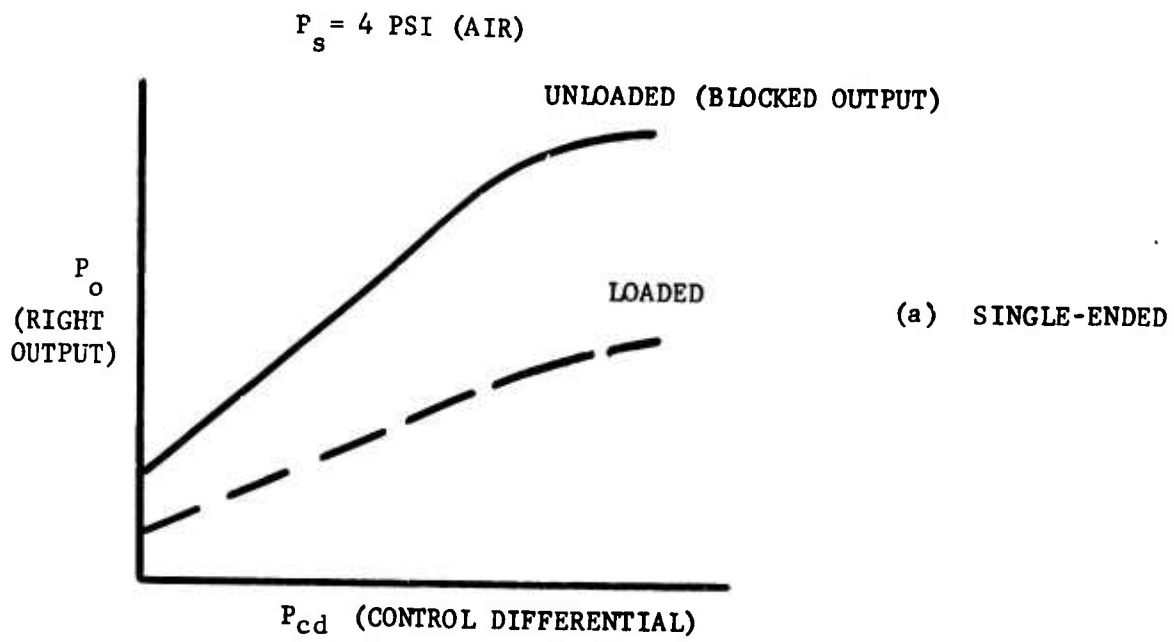


FIGURE 12 - TYPICAL TRANSFER CURVES
(DIFFERENTIAL AMPLIFIER)

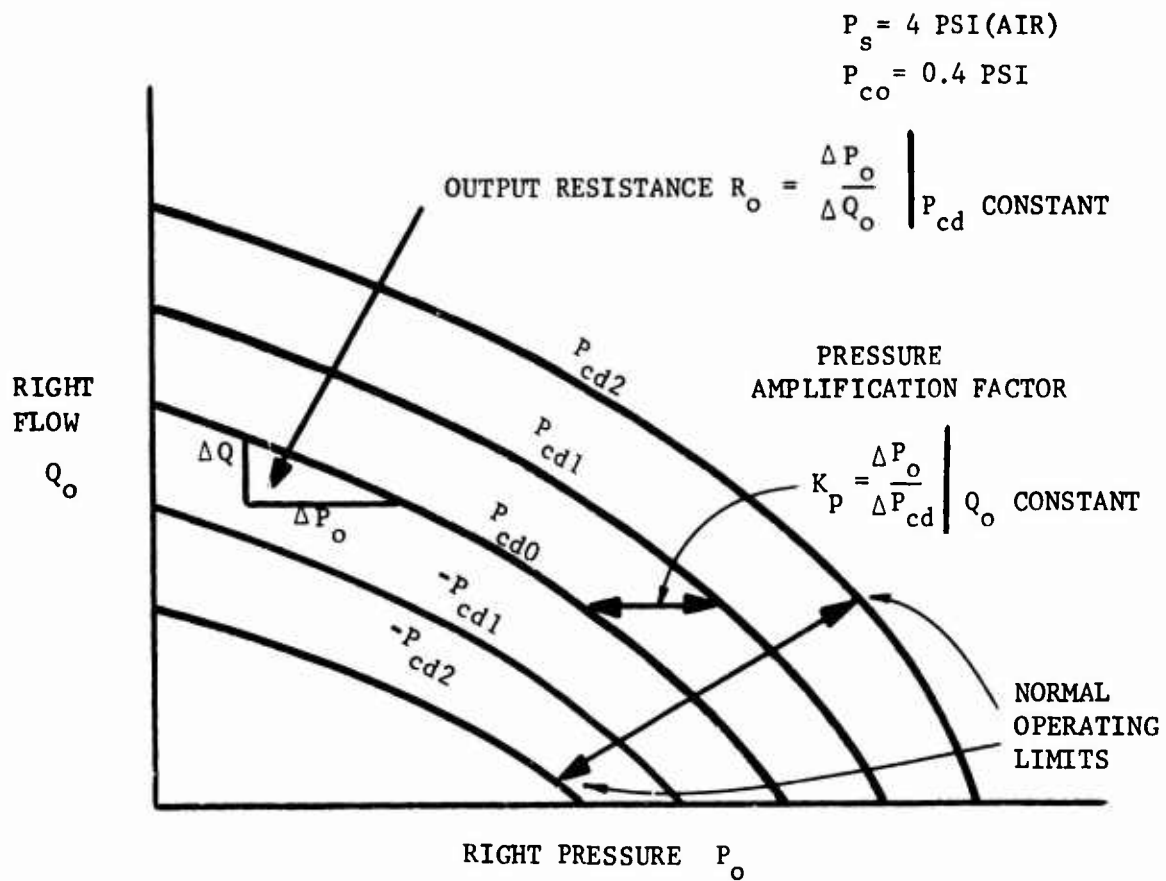


FIGURE 13 - TYPICAL STATIC OUTPUT
 CHARACTERISTICS

In summary, the total static and large-signal characteristics of a fluidic device under normal operating conditions can be described by two sets of curves: input characteristics, and output characteristics with input signal as a parameter.

2.4.1 Normalization of Characteristic Curves

The characteristic curves of fluidic devices vary with supply pressure; therefore, it is necessary to provide input and output characteristics for every allowable supply pressure. This can be done by providing individual input and output curves for a number of supply pressures. It can also be done by providing a single set of input and output characteristics normalized with respect to supply pressure and supply flow. In the latter case it is necessary to provide an additional characteristic curve describing how supply flow varies with supply pressure (power nozzle characteristic).

2.5 EQUIVALENT ELECTRIC CIRCUITS

As an equivalent electric circuit the fluidic amplifier can be represented as shown in Figure 14. The input characteristics are described in terms of simple impedances between the two control ports or between a control port and return. The transfer characteristics are represented by a pressure generator whose output pressure is a function of the net pressure appearing at the control nozzle. The output characteristics are represented as simple series and shunt impedances which are directly coupled to the load impedance.

The elements of the electrical equivalent circuits can all be calculated from the graphical characteristics, circuit dimensions and conditions at the bias (quiescent, no-signal) operating point.

In summary, the small-signal and dynamic characteristics of a fluidic device under normal operating conditions can be represented by an equivalent electric circuit containing various impedances and a simple generator.

2.6 IMPORTANT PHYSICAL QUANTITIES

In the calculation of the dynamic behavior of fluidic components, it is necessary to take into account certain physical dimensions of the circuit and certain qualities of the operating fluid.

2.6.1 Line Lengths

The lengths of lines carrying pressure waves are important in the calculation of equivalent inductance (or inertance) and resistance. This includes the lengths of interconnecting lines, coupling hardware, and passages inside the fluidic component.

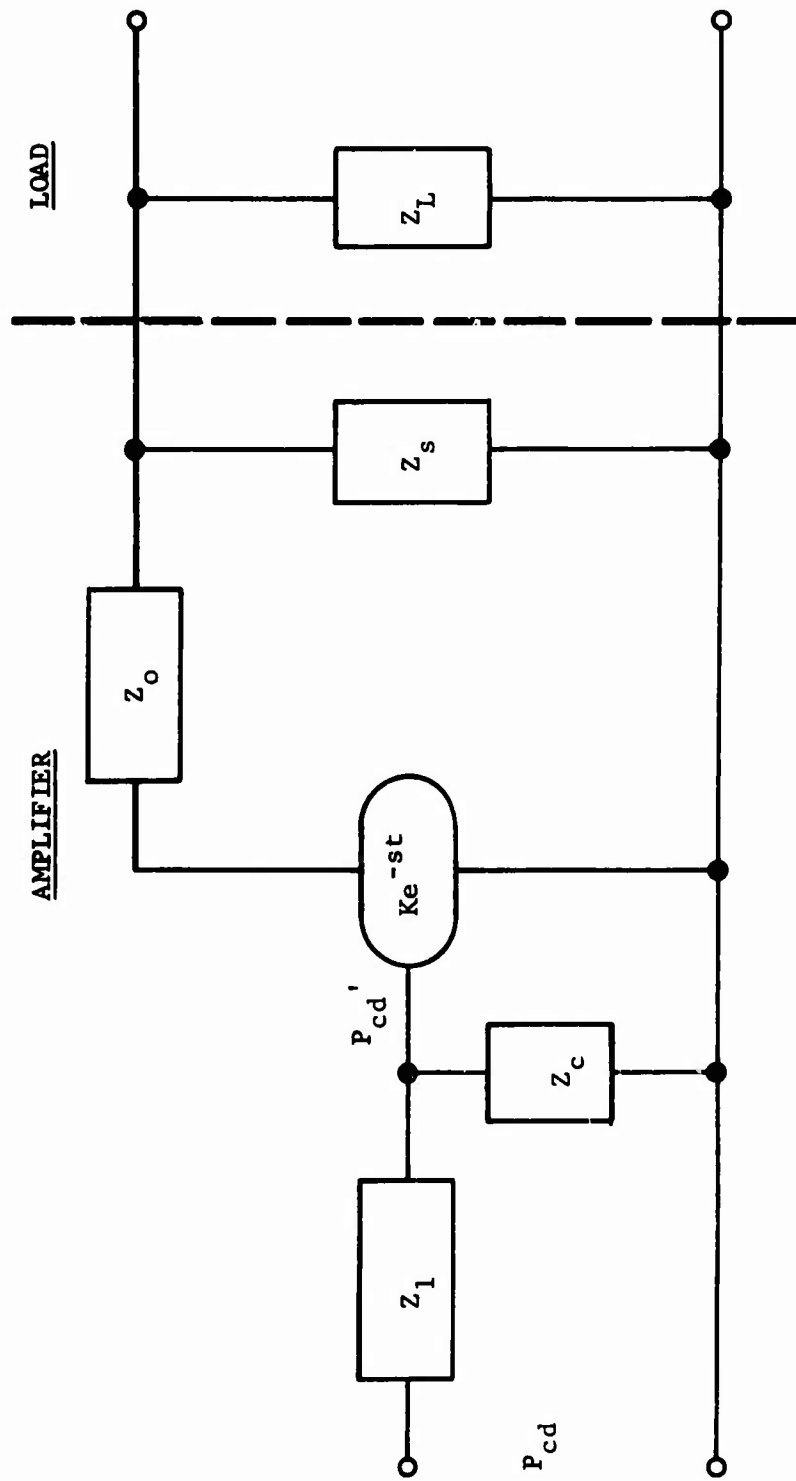


FIGURE 14 - TYPICAL ELECTRIC EQUIVALENT CIRCUIT

2.6.2 Jet Path Lengths

In passages and chamber areas where pressure waves will not propagate and the fluidic signal is transmitted as a flow variation (as in a free submerged jet), it is necessary to know the lengths of paths. From this it is possible to calculate the transit time of a signal through a fluidic component.

2.6.3 Effective Areas

In the calculation of equivalent inductance (inertance) and resistance, it is necessary to consider the effective area of the length of passage. For a fluidic component this may be presented for each different area or as an effective area based on the formula (from Reference 7)

$$A_{\text{effective}} = \frac{A_{\text{in}} - A_{\text{out}}}{\ln \frac{A_{\text{in}}}{A_{\text{out}}}}$$

where A_1 and A_2 are the areas of inlet and outlet sections. The effective areas of all control and outlet passages, coupling devices, and interconnecting lines should be given.

2.6.4 Effective Volumes

In the calculation of equivalent volume capacitances in the circuit containing the fluidic component, it is necessary to know the effective volume of fluid trapped at every level of static pressure; that is, the total volume of fluid under compression. Effective volumes of all lines, connectors, and internal passage must be given.

2.6.5 Power Jet Velocity

In the calculation of transit time, it is necessary to know the average velocity of the power jet in the interaction chamber. Either this can be measured with a pitot tube inserted up through a receiver or it can be calculated from the velocity of the power jet as it exits from the nozzle and as it enters the receiver.

2.6.6 Qualities of the Operating Fluid

In the calculation of equivalent inductance and equivalent line resistances, and in the definition of the conditions under which static characteristics are presented, it is important to know the qualities of the operating fluid. Unless the operating conditions are other than standard, ambient temperature, return and vent pressures, and type of fluid should be provided.

2.7 PERFORMANCE PARAMETERS

Performance parameters can be defined for two basic purposes: first, to describe the behavior of a device under static or dynamic conditions (like pressure gain) and, second, to provide the data necessary to calculate the behavior from basic information (like output impedance). The performance parameters most pertinent to analog fluidic control systems are defined in the following paragraphs.

2.7.1 Output Resistance R_o

Output resistance is defined as the ratio of a change in output pressure to a change in output flow for a fixed control signal; that is,

$$R_o = \frac{\Delta P_o}{\Delta Q_o} \quad \left| \quad P_{cd} \text{ constant} \right.$$

With reference to the static output characteristics of a typical amplifier (as shown in Figure 13), the output resistance is simply the slope of one of the family of curves. Thus the output characteristic curves define the output resistance under all static conditions; but because the characteristic curves are not linear, the actual output resistance is quite variable. Therefore, in determining the appropriate numerical value, the resistance must be calculated at the point at which the amplifier is operated when connected in a circuit.

2.7.2 Pressure Gain G_p

Pressure gain is defined as the ratio of the change in output pressure to the change in control pressure, when the fluidic amplifier is operating in a particular circuit (with a particular load). That is (for a differential amplifier),

$$G_p = \frac{\Delta P_{od}}{\Delta P_{cd}}$$

The transfer curve for a typical differential amplifier is shown in Figure 12. By the above definition the pressure gain is the slope of the transfer curve. Since the curve is not linear, the point at which the amplifier operates in a circuit must be specified in calculating a numerical value for pressure gain.

2.7.3 Flow Gain G_f

Flow gain is defined as the ratio of the change in output flow to the change in control flow, when the fluidic amplifier is operating in a particular circuit (with a particular load). That is (for a differential amplifier),

$$G_f = \frac{\Delta Q_{od}}{\Delta Q_{cd}}$$

By this definition the flow gain is the slope of the transfer curve plotted in units of flow. Since the curve is not linear (similar to the pressure transfer curve of Figure 12), the point at which the amplifier operates in a circuit must be specified in calculating a numerical value for flow gain.

2.7.4 Pressure Amplification Factor K_p

The pressure amplification factor for amplifiers is defined as the ratio of the change in output pressure to the change in control pressure when the output flow is constant. That is,

$$K_p = \left. \frac{\Delta P_o}{\Delta P_{cd}} \right|_{Q_o \text{ constant}}$$

In effect, this is the maximum pressure gain that an amplifier could deliver if there were no loading effects (zero amplifier output resistance). With reference to the output characteristic curves for a typical amplifier (shown in Figure 13), one can see that the amplification factor is a function of the horizontal distance between the output impedance curves. And since the curves are neither linear nor evenly spaced, it is evident that the pressure amplification factor is quite variable. Therefore, in determining the appropriate numerical value for K_p , calculations must be made in the vicinity of the point at which the amplifier operates in a circuit.

2.7.5 Sensitivity Factor K

A sensitivity factor K can be defined for any fluidic sensor in the same way that the pressure amplification factor K_p is defined for an amplifier.

The only difference is that the input variable is the quantity that the sensor measures instead of the control differential pressure. That is,

$$K = \frac{\Delta P_o}{\Delta \text{sensed variable}} \Big|_{Q_o \text{ constant}}$$

Since most output characteristic curves for fluidic sensors are nonlinear, the numerical value for the sensitivity factor must be calculated at the point at which the sensor operates when connected in a circuit.

2.7.6 Input Resistance R_c

Input resistance is defined as the ratio of the change in control pressure to the change in control flow when the bias pressure is held constant. That is,

$$R_c = \frac{\Delta P_c}{\Delta Q_c} \Big|_{(P_{c1} + P_{c2}) \text{ constant}}$$

With reference to the typical differential amplifier static input characteristics (Figure 11), the input resistance is simply the slope of the appropriate curve. And since the curves are nonlinear, the numerical value of the input resistance must be calculated at the point at which the amplifier operates when connected in a circuit.

2.7.7 Equivalent Capacitance C

Because of the compressibility of the operating fluid, there is an equivalent capacitor formed by every element of volume under pressure in the fluidic circuit. As a result, the change of pressure at every point is delayed until there is sufficient flow to satisfy the conditions of compressibility at the new pressure level. The effect is analogous to an electrical shunt capacitor and can be treated as such in equivalent circuit analysis (see section 6.0).

The equivalent capacitance of a fluidic device is defined as the ratio of the trapped volume V to the absolute static pressure P_a . That is,

$$C = \frac{V}{P_a} \quad (\text{for isothermal flow})$$

Since the passages are seldom uniform and the pressure is not the same in every section, each must be calculated as a separate element; then they must be added together to arrive at a total circuit capacitance. The pressure used in the calculation of the equivalent capacitance must of course correspond with the point at which the device operates in a circuit.

2.7.8 Equivalent Inductance L

Because of the inertance of the operating fluid, there is an equivalent inductor formed by every element of mass in the fluid circuit. As a result, the change in flow at every point is delayed until sufficient forces can build up and accelerate the flow to the new level. The effect is analogous to an electrical series inductor and can be treated as such in an equivalent circuit analysis (see section 6.0).

The equivalent inductance of a fluidic device is defined as the ratio of the product of mass density and length to the effective cross-sectional area. That is,

$$L = \frac{\rho l}{A_{\text{eff}}}$$

Since the area of the passages in fluidic circuits is seldom uniform and the density is not the same in every section, each must be calculated as a separate element; then they must be added together to arrive at a total circuit inductance. The pressure used to calculate mass density must of course correspond with the point at which the device operates in a circuit.

2.7.9 Time Delay t_d

The total time delay is made up of a transit time t_d' and a propagation time t_d'' . The transit time delay in a fluidic device is defined as the time required to transport a deflected element of fluid in the power stream from the power nozzle to a point just inside the receiver where pressure waves can propagate. It can be calculated from the ratio of the length of the interaction chamber (where the power jet is essentially free) to the average velocity of the power stream. That is,

$$t_d' = \frac{\text{length of interaction chamber}}{\text{average velocity of fluid flow}}$$

The total time delay also includes the delay in the control and outlet passages due to the finite velocity of sound. In those cases, the delay is calculated from

$$t_d'' = \frac{\text{length of aperture}}{\text{velocity of sound} + \text{velocity of steady fluid flow}}$$

and the total time delay is

$$t_d = t_d' + t_d''$$

2.7.10 Pressure Recovery Factor R_p

Because of losses in fluidic amplifiers, it is not practical to recover 100% of the total power supplied to it. In many cases the recovery is an important factor in the selection of an amplifier for a specific application. Therefore, we define the pressure recovery factor as the ratio of the maximum output pressure to the supply pressure. That is,

$$R_p = \frac{(P_o)_{\max}}{P_s}$$

Note that in the normal differential amplifier the maximum output pressure is recovered when the power stream is in a deflected condition. Note also that similar recovery factors can be defined for flow and power.

2.7.11 Signal-to-Noise Ratio S/N

Signal-to-noise ratio in fluidic circuits has the same meaning that it has in electronic circuits. Expressed in decibels, it is the ratio of the maximum signal capability to the noise at one point in the circuit. That is,

$$S/N = 20 \log_{10} \frac{\text{maximum useable signal}}{\text{noise}}$$

In fluidic amplifiers, the major source of noise is from turbulence and instability of the power stream; therefore, a reasonable measure of the noise can be made at the operating bias point.

3.0 TEST METHODS AND INSTRUMENTATION

3.1 STATIC

3.1.1 Amplifier Static Characteristics (Paragraph 2.4)

The circuit for measuring the static characteristics of a differential fluidic amplifier is shown in Figure 15. Note that flowmeters are required for one output side only, providing that the second output port is connected to a dummy load with the same impedance as the flowmeter.

The circuit contains, in addition to the amplifier under test, a regulated supply of air, manually controlled valves in the lines leading to the control ports, and identical manually controlled valves in the lines from the output ports. The flowmeter in the output circuit should be chosen for low pressure drop. The pressure meters at the supply, control, and output ports can be simple U-tube manometers containing a fluid (mercury or water) suitable for the pressures being measured. Expansion tanks are used at each port to measure the approximate total pressure. Data can be recorded directly onto properly scaled graphs labeled output flow versus output pressure and input flow versus input pressure.

The amplifier is tested as follows: A nominal supply pressure (one for which the amplifier was designed) is applied, and the pressures at the control ports are adjusted to 10% of the supply pressure. (This is the control bias pressure where most jet-interaction amplifiers perform best, but other bias pressures may be appropriate for a particular case.)

The first run (with wide-open load valve) is made by varying the control differential pressure from zero to +10% of supply pressure and from zero to -10% of supply pressure. Note that the bias (the average of the two control pressures) must always remain at 10% of supply pressure. For example, when the right control pressure is raised to 11%, the left control pressure is lowered to 9%, thereby generating +2% control differential while maintaining the bias at 10%. At each point of control differential, the output flow and pressure define a point on the output graph and the input flow and pressure define a point on the input graph.

When the first run is complete, the load circuit valves are closed an equal amount, giving roughly 1/4 of the supply pressure at the output ports with zero control differential. The second run, varying the control differential pressure from zero to +10% of supply and from zero to -10% of supply, yields a new set of points on the output graph. The input points should be checked against the results of the first run to determine if it is necessary to record them.

Additional runs are made in an identical manner: the load valves are closed in increments until the final run with blocked output ports.

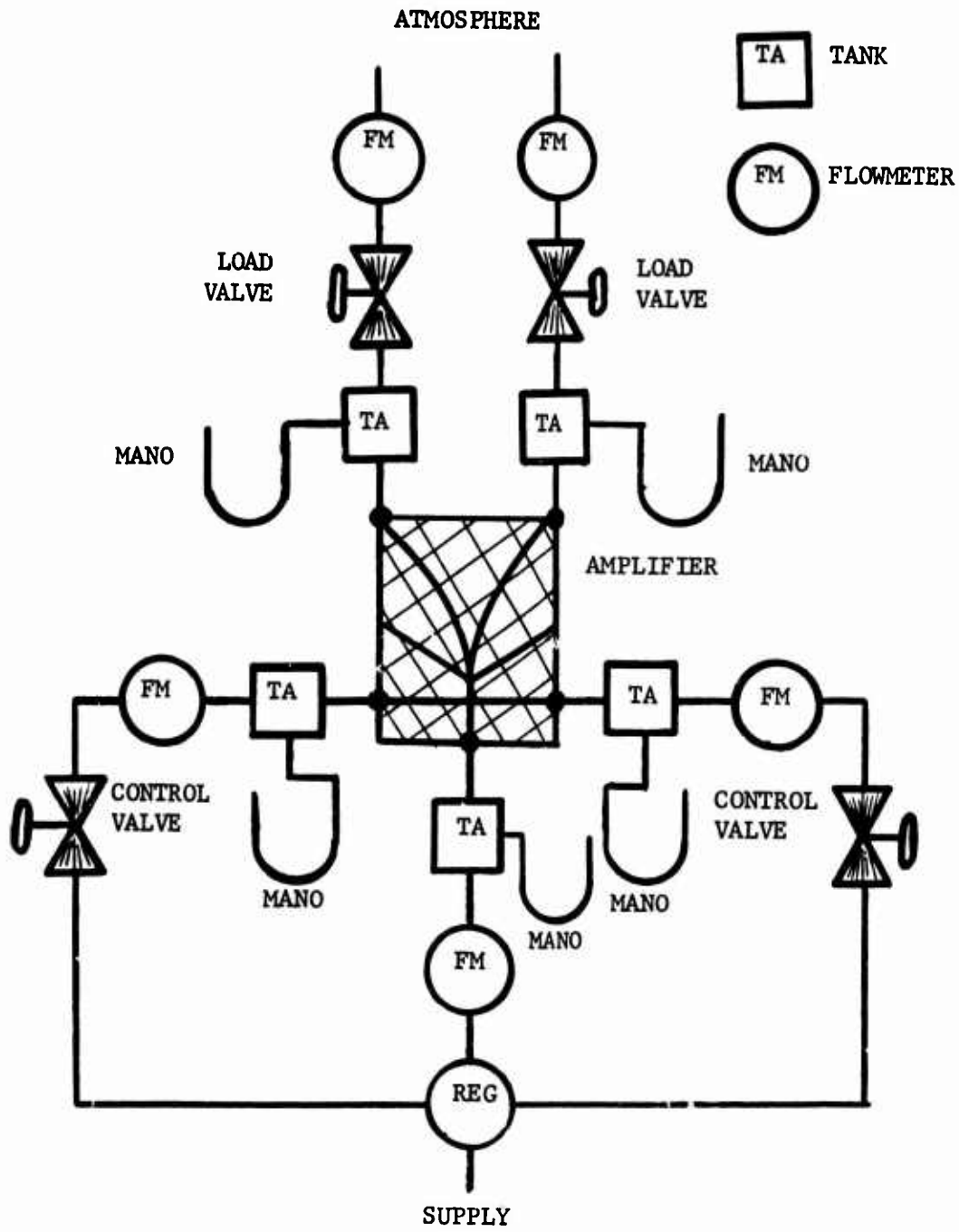


FIGURE 15 - CIRCUIT FOR MEASURING DIFFERENTIAL
FLUIDIC AMPLIFIER

Finally, points of equal control differential pressure are connected with smooth curves. A typical set of output characteristic curves for a jet interaction amplifier is shown in Figure 16. Note that, although they represent a differential amplifier, they are actually measured on one side only, if the amplifier is reasonably well balanced.

A second and third set of output and input characteristics should be taken with the same supply pressure but with control bias pressures of 5% of supply and 20% of supply respectively. A fourth and fifth set, taken at supply pressures above and below the nominal, and with control bias at 10% of supply, will complete the characteristics necessary for matching operating points and analyzing the response to large signals.

The static characteristics of other types of fluidic amplifiers are measured in a similar manner. It should be emphasized that, when many characteristics are to be recorded, it is most convenient to automate the process, using electronic transducers and a graphical XY plotter.

3.1.2 Sensor Static Characteristics (Paragraph 2.4)

The circuit for measuring the static output characteristics of a push-pull vortex rate sensor is shown in Figure 17. Note that a flowmeter is required in only one of the output lines, providing that the adjacent line contains an equivalent dummy impedance.

The circuit contains, in addition to the rate sensor under test, a regulated supply of air, a means for rotating the sensor at a known rate increment, manually controlled valves in the output, a flowmeter of low pressure drop, and U-tube manometers containing appropriate fluids (typically water).

The rate sensor is tested as follows. A nominal supply pressure is applied, and the load valve is opened wide. The rate sensor is rotated at a known rate, and the output conditions are recorded as a point on an appropriately scaled graph of output flow versus output pressure. The rate of turn is changed by a known increment, and the resulting output circuit conditions are recorded as a point on the output graph.

When a predetermined number of values of rate of turn have been tested, the load circuit valves are closed by equal increments, the range of rate increments is repeated, and the resulting output pressures are recorded. Additional runs are made with load valves set at increments giving uniformly spaced points on the output graph until the loads are completely blocked. Finally, points of equal rates of turn are connected with smooth curves. The result is a set of output characteristics, shown in Figure 18, which are typical of many vortex rate sensors.

The static characteristics of other types of fluidic sensors are measured in a similar manner.

MODEL 1602-A AMPLIFIER $P_s = 8$ PSI (AIR) $P_{co} = 0.8$ PSI

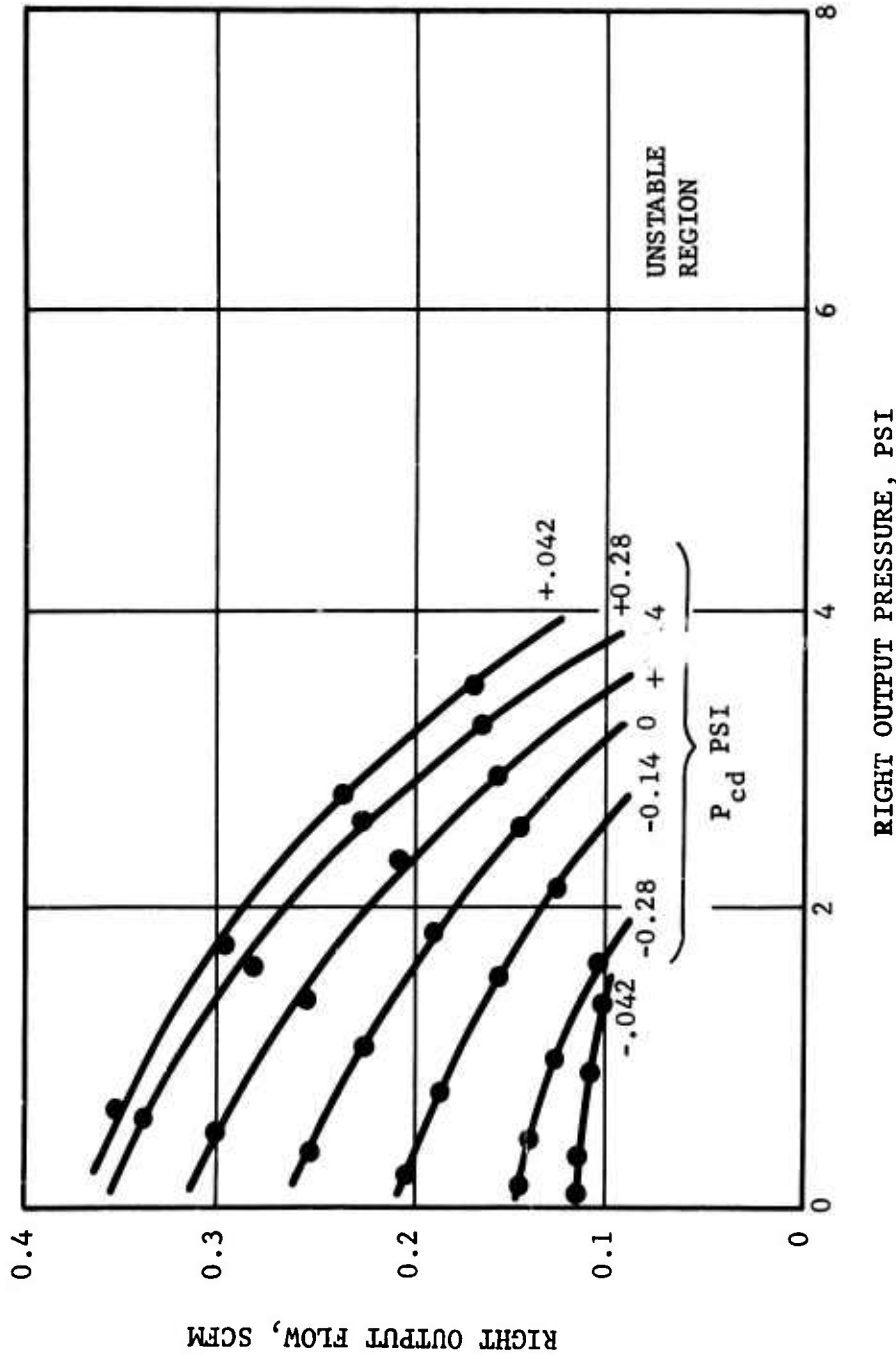


FIGURE 16 - TYPICAL STATIC OUTPUT CHARACTERISTICS OF
A JET-INTERACTION AMPLIFIER

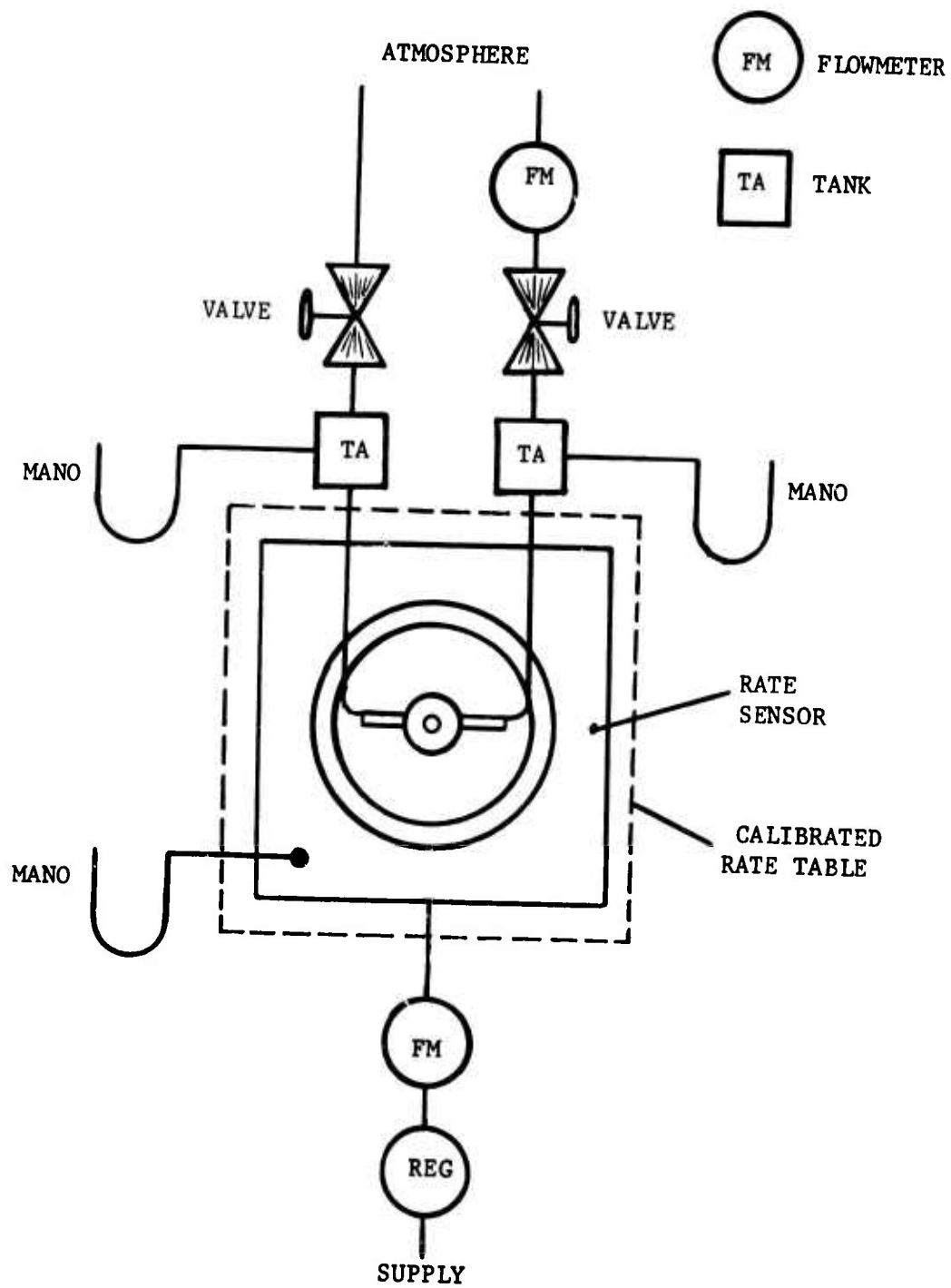


FIGURE 17 - CIRCUIT FOR MEASURING STATIC
OUTPUT CHARACTERISTICS OF A VORTEX RATE SENSOR

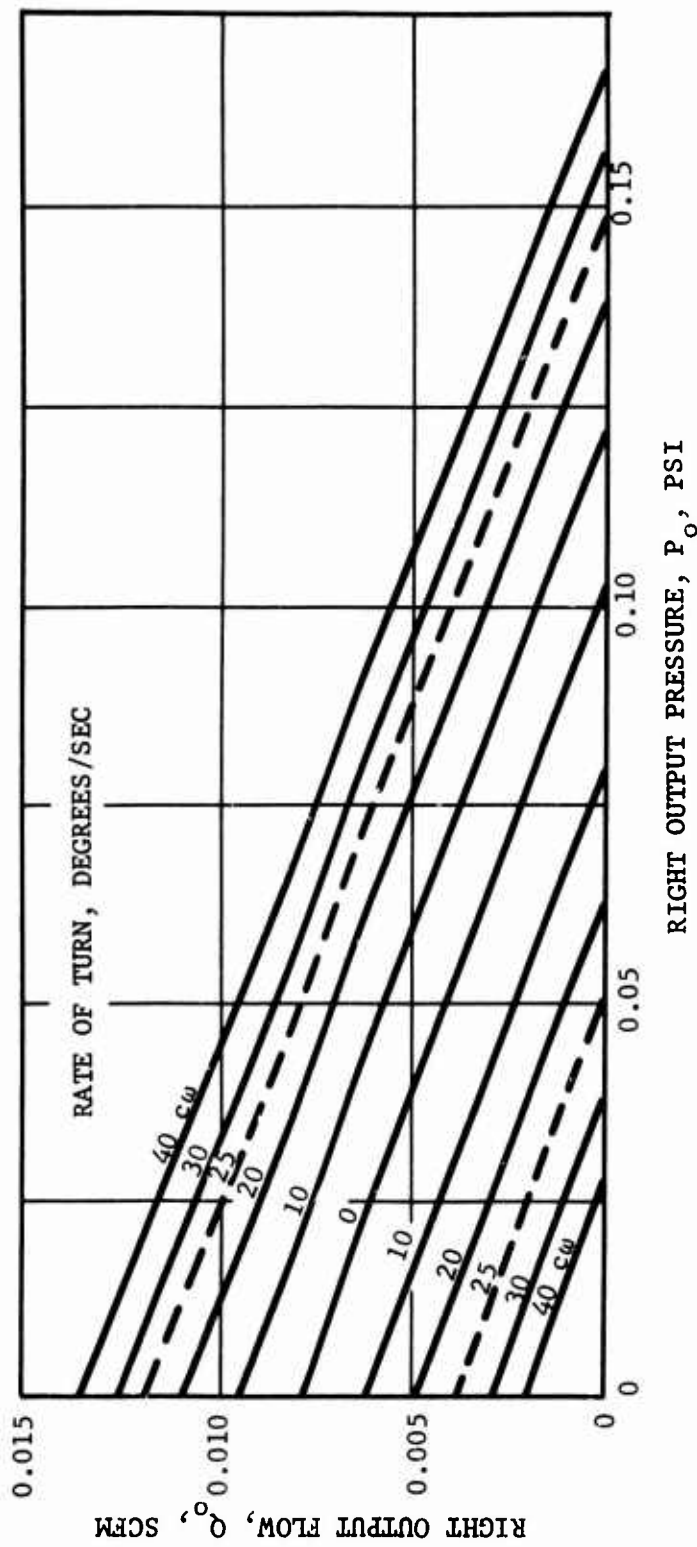


FIGURE 18 - TYPICAL STATIC CHARACTERISTICS OF A VORTEX RATE SENSOR

3.1.3 Passive Element Static Characteristics (Paragraph 2.4)

The circuit for measuring the static characteristics of any fluidic passive element is shown in Figure 19. The circuit contains, in addition to the element under test, a regulated supply pressure, a manually controlled valve, a U-tube manometer connected across the resistor, and a low-pressure-drop flowmeter on the exhaust side of the circuit.

A resistor is tested as follows. The supply pressure is set at a value slightly above the maximum which the resistor will be exposed to in use. The manual valve is opened wide, resulting in a particular combination of pressure drop and flow which is recorded as a point on an appropriately scaled graph of flow versus pressure drop. The manual valve is closed a given increment, causing a new combination of pressure drop and flow which is recorded as a new point. The valve is closed by increments, until it blocks the flow to the element, and the resulting points are plotted on the graph. Finally, the points are connected to form a smooth curve representing the static characteristics of the element. The result is a characteristic typically as shown in Figure 20.

3.2 DYNAMIC

3.2.1 Amplifier Dynamic Characteristics (Section 6.0)

3.2.1.1 Adjusting the Test Circuit and Interpreting Data Displayed

The circuit for measuring the dynamic characteristics of a push-pull (differential) fluidic amplifier is shown in Figure 21. Note that the use of pressure instrumentation is illustrated. Flow transducers could be used if preferred.

The test circuit contains, in addition to the amplifier under test, a source of supply, a pneumatic sinusoidal signal generator with separately adjustable bias and amplitude levels (to be described in detail in paragraph 3.3.1), manometers containing appropriate fluids connected at the control and output ports, equal loads connected at the output ports, identical minimum-volume differential pressure transducers connected between the control ports and between the output ports (paragraph 3.3.2), an electrical power supply (typically two 3-volt dry-cell batteries), and a high-sensitivity XY plotting oscilloscope with identical X and Y amplifiers (paragraph 3.3.4). The X axis is connected to the input transducer, and the Y axis is connected to the output transducer.

The amplifier is adjusted for test as follows. Supply pressure (typically 8 psig) is applied to the amplifier circuit and the pneumatic sinusoidal signal generator. The signal generator is set to run at a speed producing 5-10 cps, while the control circuit bias pressure is adjusted to 10% of the

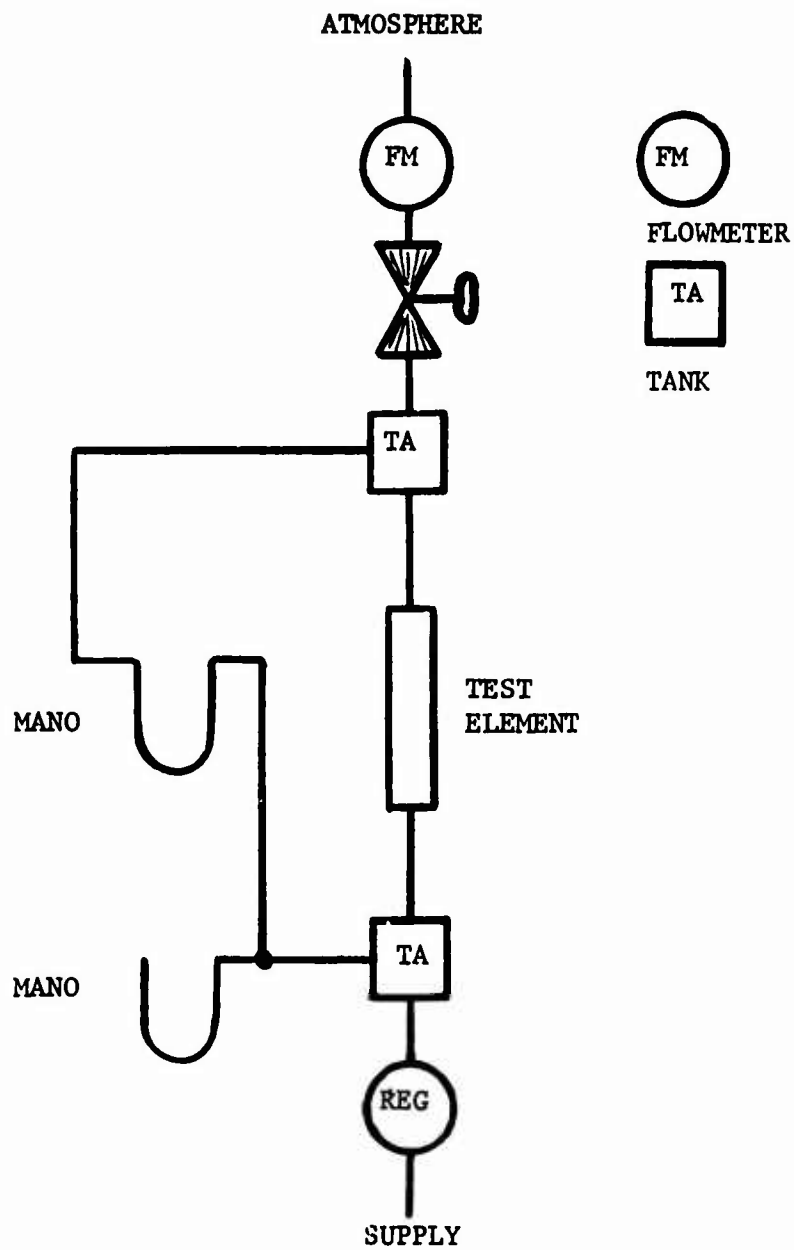


FIGURE 19 - CIRCUIT FOR MEASURING STATIC CHARACTERISTICS OF A PASSIVE ELEMENT

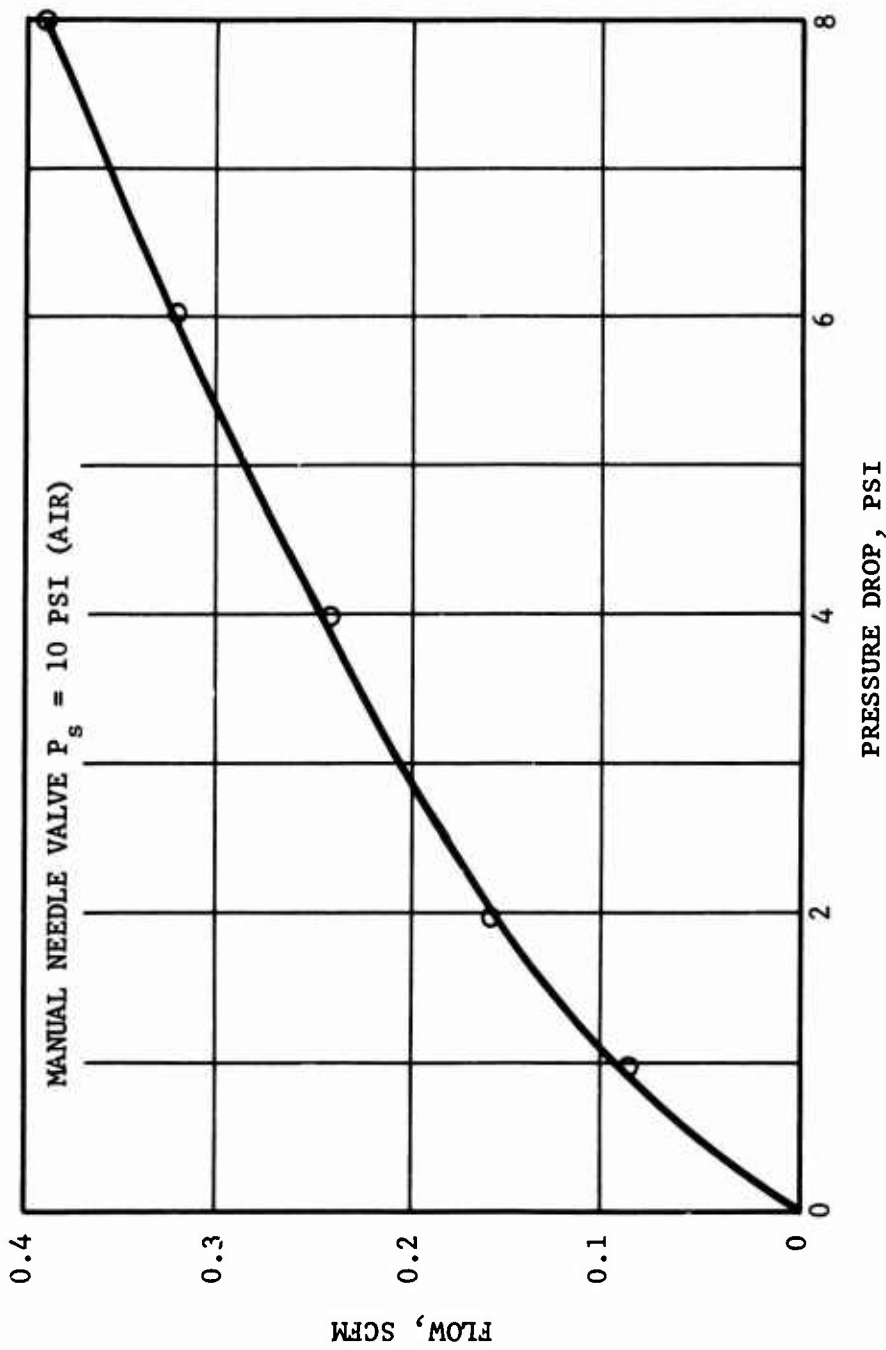


FIGURE 20 - TYPICAL STATIC CHARACTERISTICS OF A
FLUIDIC RESISTOR

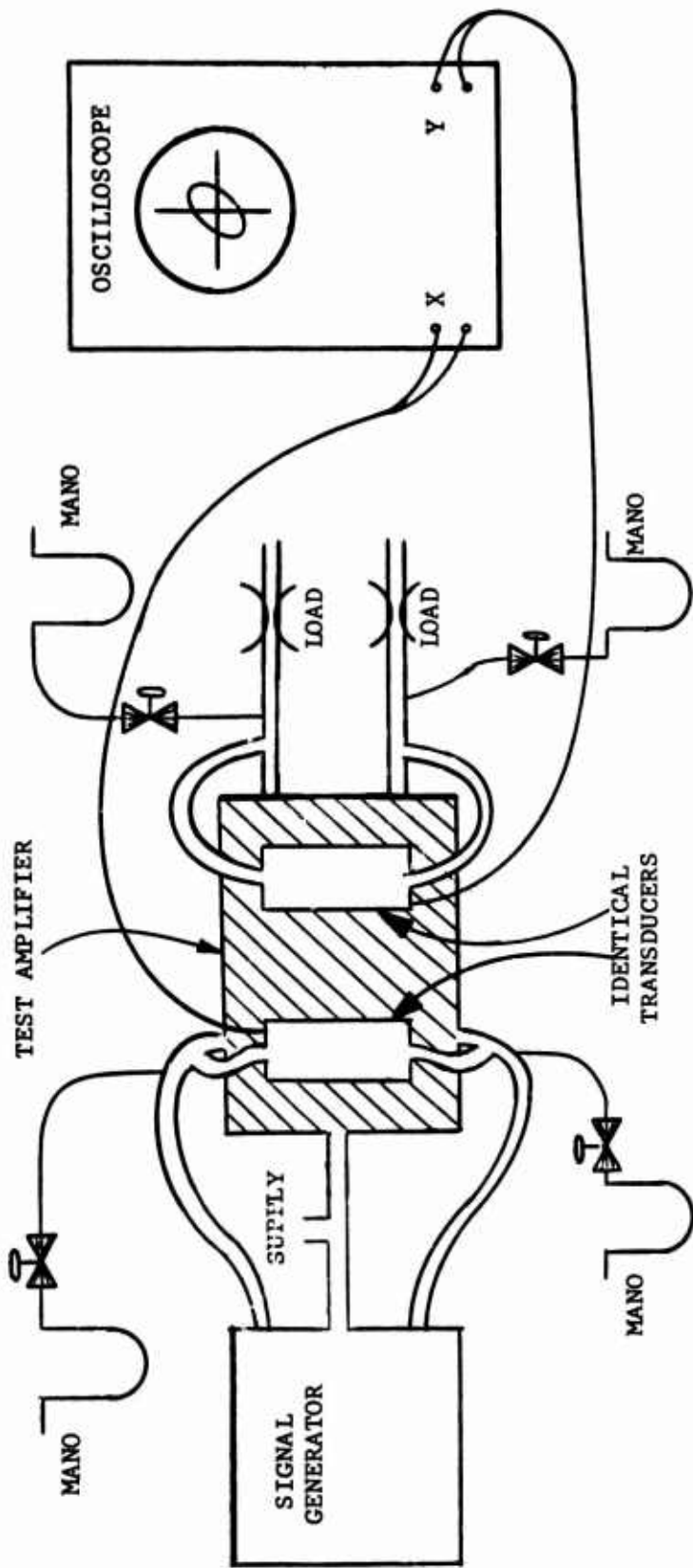


FIGURE 21 - CIRCUIT FOR MEASURING DYNAMIC CHARACTERISTICS OF A DIFFERENTIAL AMPLIFIER

supply pressure (or any other appropriate bias level). The signal generator drive motor is then shut off; and by advancing the generator rotor disc slowly by hand, the amplitude of the sinusoidal differential pressure signal is measured. The amplitude is then adjusted (typically 10% of supply pressure, peak to peak) to the proper level. If an adjustment is made, it is necessary to repeat the bias adjustment again, then the amplitude adjustment, until both requirements are satisfied. The bias and the amplitude pressures are noted, and the control circuit manometers are cut off. The load bias pressures are noted, and the load circuit manometers are cut off.

With the signal generator running at low speed (typically 1 to 2 cps) and the transducer power supply connected, the oscilloscope sensitivities are adjusted (in the XY mode) for good readability (as illustrated in Figure 22a). The figure on the oscilloscope is obviously a plot of the output pressure (Y axis) versus the input pressure (X axis); and if the oscilloscope amplifiers have been set for equal sensitivity, the slope of the figure is the pressure gain of the amplifier circuit.

At higher frequencies, when there is a significant amount of phase shift between the output signal (Y axis) and the input signal (X axis), the figure appearing on the oscilloscope is not a single line, but rather a closed figure. If the amplifier (or circuit element) under test is ideally linear, the figure is a straight line for zero phase difference, an ellipse with its major axis greater than the slope of the straight line for phase differences between 0 and 90°, and an ellipse with its major axis exactly vertical for a phase difference of 90°. For phase differences greater than 90°, the major axis of the ellipse rotates into the second, third, and fourth quadrants. These situations are illustrated in Figure 22 for phase differences of less than 180°.

Both gain and phase difference can be read from the oscilloscope display. Gain is the ratio of the maximum excursion in the Y direction to the maximum excursion in the X direction, as illustrated in Figure 23. The phase difference is calculated from the ratio of the width of the ellipse in the Y direction to the maximum excursion in the Y direction; that is,

$$\text{sine of phase angle difference} = \frac{\text{width of ellipse}}{\text{maximum Y deflection}}$$

or

$$\theta = \sin^{-1} \frac{A}{B}$$

3.2.1.2 Frequency Response Testing (Section 6.0)

The amplifier circuit is now ready for frequency response testing. The first point is measured with the signal generator set at a very low frequency (less than 1 cps). The gain and phase shift are calculated from the figure on the oscilloscope. The frequency (which can also be measured

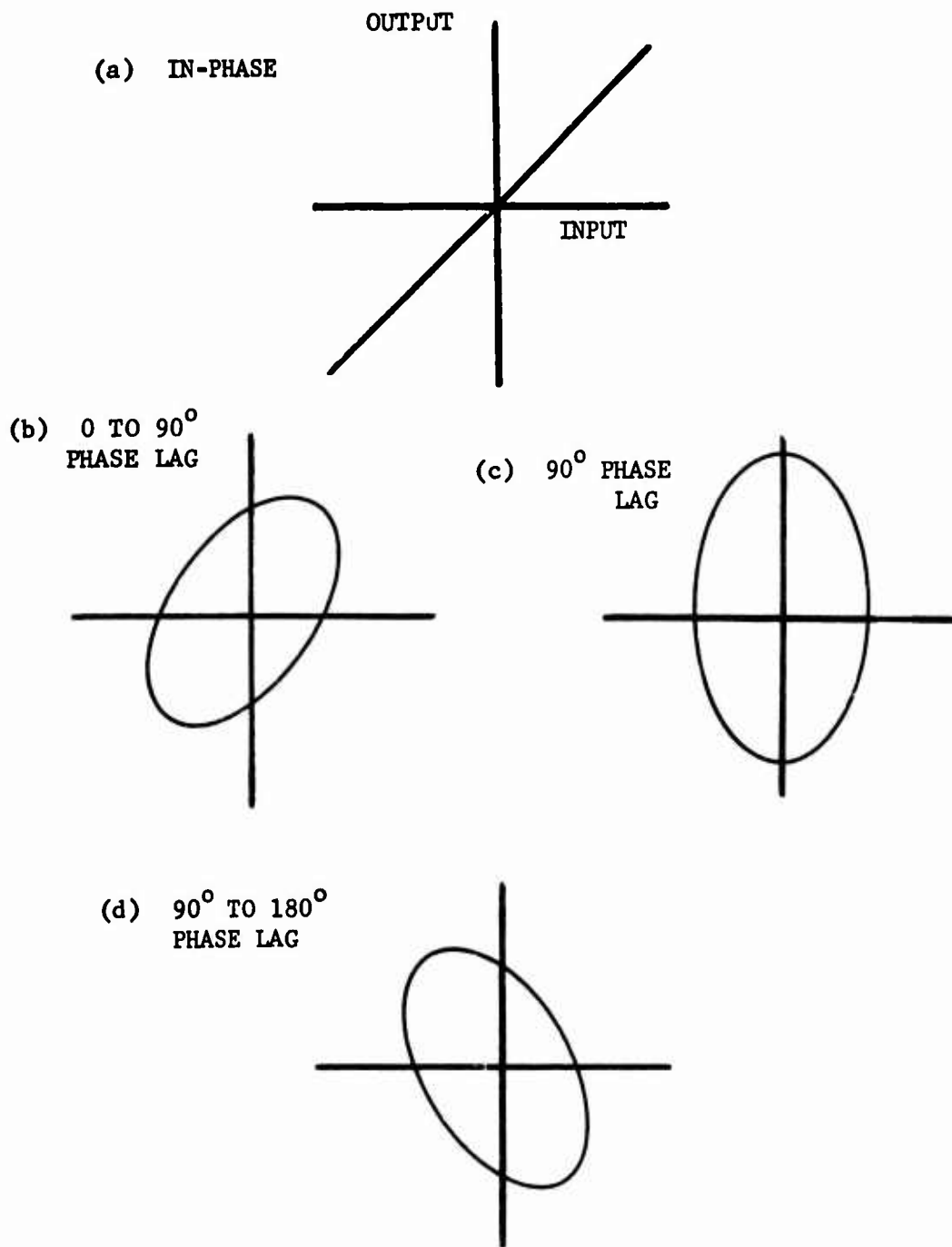


FIGURE 22 - TYPICAL OSCILLOSCOPE DISPLAYS
OF SINUSOIDAL RESPONSE (XY MODE)

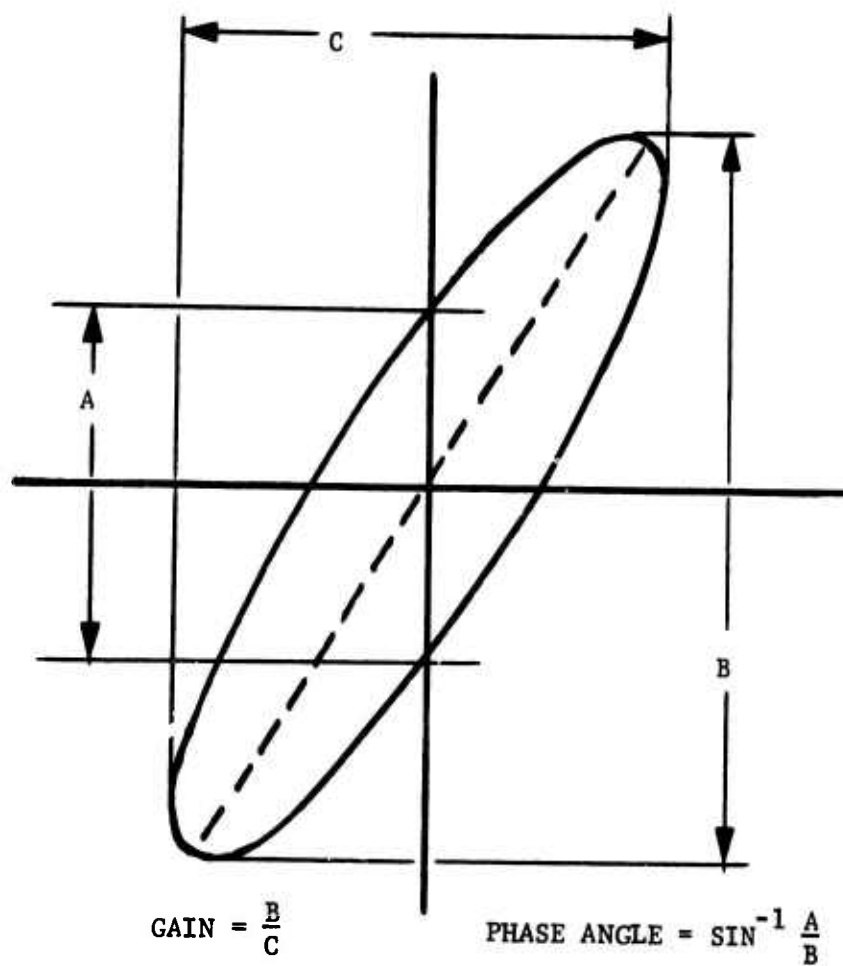


FIGURE 23 - MEASURING GAIN AND
PHASE ANGLE FROM OSCILLOSCOPE DISPLAY

on the oscilloscope by temporarily switching to the time base mode of display), the gain, and the phase shift are recorded. Other points are measured at convenient increments of frequency (typically 1, 2, 5, 7, 10, 20, and so on) up to frequency where the output is so attenuated that the response cannot be separated from the noise appearing on the oscilloscope.

From these data, the gain is calculated in decibels = $20 \log_{10} \frac{P_{out}}{P_{in}}$.

The results are plotted as a familiar Bode diagram (Figure 24), which shows how the magnitude of the gain and the phase shift of the amplifier circuit vary with frequency of the incoming sinusoidal pressure signal.

3.2.1.3 Measuring Total Time Delay (Paragraph 2.7.9)

For measuring the time delay (transport time) of a fluidic amplifier, it is convenient to substitute a square-wave signal generator for the sinusoidal signal generator used in the frequency response tests (Figure 21). The transient response is then displayed on the oscilloscope used in its two-trace mode (both input and output pressures displayed on a common time base). A typical response is shown in Figure 25. The time delay (transport time) is then measured as the time difference between the initial rise of the square-wave input signal and the initial rise of the output pressure. The measurement is made more convenient by photographing the oscilloscope display and reading the resulting print.

The time delay appears in the frequency response as a phase difference directly proportional to frequency. The phase contributed by the time delay can be calculated from

$$\theta = 360 \times \text{time delay} \times \text{frequency}$$

3.2.2 Sensor Dynamic Characteristics (Section 6.0)

The circuit for measuring the dynamic characteristics of a typical fluidic sensor (rate sensor) is shown in Figure 26. The circuit contains in addition to the sensor under test, a source of supply pressure, a means for introducing a dynamic change in the sensed variable (such as a sinusoidally driven rate table), a transducer to measure the sensed variable independently (such as a high-performance electromechanical rate gyro), a minimum volume differential pressure transducer (paragraph 3.3.2), a source of power for the transducers, an appropriate load on the rate sensor outputs, and an XY oscilloscope (paragraph 3.3.4).

The input transducer is connected to the X axis of the oscilloscope, and the output transducer is connected to the Y axis of the oscilloscope. With the oscilloscope in the XY mode the input is varied sinusoidally at a relatively small peak-to-peak amplitude at various frequencies of interest.

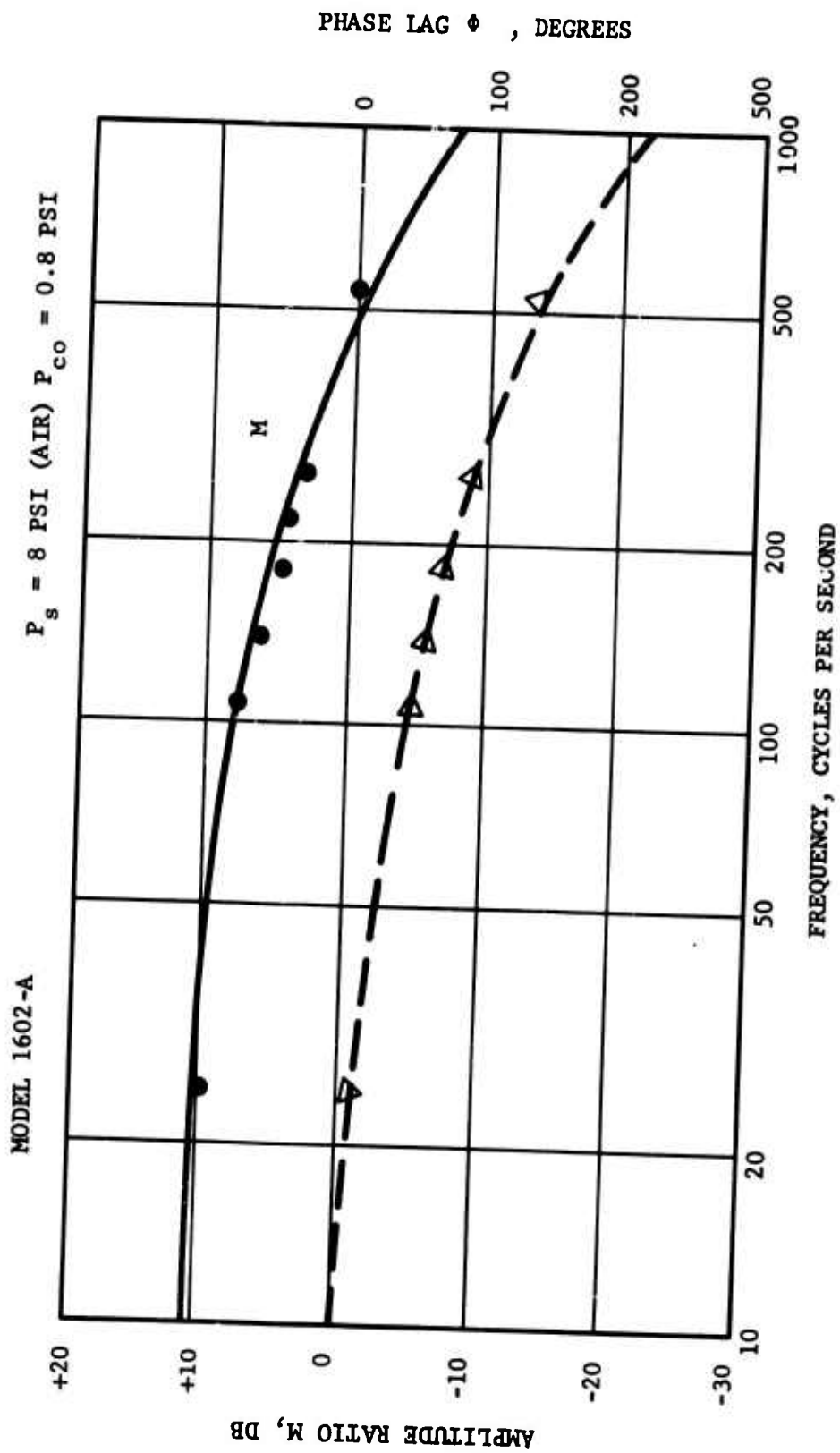


FIGURE 24 - TYPICAL FREQUENCY RESPONSE OF AN AMPLIFIER

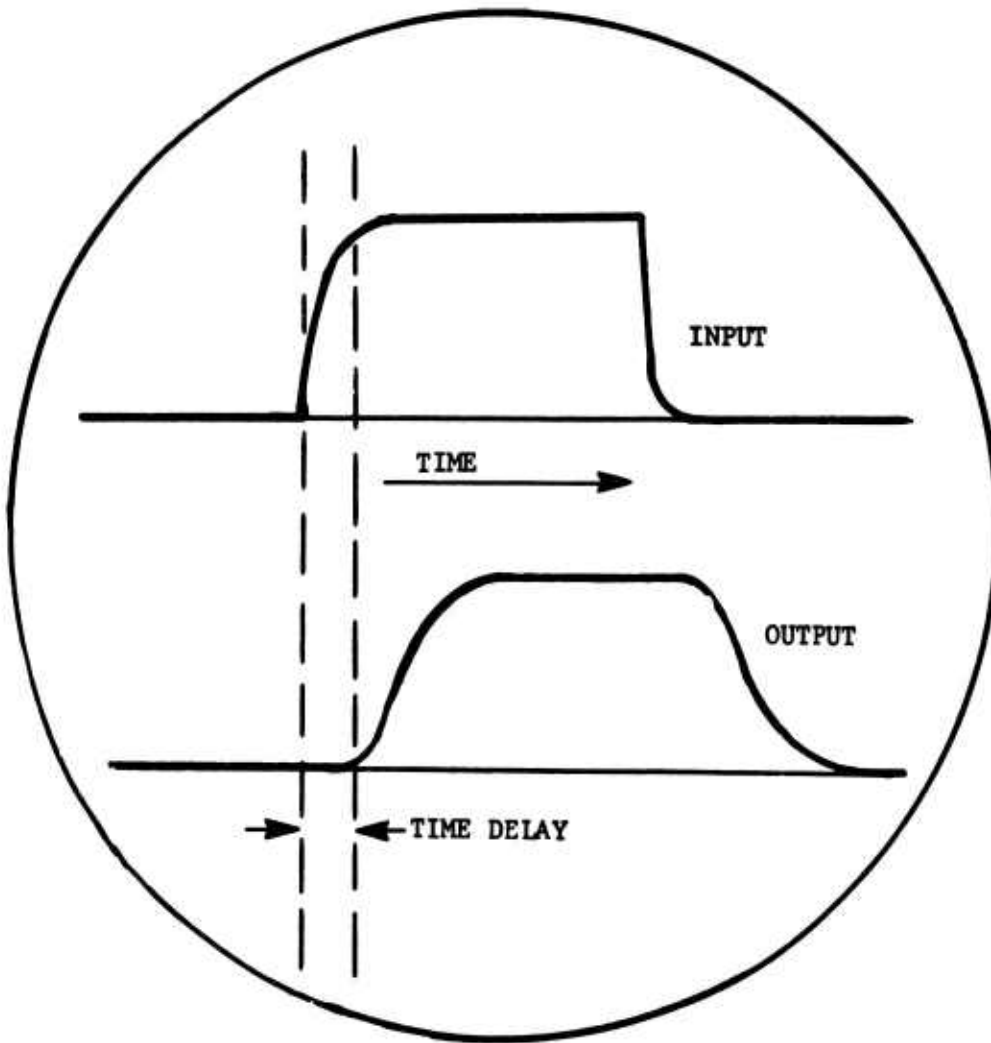


FIGURE 25 - TYPICAL OSCILLOSCOPE DISPLAY
OF STEP RESPONSE (COMMON TIME BASE)

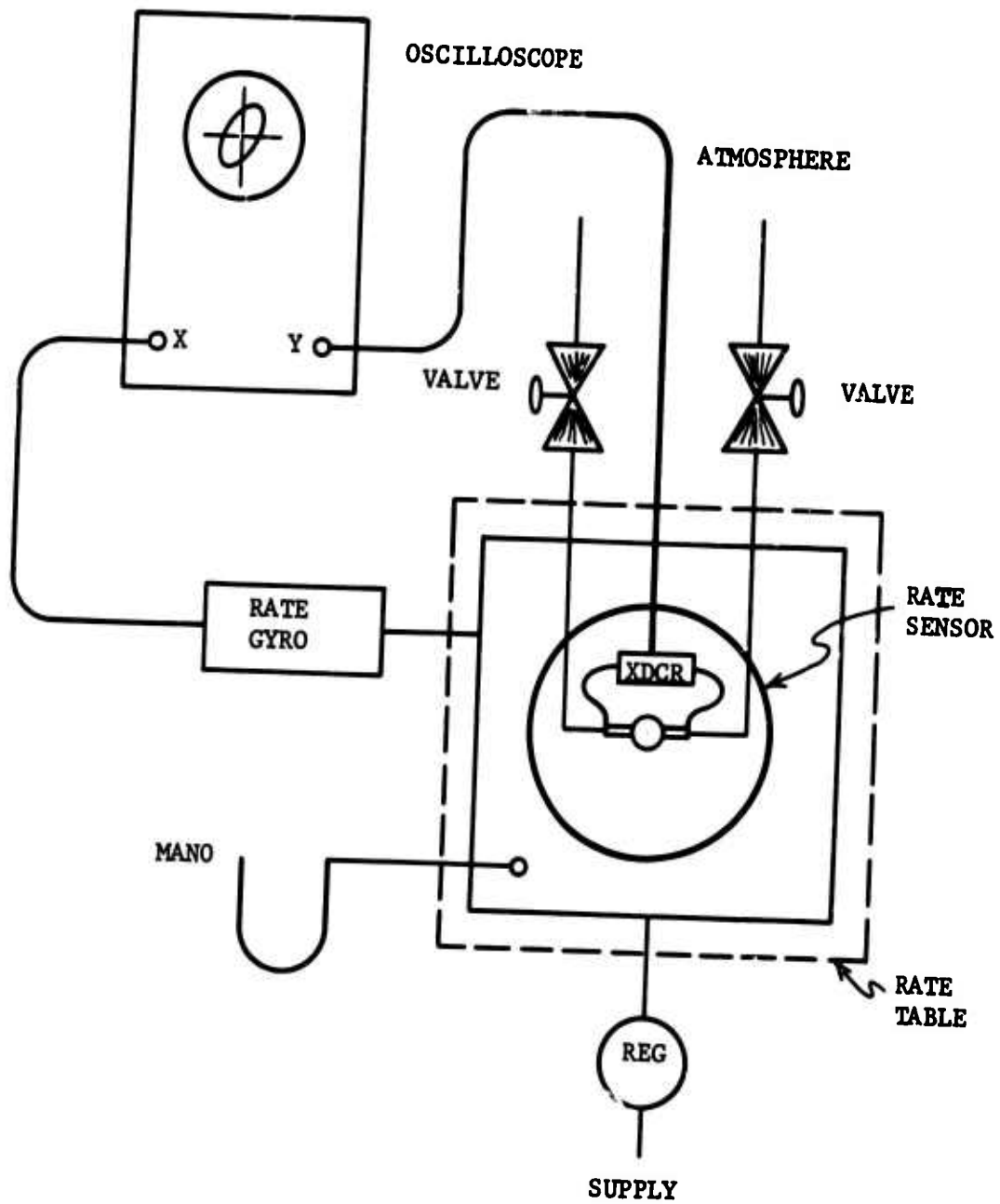


FIGURE 26 - CIRCUIT FOR MEASURING
 DYNAMIC CHARACTERISTICS OF
 A VORTEX RATE SENSOR

The amplitude and phase response of the sensor can then be measured directly from the oscilloscope display, as described in section 3.2.1.2. The results are plotted as a familiar Bode diagram showing the variation of amplitude and phase with frequency.

The time delay (transport time) of the sensor is measured from the response to a step input. The results are displayed on the oscilloscope in the two-trace mode with both input and output signals plotted on a common time base. The time delay is measured as the difference between the initial rise of the input signal and the initial rise of the output signal. The measurement is more convenient if the oscilloscope display is photographed and the reading taken from the resulting print (as described in section 3.2.1.3).

3.2.3 Passive Element Dynamic Characteristics (Section 6.0)

The circuit for measuring the dynamic characteristics of any passive fluidic element is shown in Figure 27. In addition to the element being tested, the circuit requires a source of fluid supply, a sinusoidal differential pressure signal generator (described in section 3.3.1), a minimum-volume differential pressure transducer (paragraph 3.3.2), a source of power for the transducer (3-volt battery), a miniature dynamic flow probe (hot-wire anemometer) (paragraph 3.3.3), and an XY plotting oscilloscope (paragraph 3.3.4).

In running a frequency response test of an impedance element, it may be desirable to have a biased differential pressure signal, simulating the conditions encountered in most fluidic amplifier circuits. The signal generator can be unbalanced to provide this bias flow.

To measure the dynamic characteristics, the flow transducer is connected to the Y axis of the oscilloscope and the pressure transducer is connected to the X axis. The signal generator is adjusted for a peak-to-peak amplitude representing typical conditions (say, 1 psi). The signal generator is then set to run at a low frequency (below 1 cps). The figure displayed on the oscilloscope in the XY mode is obviously a plot of the pressure-flow static characteristics. (Typically, an orifice would display a square-law relationship; a capillary would show a linear relationship.) Thus, the impedance of the passive element would be a function of the slope of the curve around the bias point. With properly calibrated transducers, the impedance at that frequency can be calculated directly from the oscilloscope display.

The frequency can be increased in convenient increments, and the magnitude and phase angle of the impedance can be measured from the oscilloscope display as described in section 3.2.1.1. The results are plotted in the form of a Bode diagram, showing how the magnitude of the impedance and the phase angle of the impedance vary with frequency of the applied pressure.

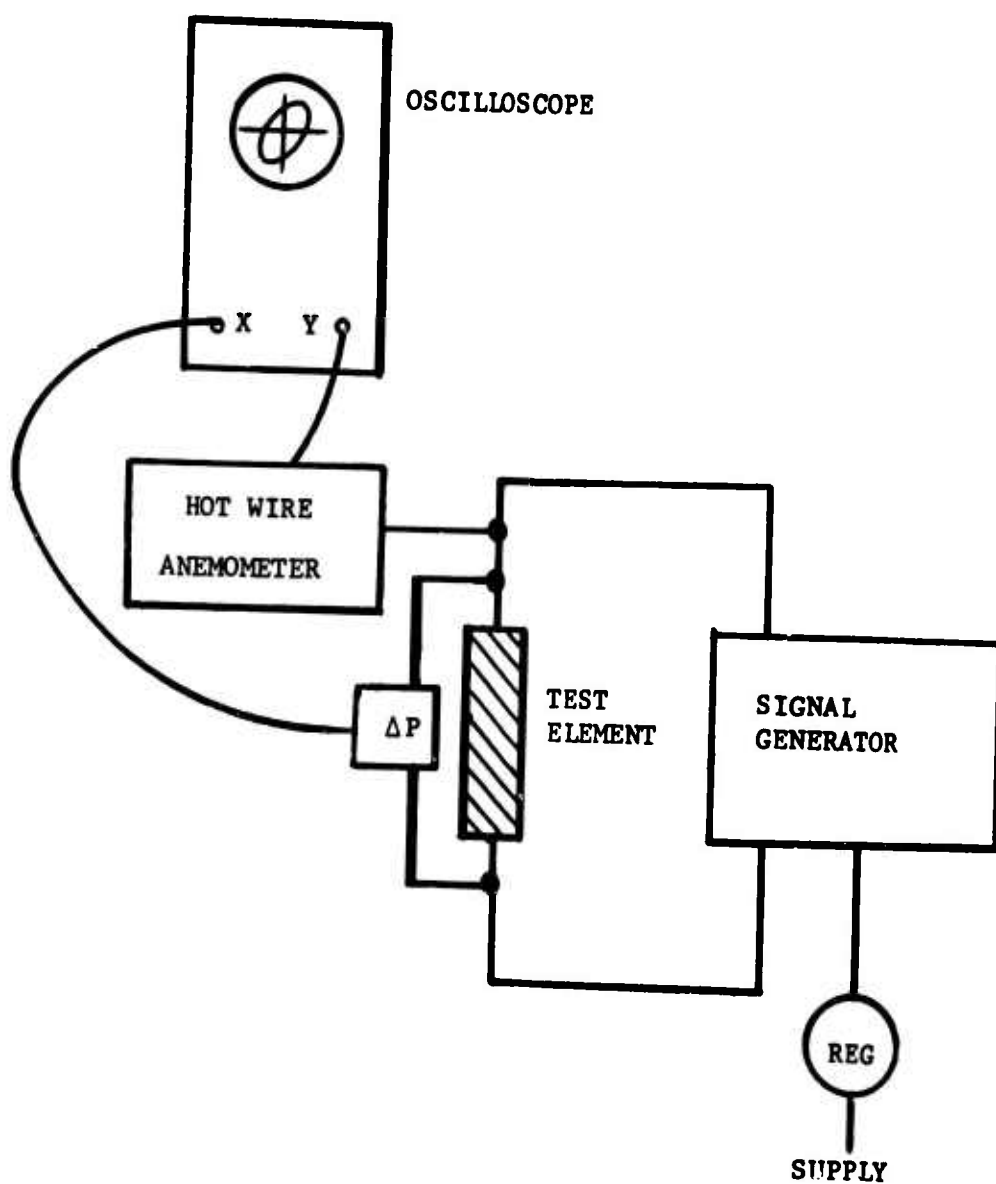


FIGURE 27 - CIRCUIT FOR MEASURING DYNAMIC CHARACTERISTICS OF A PASSIVE ELEMENT

3.3 SPECIAL TEST EQUIPMENT

3.3.1 Pneumatic Pressure Signal Generator

The pneumatic signal generator required to implement the foregoing dynamic tests must have the following specifications:

1. Deliver a differential pressure signal.
2. Include an independently adjustable bias pressure in both output lines.
3. Include an adjustment for peak-to-peak amplitude of the output signal.
4. Have a continuously adjustable frequency from 1 cps to 300 cps.
5. Generate either a sine wave or a square wave ($\pm 5\%$ distortion) with a minimum of changeover effort.
6. Maintain a relatively constant ($\pm 10\%$) output over the specified frequency range.
7. Require standard pneumatic and electrical power inputs.

3.3.2 Pressure Transducers

The pressure transducers necessary to implement the test circuits such as those shown in Figures 21, 26, and 27 have one major physical requirement. That is, they must be capable of measuring pressures in a physical circuit without introducing a large volume capacitance. Therefore, they must have a minimum-diameter flush-mounted diaphragm and be connected into the test circuit by means of a minimum-volume adapter similar to the one illustrated in Figure 28, using the shortest possible lines. It should be noted that in a differential pressure transducer, the dynamics of the two sides are not identical and can never be made so. Therefore, they should be connected into the test circuit in the same phase (that is, high pressure on the same sides at the same time) so that the effect will be partially cancelled.

3.3.3 Flow Transducers

For dynamic testing, the only practical flow sensor known is the hot wire. However, there are many levels of sophistication in the instrumentation circuits necessary to provide an indication of the instantaneous flow. Again, since the dynamic behavior of any fluidic circuit is so highly dependent on the associated lines and volumes, the hot-wire sensor should be arranged so that it introduces a minimum of additional volume and restriction into the test circuit. The sensors should also be properly phased to minimize any resulting nonlinear effects. That is, they should be so arranged that high flow occurs at the same instant at each sensor.

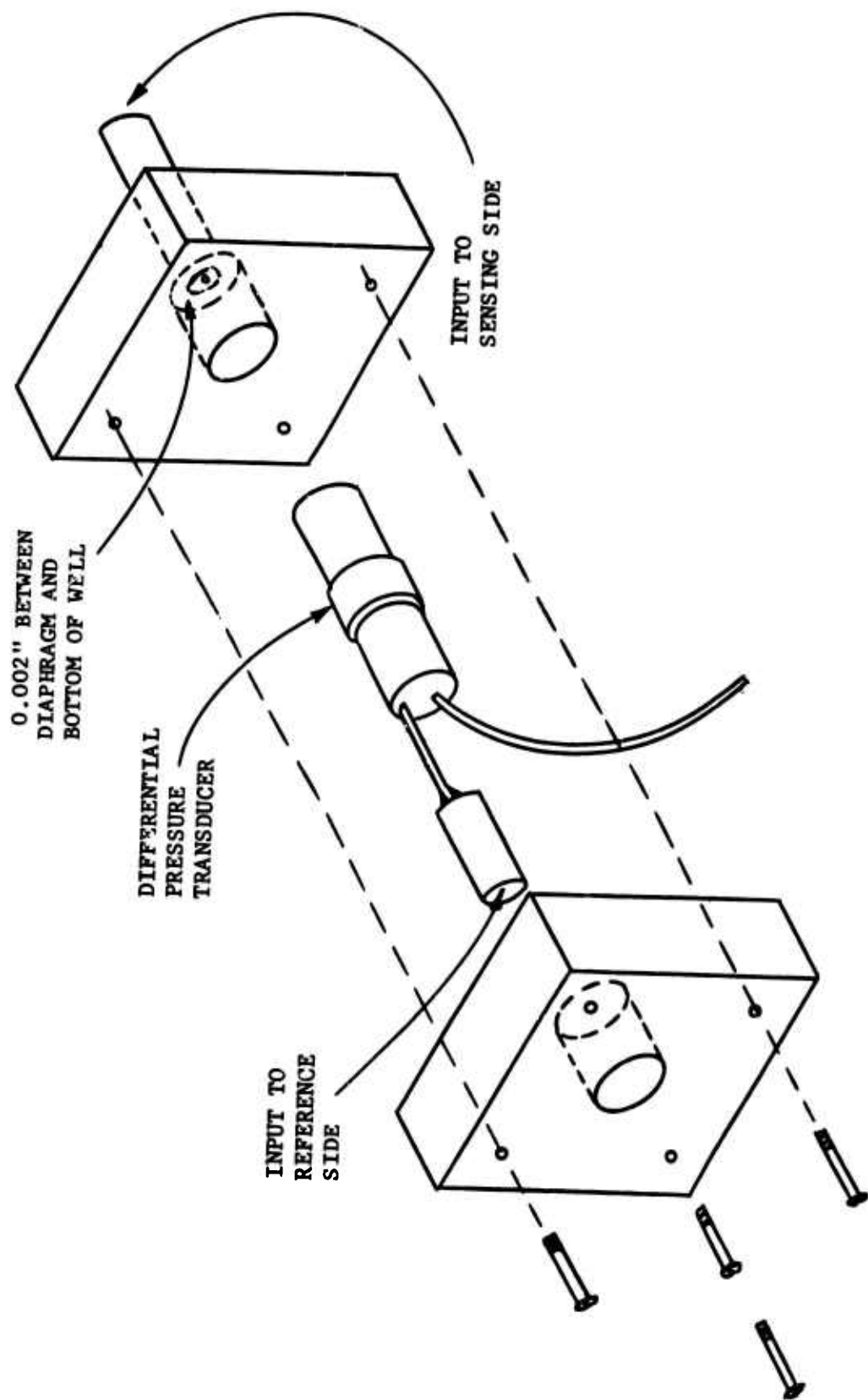


FIGURE 28 - PRESSURE TRANSDUCER WITH MINIMUM-VOLUME ADAPTER

3.3.4 XY Oscilloscope

For measuring the frequency response characteristics of fluidic devices, it is most convenient to use an oscilloscope with the following characteristics:

1. Two beams synchronized to common time base.
2. Calibrated time base.
3. Identical amplifiers on both channels.
4. High sensitivity (2 mv/cm).
5. Convertible for XY plotting.

4.0 GRAPHICAL CHARACTERISTICS OF TYPICAL FLUIDIC DEVICES

Graphical characteristics for general classes of active fluidic devices were defined and discussed in sections 2.4 and 3.1. In this section, actual graphical characteristics of typical active and passive fluidic devices will be illustrated. These characteristics will show what is to be expected in the "real world".

4.1 TURBULENT (NONLINEAR) RESTRICTORS

Turbulent restrictors are most common in fluidic circuits. Various types operate with various degrees of turbulence; therefore, their characteristics differ. Shown in Figure 29 are three typical examples of the characteristics of turbulent restrictors: a sharp-edged orifice, a standard needle valve, and a short length of plastic tubing. Note that the characteristics of the most turbulent, the sharp-edged orifice, closely approach a square law. That is,

$$Q^2 = K(\Delta P)$$

Since incremental resistance is defined from the slope of these curves it is important to note that the numerical value of resistance is not constant (the resistance is nonlinear). It must be calculated at the point where it is to be operated in a circuit.

4.2 LAMINAR (LINEAR) RESTRICTORS

Laminar restrictors are sometimes needed in a fluidic circuit to avoid the effects of nonlinear resistance. Various types are used, all of them based on laminar flow through very small passages. Shown in Figure 30 are typical characteristics of several available types: Fotoceram,* extruded ceramic rod, and bundled stainless steel capillary tubes. Note that over a considerable range of pressure, the characteristic of the bundled capillary tubes is a straight line. That is,

$$Q = K(\Delta P)$$

Since resistance is defined from the slope of the characteristic curve, the resistance is constant over this range; therefore, the specific point of operation need not be known (so long as it is within the linear range).

4.3 FLUIDIC AMPLIFIERS

4.3.1 Vented Jet-Interaction Amplifier Output Characteristics

The output characteristics of a typical vented jet-interaction differential amplifier are shown in Figure 31. Note that the amplifier is not stable with blocked loads.

*Trademark of Corning Co.

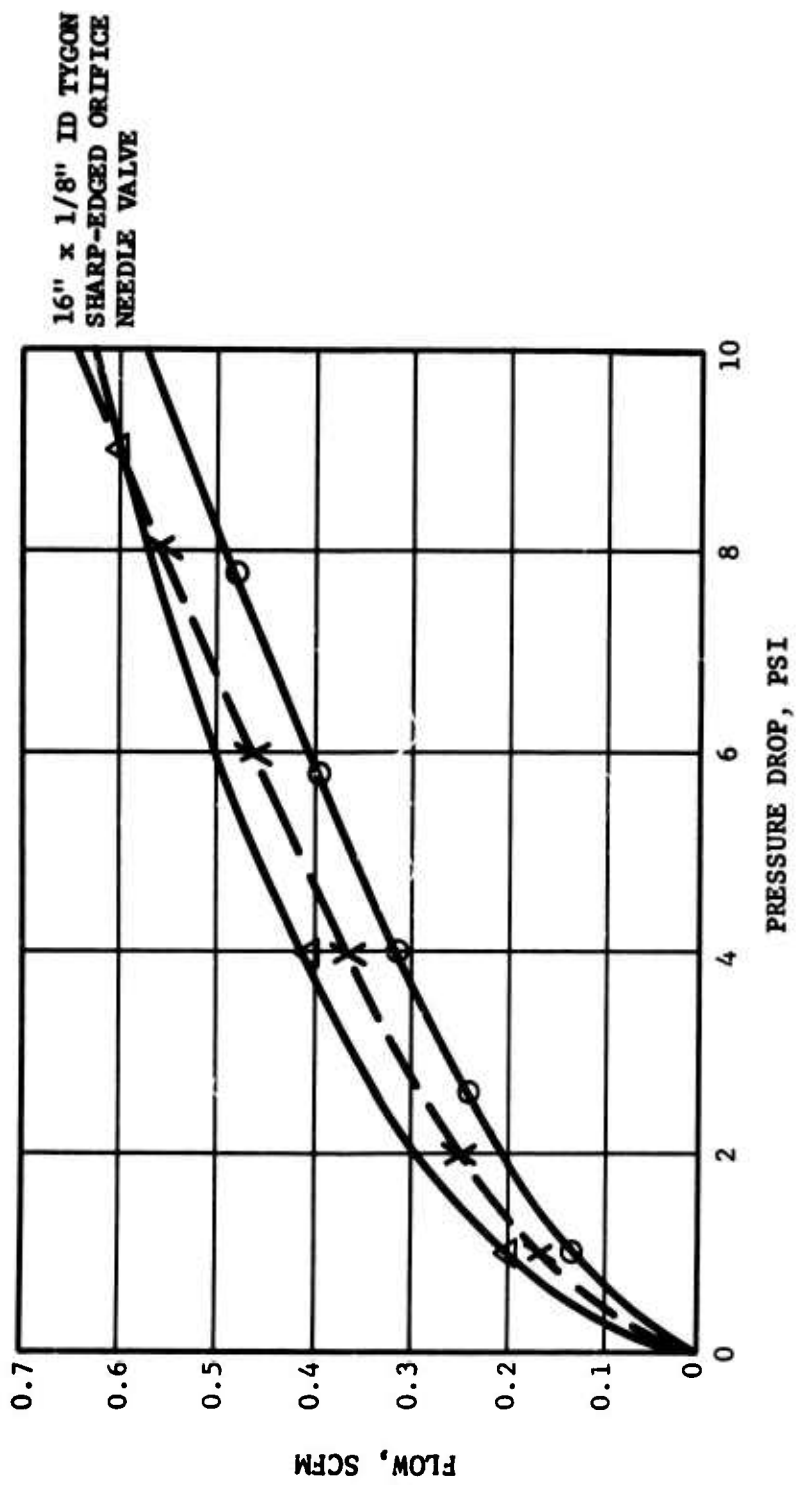


FIGURE 29 - STATIC CHARACTERISTICS OF
TYPICAL TURBULENT-FLOW RESTRICTORS

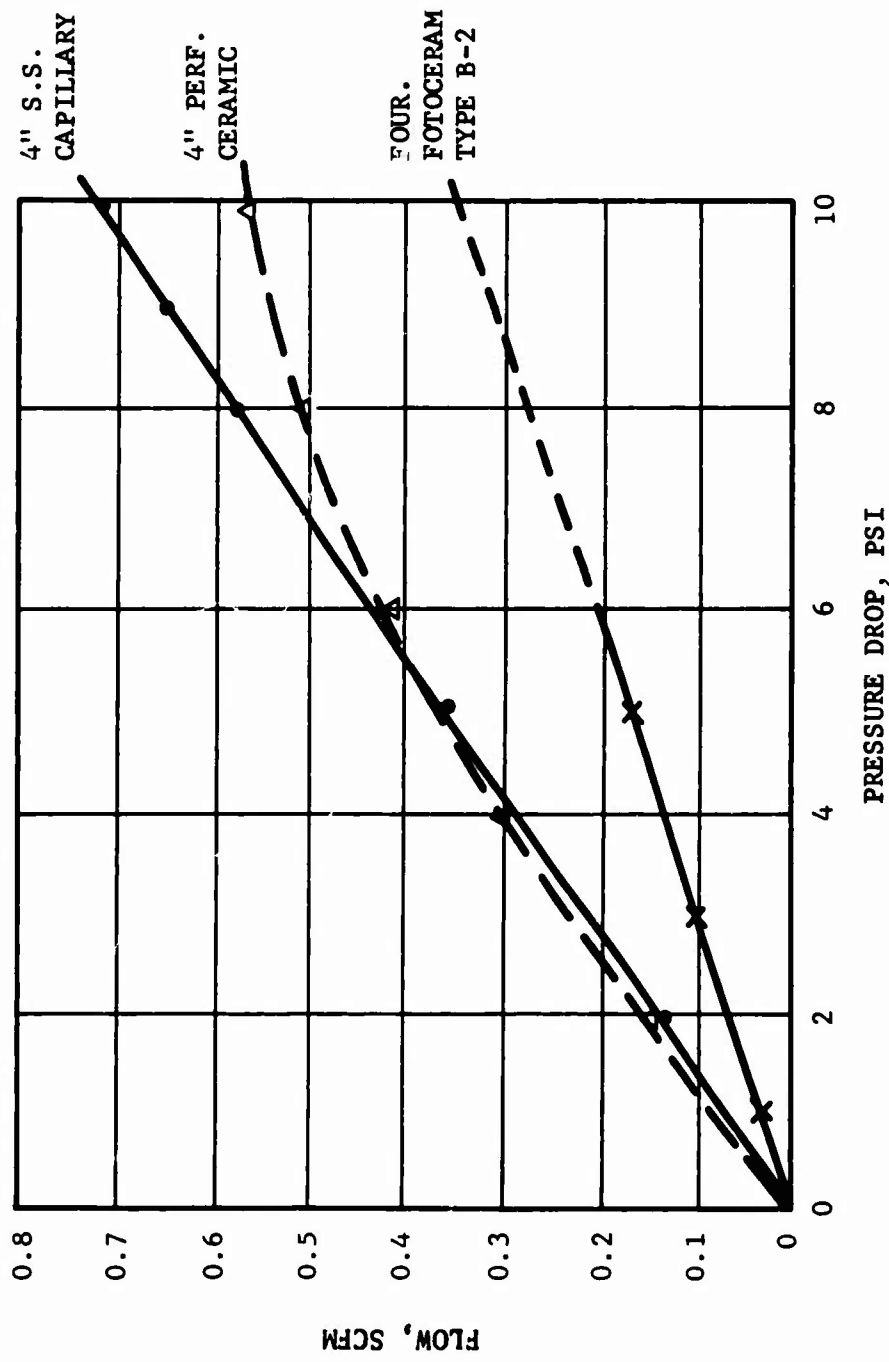


FIGURE 30 - STATIC CHARACTERISTICS OF
TYPICAL LAMINAR-FLOW RESTRICTORS

MODEL 1602-A $P_s = 8 \text{ PSI (AIR)}$ $P_{co} = 0.8 \text{ PSI}$

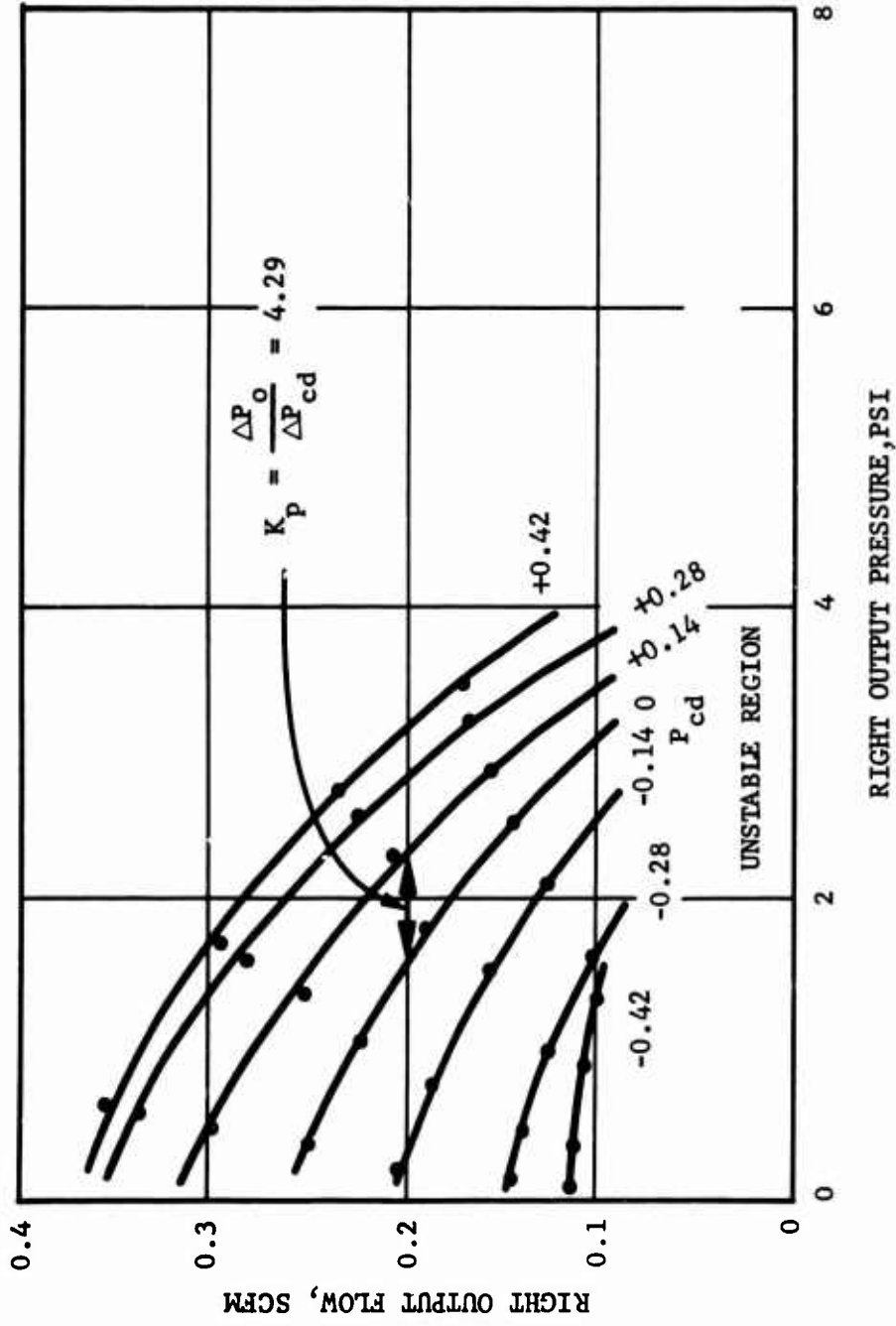


FIGURE 31 - STATIC OUTPUT CHARACTERISTICS OF VENTED
JET-INTERACTION AMPLIFIER

4.3.2 Vented Jet-Interaction Amplifier Input Characteristics

The input characteristics of a typical vented jet-interaction amplifier are shown in Figure 32.

4.3.3 Vented Jet-Interaction Amplifier Transfer Characteristics

The transfer characteristics of a typical jet-interaction amplifier are shown in Figure 33. Note that these apply to only one circuit connection; if the circuit is changed, the transfer characteristics change.

4.3.4 Closed Jet-Interaction Amplifier Output Characteristics

The output characteristics of a typical closed jet-interaction amplifier are shown in Figure 34. Note that by comparison with Figure 31, the use of vents avoids the complete loss of gain (distance between curves) at low output flows.

Note that in the closed amplifier, the effects of loading are reflected back to the input ports. Therefore, the input characteristics will be a family of curves similar to Figure 32, with load resistance as the parameter.

4.3.5 Vented Elbow Amplifier Output Characteristics

The output characteristics of a typical vented elbow amplifier are shown in Figure 35. Note that this type of amplifier is characterized by very low output resistance ($\Delta P_o / \Delta Q_o$).

4.4 SENSORS

As described in section 3.1.2, the characteristics of sensors can be described by a set of output curves with the sensed variable as a parameter.

4.4.1 Vortex Rate Sensor

The output characteristics of a typical vortex rate sensor are shown in Figure 36. Note that the parameter is the rate of turn of the sensor. Note also that because of the type of pickoff used, the characteristics are very nearly straight lines.

4.5 ACTUATORS

Actuators are defined as the end loads on the fluidic control system which convert fluidic power into mechanical power. Therefore, we will be concerned only with input characteristics. The most common forms are rectilinear and rotary actuators and fluid motors.

MODEL 1602A $P_s = 8$ PSI (AIR) $P_{co} = 0.8$ & 0.4 PSI

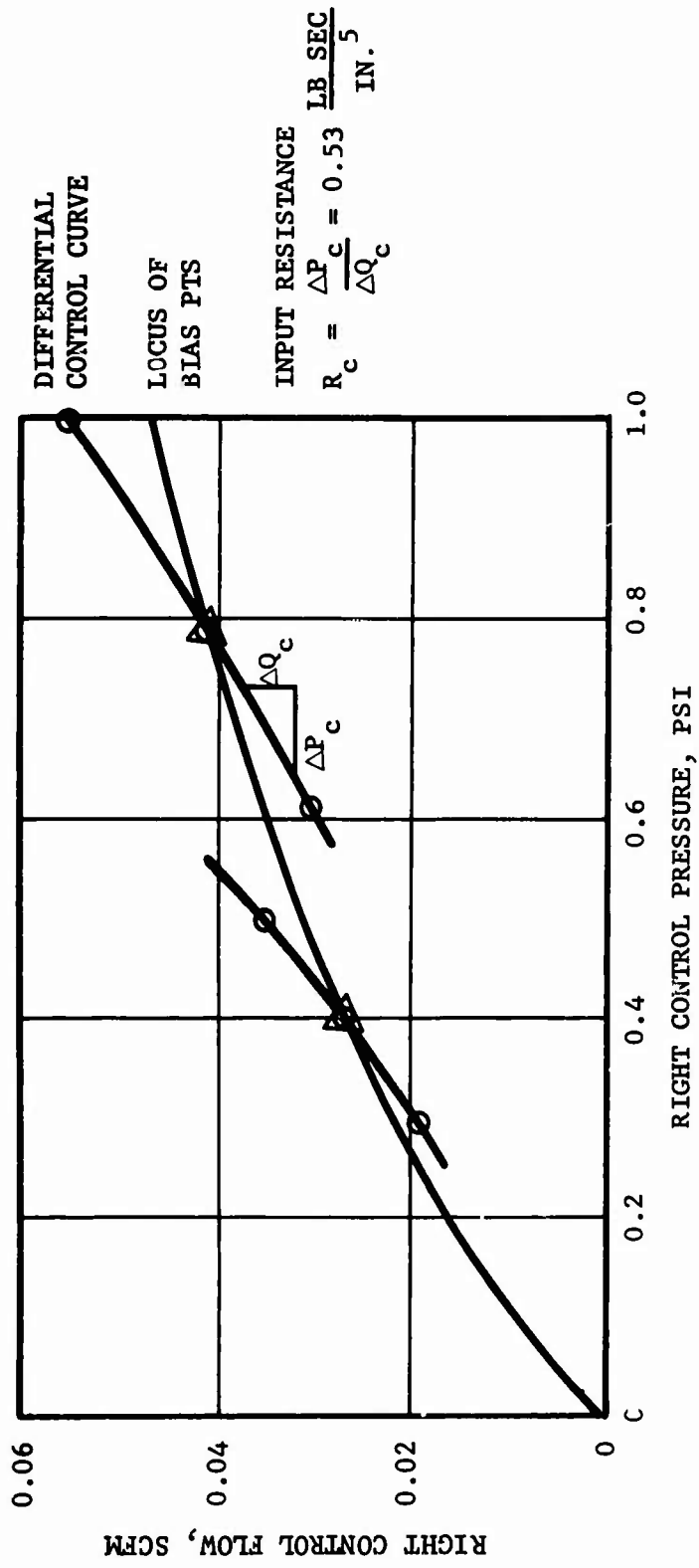


FIGURE 32 - STATIC INPUT CHARACTERISTICS OF VENTED JET-INTERACTION AMPLIFIER

MODEL 1602-A $P_s = 8 \text{ PSI (AIR)}$ $P_{co} = 0.8 \text{ PSI}$ LOAD $R_c = 0.7 \frac{\text{LB SEC}}{\text{IN}^5}$

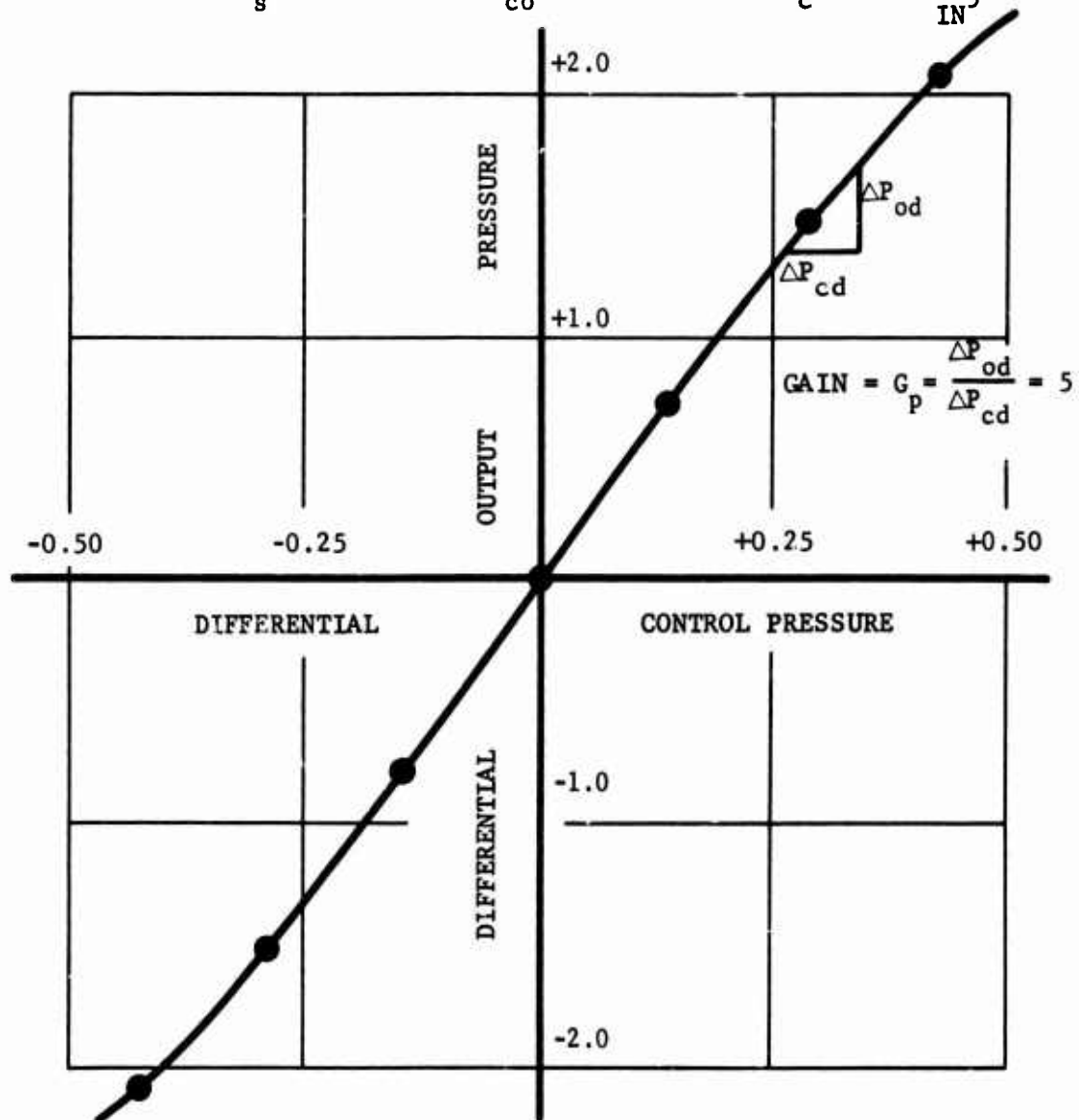


FIGURE 33 - STATIC TRANSFER CHARACTERISTICS
OF VENTED JET-INTERACTION AMPLIFIER

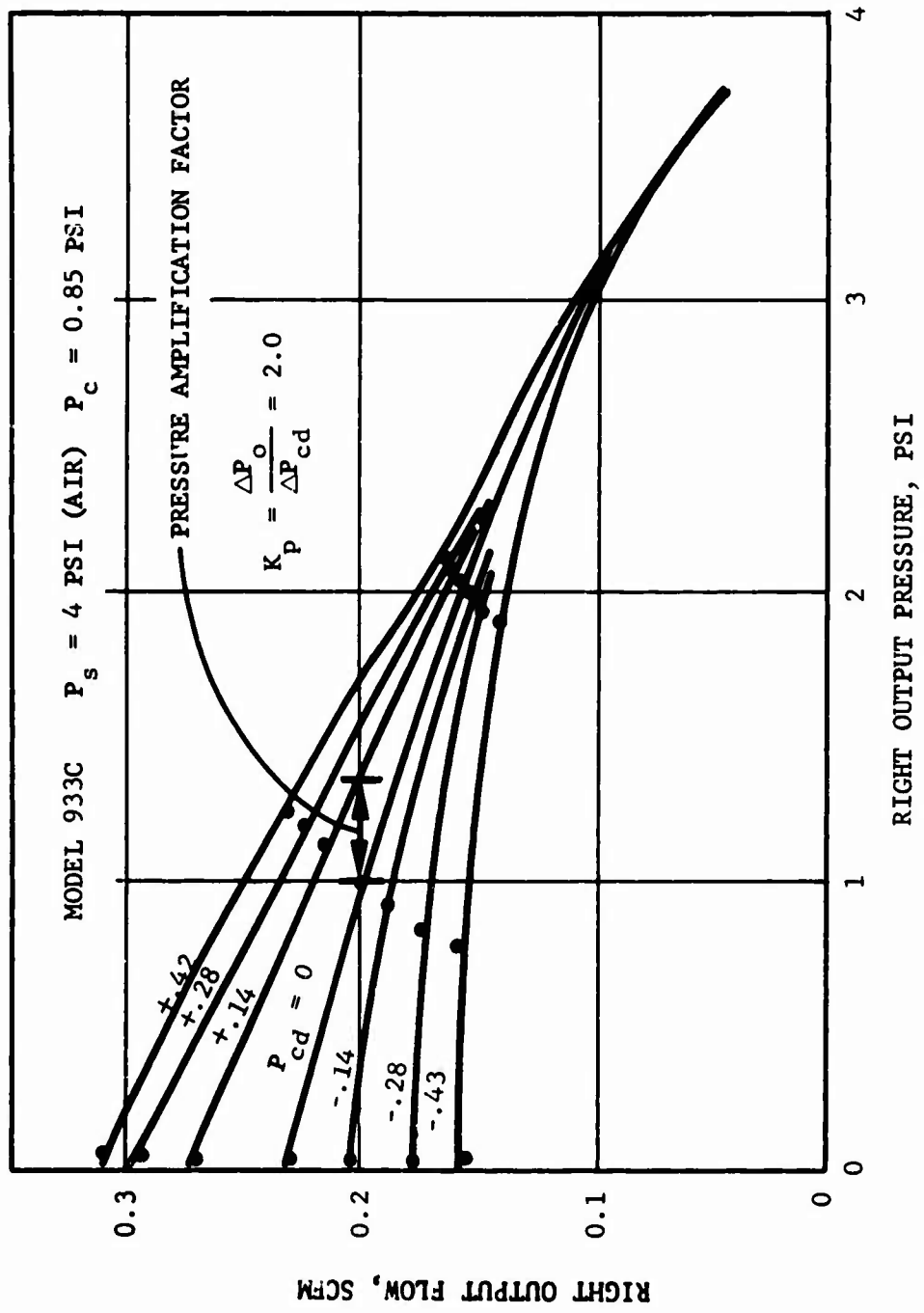


FIGURE 34 - STATIC OUTPUT CHARACTERISTICS OF CLOSED JET-INTERACTION AMPLIFIER

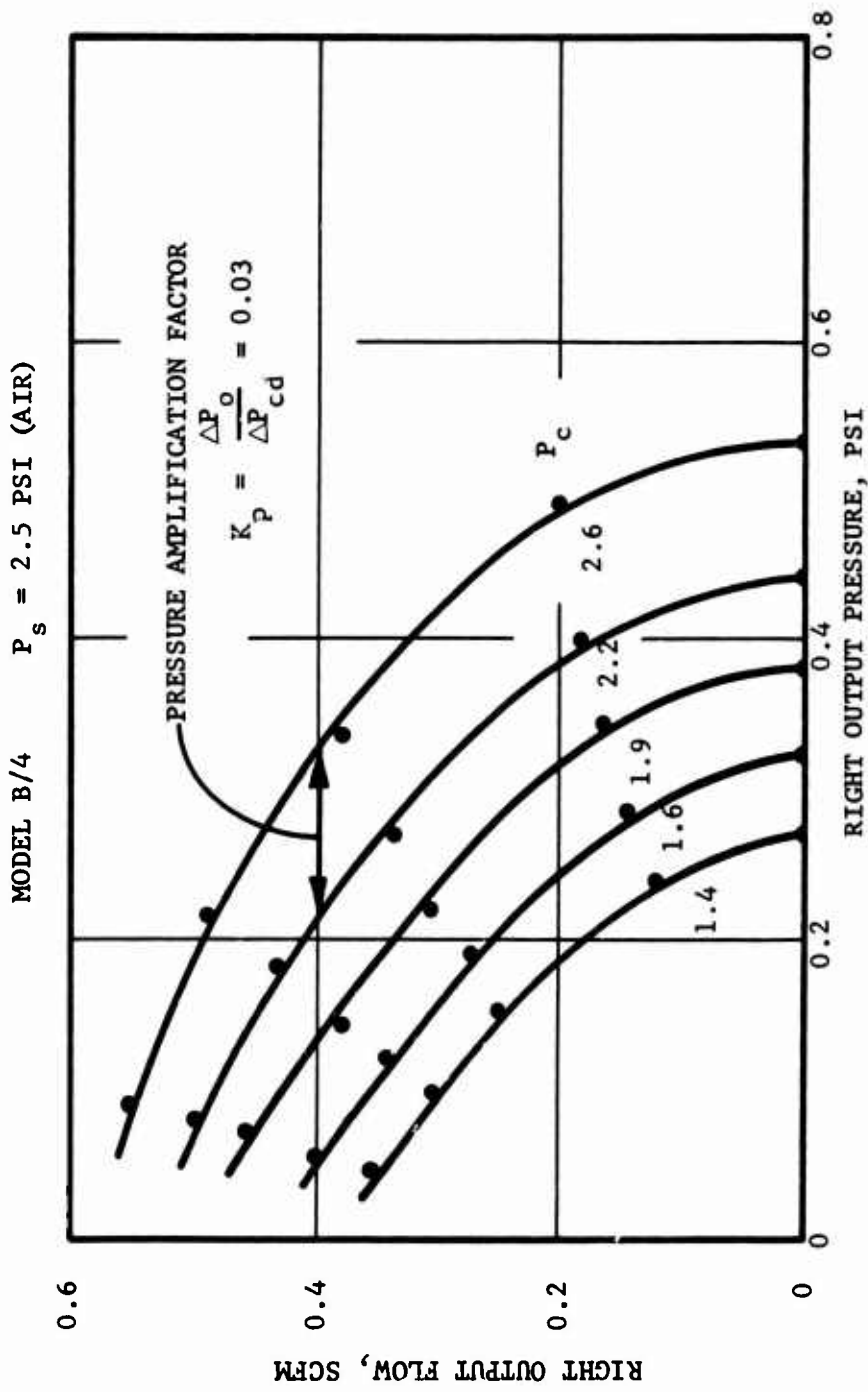


FIGURE 35 - STATIC OUTPUT CHARACTERISTICS OF
VENTED ELBOW AMPLIFIER

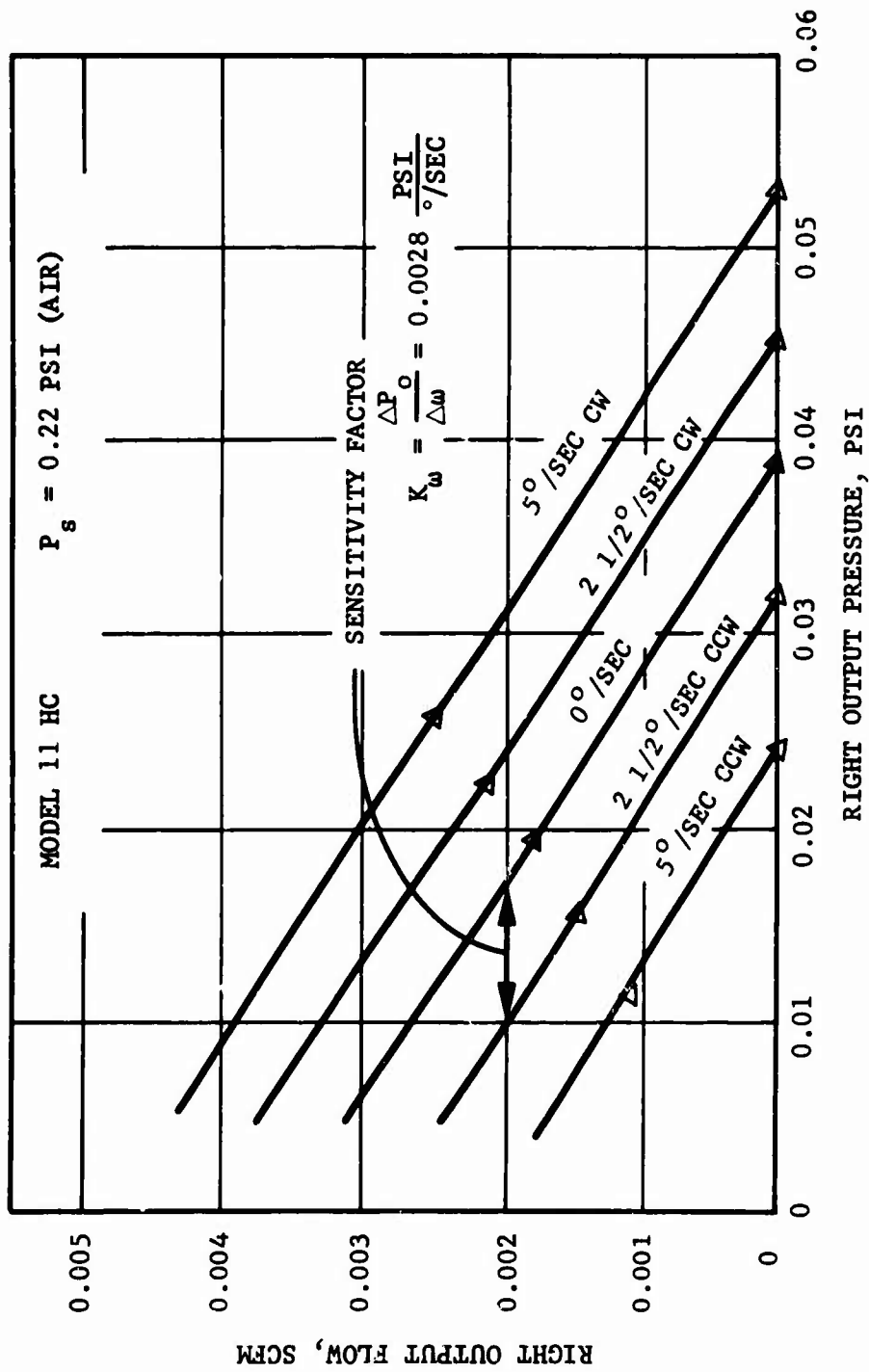


FIGURE 36 - STATIC OUTPUT CHARACTERISTICS OF
 VORTEX RATE SENSOR

The dynamic characteristics of actuators and reflected loads are extremely important to the design of a stable, high-performance fluidic control system. Actuator and load dynamics are covered in sections 6.1.5 and 6.1.6.

4.5.1 Rectilinear and Rotary Actuators

Rectilinear and rotary actuators are piston-type devices with very low leakage, designed for limited motion. Therefore, the static input characteristics for a blocked mechanical load, typically as shown in Figure 37, are straight lines very nearly on the pressure axis. With no mechanical load, the flow (and velocity) is limited only by the friction and internal resistance of the actuator; but because of limited motion, this condition can exist only for a short period.

4.5.2 Fluid Motors

Fluid motors may be piston- or vane-type devices designed for continuous rotation and may have considerable leakage. Typical static input characteristics with a blocked rotor are shown in Figure 38 for a low-leakage piston-type motor and for a high-leakage vane-type motor. When the motors are running at constant velocity, the characteristics are raised parallel to themselves.

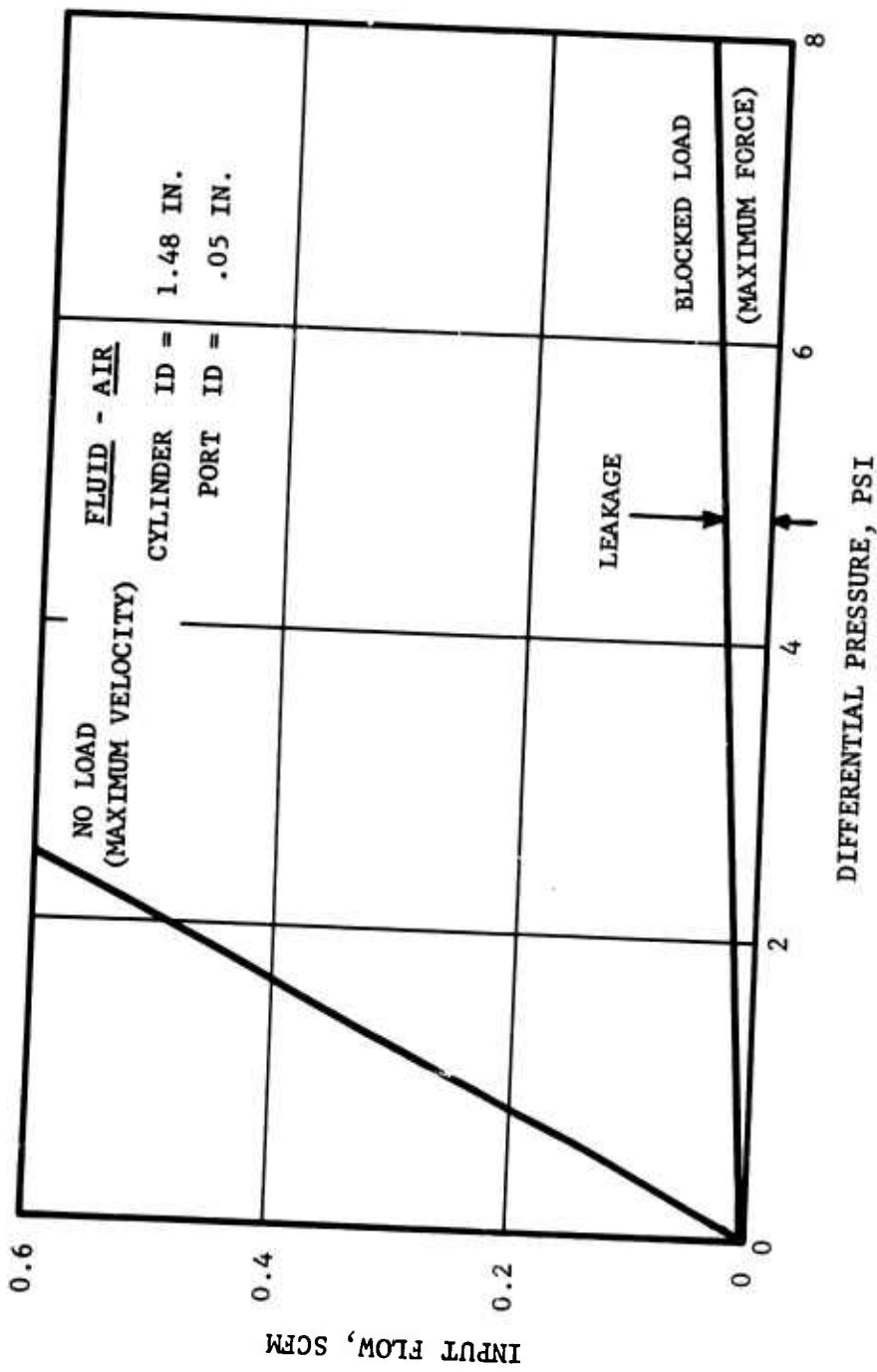


FIGURE 37 - STATIC INPUT CHARACTERISTICS OF
PISTON - TYPE ACTUATOR (TYPICAL)

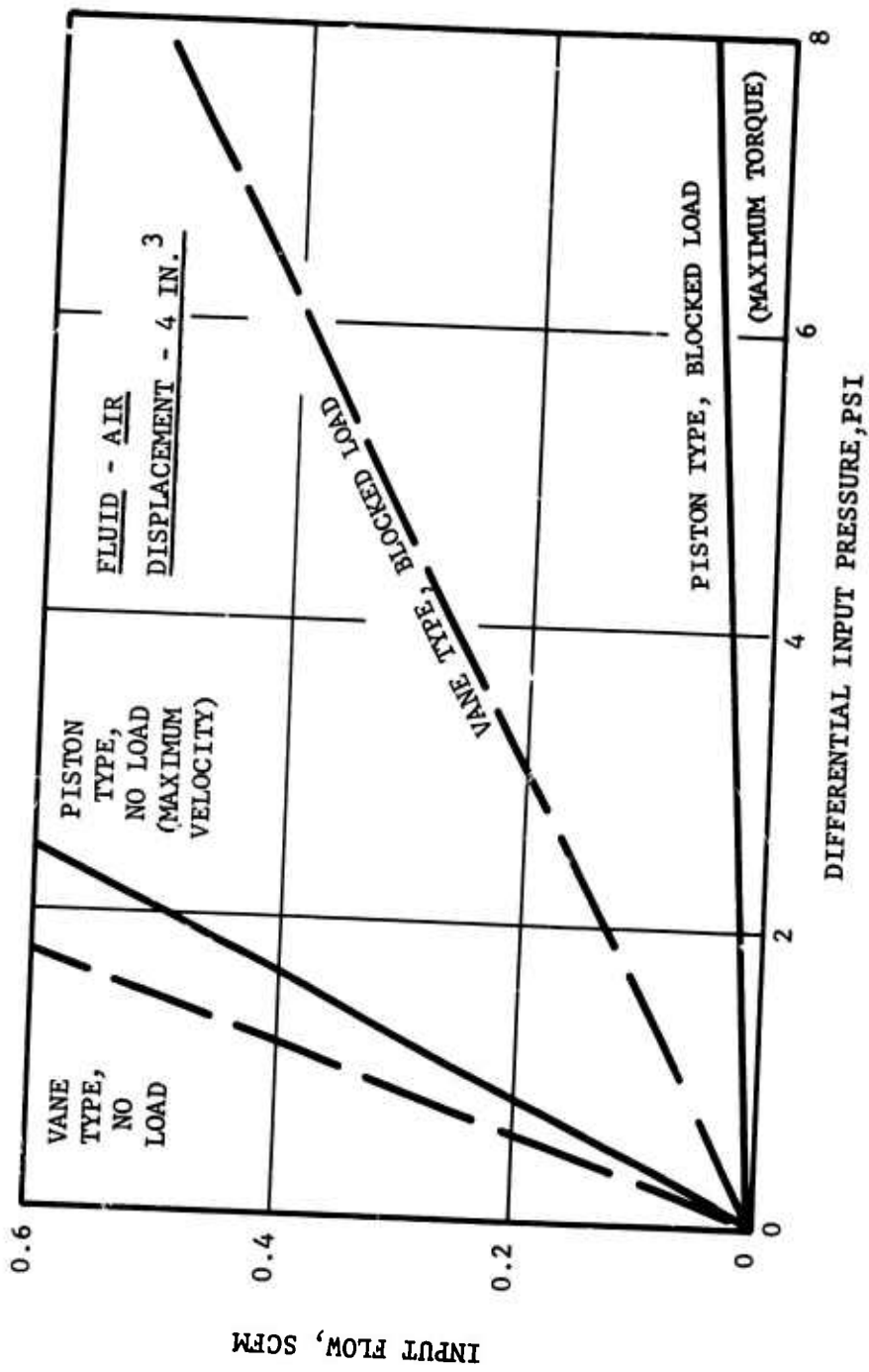


FIGURE 38 - STATIC INPUT CHARACTERISTICS OF
PISTON-TYPE AND VANE-TYPE FLUID MOTORS (TYPICAL)

5.0 LARGE SIGNAL PERFORMANCE ANALYSIS

Not unlike most electronic and hydraulic components, the characteristics of fluidic devices are nonlinear. When operated at extremes or when driven by a large signal, the performance parameters cannot be considered constant, and the output will be a distorted reproduction of the input. In this case the graphical method of performance analysis is most convenient because it permits the system designer to account for the nonlinearities without the use of complex mathematics (Reference 12).

5.1 THE LOAD LINE

Consider first the case of the differential fluidic amplifier with a passive load having characteristics as shown in Figure 39b. The output characteristics of the amplifier would appear as in Figure 39a. The problem is to find out what will happen when the amplifier is connected to the passive load.

The first point that the circuit designer must realize is that the output characteristics show how the amplifier will behave with any load. In fact, the curves were plotted from the performance of the amplifier for a number of loads, from open outlet port (zero impedance) to blocked output point (infinite impedance).

The second point is that the load characteristic is a single line; that is, there is only one flow level for each pressure applied.

Finally, one must realize that when the load is connected to the amplifier, the pressures and flows are common to the two; that is, the amplifier output pressure is identical with the passive load pressure and the amplifier output flow is identical with the passive load flow.

Because of these points, the combined behavior of an amplifier with passive load can be found simply by plotting their characteristics on the same graph as shown in Figure 39c. The passive load characteristics are superimposed on the amplifier output characteristics as a "load line". Since pressures and flows must be identical in both components, the points of intersection of the curves can be the only operating points.

Consider the case of cascading two differential fluidic amplifiers. For the driving amplifier we would have a set of output characteristics as shown in Figure 40a. For the driven amplifier we would be concerned with its input characteristics as shown in Figure 40b. Now how can we tell how the amplifiers will behave when they are connected together?

When the output of the driver is connected to the input of the driven amplifier, the output pressure and flow of the driver must be identical with the input pressure and flow of the driven. That is, the only possible operating conditions are those where the output pressure and flow of the driver amplifier coincide with the input pressure and flow of the driven

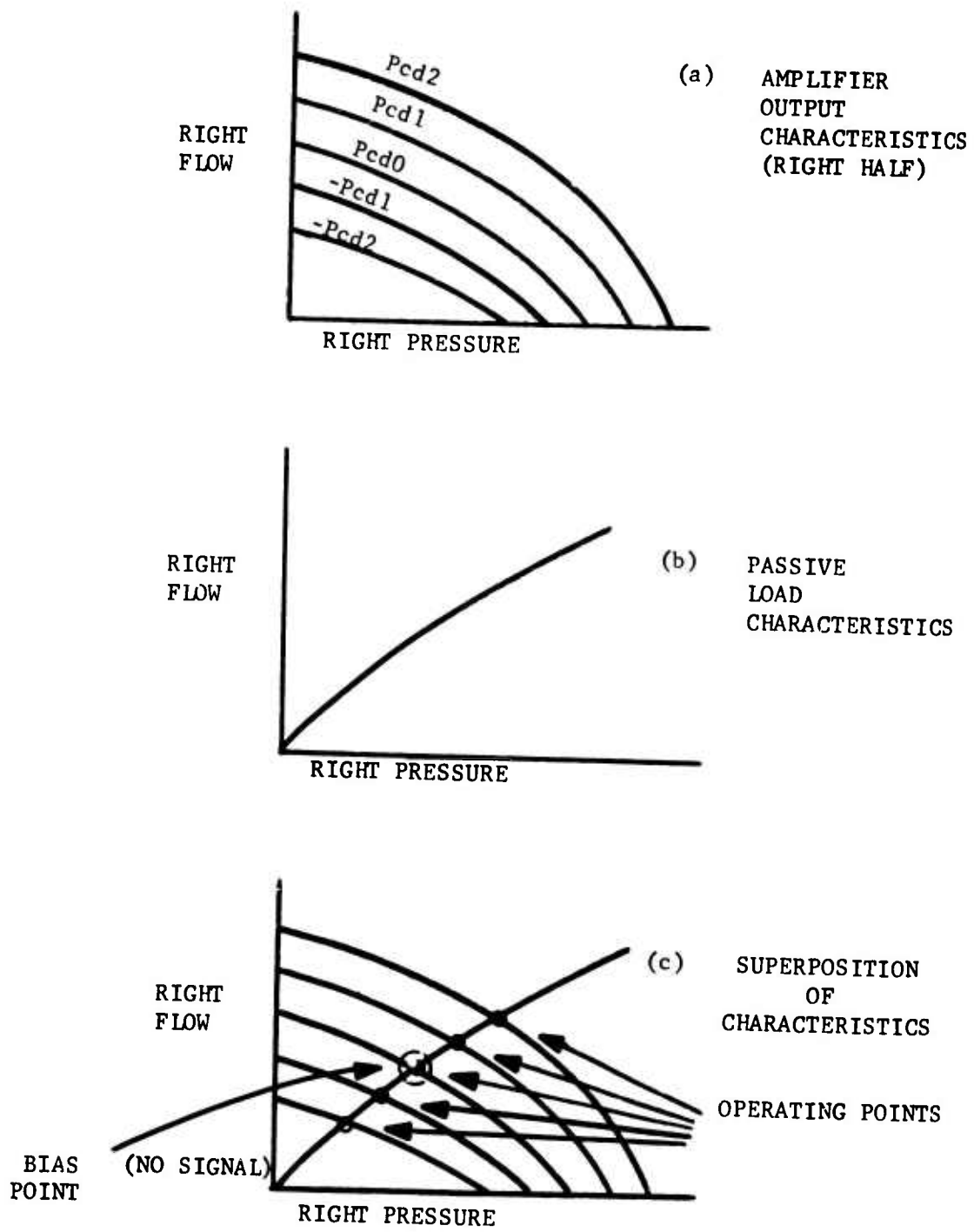


FIGURE 39 - COUPLING A DIFFERENTIAL FLUIDIC AMPLIFIER TO A PASSIVE LOAD

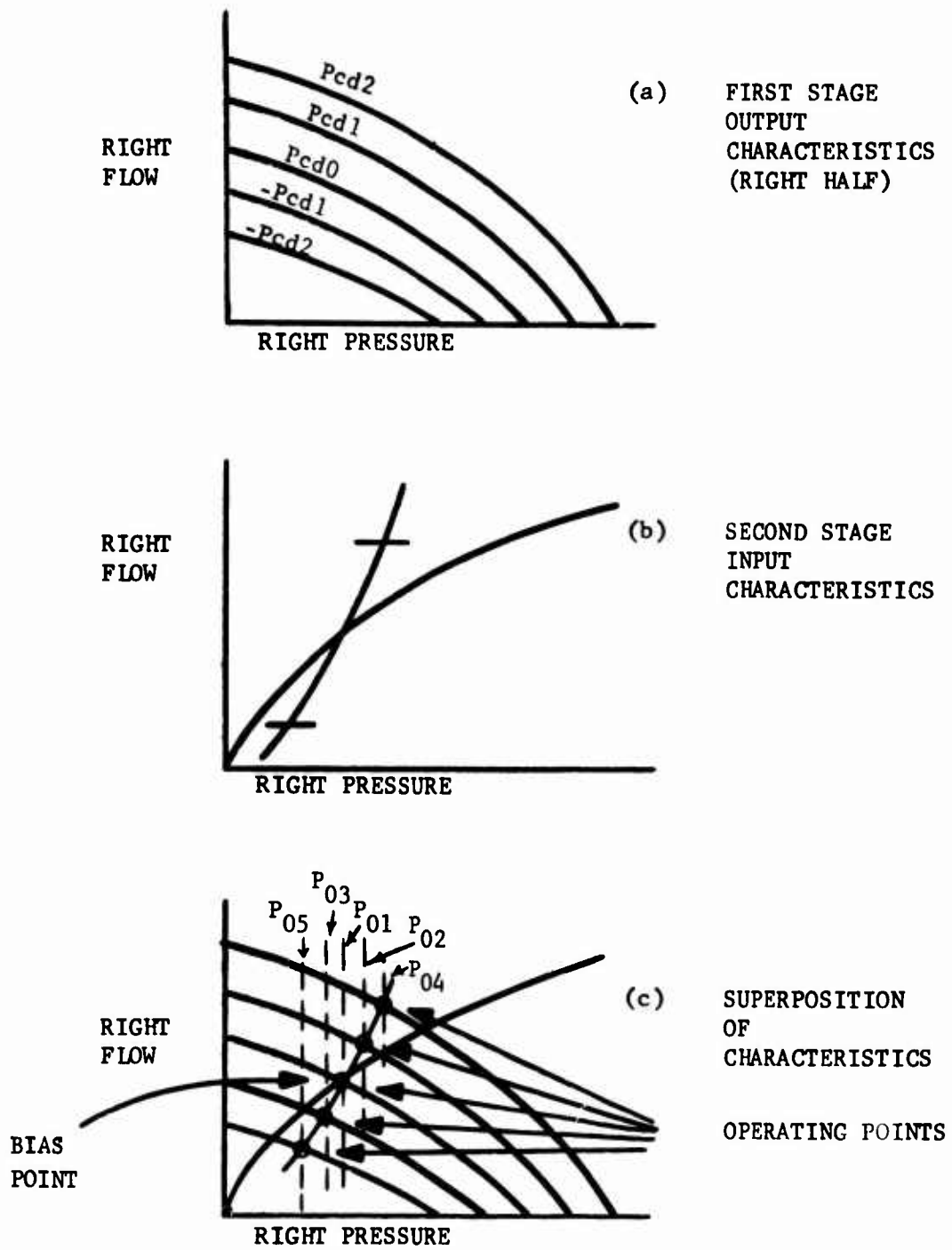


FIGURE 40 - COUPLING TWO DIFFERENTIAL FLUIDIC AMPLIFIERS

amplifier. These points are easily found by superimposing the input characteristics of the driven amplifier as a "load line" on the output characteristics of the driver, as shown in Figure 40c. The points where the characteristics intersect are the only stable operating points. (Note that even in the case of a differential connection, it is necessary to consider each side separately.) Once the range of operating points is defined on the input characteristic, the points may be entered on the output characteristics of the second stage, and the output of the second stage is then determined by the same "load line" method.

The load line concept can be generalized as follows. Whenever two fluidic components are connected together, the coupled behavior can be defined by superimposing the appropriate characteristic curves for the two components. The only stable operating points are where the characteristics intersect.

5.1.1 Load Line Design Procedure

To determine the characteristics of two coupled active or passive fluidic components, two sets of information must be obtained. They are (1) the output characteristics of the driving component (with control variable as a parameter) and (2) the input characteristics of the driven component (with normal operating range marked on the curves).

The procedure is as follows:

1. Plot the driving amplifier output characteristics to a convenient scale (paragraph 4.3).
2. Convert the input characteristics of the driven component to a similar scale (paragraph 4.3).
3. Plot the input characteristics of the driven component on the output characteristics of the driving component (paragraph 5.1).
4. Note the points at which the curves intersect.
5. The intersecting points determine the operating characteristics of the two coupled fluidic components.

5.2 CALCULATION OF THE TRANSFER (GAIN) CURVE (Paragraph 4.3.3)

Once the operating conditions have been defined by the superposition of characteristic curves, the gain (or performance) curve can be calculated. Referring again to Figures 39c and 40c, it is first necessary to determine the bias (or quiescent) point. This is given at the intersection of the zero control curve of the driver amplifier with the passive load characteristic or the bias curve of the driven amplifier. This is the point at which the pressure and flow will be when there is no signal into the driver amplifier.

When the differential amplifier receives an input signal, one output port pressure increases while the other output port pressure decreases. Since this is the condition that is applied at the input of our driven amplifier, it is appropriate to use the differential curve for the "incremental" load

line; that is, for changes about the operating bias point (see paragraph 3.1.1).

To plot the differential pressure gain curve for the driver amplifier loaded with the second differential amplifier, the coordinates shown in Figure 41 are used. Where $P_{cd} = 0$, the output pressure of the right port is P_{o1} and the output pressure of the left port (if the amplifier is perfectly balanced) is P_{o1} . Therefore, the differential output P_{od} is zero. When $P_{cd} = +1$, the right output is P_{o2} , the left output is P_{o3} , and the difference is $P_{od} = +2$. When $P_{cd} = -1$, the right output is P_{o3} , the left output is P_{o2} , and the difference is $P_{od} = -2$. Continuing this procedure of taking increments of P_{cd} and calculating the value of P_{od} from the curves leads to a complete transfer (gain) curve as shown in Figure 41. Note that this defines the pressure gain of the driver amplifier only when it has the driven amplifier as a load.

If the amplifier is not perfectly balanced, then different output characteristics for the right output and the left output are used in a way similar to that above.

5.2.1 Transfer Curve Design Procedure

To determine the sensitivity or gain of coupled fluidic components, the plot of output characteristics of the driving component with the input characteristics of the driven component superimposed must be available.

The procedure is as follows:

1. Select the input and output variables of interest (pressure, flow, rate of turn, etc.).
2. Prepare a graph with scales to conveniently cover the range of variables.
3. Find the no-signal operating (bias) point from the intersection of the zero-control output curve with the load line (paragraph 5.1.1).
4. Take a number of positive and negative increments of input signal, and determine from the intersection of the appropriate output curves with the load line a number of points along the transfer curve.
5. Plot the results on the previously prepared graph.
6. The resulting transfer curve defines the specific performance of the coupled components under the given conditions of supply bias and load.
7. The slope of the transfer curve is the gain (of an amplifier) or sensitivity (of a transducer).

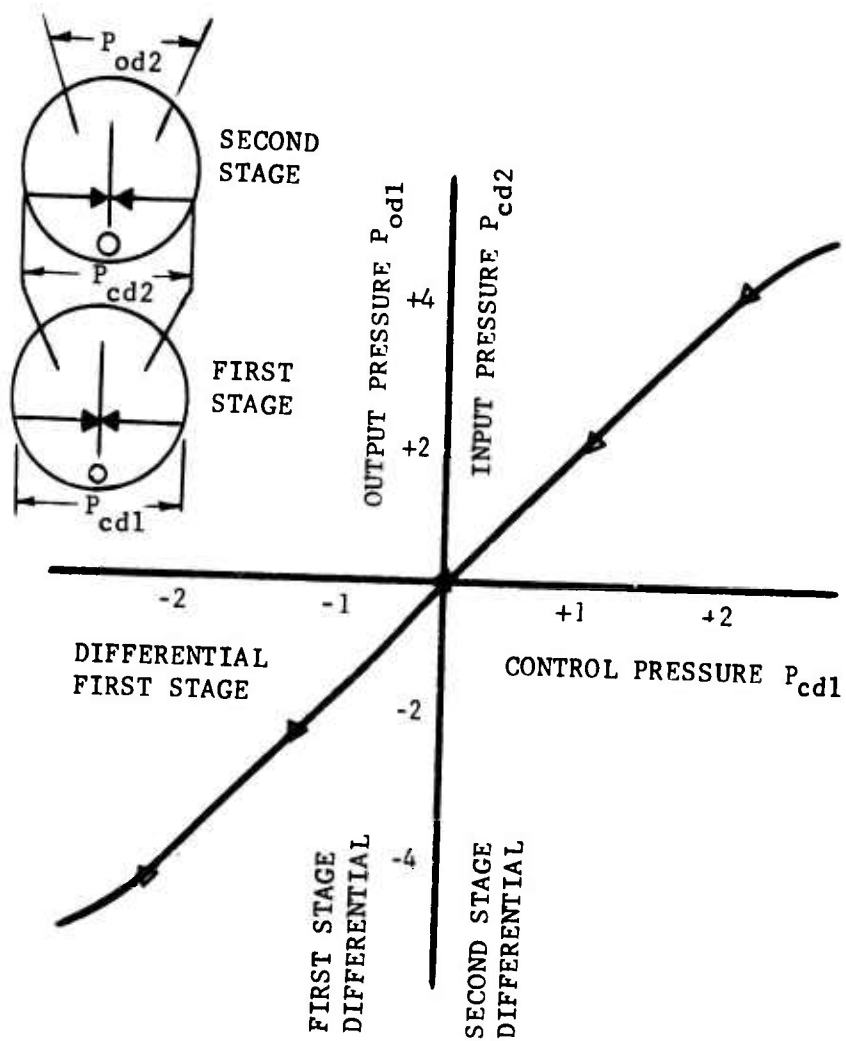


FIGURE 41 - PRESSURE TRANSFER CURVE OF DIFFERENTIAL AMPLIFIER LOADED WITH SECOND DIFFERENTIAL STAGE

5.3 STATIC MATCHING OF CASCADED FLUIDIC COMPONENTS

In the foregoing paragraph (5.1), the load line method for determining the performance of cascaded fluidic components was introduced. In the illustration given (Figure 40), the ideal case was assumed; that is, no matching problems arose. In this paragraph the more probable situation, when matching problems do arise, is covered.

5.3.1 Objectives

The objectives in properly cascading fluidic components are:

1. Providing proper gains
2. Matching operating bias points
3. Matching operating ranges

Let us first define each objective in more detail.

Proper gains are, after all, what the circuit is usually in existence to provide. However, the designer may want primarily flow gain, leaving pressure gain and power gain as secondary considerations. Or he may want to optimize pressure gain instead.

Operating bias (quiescent) points are the pressures and flows defining the desired conditions in the component with no signal applied.

Operating ranges are the ranges of pressures and flows over which the component can be operated with good results.

5.3.2 Matching a Vortex Rate Sensor and Differential Amplifier

Now consider the matching problem in more detail. Suppose we are given an existing vortex rate sensor to measure rates of turn from 10 degrees per second counterclockwise to 10 degrees per second clockwise. Our task is to amplify the output using available "off-the-shelf" amplifiers.

Vortex rate sensors are inherently low-pressure, high-output-impedance devices. Typical output characteristics are shown in Figure 42. Although push-pull differential circuits are to be used in this application, it is necessary to match the operating characteristics of each half; therefore, we will be concerned with single-ended characteristics in the matching process.

Vented jet-interaction amplifiers are available in a limited number of standard sizes. An amplifier of high input impedance is necessary to match the high output impedance of the rate sensor. This implies an amplifier with small control nozzles, therefore an amplifier of small overall size. Figure 43 shows the input characteristics of a typical small jet-interaction amplifier with power nozzle 0.010 x 0.025. Note that the preferred bias operating point is 10% of supply pressure, and the linear

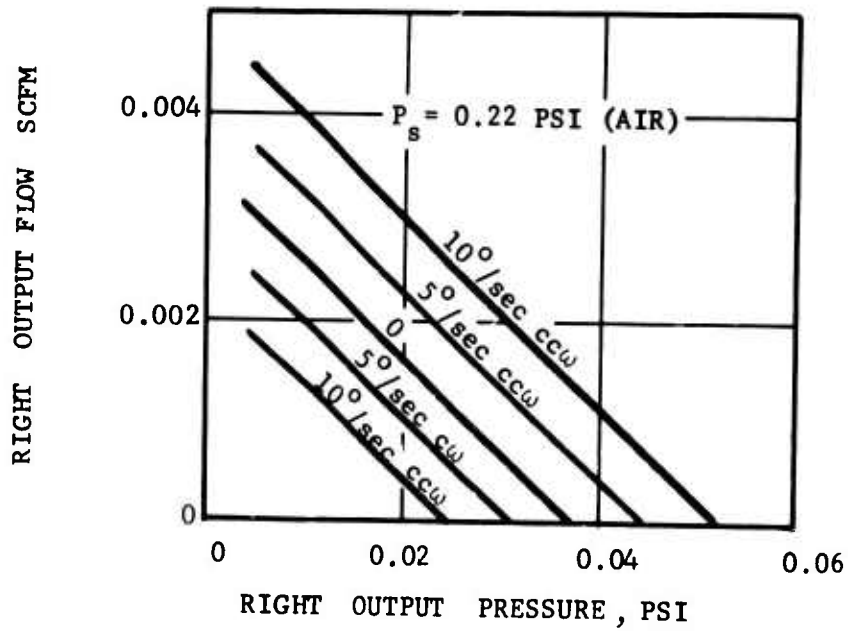


FIGURE 42 - STATIC OUTPUT CHARACTERISTICS OF VORTEX RATE SENSOR

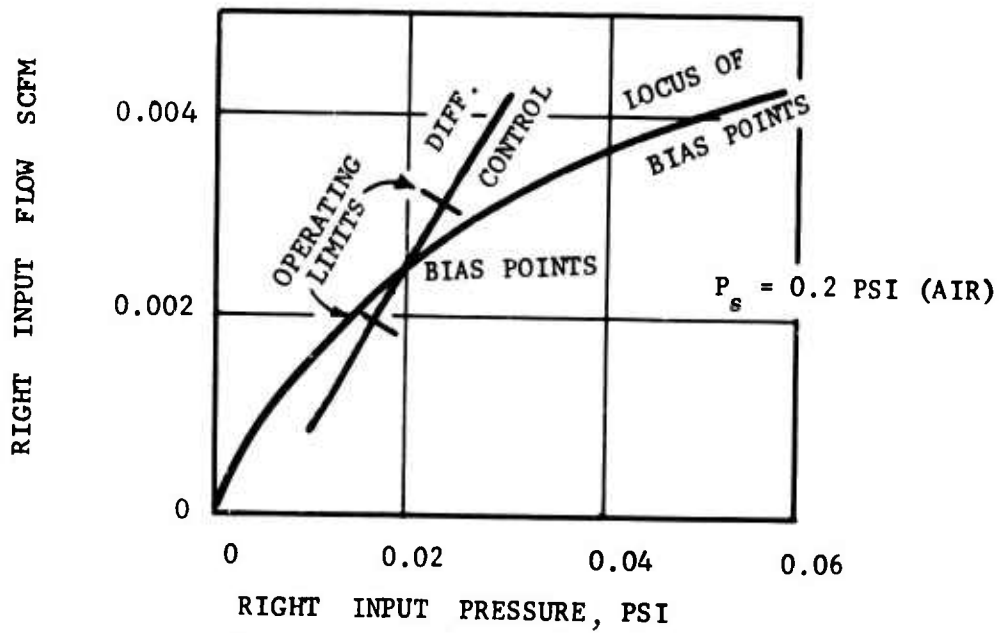


FIGURE 43 - STATIC INPUT CHARACTERISTICS OF SMALL VENTED JET-INTERACTION AMPLIFIER

range of amplification is about $\pm 5\%$ of supply pressure.

Following the procedures for determining the operating characteristics of the rate sensor and amplifier when they are connected together (paragraph 5.1.1), the input characteristics of the amplifier are superimposed as a load line on the output characteristics of the rate sensor, as shown in Figure 44.

5.3.2.1 Providing Proper Gains

Again referring to Figure 44, it is apparent that taking increments of rate of turn to plot the transfer curve (paragraph 5.2) yields relatively small increments of input pressure. This condition is evidently a result of the fact that the input characteristic of the amplifier is relatively steep when compared with the rate sensor output characteristics; that is, the impedance match is poor.

Now suppose it were necessary to optimize pressure sensitivity of the amplifier rate-sensor circuit. It is apparent that we would require an amplifier input characteristic with relatively low slope (high impedance) as illustrated in Figure 45. Then when increments of rate of turn were taken to determine the resulting increments of amplifier input pressure, the pressure sensitivity would be vastly increased.

5.3.2.2 Matching Operating Bias Points

Since the preferred bias point for the amplifier does not coincide with the zero rate of turn curve of the rate sensor, Figure 44 illustrates a case of mismatch of the bias points. There are at least three ways to be explored to correct the situation. The output bias level of the rate sensor can be increased, as in Figure 46. Or the amplifier supply pressure can be reduced, maintaining the input bias at 10% of the supply, as in Figure 47. Or the effective load line of the rate sensor can be shifted by the addition of restrictors in series or in parallel with the amplifier input, as in Figure 48. (The latter method is obviously not suitable for correcting the type of mismatch illustrated in this example problem.)

5.3.2.3 Matching Operating Ranges

With reference to Figure 44, it is apparent that there is also a mismatch of optimum operating ranges. The rate sensor, in the situation illustrated, is capable of overdriving the amplifier into its nonlinear range. Again, there are at least three methods to be investigated for correcting the situation: adding series or shunt resistance in the differential circuit, changing the output bias of the rate sensor, and changing the amplifier supply pressure. Note that resistances across the differential lines will affect the slope and length of the differential load line but not the operating point.

It is evident that two of these steps are also used to match the operating

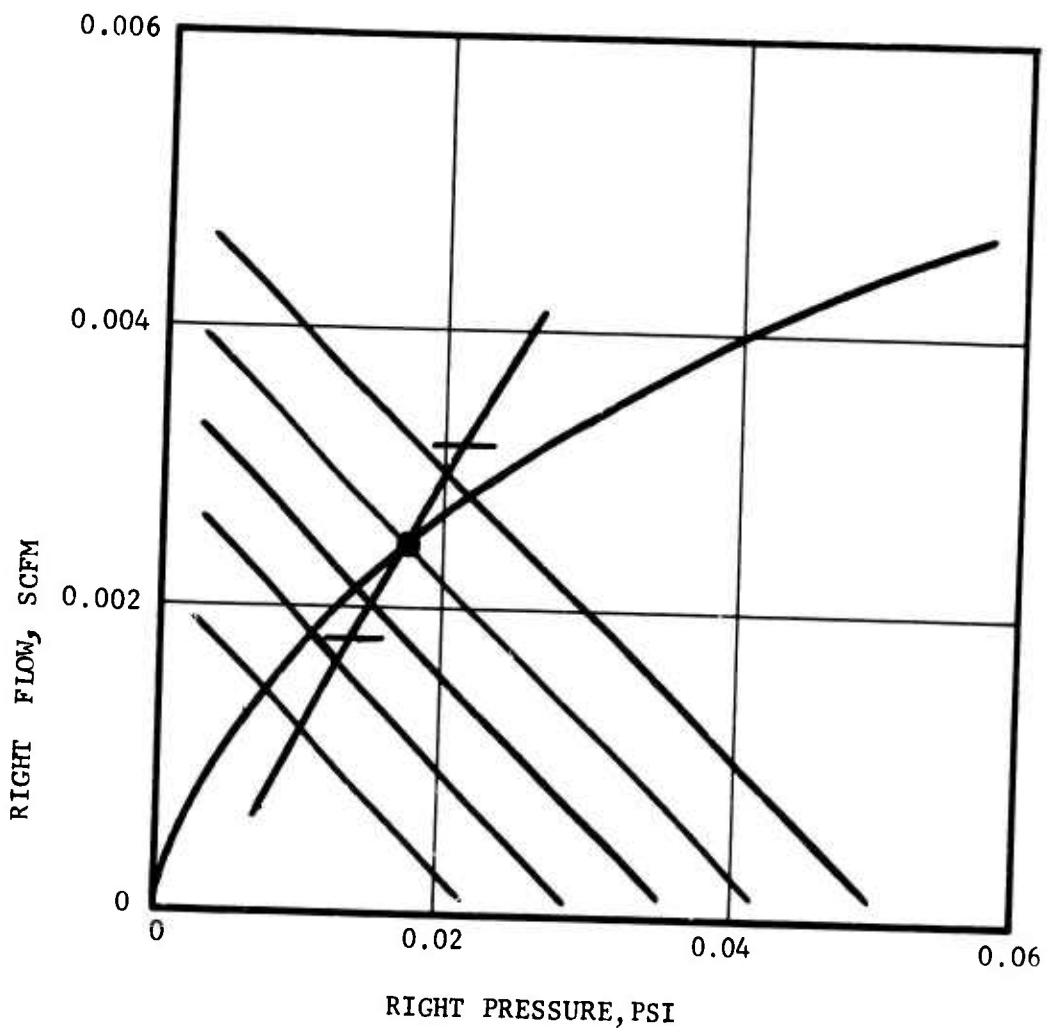


FIGURE 44 - SUPERPOSITION OF STATIC CHARACTERISTICS OF VORTEX RATE SENSOR AND VENTED JET-INTERACTION AMPLIFIER

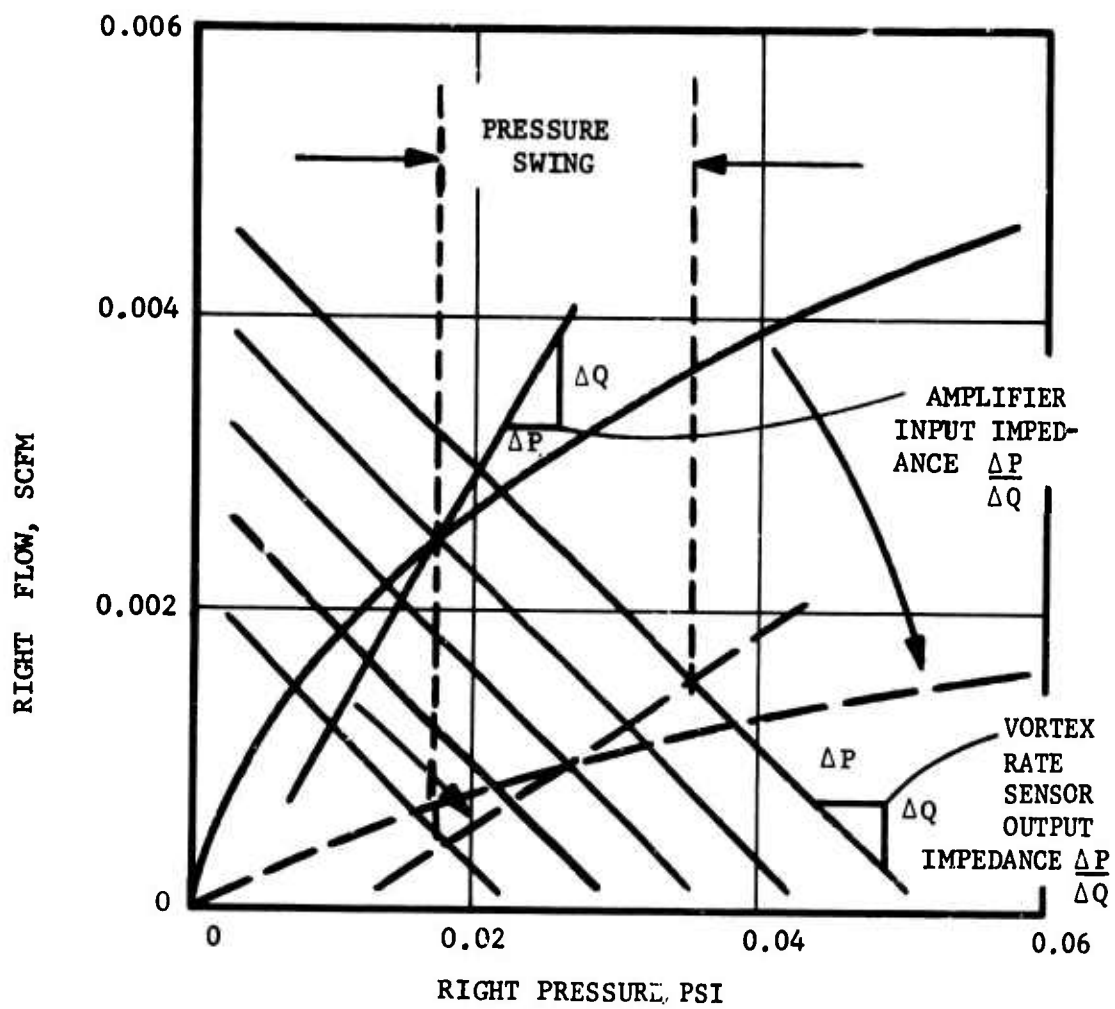


FIGURE 45 - IMPEDANCE MATCHING FOR
HIGH STATIC PRESSURE GAIN

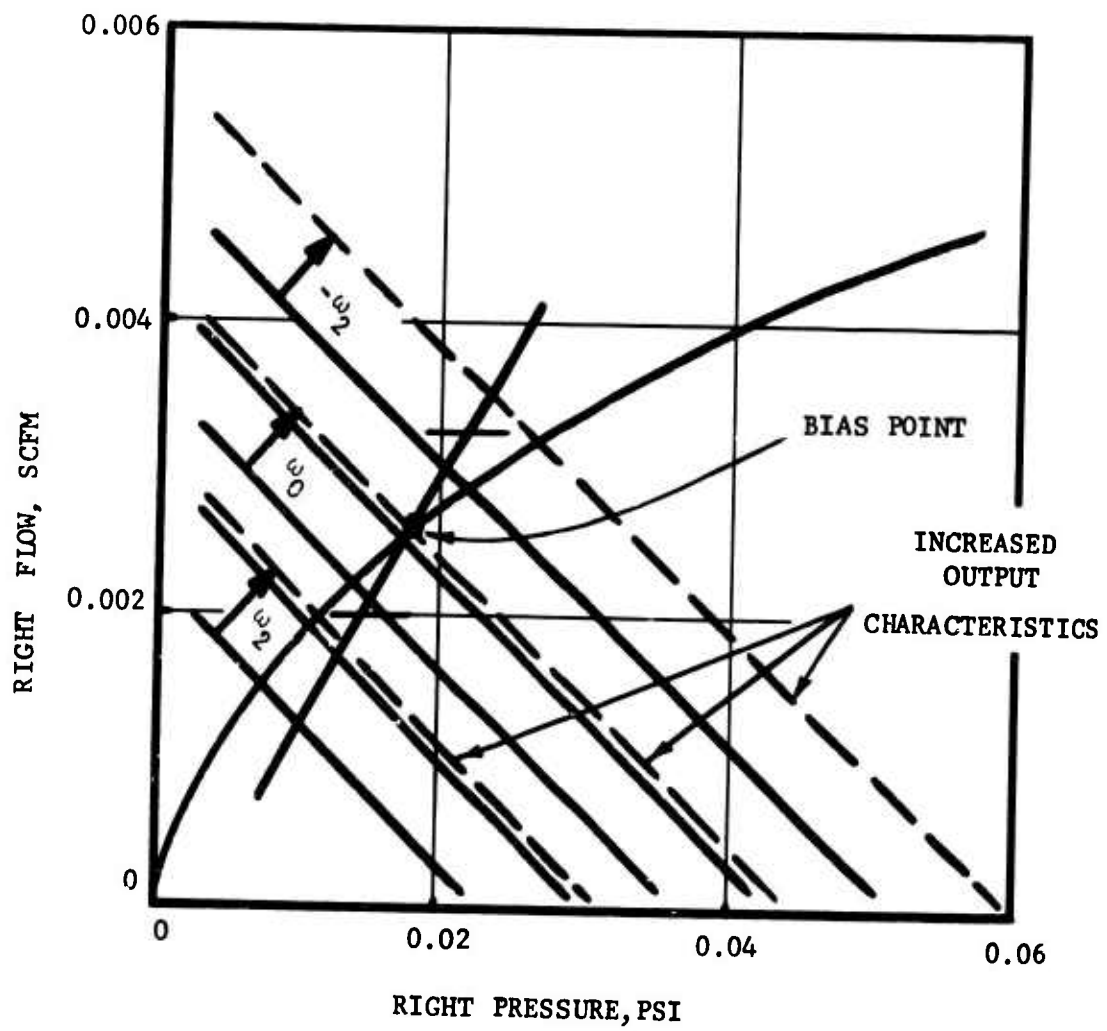


FIGURE 46 - MATCHING OPERATING POINTS
BY RAISING RATE SENSOR OUTPUT BIAS

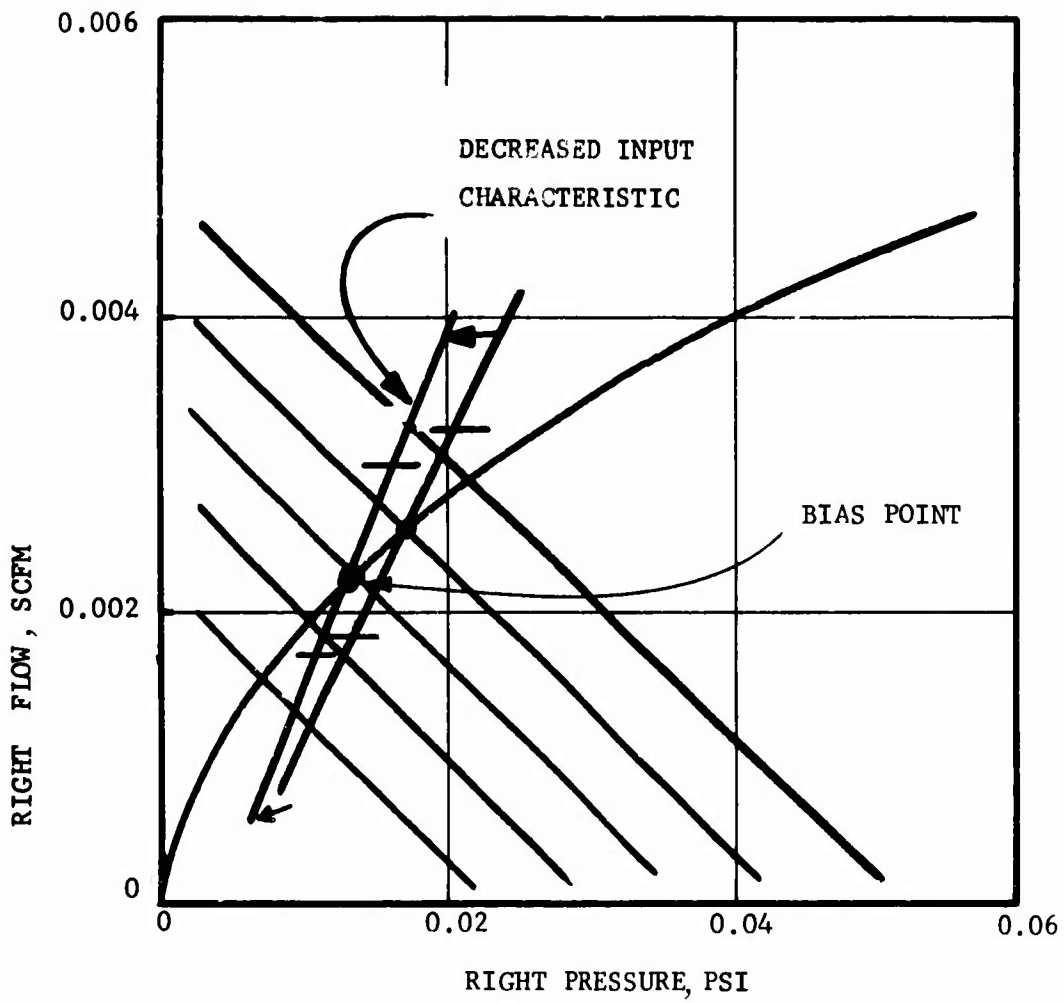


FIGURE 47 - MATCHING OPERATING POINTS
BY REDUCING AMPLIFIER SUPPLY PRESSURE

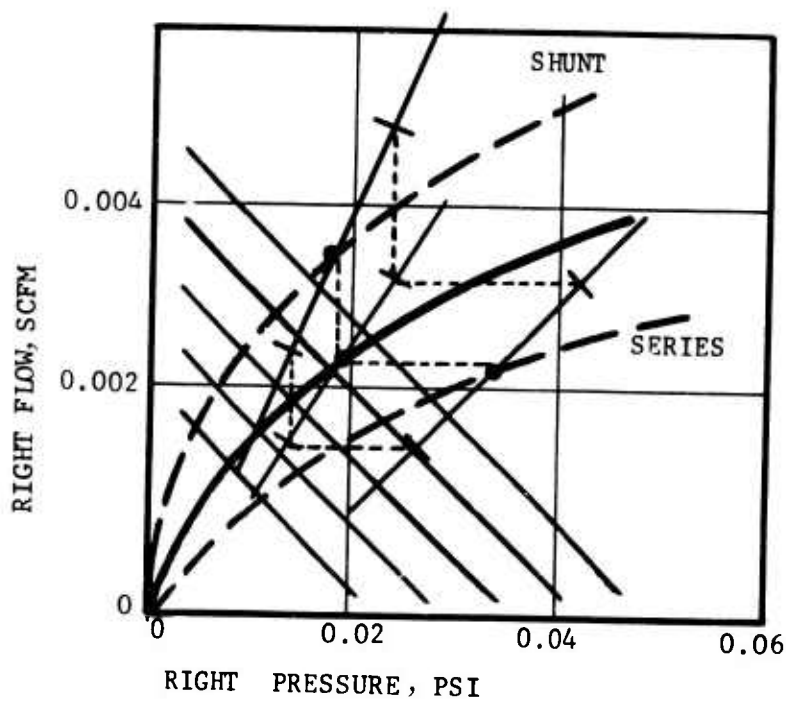
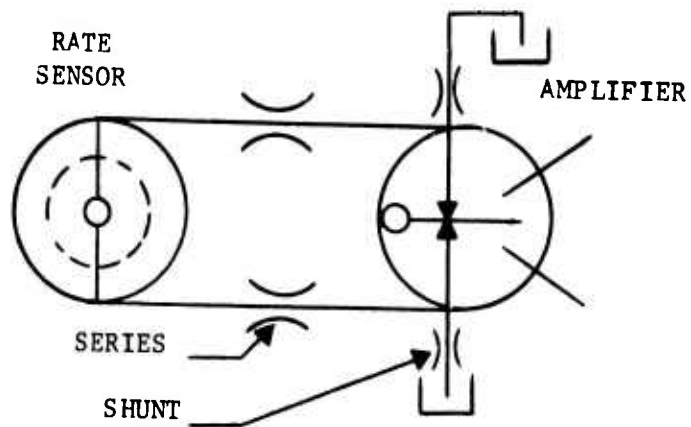


FIGURE 48 - MATCHING OPERATING POINTS BY
 ADDING RESTRICTORS IN EACH SIDE OF
 THE CIRCUIT

points, and therefore the effect of one upon the other must be considered. It turns out that static matching of fluidic components is a series of compromises based on a thorough understanding of their behavior.

5.3.3 Procedure for Matching

To properly match fluidic components for optimum performance, it is necessary to:

1. Provide proper gain
2. Match operating bias points
3. Match operating ranges

The procedure for doing this is as follows:

1. Obtain a plot of the output of the driving component with preferred operating bias points and operating ranges marked.
2. Choose a driven component whose input characteristics have a slope (impedance) which will optimize the gain variable of interest (pressure, flow, or power).
3. Match operating bias points by adjusting output pressure levels, changing supply pressures, or connecting passive restrictors in series or in parallel with the single-ended circuit.
4. Match operating ranges by changing supply pressures, adjusting bias points, and connecting passive restrictors in series or in parallel with the differential circuit.

6.0 SMALL SIGNAL PERFORMANCE ANALYSIS

Graphic methods of performance analysis are truly general; and if complete data are available, they are valid in all situations. However, for small signals, the reading of graphs becomes inaccurate. In this case a more exact and convenient method of calculating performance is by linearizing parameters around the operating bias point and employing them in an equivalent electrical circuit. This approach is widely used in all forms of engineering analysis, including electronics, acoustics, pneumatics, hydraulics, and mechanics. Therefore, by applying this approach in fluidics, all the mathematical tools developed for those forms over so many years can also be used to advantage in the analysis of fluidic systems.

The process of developing an equivalent electrical circuit for a fluidic component can be a difficult analytical task. Fortunately, useful mathematical models can also be developed through a process of logic and validated through comprehensive experimental tests. To date, this has been the only known approach which has produced useful results (Reference 2).

6.1 DEVELOPMENT OF THE EQUIVALENT CIRCUITS FOR FLUIDIC COMPONENTS

As an illustration of the approach, we will consider the case of the vented jet-interaction amplifier in some detail. Mainly by a process of logic, a direct lumped model of the amplifier can be fabricated as shown in Figure 49, using Z to represent fluid impedance. Each element in the circuit represents a measurable fluid phenomenon in the amplifier, and each is nonlinear. If each nonlinearity were fully described, the circuit could be used for large-signal performance analysis. However, they have not yet been fully described, so the circuit of Figure 49 is most useful for the insight it provides into the factors involved in cascading amplifiers and as the basis for deriving the simplified linearized equivalent circuit for small-signal performance analysis.

The complete set of equations was written to describe, in analytical form, the behavior of the circuit of Figure 49. The effect of incremental changes in control signal was then investigated, leading to the linearized small-signal equivalent circuit shown in Figure 50. Note that the equivalent circuit eliminates bias conditions, supply pressure, and, in this case, bleed impedance. Note also that the equivalent circuit elements are now treated as constants, calculated for incremental changes around the operating bias point. The load circuit equivalent generator (representing pure amplifier gain) is represented by $2K_p$; the impedance in series with the output is $2Z_o$ and the effective load impedance between output ports is $2Z_L$. The input circuit, neglecting any impedance in the line leading to the control nozzles, is represented as a shunt impedance $2Z_c$.

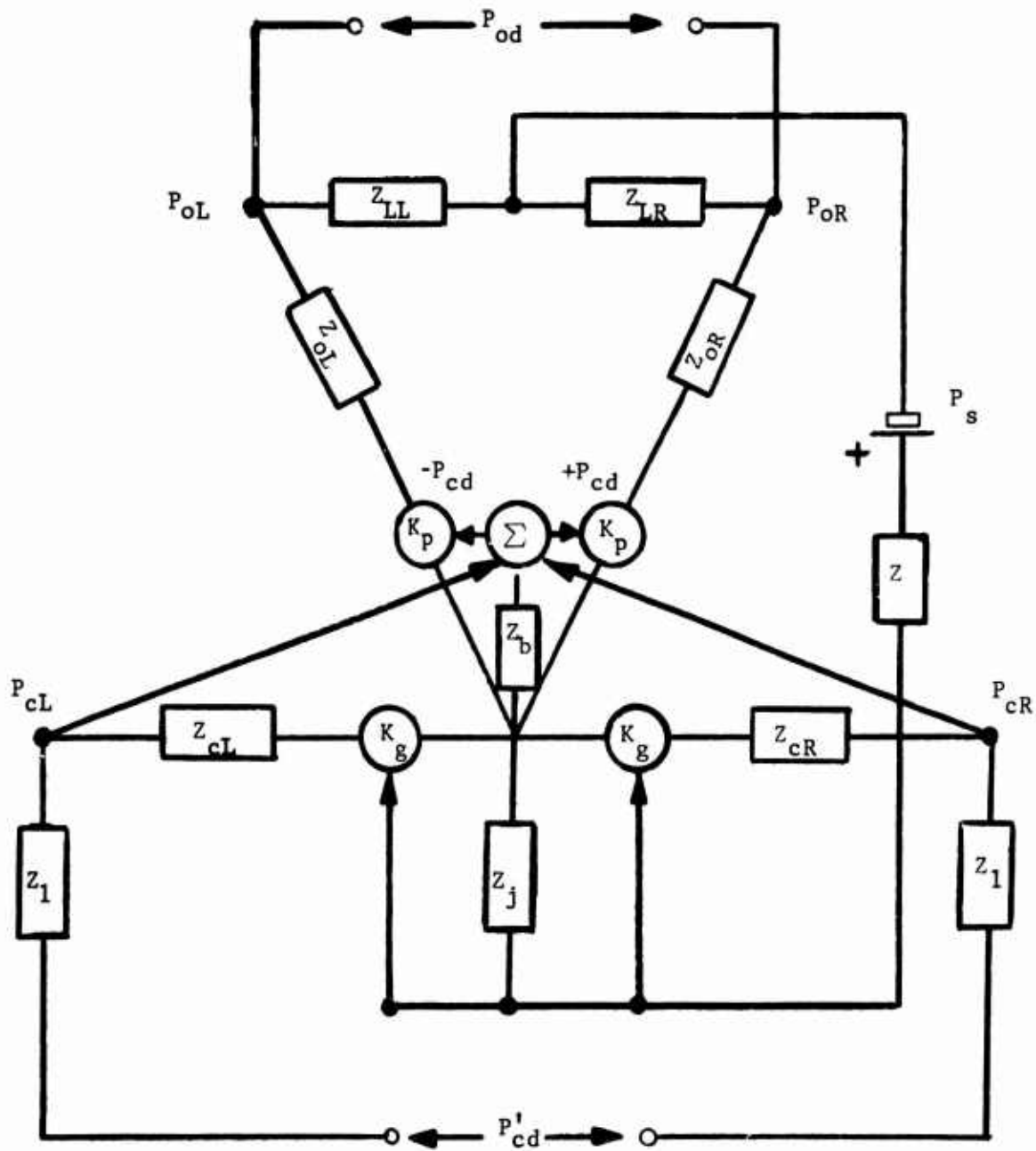


FIGURE 49 - LUMPED ELECTRICAL MODEL OF
VENTED JET - INTERACTION AMPLIFIER

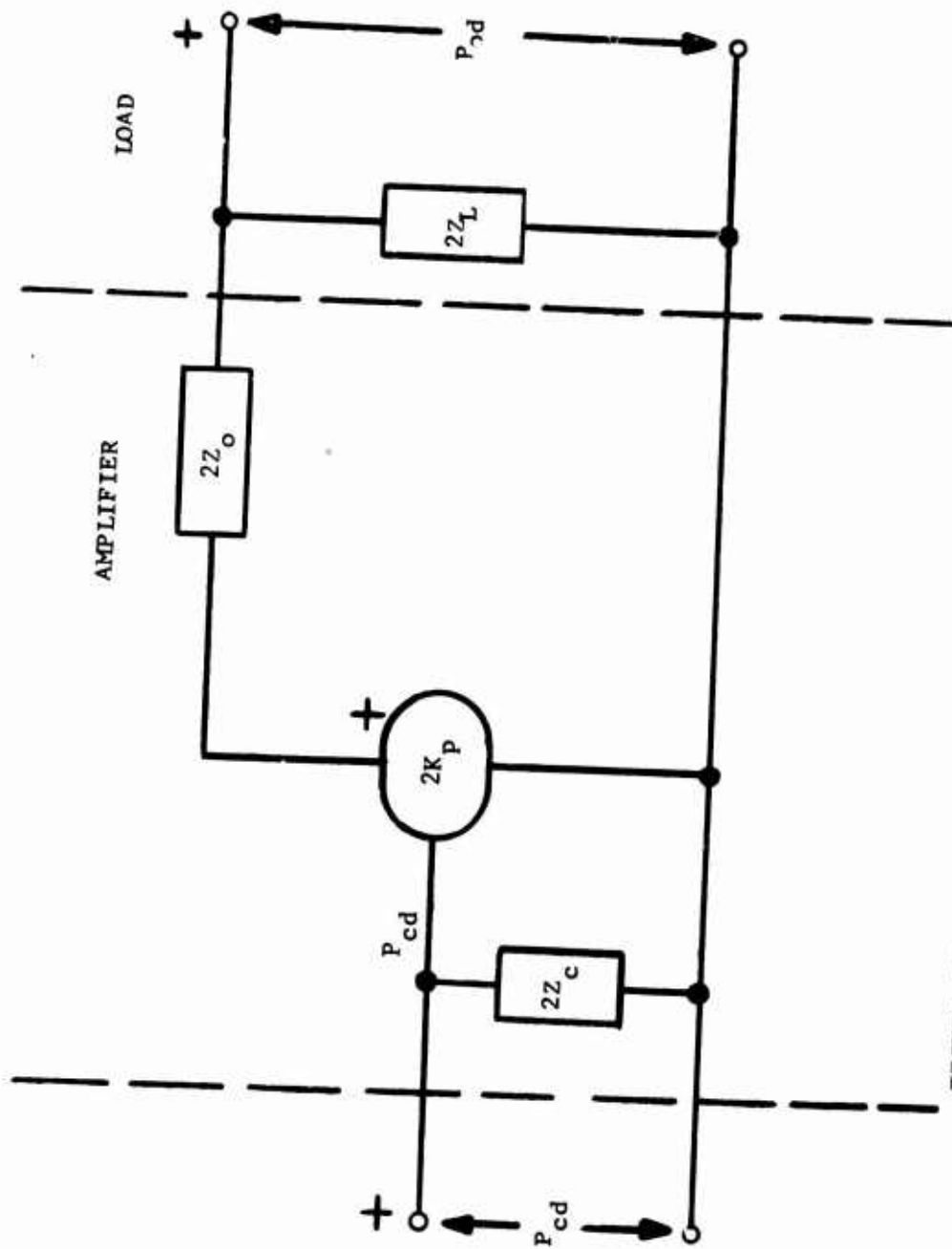


FIGURE 50 - LINEARIZED SMALL-SIGNAL EQUIVALENT
 CIRCUIT OF VENTED JET-INTERACTION AMPLIFIER
 (VALID FOR STATIC AND LOW FREQUENCY CASES)

The equivalent circuit of Figure 50 is valid for small signal analysis at low frequencies, providing that the impedances are properly defined at the frequencies of interest. If only the "resistive" components of the impedance are used, the circuit is good for the static case only.

6.1.1 Equivalent Circuit for a Vented Jet-Interaction Amplifier (Reference 2)

At higher frequencies where resistive elements no longer satisfactorily describe the behavior, the time delays due to transit time, wave propagation, and the presence of "reactive" circuit elements (like volume capacitance) must be considered. Figure 51 defines the equivalent electrical circuit for higher frequencies. The element in series with the input circuit $2L_c$ is due to inertance in the line to the control nozzle. The shunt elements $2R_c$ and $C_c/2$ are effective control nozzle resistance and volume capacitance of the control line. The equivalent generator $2K_p$ contains a delay factor (e^{-st_d}) which includes wave propagation and transit times in the total path from the control port to the load terminals. The output circuit contains a series inductor $2L_o$ and resistor $2R_o$ and a shunt volume capacitor $C_o/2$. If the lines to the load are short, the load volume capacitance $C_L/2$ is directly parallel with the amplifier capacitance, and the load resistance $2R_L$ parallels both. The transfer function for this amplifier is

$$\frac{P_{od}}{P_{cd}} = \frac{2K_p R_L}{R_o + R_L} \frac{e^{-st_d}}{\left(1 + s \frac{L_c}{R_c} + s^2 L_c C_c\right) \left[1 + s \left(\frac{C_t 2R_o R_L}{R_o + R_L} + \frac{L_o}{R_o + R_L}\right) + s^2 \frac{2C_t L_o R_L}{R_o + R_L}\right]}$$

The overall high-frequency transfer function from Figure 51 contains an attenuation due to the output circuit resistor network, a gain factor equal to twice the amplification factor, the time delay, and quadratic factors resulting from the combination of time constants in the input and output networks.

The equivalent circuit for the vented jet-interaction amplifier has been proven by experiment to be valid to frequencies above 400 cycles per second.

6.1.2 Equivalent Circuits for a Closed Jet-Interaction Amplifier (Reference 2)

The equivalent circuit for the closed jet-interaction amplifier is shown in Figure 52. It is similar to the circuit for the vented amplifier except that it includes an internal feedback loop. The feedback loop is present as a result of the backup of output pressures into the interaction

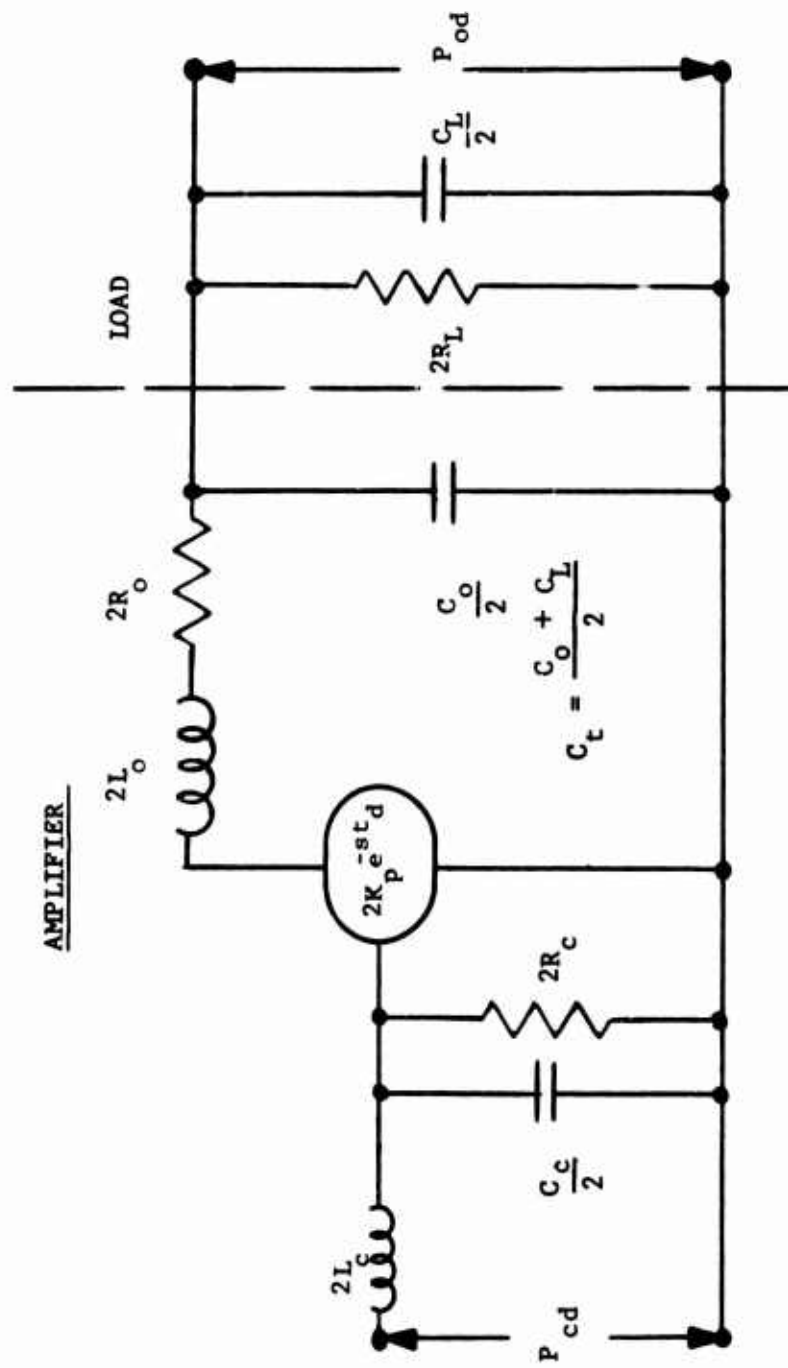


FIGURE 51 - EQUIVALENT CIRCUIT OF VENTED JET -
INTERACTION AMPLIFIER (VALID TO 400 CPS)

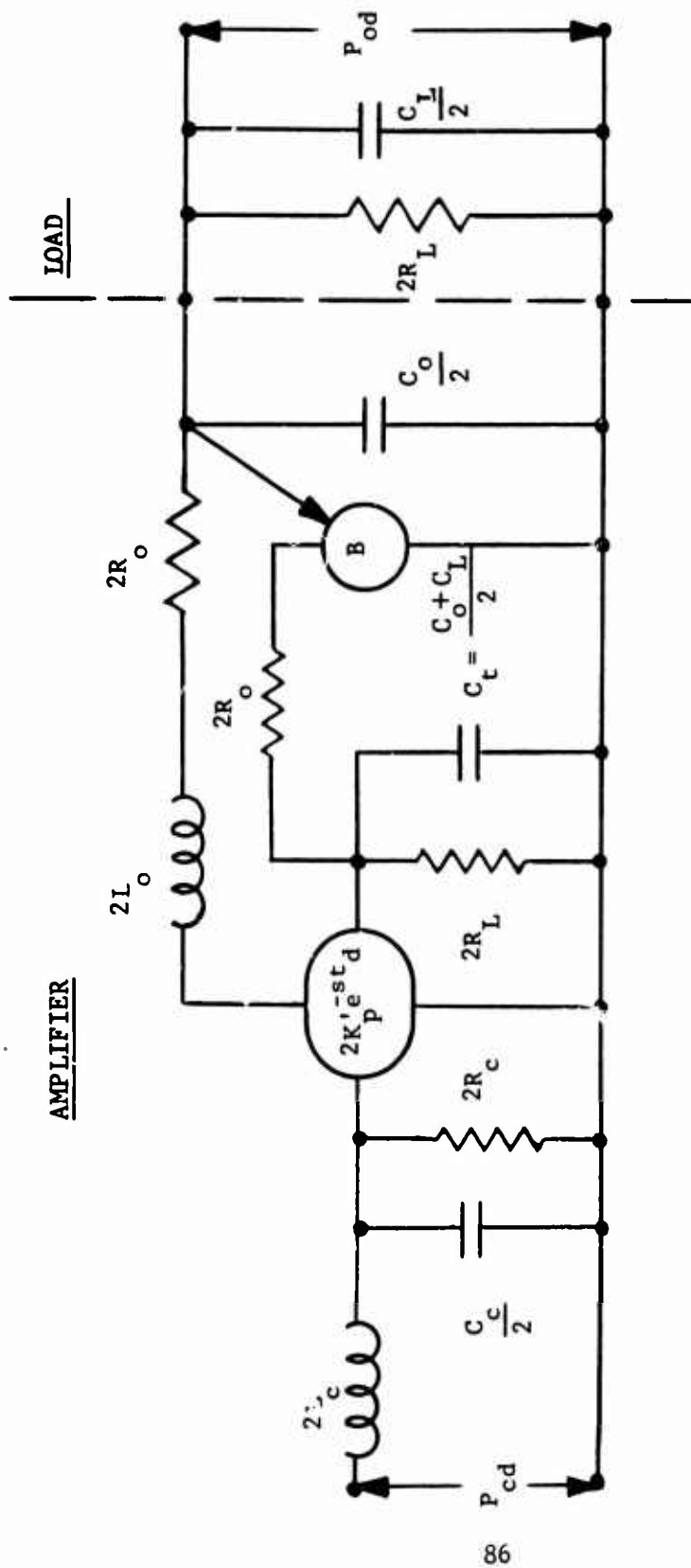


FIGURE 52 - EQUIVALENT CIRCUIT OF CLOSED JET-INTERACTION
AMPLIFIER (VALID TO 400 CPS)

chamber, where they act to reduce the gain of the amplifier circuit. The transfer function for this amplifier is

$$\frac{P_{od}}{P_{cd}} \approx \frac{2K_p R_L}{R_o + R_L} \frac{\left(1 + sC_t \frac{2R_o R_L}{R_o + R_L}\right) e^{-std}}{\left(1 + s\frac{L_c}{R_c} + s^2 L_c C_c\right) \left[1 + s \frac{4C_t R_o R_L}{(1 + 2K'_p B)(R_o + R_L)} + \frac{s^2 \frac{4C_t^2 R_o^2 R_L^2}{(1 + 2K'_p B)(R_o + R_L)^2} + s^3 \frac{4L_o C_t^2 R_L^2 R_o}{(1 + 2K'_p B)(R_o + R_L)^2}\right]}$$

The equivalent circuit for the closed jet-interaction amplifier has been validated by experiment to frequencies above 400 cycles per second.

6.1.3 Equivalent Circuit for Vented Elbow Amplifier (Reference 2)

The equivalent circuit for a typical vented elbow amplifier is shown in Figure 53. Note that this amplifier is essentially a flow amplifier; hence, the equivalent generator is a flow generator. Otherwise, the circuit is similar in form to the jet-interaction amplifier circuits. The transfer function for this amplifier is

$$\frac{P_o}{P_c} = \frac{K_f R'_L}{R_c (R_o + R_L)} \frac{e^{-std}}{\left(1 + s\frac{L_c}{R_c} + s^2 L_c C_c\right) (1 + sC'R')} \left[1 + s \frac{C_t R_o R_L + L_o}{R_o + R_L} + s^2 \frac{L_o C_t R_L}{R_o + R_L}\right]$$

The equivalent circuit for the vented elbow amplifier has been validated by experiment to frequencies above 400 cycles per second.

6.1.4 Equivalent Circuit of a Vortex Rate Sensor (Reference 3)

The equivalent circuit for a typical vortex rate sensor is shown in Figure 54. The rate of turn drives an equivalent generator containing the sensitivity factor. In the process it is subject to a time delay due to the time that it takes for the angular momentum at the rim to be transported through the vortex to the pickup in the drain tube. The resulting pressure signal is then applied to an output circuit containing the same arrangement of elements that appear in the amplifier output circuits. The transfer function for the vortex rate sensor is

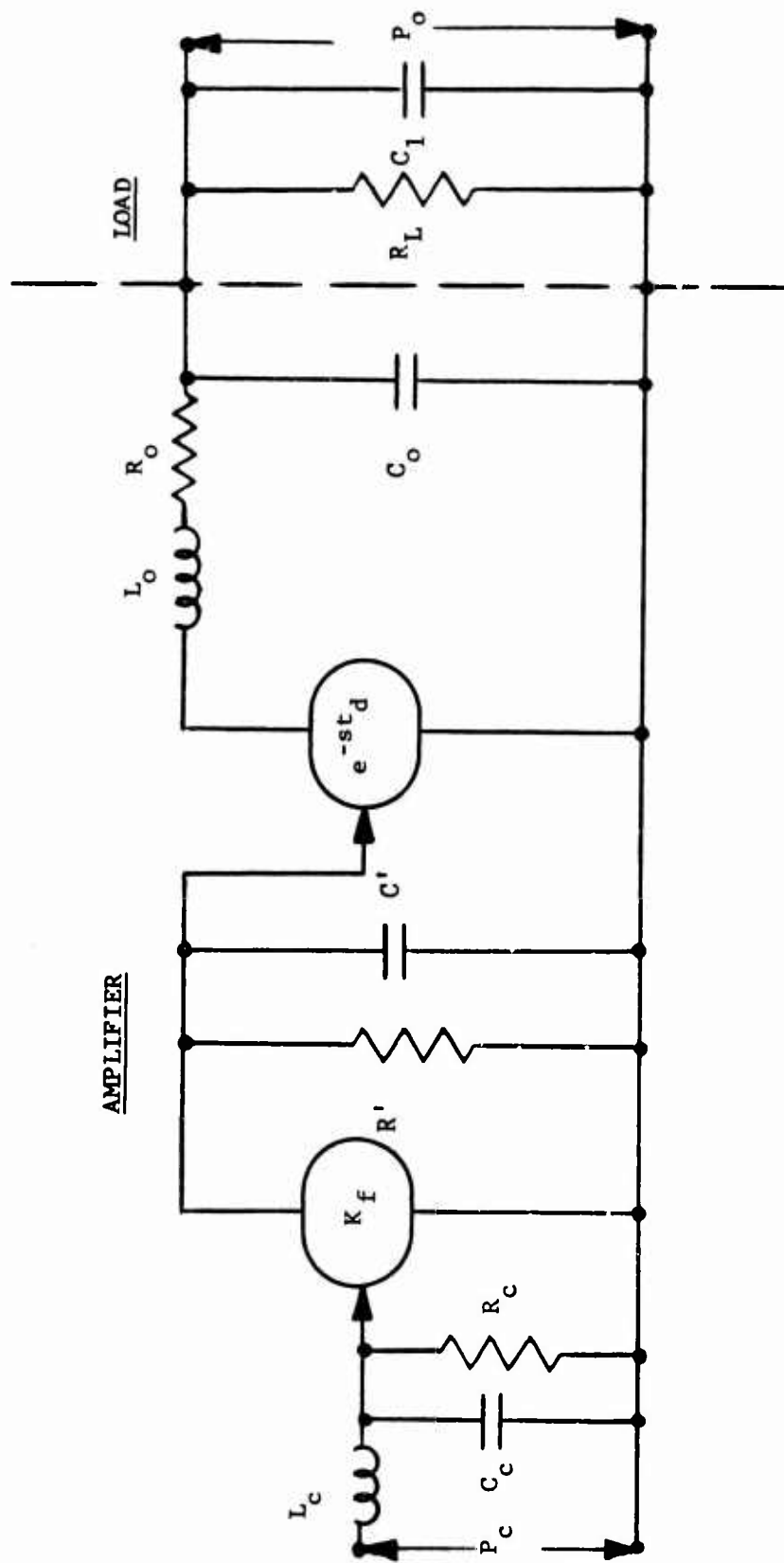


FIGURE 53 - EQUIVALENT CIRCUIT OF VENTED ELBOW
AMPLIFIER (VALID TO 400 CPS)

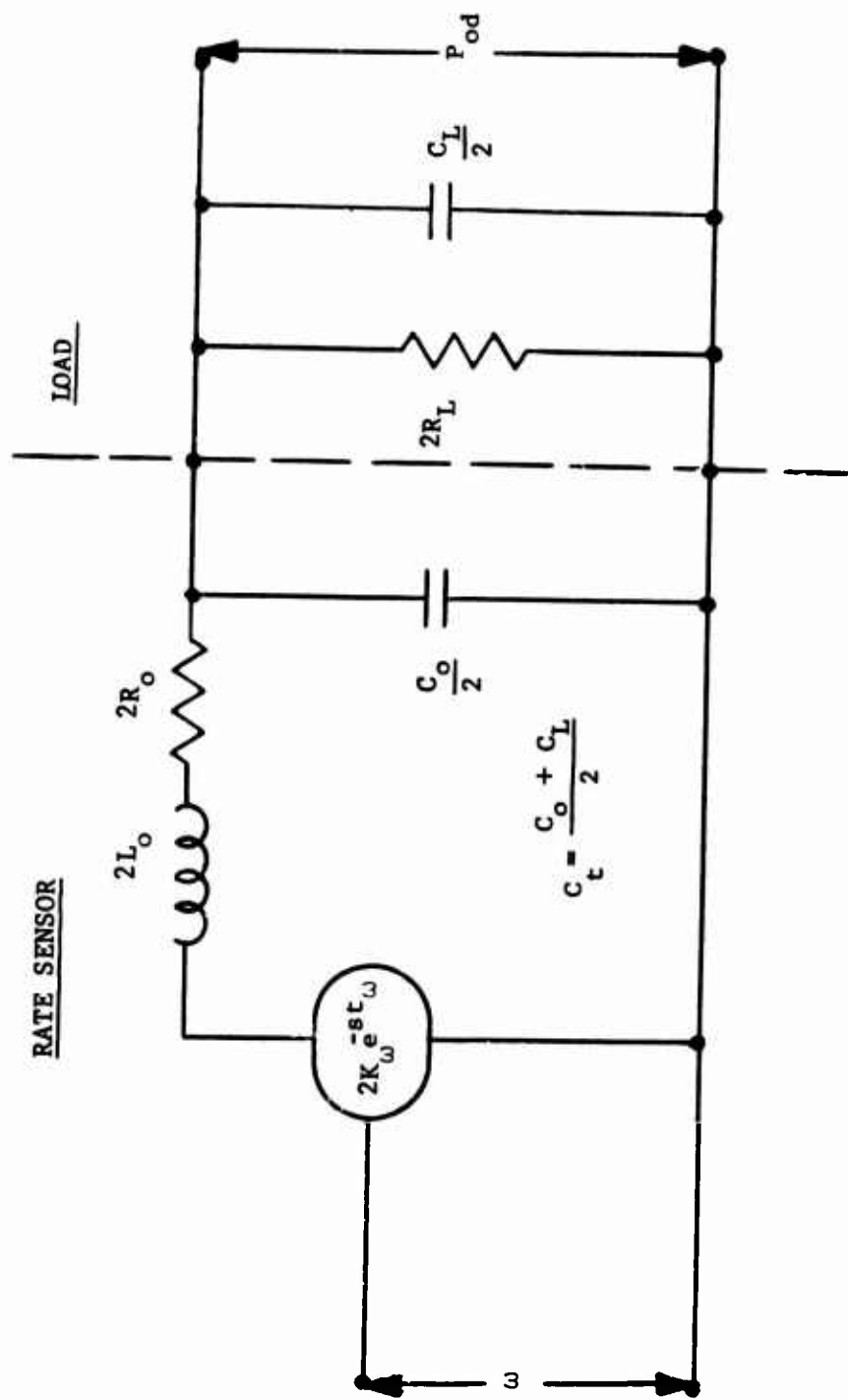


FIGURE 54 - EQUIVALENT CIRCUIT OF VORTEX RATE SENSOR

$$\frac{P_{od}}{\omega} = \frac{2K_{\omega} R_L}{R_o + R_L} \frac{e^{-st_{\omega}}}{1 + s \left(\frac{2C_t R_o R_L}{R_o + R_L} + \frac{L_o}{R_o + R_L} \right) + s^2 \frac{2C_t L_o R_L}{R_o + R_L}}$$

6.1.5 Equivalent Circuit For a Piston-Type Actuator

The equivalent electrical circuit for a typical piston-type (or bellows-type) actuator is shown in Figure 55. Pressure applied to the actuator causes flow in the equivalent capacitor because of compressibility, and flow through the leakage resistance (if present). A reduced pressure is also applied to a series network containing the reflected acceleration, velocity, and position characteristics of the load. All of these flows must be conducted through the internal resistance of the actuator and its associated connections which limit the maximum available velocity and acceleration of the actuator - load combination (Reference 6).

6.1.6 Equivalent Circuit For Piston-Type and Vane-Type Motors

The equivalent circuit for a typical piston-type or vane-type motor is shown in Figure 56. Pressure applied to the motor causes flow due to compressibility of the trapped fluid and due to leakage (which is considerable in the vane-type motor). A reduced pressure is also applied to a series network containing the reflected acceleration and velocity characteristics of the load. (The resulting flows through the internal resistance of the motor and its associated connections cause a pressure drop which limits the top speed and acceleration of the motor and its load.)

6.2 CASCADING EQUIVALENT CIRCUITS

When fluidic components are cascaded (that is, one becomes the load on the other), their equivalent electrical circuits will be cascaded in a similar way. Figure 57 illustrates the connection of a vented jet-interaction amplifier to the output of a vortex rate sensor for the purpose of amplifying the signal. The cascading of the equivalent circuits simply involves the connection of the output terminals of the rate sensor circuit (Figure 54) to the input terminals of the amplifier (Figure 51). Note that in the interconnecting lines we have added a resistance R_1 to represent any additional resistance due to unusual line lengths.

6.3 DERIVATION OF THE TRANSFER FUNCTION FOR CASCADED FLUIDIC COMPONENTS

The derivation of the transfer function for the cascaded fluidic components involves the straightforward analysis of the equivalent electrical circuits by well-known mathematical methods (Reference 10). Specifically, it involves the loop analysis of each set of coupled circuits using the Laplace transform notation, and the combination of the results into a single transfer function representing the overall dynamic response of the

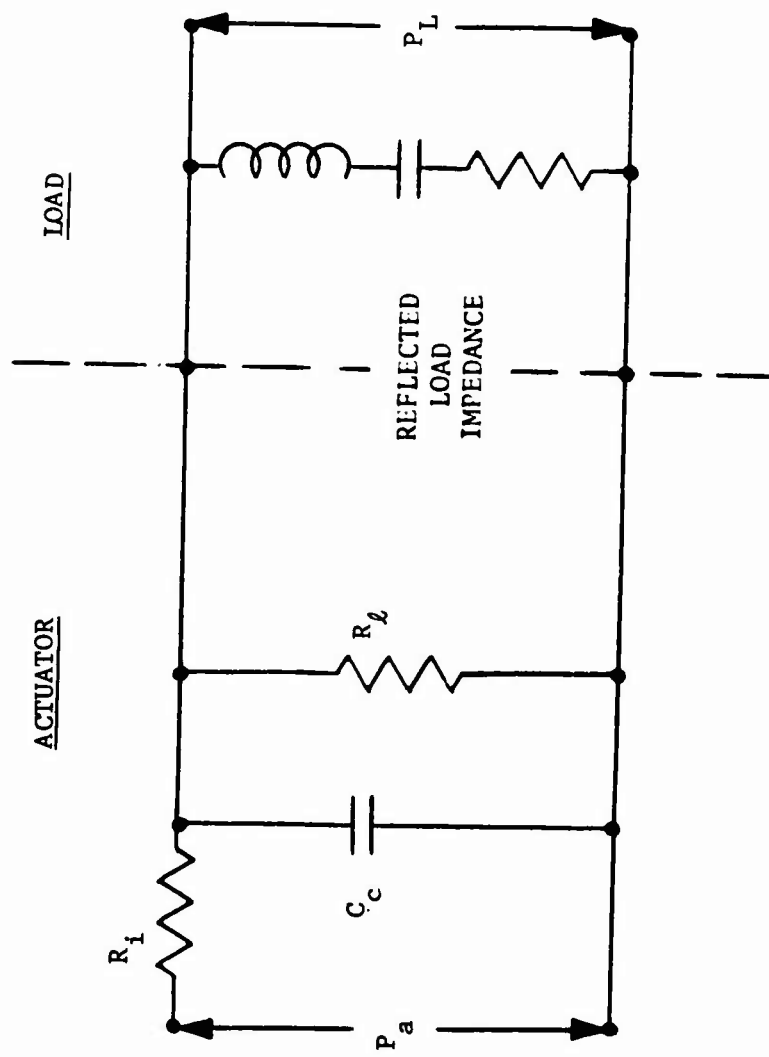


FIGURE 55 - EQUIVALENT CIRCUIT OF PISTON-TYPE ACTUATOR

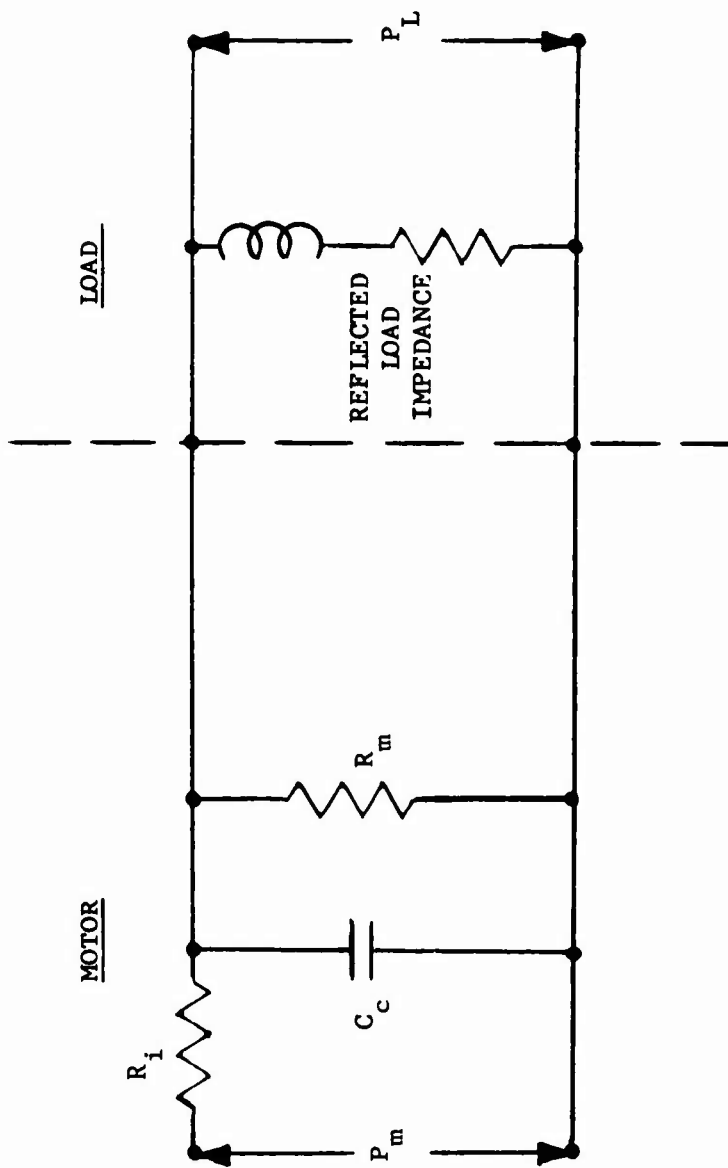


FIGURE 56 - EQUIVALENT CIRCUIT OF PISTON-TYPE AND VANE-TYPE FLUID MOTORS

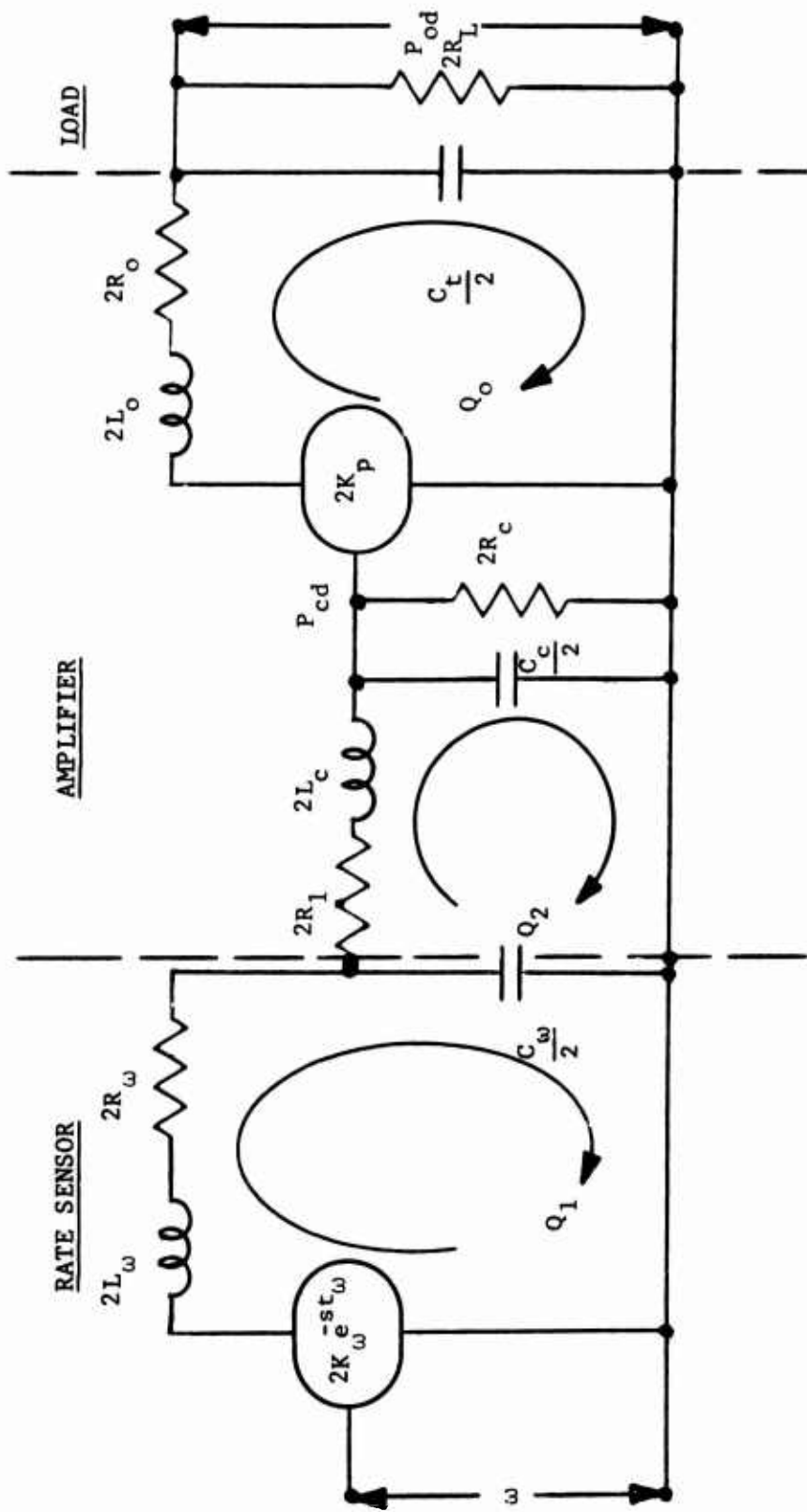


FIGURE 57 - CASCADING EQUIVALENT CIRCUITS OF VORTEX RATE SENSOR AND VENTED JET-INTERACTION AMPLIFIER

cascaded fluidic components. The procedure is perhaps best communicated by means of an example.

Consider the circuit illustrated in Figure 57 and described in paragraph 6.2. We must first generate the array of loop equations in the form of

$$P_1 = Z_{11}Q_1 + Z_{12}Q_2 + Z_{13}Q_3$$

$$P_2 = Z_{21}Q_1 + Z_{22}Q_2 + Z_{23}Q_3$$

$$P_3 = Z_{31}Q_1 + Z_{32}Q_2 + Z_{33}Q_3$$

In this case we have only two coupled loops: those involving Q_1 and Q_2 . From these we are to derive the transfer function for the first coupled section P_{cd}/ω . The loop equations, assuming zero initial conditions, are

$$2K_\omega e^{-st_\omega} = (2R_\omega + 2sL_\omega + 2/sC_\omega)Q_1 + (2/sC_\omega)(-Q_2)$$

$$0 = (2/sC_\omega)(-Q_1) + (2/sC_\omega + 2sL_c + 2R_1 + \frac{4R_c/sC_c}{2R_c + 2/sC_c})(Q_2)$$

Solving for Q_2 by determinants, we have

$$Q_2 = \frac{\begin{vmatrix} (2R_\omega + 2sL_\omega + 2/sC_\omega) & 2K_\omega e^{-st_\omega} \\ -(2/sC_\omega) & 0 \end{vmatrix}}{D}$$

where

$$D = \begin{vmatrix} (2R_\omega + 2sL_\omega + 2/sC_\omega) & -(2/sC_\omega) \\ -(2/sC_\omega) & (2/sC_\omega + 2sL_c + 2R_1 + \frac{4R_c/sC_c}{2R_c + 2/sC_c}) \end{vmatrix}$$

Then

$$Q_2 = \frac{K_\omega e^{-st_\omega}(1/sC_\omega)}{(R_\omega + sL_\omega + 1/sC_\omega)(1/sC_\omega + sL_c + R_1 + \frac{R_c/sC_c}{R_c + 1/sC_c}) - (1/sC_\omega)^2}$$

For simplicity in the algebraic solution for Q_2 , let us assume that all the inductances L_ω , L_c , and L_o are negligible. One should keep in mind the fact that we can reintroduce these terms into the solution whenever desired simply by adding the appropriate sL term to each of the associated R terms.

$$\text{Then } Q_2 = \frac{K_\omega e^{-st_\omega} (1/sC_\omega)}{(R_\omega + 1/sC_\omega)(1/sC_\omega + R_1 + \frac{R_c/sC_c}{R_c + 1/sC_c}) - (1/sC_\omega)^2}$$

We are attempting to define the transfer function for P_{cd}/ω as a first step, but

$$P_{cd} = Q_2 \frac{2R_c/sC_c}{R_c + 1/sC_c}$$

Substituting the equation for Q_2 gives

$$\frac{P_{cd}}{\omega} = \frac{2K_\omega e^{-st_\omega} (1/sC_\omega) (\frac{R_c/sC_c}{R_c + 1/sC_c})}{(R_\omega + 1/sC_\omega)(1/sC_\omega + R_1 + \frac{R_c/sC_c}{R_c + 1/sC_c}) - (1/sC_\omega)^2}$$

This expression then is reduced algebraically to

$$\frac{P_{cd}}{\omega} = \frac{K_\omega e^{-st_\omega} R_c}{(R_\omega + R_1 + R_c)} \frac{1}{s^2 C_\omega R_\omega C_c R_c (\frac{R_1}{R_\omega + R_1 + R_c}) + \frac{1}{s C_c R_c (\frac{R_\omega + R_1}{R_\omega + R_1 + R_c}) + s C_\omega R_\omega (\frac{R_1 + R_c}{R_\omega + R_1 + R_c}) + 1}}$$

This defines the transfer function for the first section of the equivalent circuit involving the coupled rate sensor output and amplifier input circuits.

The second section of the complete equivalent circuit involving the flow Q_o is described by the following two equations.

$$Q_o = \frac{K_p e^{-st_o} P_{cd}}{sL_o + R_o + \frac{R_L/sC_t}{R_L + 1/sC_t}}$$

and

$$P_{od} = Q_o \frac{2R_L/sC_t}{R_L + 1/sC_t}$$

Combining gives

$$P_{od} = \frac{K_p e^{-st_o} P_{cd} \frac{R_L/sC_t}{R_L + 1/sC_t}}{sL_o + R_o + \frac{R_L/sC_t}{R_L + 1/sC_t}}$$

Again neglecting L_o for simplicity,

$$\frac{P_{od}}{P_{cd}} = \frac{2K_p e^{-st_o} \frac{R_L/sC_t}{R_L + 1/sC_t}}{R_o + \frac{R_L/sC_t}{R_L + 1/sC_t}}$$

This expression is reduced algebraically to

$$\frac{P_{od}}{P_{cd}} = \frac{2K_p e^{-st_o} R_L}{R_o + R_L} \frac{1}{sC_t \frac{R_o R_L}{R_o + R_L} + 1}$$

Now we have the transfer functions P_{cd}/ω and P_{od}/P_{cd} . We want the overall transfer function P_{od}/ω .

But

$$P_{od}/\omega = P_{cd}/\omega \times P_{od}/P_{cd}$$

Then

$$\frac{P_{od}}{\omega} = \frac{4K_{\omega} e^{-st_{\omega}} K_c K_p e^{-st_o} R_L}{(R_{\omega} + R_1 + R_c)(R_o + R_L)} \left[\frac{1}{sC_t \left(\frac{R_o R_L}{R_o + R_L} \right) + 1} \right]$$

$$\left[\frac{1}{s^2 C_{\omega} R_{\omega} C_c R_c \left(\frac{R_1}{R_{\omega} + R_1 + R_c} \right) + sC_c R_c \left(\frac{R_{\omega} + R_1}{R_{\omega} + R_1 + R_c} \right) + sC_{\omega} R_{\omega} \left(\frac{R_1 + R_c}{R_{\omega} + R_1 + R_c} \right) + 1} \right]$$

Describes the small-signal static and dynamic behavior of the cascaded rate sensor and amplifier. To calculate the behavior in numerical form, it will first be necessary to evaluate each of the equivalent circuit parameters contained in the above transfer function.

6.4 CALCULATION OF EQUIVALENT CIRCUIT PARAMETERS

6.4.1 Vortex Rate Sensor

The performance parameters for the vortex rate sensor are calculated from the graphical output characteristics and the circuit dimensions at the operating point. Starting with the combined rate sensor - amplifier static characteristics as shown in Figure 58, it is possible to define the operating bias point at $P_1 Q_1$. From here we can proceed with the calculation of circuit parameters.

6.4.1.1 Sensitivity Factor K_{ω}

The sensitivity factor (defined in paragraph 2.6.4) is calculated from the horizontal spacing between rate sensor output characteristics at the operating bias point (see Figure 58).

6.4.1.2 Time Delay t_{ω}

The time delay of the rate sensor (defined in paragraph 2.6.8) is calculated from the dimensions of the rate sensor and output circuit and the flow and pressure conditions at the operating point. It can also be measured directly (paragraph 3.2.1.3).

6.4.1.3 Output Resistance R_{ω}

The output resistance (defined in paragraph 2.6.1) is calculated from the slope of the zero signal output characteristic curve at the operating point (see Figure 58).

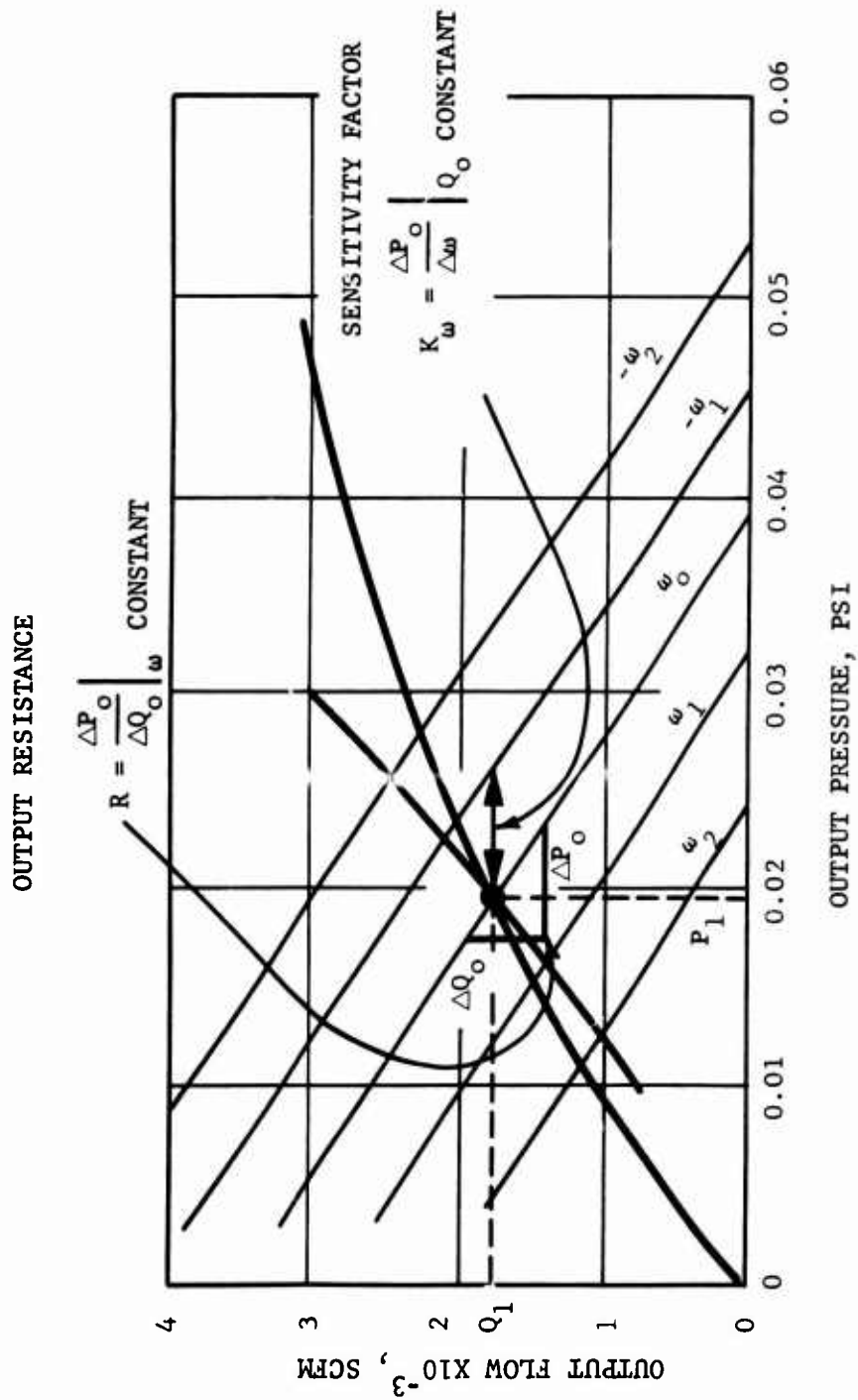


FIGURE 58 - EQUIVALENT CIRCUIT PARAMETERS DEFINED FROM STATIC OUTPUT CHARACTERISTICS OF VORTEX RATE SENSOR

6.4.1.4 Output Inductance L_{ω}

The output inductance of the rate sensor (defined in paragraph 2.6.7) is calculated from the density at the operating point and the dimensions of the output circuit.

6.4.1.5 Output Capacitance C_{ω}

The output capacitance of the rate sensor (defined in paragraph 2.6.6) is calculated from the dimensions of the output circuit and the pressure at the operating point.

6.4.2 Amplifier

The parameters in the amplifier input circuit are calculated from the graphical characteristics that define the conditions in the coupled rate sensor output - amplifier input circuits (see Figure 59). The parameters in the amplifier output circuit are calculated from the graphical characteristics that define the conditions in the amplifier output circuit with the resistance R_L as a load line.

6.4.2.1 Input Inductance L_c

The input inductance of the amplifier (defined in paragraph 2.6.7) is calculated from the dimensions of the input circuit and the control operating point pressure.

6.4.2.2 Input Resistance R_c

The input resistance of the amplifier (defined in paragraph 2.6.5) is calculated from the slope of the input characteristic at the operating point (see Figure 59).

6.4.2.3 Input Capacitance C_c

The input capacitance of the amplifier (defined in paragraph 2.6.6) is calculated from the dimensions of the input circuit and the control pressure at the operating point.

6.4.2.4 Line Resistance R_l

The line resistance in the input circuit is calculated from the line dimensions and the pressure and flow conditions at the operating point by using standard formulae or measuring as described in paragraphs 3.1.3 and 3.2.3.

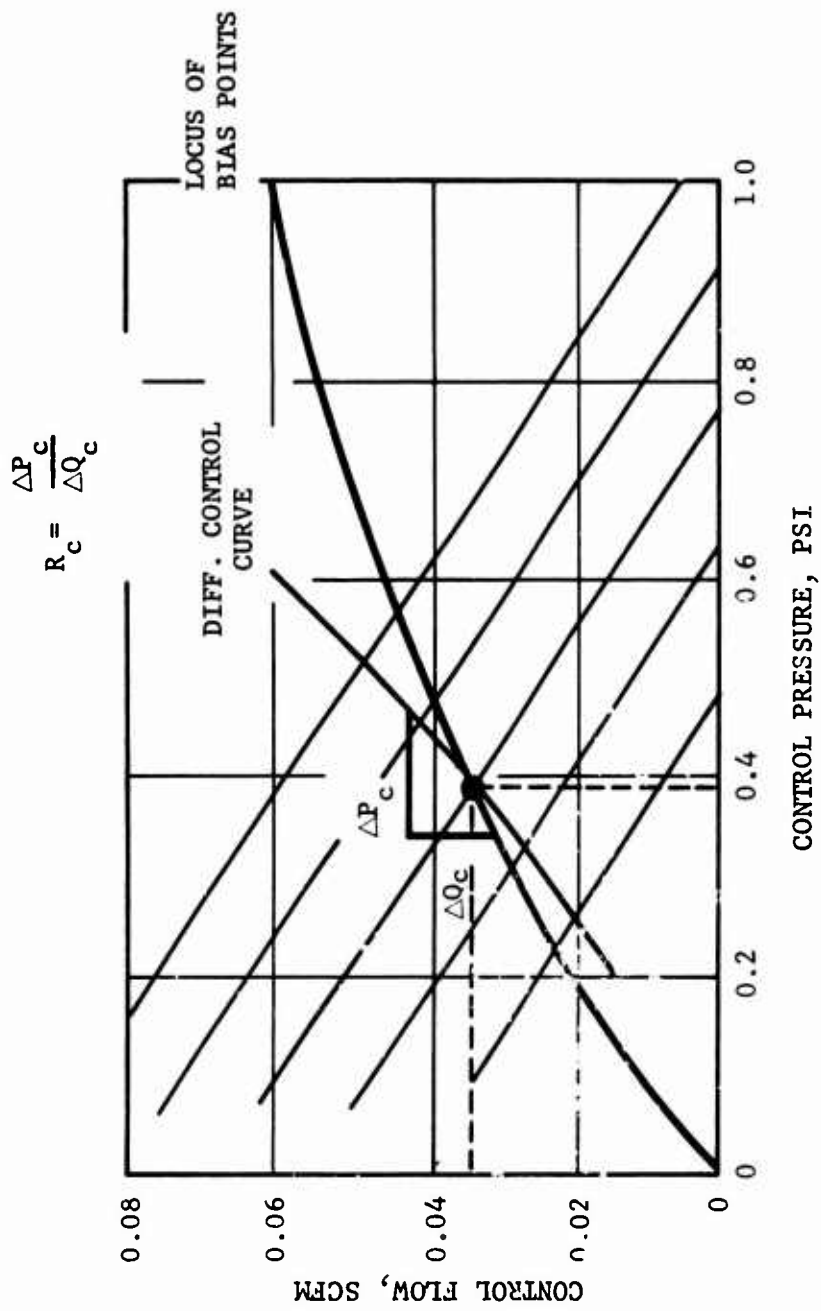


FIGURE 59 - EQUIVALENT CIRCUIT PARAMETERS DEFINED FROM STATIC INPUT CHARACTERISTICS OF JET-INTERACTION AMPLIFIER

6.4.2.5 Amplification Factor K_p

The pressure amplification factor (defined in paragraph 2.6.3) is calculated from the horizontal spacing between curves of the amplifier output characteristics at the operating point (see Figure 60).

6.4.2.6 Time Delay t_o

The amplifier time delay (defined in paragraph 2.6.8) is calculated from the dimensions of the amplifier circuits and the pressure and flow conditions at the operating point. It can also be measured directly (paragraph 3.2.1.3).

6.4.2.7 Output Resistance R_o

The amplifier output resistance (defined in paragraph 2.6.1) is calculated from the slope of the zero signal output characteristic at the operating point (see Figure 60).

6.4.2.8 Output Inductance L_o

The amplifier output inductance (defined in paragraph 2.6.7) is calculated from the amplifier output circuit dimensions and the density at the operating point.

6.4.2.9 Output Capacitance C_t

The output capacitance (defined in paragraph 2.6.6) of the amplifier and its load circuit is calculated from the dimensions of the amplifier and load circuits and the pressure at the operating point.

6.4.2.10 Load Resistance R_L

The load resistance on the amplifier is calculated from the slope of the load line (load restrictor characteristic) at the operating point (see Figure 60).

6.5 CALCULATION OF FREQUENCY RESPONSE

6.5.1 Substitution of the Variable

To calculate the frequency response of cascaded fluidic components, we must first generate the coupled equivalent circuit (paragraph 6.2), derive the transfer function (paragraph 6.3), calculate the performance parameters (paragraph 6.4), and substitute them into the transfer function. The result would be a numerical equivalent of the transfer function containing the Laplace transform variable, s , typically as follows:

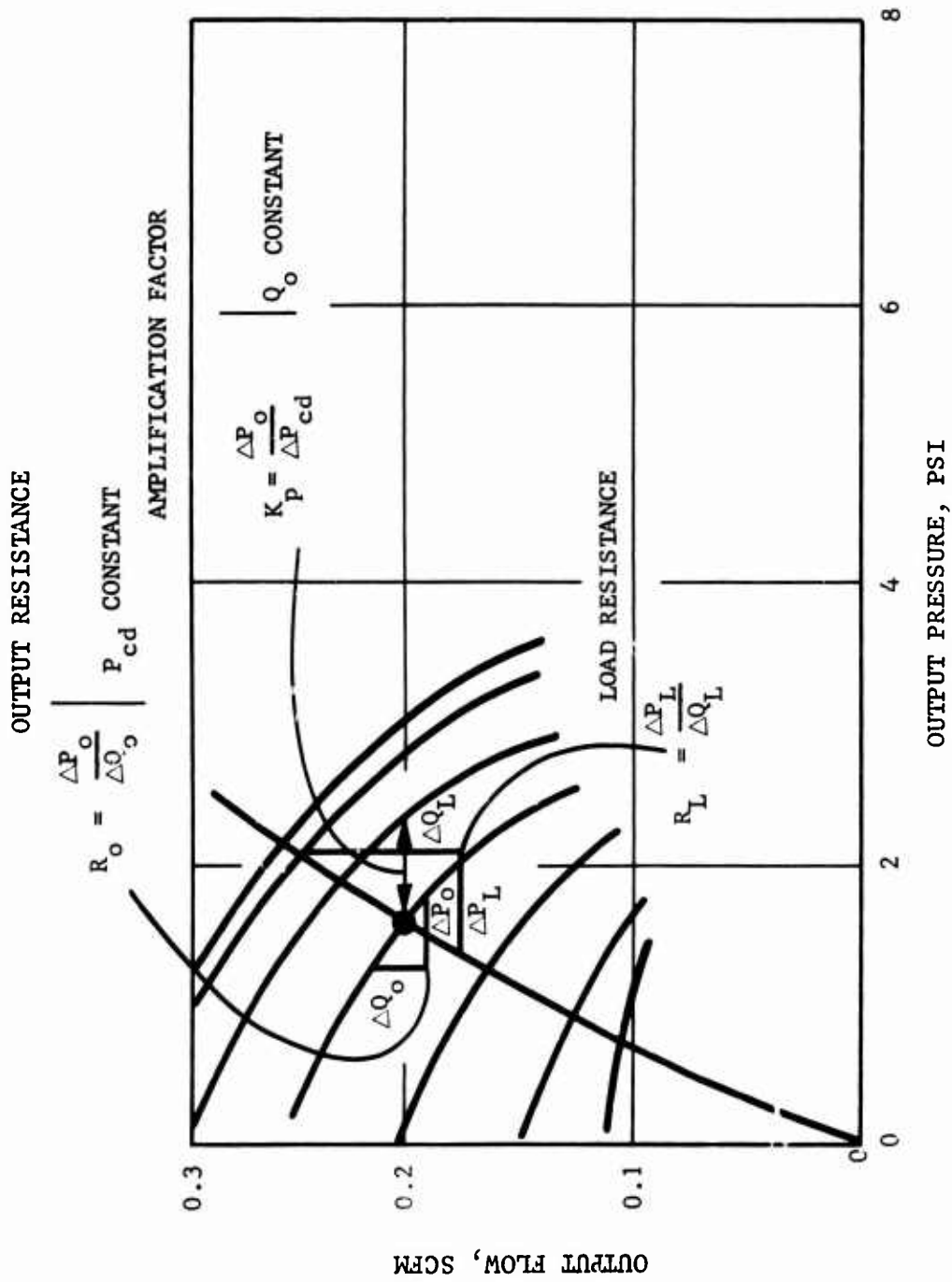


FIGURE 60 - EQUIVALENT CIRCUIT PARAMETERS DEFINED FROM STATIC OUTPUT CHARACTERISTICS OF AMPLIFIER

$$\frac{P_{od}}{\omega} = 0.05 \frac{e^{-0.01s}}{(8 \times 10^{-6} s^2 + 5 \times 10^{-3} s + 1)(2 \times 10^{-3} s + 1)}$$

With reference to Chestnut and Mayer, Servomechanisms and Regulating System Design, Volume I, one of the properties of the Laplace transform is direct conversion into the frequency plane. That is, the frequency characteristics of the transfer function above can be determined simply by substituting the variable $j2\pi f$ for the Laplace transform variable s . The factor $2\pi f$ is the radian frequency, and $j = \sqrt{-1}$.

Therefore, to determine the frequency response of the above transfer function defining the behavior of the cascaded vortex rate sensor and amplifier, we substitute $j2\pi f$ for s (except in the delay factor $e^{-0.01s}$).

$$\frac{P_{od}}{\omega} = 0.05 \frac{e^{-0.01s}}{(-3.2 \times 10^{-4} f^2 + j3.1 \times 10^{-2} f)(j1.3 \times 10^{-2} f + 1)}$$

Now the calculation must be separated into two parts, one involving the linear system response and one involving the time delay (which we will consider a nonlinear system response); schematically,

$$\frac{P_{od}}{\omega} = \frac{\text{linear} \quad 0.05}{(1 - 3.2 \times 10^{-4} f^2 + j3.1 \times 10^{-2} f)(j1.3 \times 10^{-2} f + 1)} \quad \text{nonlinear} \quad e^{-0.01s}$$

6.5.2 Calculation of Linear Response

For the purpose of illustration, let us calculate the response of the cascaded rate sensor and amplifier at a frequency of 100 cycles per second.

In the linear portion of the transfer function, the frequency is substituted directly:

$$\frac{P_{od}}{\omega} = \frac{0.05}{(1 - 3.2 \times 10^{-4} \times 10^4 + j3.1 \times 10^{-2} \times 10^2)(j1.3 \times 10^{-2} \times 10^2 + 1)}$$

$$\frac{P_{od}}{\omega} = \frac{0.05}{(-2.2 + j3.1)(j1.3 + 1)}$$

Converting the complex numbers to vectors,

$$\frac{P_{od}}{\omega} = \frac{0.05}{3.8 \angle 124^\circ \times 1.6 \angle 39^\circ} = \frac{0.05}{6.1 \angle 163^\circ}$$

$$\frac{P_{od}}{\omega} = 0.008 \angle -163^\circ \quad \text{at 100 cps}$$

and converting to decibels,

$$\frac{P_{od}}{\omega} = -42\text{db} \angle -163^\circ \quad \text{at 100 cps}$$

6.5.3 Calculation of the Response to Time Delay

The factor $e^{-0.01s}$ in the transfer function of the cascaded rate sensor and amplifier represents a dead-time delay: a nonlinear condition. Fortunately, its effect on frequency response is not difficult to analyze.

Consider the illustration of Figure 61. It is evident that the effect of dead time is to delay the sine wave a fixed time without affecting the amplitude. However, it is also to be recognized that a fixed delay time represents a different phase shift (in terms of number of degrees), depending on the frequency of the sine wave. In fact, it turns out that the effective phase shift in degrees is a linear function of frequency; that is,

$$\theta = -360 f t_d \text{ degrees}$$

which is logical because if the frequency is 1 cycle per second and the time delay is 1 second, the wave would appear to be shifted 360° .

Thus, with the given time delay of 0.01 second, the effective phase shift at 100 cps is

$$\theta = -360 \times 100 \times 0.01$$

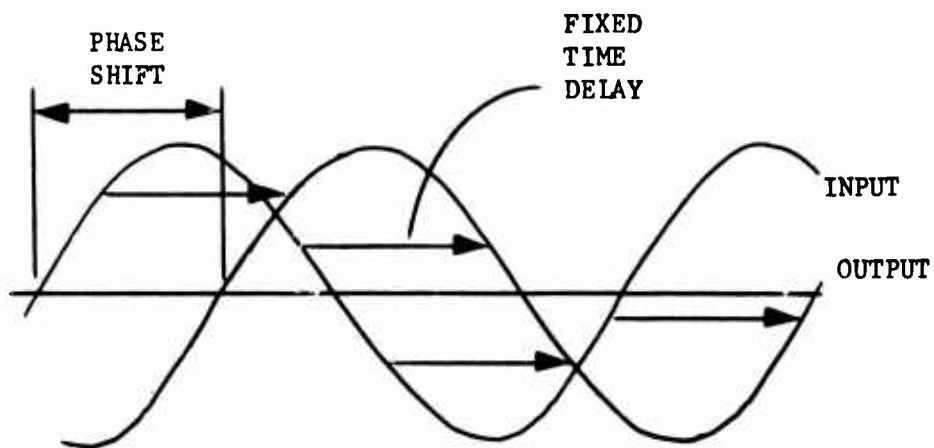
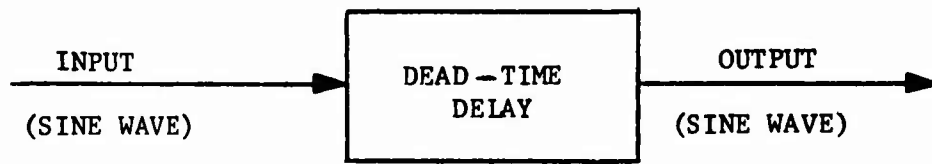
$$\theta = -360^\circ$$

6.5.4 The Total Frequency Response

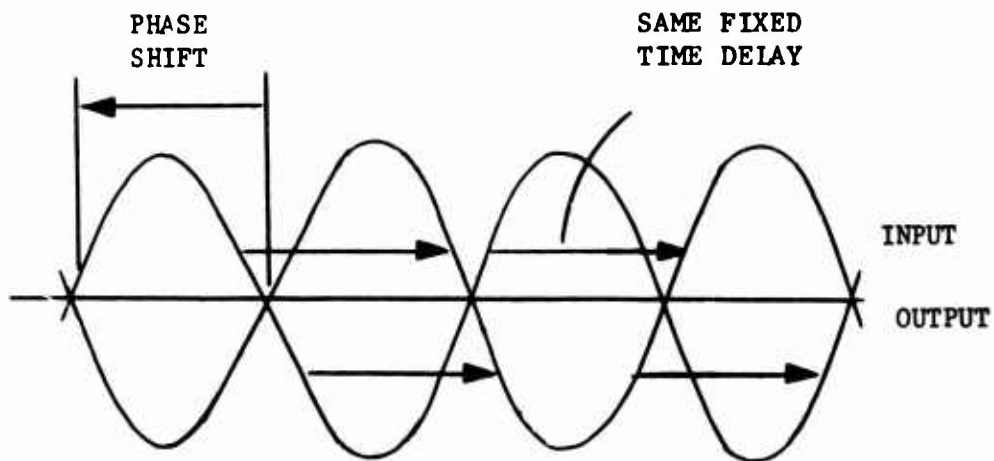
Considering the response to both the linear and the nonlinear portions of the transfer function, the value of the complete transfer function is the direct cascade of the response of each alone. That is,

$$\frac{P_{od}}{\omega} = -42\text{db} \angle -163^\circ \angle -360^\circ$$

$$\frac{P_{od}}{\omega} = -42\text{db} \angle -523^\circ \quad \text{at 100 cps}$$



AT LOW FREQUENCY



AT HIGHER FREQUENCIES

FIGURE 61 - EFFECT OF DEAD TIME ON
SINUSOIDAL RESPONSE

Other values of frequency are inserted into the transfer function to calculate the linear response (paragraph 6.5.2) and the nonlinear response (paragraph 6.5.3), which combine (paragraph 6.5.4) to give the total response at each point. The results are plotted as a Bode diagram in Figure 62.

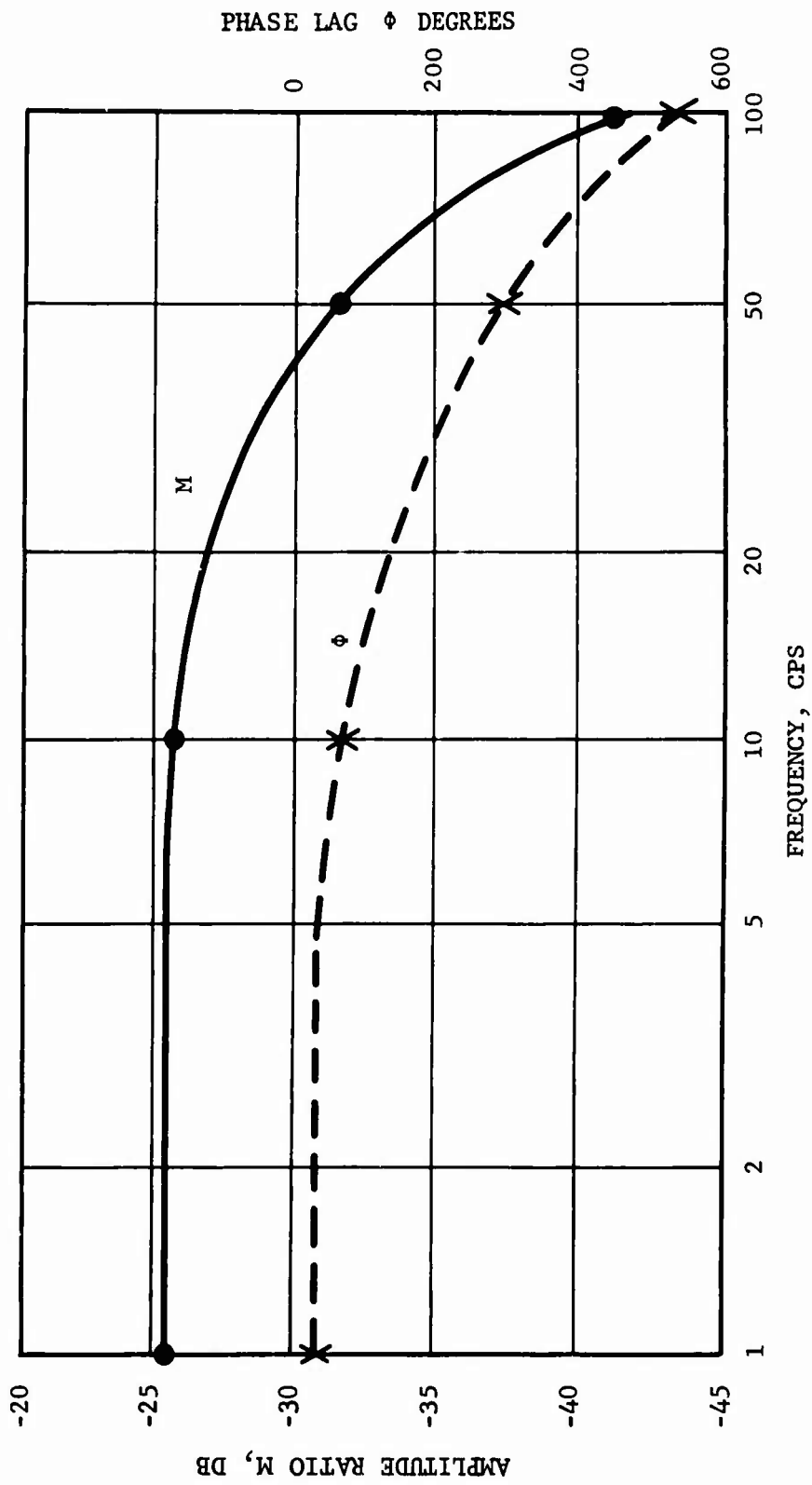


FIGURE 62 - FREQUENCY RESPONSE OF COMBINED RATE SENSOR AND VENTED JET-INTERACTION AMPLIFIER (BODE DIAGRAM)

7.0 DETAILED SYSTEM DESIGN PROCEDURE

Refer to the appropriate paragraph in this manual for information related to each of the items of the following.

7.1 REQUIRED INFORMATION

1. Performance specification for the system
2. Characteristics of available supplies, signal sources, and driven loads
3. Static characteristics on available fluidic and interface system components (input and output)
4. Internal dimensional characteristics of available fluidic and interface system components (effective volumes, lengths, and areas)

7.2 STEP-BY-STEP DESIGN

1. Choose final control element suitable for driving the given load (actuator, indicator).
The choice is a function of the available supply, the required force and velocity levels, and the function to be performed.
2. Determine its input characteristics (pressure, flow, volume, compliance).
This includes the static characteristics, the physical dimensions, and the reflected dynamics of the load.
3. Choose a sensor suitable for detecting the input variable (sensitivity, signal-to-noise ratio).
In some cases the input variable may be given as a part of the system specifications.
4. Determine its output characteristics (static characteristics, effective volumes, lengths, time delay).
When the input variable is specified, the static loading characteristics and the physical dimensions must also be specified.
5. Block out the system between sensor and final control element with appropriate functional components (impedance level, pressure gain, power capacity, speed of response, compensation, computation).
6. Tentatively choose fluidic devices with the potential for satisfying the functional requirements of the system.
Where standard devices are available, they should be used; where standard devices are not available, their characteristics must be defined.

7. Explore the operating bias point matching problem by superimposing the input characteristics of each driven component onto the output characteristics of each driving component. The operating bias point is at the intersection of the zero control parameter curve with the effective load line.
8. Explore the matching of preferred operating ranges using the same superimposed characteristics. Matching operating ranges is in some ways, similar to the operating bias point matching problem, except restrictors can now be connected across the differential circuit without affecting the bias point.
9. Make the operating bias points coincide and the operating ranges compatible by suitable trade-offs and adjustments (supply pressure, bias level, shunt and series resistances).
10. Calculate the transfer curve of the system in steps beginning from the sensor and including required matched gain stages as needed to provide the necessary signal level at the final control element.
11. Investigate and correct for tendencies toward nonlinearity, saturation, and inefficient use of operating ranges.
12. Select the appropriate equivalent electrical circuit for each component of the system.
13. Prepare an equivalent electrical circuit of the entire coupled system.
14. Derive the transfer function of each isolated portion of the system equivalent circuit.
15. Cascade the partial system transfer functions to generate the transfer function of the entire system.
16. Calculate the equivalent circuit performance parameters from static characteristics and pressures and flows at the operating bias points combined with effective dimensions of the components and their interconnections.
17. Substitute the calculated performance parameters in the transfer functions.
18. Calculate the system frequency response.
19. Compare the calculated response with the required performance specification.
20. Investigate individual component transfer functions and make the

changes necessary to correct for deviations from desired performance.

21. Finalize preliminary design and calculate performance.
22. Generate a listing of factors important to achieving design goals (short small lines, symmetry, isolated supplies, adequate vents).

7.3 DESIGN CHECKLIST

A design checklist is given below for the convenience of the system designer who is intimately familiar with the detailed design procedure.

1. Choose Final Control Element.
2. Determine its Input Characteristics.
3. Choose Suitable Sensor (Input).
4. Determine its Output Characteristics.
5. Block Out System.
6. Choose Fluidic Devices.
7. Superimpose Mating Characteristics.
8. Explore Matching Problems.
9. Make Operating Points and Ranges Coincide.
10. Calculate Transfer Curves.
11. Investigate Nonlinearities.
12. Develop Equivalent Circuits of Components.
13. Prepare Equivalent Circuit of System.
14. Derive Transfer Functions of Isolated Networks.
15. Generate Transfer Function of System.
16. Calculate Equivalent Circuit Parameters.
17. Substitute into Transfer Function.
18. Calculate System Response.
19. Compare With Specifications.
20. Make Necessary Changes.
21. Finalize Design.
22. Generate List of Critical Factors.

8.0 ILLUSTRATIVE EXAMPLE OF V/STOL CONTROL SYSTEM DESIGN

8.1 DESCRIPTION OF THE UH-1B YAW DAMPER SYSTEM

To illustrate the procedures described in this manual, we have chosen to design a fluidic system to implement the UH-1B yaw damper. The complete system is shown in Figure 63 in block diagram form.

The fluidic portion of the system is redrawn in Figure 64 with functional specifications noted.

Now to proceed with the design according to the methods given in the manual; we will refer to section 7.0 and follow the sequence outlined there.

8.2 REQUIRED INFORMATION

1. Performance Specifications for the System

- a. Input range = $\pm 25^\circ/\text{sec}$ yaw rate (nominal)
- b. Output range = ± 0.38 inch deflection of servo
- c. Frequency response — characteristics of a highpass network with a time constant of 3.0 seconds and less than 180° phase shift at 10 cps
- d. Linearity + 20%
- e. Threshold $0.10^\circ/\text{sec}$

2. Characteristics of Available Supply Signal Sources and Driven Load

- a. Supply — 10 psi air at standard conditions
- b. Signal source — yaw rate of aircraft $\pm 25^\circ/\text{sec}$ with maximum of $40^\circ/\text{sec}$
- c. Driven load — mechanical linkage requiring ± 0.38 inch of deflection against a force matched by existing servo

3. Static Characteristics of Available Fluidic and Interface Components

- a. Rate sensor — output characteristics shown in Figure 65 (assumed balanced)
- b. Amplifier A —
 - Normalized output characteristics shown in Figure 66 (assumed balanced)
 - Normalized input characteristics shown in Figure 67 (assumed balanced)
 - Power nozzle characteristics shown in Figure 68
- Amplifier B —
 - Normalized output characteristics shown in Figure 69 (assumed balanced)
 - Normalized input characteristics shown in Figure 70 (assumed balanced)

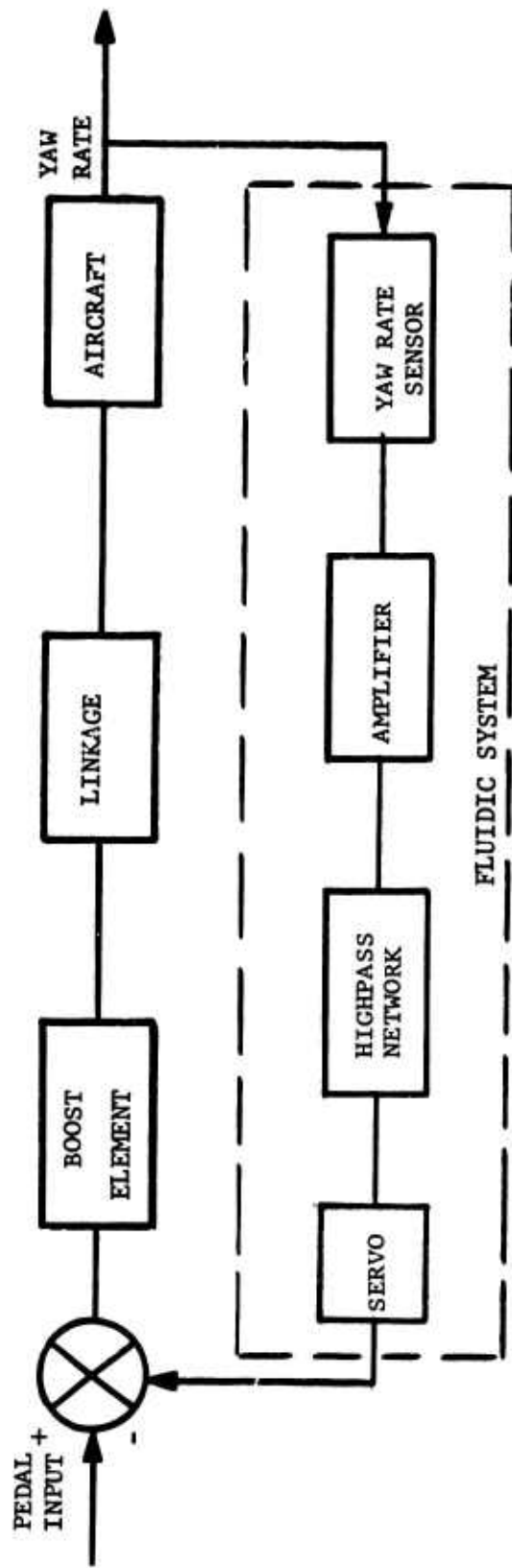
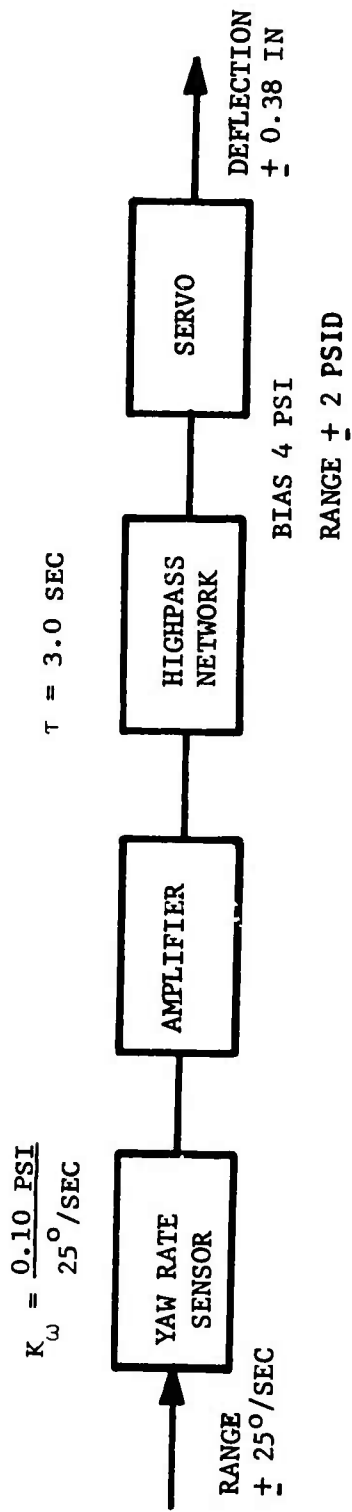


FIGURE 63 - BLOCK DIAGRAM OF UH-1B YAW DAMPER SYSTEM



LINEARITY + 20%

THRESHOLD $0.10^{\circ}/\text{SEC}$

FIGURE 64 - FUNCTIONAL REQUIREMENTS OF FLUIDIC SYSTEM

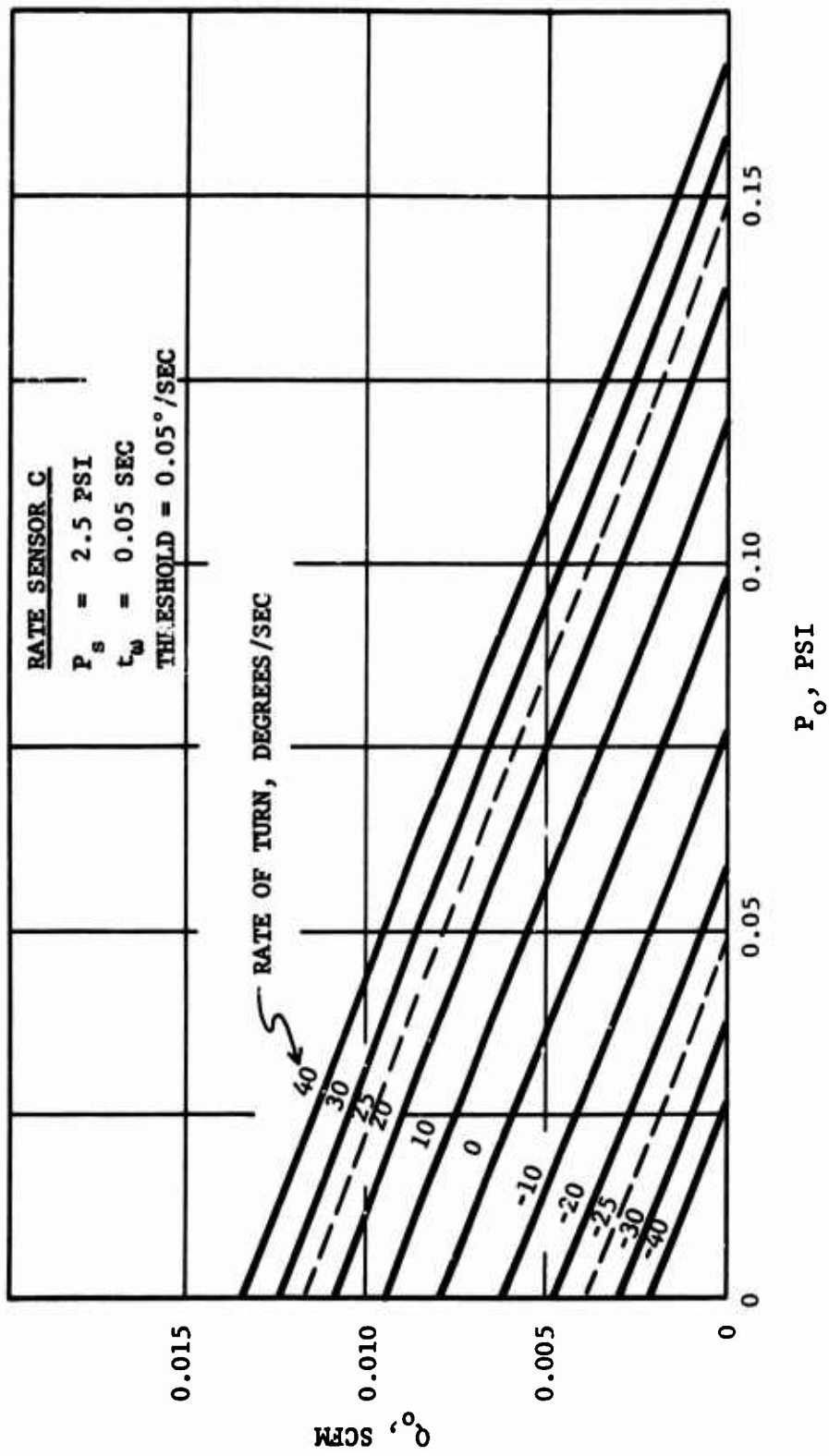


FIGURE 65 - STATIC OUTPUT CHARACTERISTICS OF RATE SENSOR

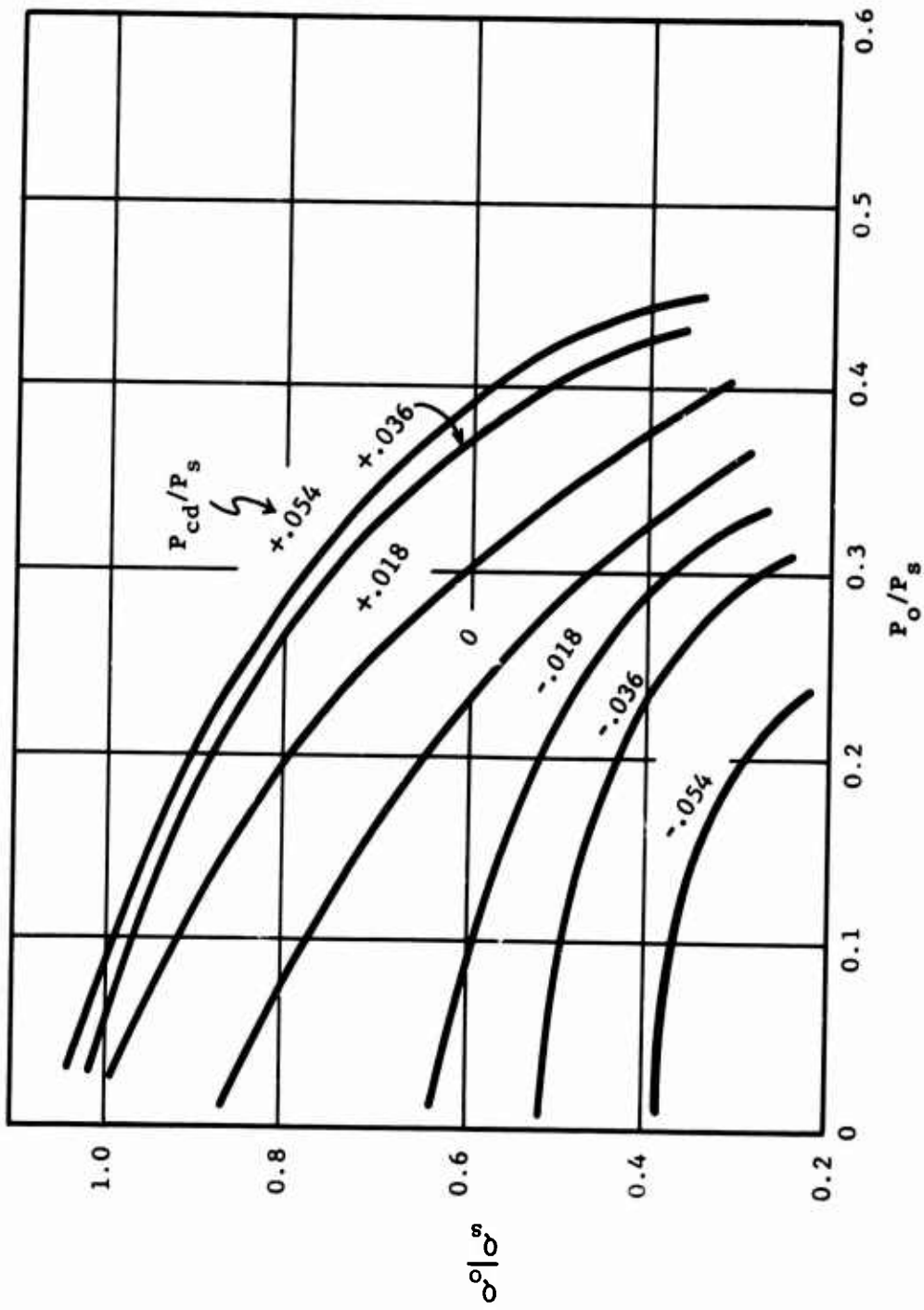


FIGURE 66 - NORMALIZED OUTPUT CHARACTERISTICS OF AMPLIFIER A

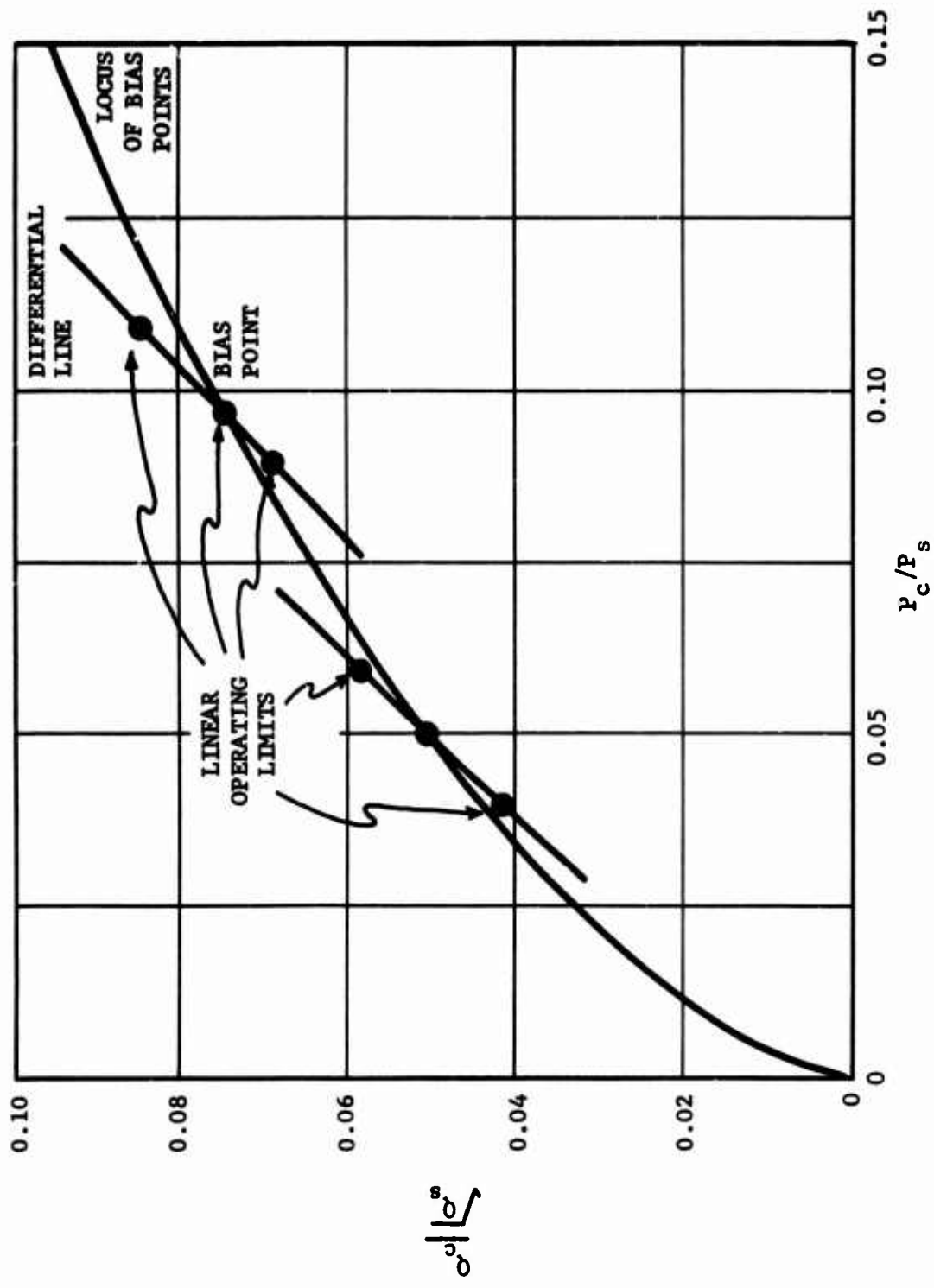


FIGURE 67 - NORMALIZED INPUT CHARACTERISTICS OF AMPLIFIER A

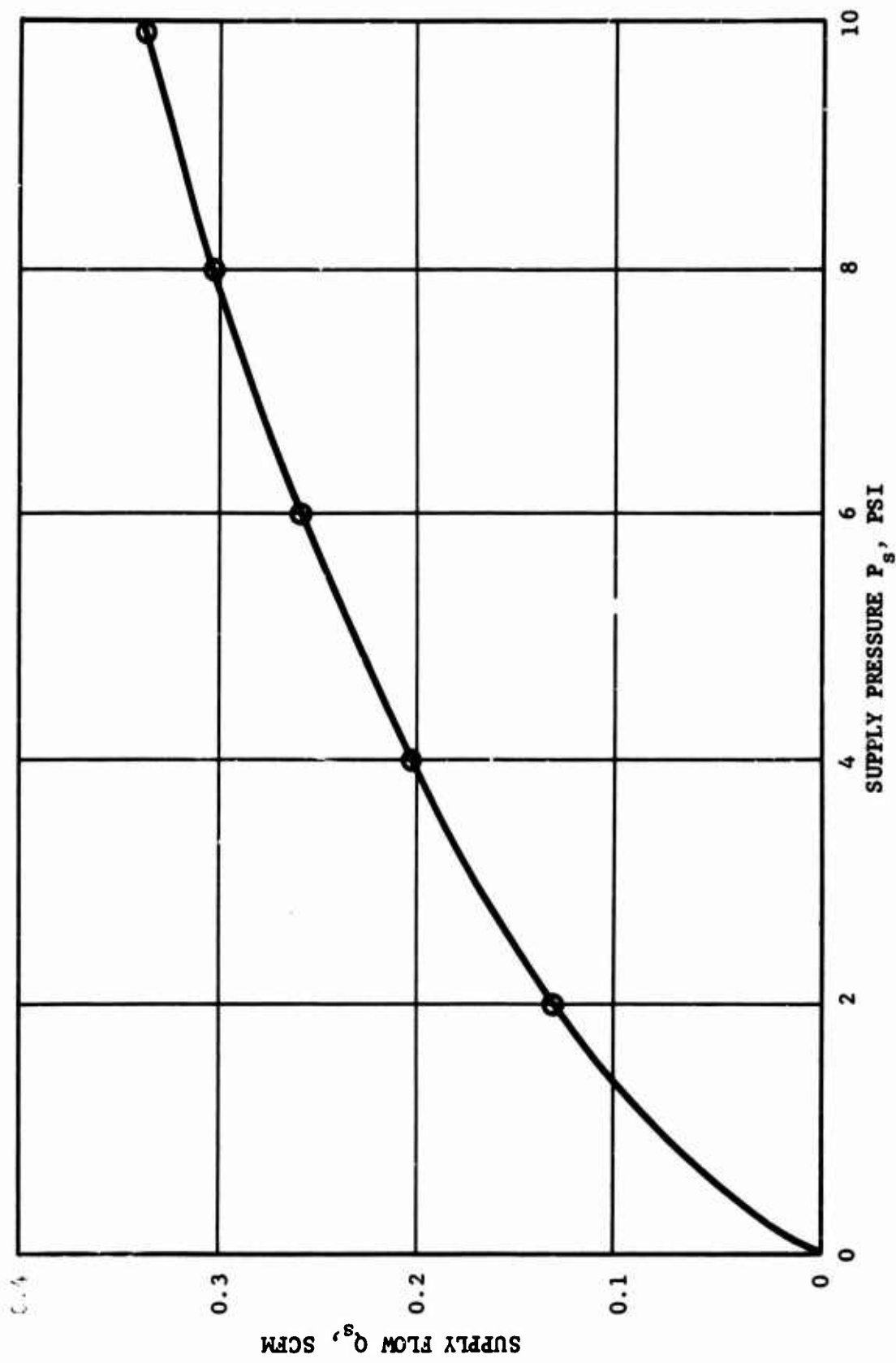


FIGURE 68 - POWER NOZZLE CHARACTERISTICS OF AMPLIFIER A

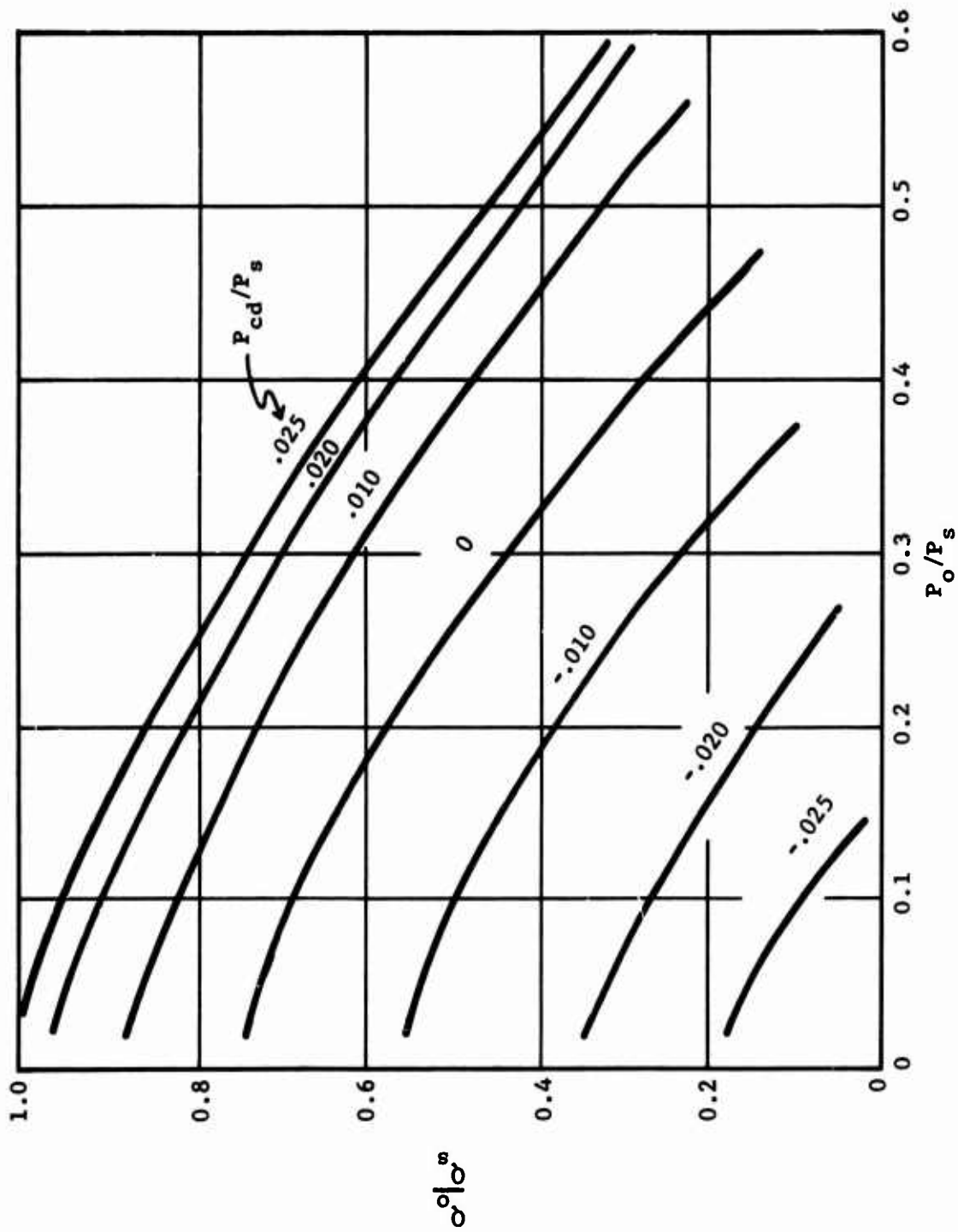


FIGURE 69 - NORMALIZED OUTPUT CHARACTERISTICS OF AMPLIFIER B

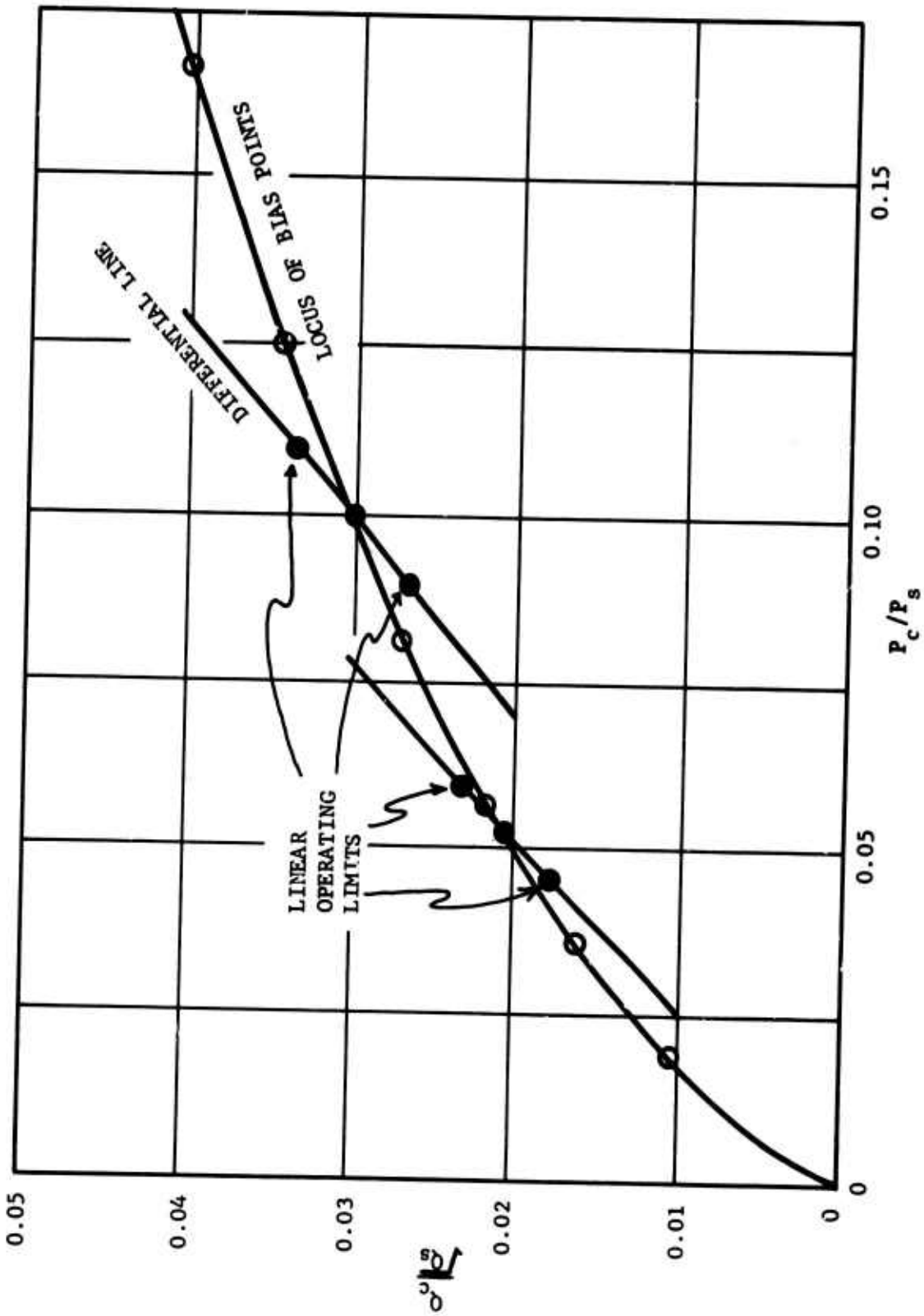


FIGURE 70 - NORMALIZED INPUT CHARACTERISTICS OF AMPLIFIER B

- Power nozzle characteristics shown in Figure 71
- c. Output servo actuator — input characteristics shown in Figure 72 (essentially infinite input resistance)
- d. Laminar-flow restrictors — characteristics shown in Figure 73 typical of all values of linear restrictors available

4. Internal Dimensional Characteristics of Available Fluidic and Interface Components

- a. Rate sensor — time delay is given on the static characteristics, so vortex chamber dimensions are not necessary. Output tubes are 0.060 inch inside diameter and 2 inches long.
- b. Amplifier A —
 - Dimensional sketch is shown in Figure 74.
 - Ferrules connected to input and output passages 0.5 inch long, 0.19 inch inside diameter.
 Amplifier B —
 - Dimensional sketch is shown in Figure 75.
 - Ferrules connected to input and output passages 0.44 inch long, 0.13 inch inside diameter.
- c. Output servo actuator — input volume approximately 0.001 inch³. Ferrules connected to input 0.44 inch long, 0.13 inch inside diameter.
- d. Laminar restrictors — assume negligible delay time, volume, and length.

8.3 STEP-BY-STEP DESIGN

1. Choose final control element — The servo actuator for the fluidic UH-1B yaw damper is fixed by existing system considerations.
2. Determine its input characteristics — As given, the static input characteristics (Figure 72) appear as an infinite resistance (no flow). Reflected load dynamics are negligible.
3. Choose a suitable sensor — The static characteristics of the available rate sensor (Figure 65) show that it has the required sensitivity, linearity, range, and threshold.
4. Determine its output characteristics — The static characteristics are given in Figure 65. The time delay is given as measured by the supplier (50 milliseconds). The output capacitance and inductance can be calculated (paragraphs 2.7.7 and 2.7.8) from the dimensions of the output tubing.
5. Block out the system between sensor and final control element — A preliminary schematic diagram of the fluidic system is shown in Figure 76. Referring to Figure 64, we see that the rate sensor has a maximum (blocked load) differential output of 0.10 psi for an input of 25°/sec. The performance specifications call for a servo output deflection of 0.38 inch for an input yaw rate of 25°/sec,

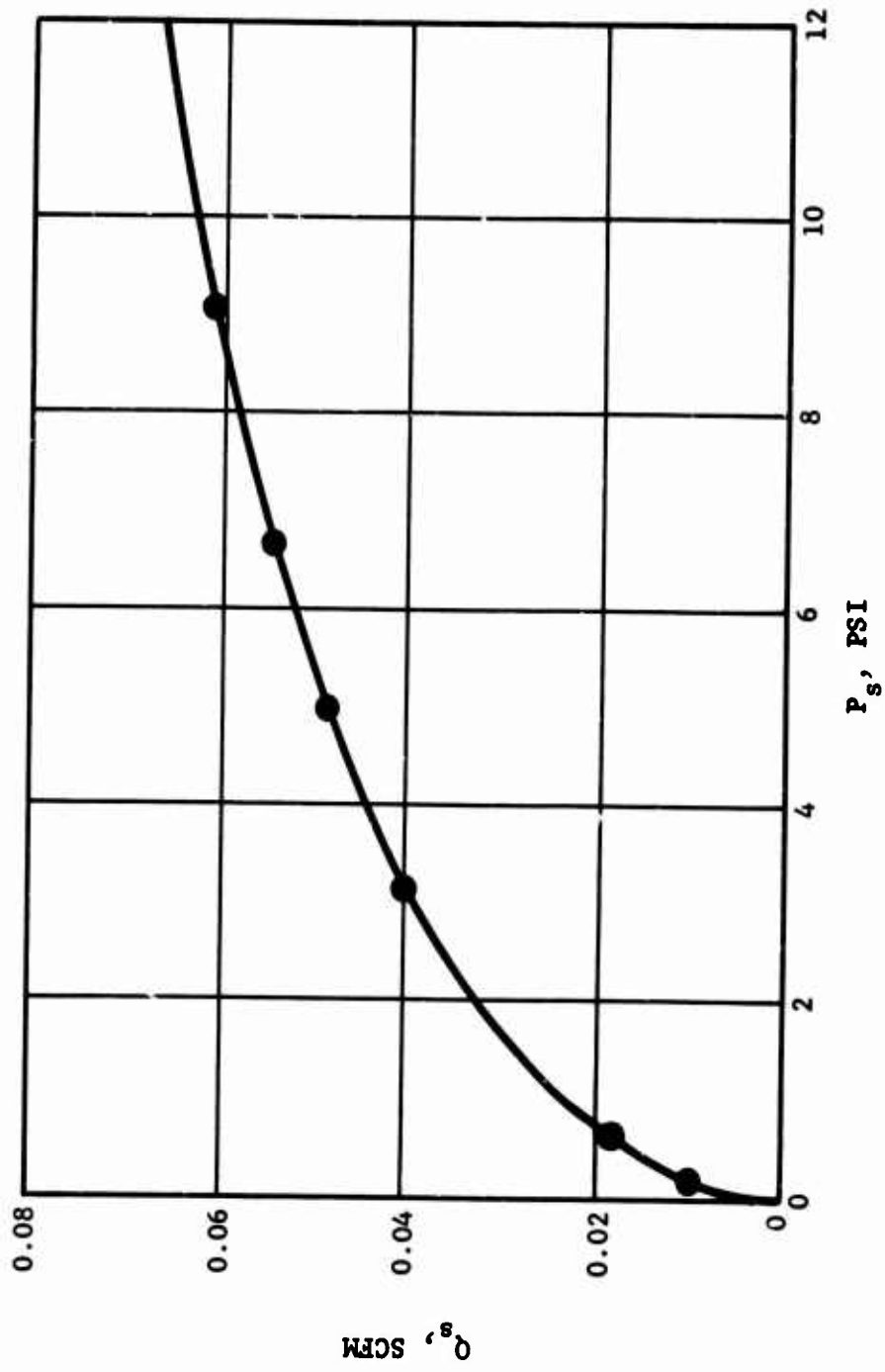


FIGURE 71 - POWER NOZZLE CHARACTERISTICS OF AMPLIFIER B

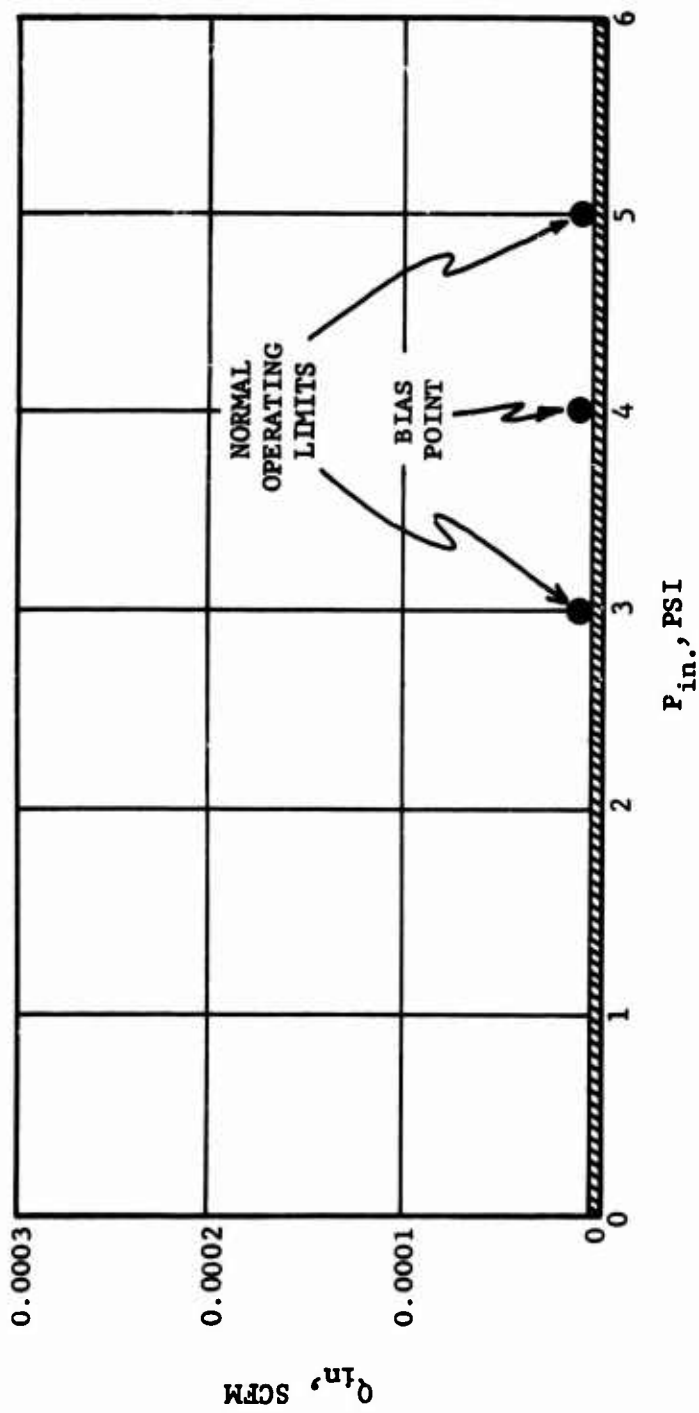


FIGURE 72 - INPUT CHARACTERISTICS OF SERVO ACTUATOR

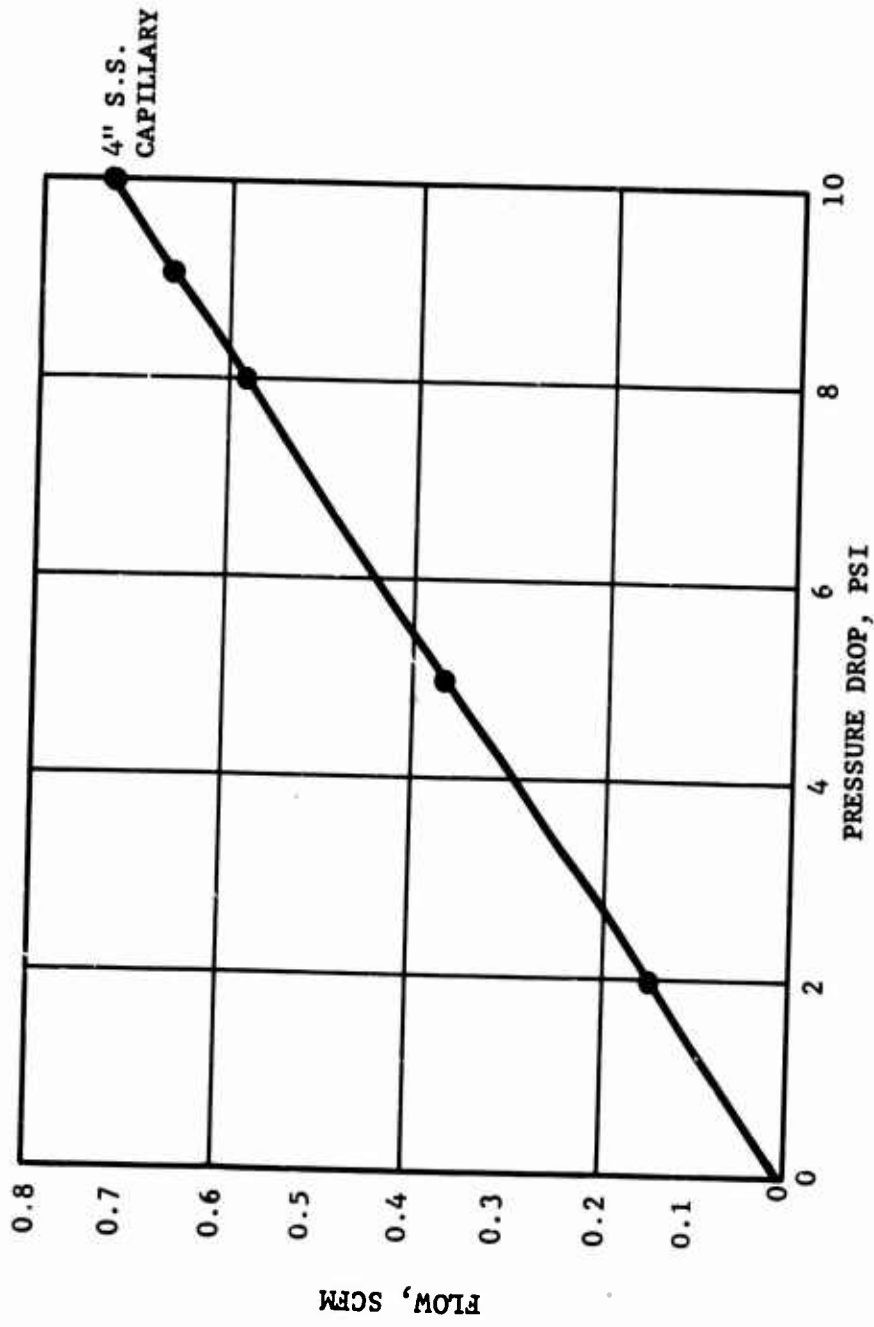


FIGURE 73 - CHARACTERISTICS OF TYPICAL LAMINAR-FLOW RESTRICTOR

SCALE 1" = 1/8"

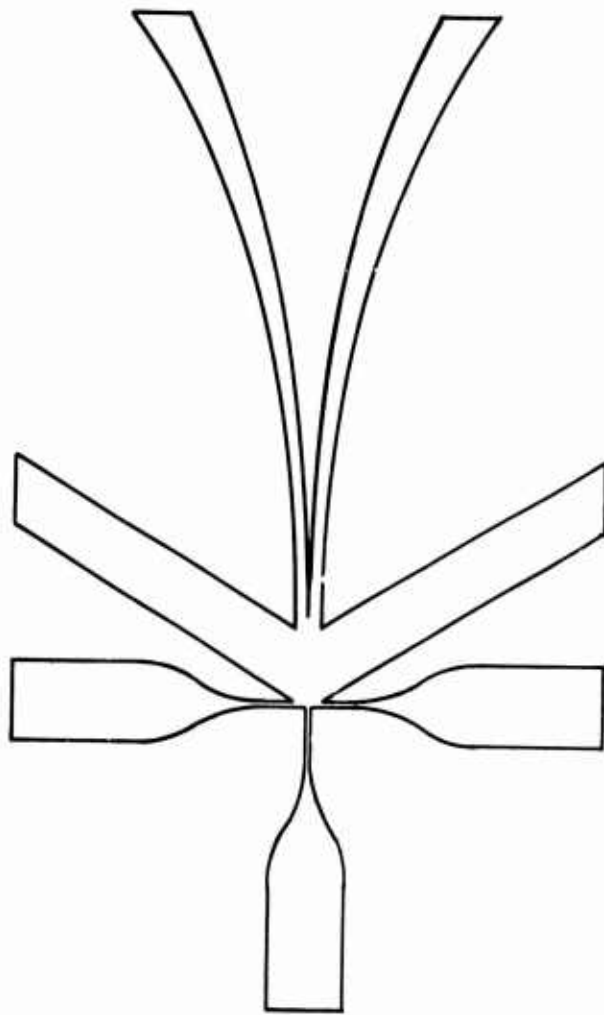


FIGURE 74 - DIMENSIONAL SKETCH OF AMPLIFIER A
(DEPTH OF CHANNELS 0.050)

SCALE 1" = 1/16"

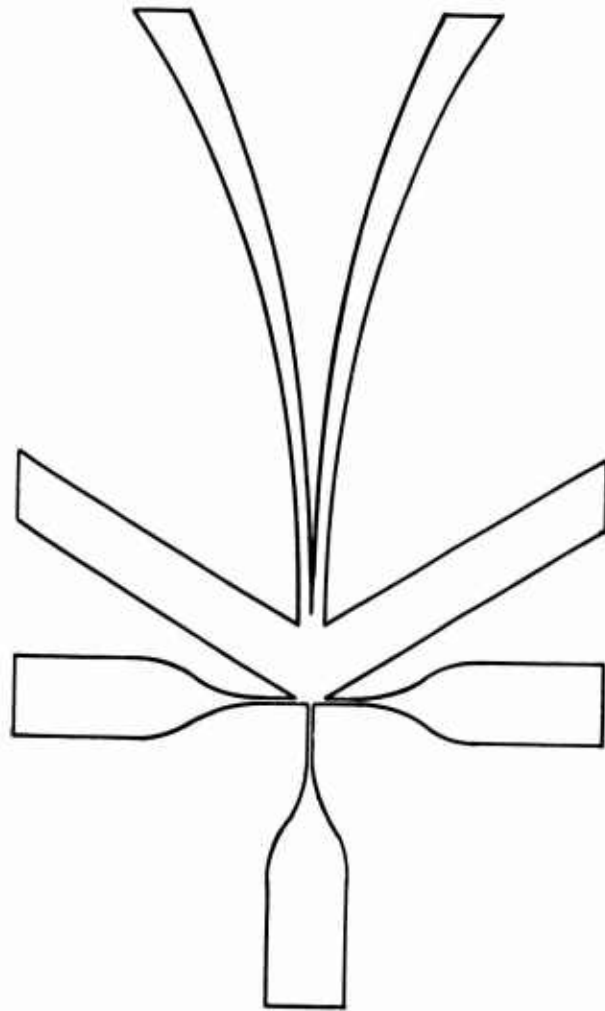


FIGURE 75 - DIMENSIONAL SKETCH OF AMPLIFIER B
(DEPTH OF CHANNELS 0.025)

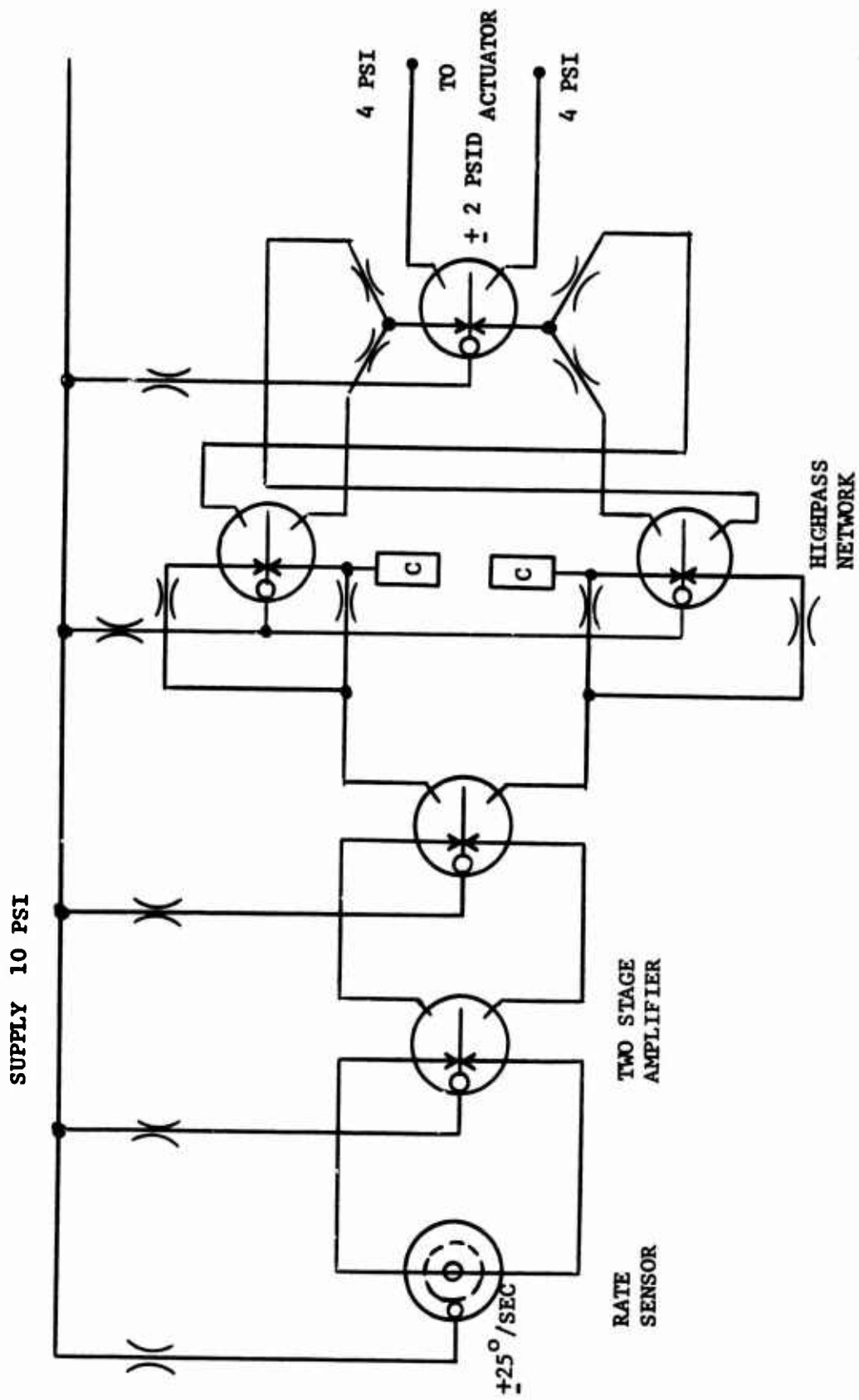


FIGURE 76 - PRELIMINARY SCHEMATIC DIAGRAM OF FLUIDIC YAW DAMPER

which corresponds with a differential pressure at the servo input of 2 psi. In other words, we get 0.1 psi out of the rate sensor and we need 2 psi out of the fluidic amplifiers; therefore, with ideal matching, the minimum amplifier pressure gain must be 20.

6. Tentatively choose fluidic devices — We have tentatively selected two fluidic amplifiers, either of which may satisfy the requirements for pressure gain and matching. These are designated Amplifier A and Amplifier B, and their characteristics are described in paragraph 8.2, item 3b, and paragraph 8.2, item 4b. They are illustrated in Figures 66 through 71.

8.3.1 Rate Sensor and First Stage Amplifier

7. Explore the Operating Bias Point Matching Problem

Examination of the rate sensor output characteristics (Figure 65) for maximum pressure sensitivity reveals that we should operate near 0.10 psi. If we do so, the amplifier connected to it must have a bias pressure of 0.10 psi and require no flow. This is not realistic, so we will compromise for a bias point at 0.07 psi. Assuming a supply pressure of 10 times the input bias pressure (0.7 psi), we can calculate the input flow required by Amplifier A at an input bias pressure of 0.07 psi. That is,

$$\begin{aligned} \text{for } P_s &= 0.7 \text{ psi} \\ Q_s &= 0.60 \text{ scfm (see Figure 68)} \\ \text{and } \sqrt{Q_s} &= 0.245 \\ \text{when } P_c/P_s &= 0.10 \\ Q_c/\sqrt{Q_s} &= 0.077 \text{ (see Figure 67)} \\ \text{then } Q_c &= 0.077 \times 0.245 \\ Q_c &= 0.0189 \text{ scfm} \end{aligned}$$

Superimposing this point ($P_c = 0.07$ psi, $Q_c = 0.0189$ scfm) on the rate sensor characteristics (see Figure 77) shows that the input flow required cannot be supplied by the rate sensor, and that the impedance match (relative slopes) is poor.

Drawing a rough square-law curve between the origin and the point just calculated ($P_c = 0.07$ psi, $Q_c = 0.018$ scfm) shows that the amplifier input bias will probably match the rate sensor output bias (zero signal line) around 0.01 psi. Again assuming that the amplifier would have a supply pressure 10 times the input bias,

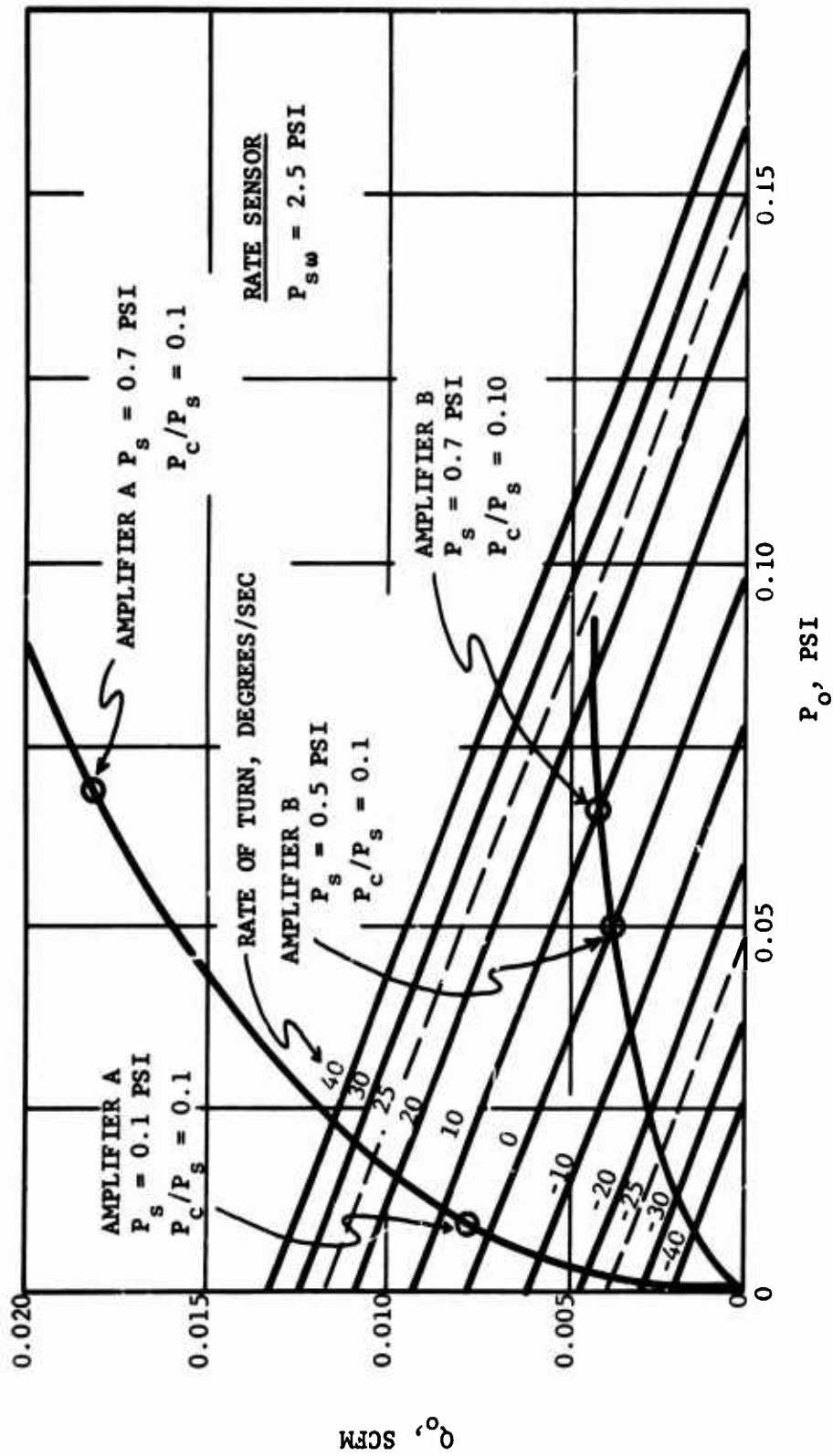


FIGURE 77 - RATE SENSOR OUTPUT CHARACTERISTICS WITH FIRST STAGE INPUT BIAS CHARACTERISTICS SUPERIMPOSED

$$\begin{aligned}
P_s &= 0.1 \text{ psi} \\
\text{then } Q_s &\approx 0.01 \text{ scfm (see Figure 68)} \\
\sqrt{Q_s} &= 0.1 \\
\text{when } P_c/P_s &= 0.10 \\
Q_c/\sqrt{Q_s} &= 0.077 \text{ (see Figure 67)} \\
\text{then } Q_c &= 0.077 \times 0.1 \\
Q_c &= 0.0077 \text{ scfm}
\end{aligned}$$

Plotting this point ($P_c = 0.01$ psi, $Q_c = 0.0077$ scfm) on the rate sensor characteristics (Figure 77) shows that Amplifier A could be matched to the rate sensor using an amplifier supply pressure of 0.01 psi. However, with an amplifier supply pressure of 0.01 psi it would be impossible to get more than about 0.005 psi out of it. Therefore, we would be throwing away too much pressure sensitivity.

9. Make the Operating Bias Points Coincide

To rectify this situation, we will choose Amplifier B, which has smaller control nozzles and therefore higher input resistance (less input flow).

Assuming a bias point of 0.07 psi, the supply will be 0.7 psi

$$\begin{aligned}
\text{for } P_s &= 0.7 \text{ psi} \\
\text{then } Q_s &= 0.019 \text{ scfm (see Figure 71)} \\
\sqrt{Q_s} &= 0.138 \\
\text{when } P_c/P_s &= 0.10 \\
Q_c/\sqrt{Q_s} &= 0.030 \text{ (see Figure 70)} \\
\text{then } Q_c &= 0.030 \times 0.138 \\
Q_c &= 0.0042 \text{ scfm}
\end{aligned}$$

Plotting this point ($P_c = 0.07$ psi, $Q_c = 0.0042$ scfm) on the rate sensor output characteristics (Figure 77) shows that the amplifier bias is too high. Drawing a rough square-law curve from the origin through this point will help to "zero-in" on the correct match. It appears at approximately 0.05 psi, where the amplifier input locus of bias points crosses the zero signal output line of the rate sensor. At this point

$$P_s = 0.5 \text{ psi (10 times input bias)}$$

then $Q_s = 0.016$ scfm (see Figure 71)

$$\sqrt{Q_s} = 0.127$$

when $P_c/P_s = 0.10$

$$Q_c/\sqrt{Q_s} = 0.030 \text{ (see Figure 70)}$$

then $Q_c = 0.030 \times 0.127$

$$Q_c = 0.0039 \text{ scfm}$$

Plotting this point ($P_c = 0.05$ psi, $Q_c = 0.0039$ scfm) on the rate sensor output characteristics (Figure 77) shows that the operating bias points of the rate sensor and amplifier are now properly matched.

8. Explore the Matching of Preferred Operating Ranges

Figure 78 is a replot of the rate sensor output characteristics with the input characteristics superimposed, including the differential input curve with preferred operating limits. Note that to stay within a reasonably linear range of operation of Amplifier B, the input swing must be limited to $\pm 1\% P_s$ ($\pm 2\% P_s$ control differential P_{cd}). However, as illustrated in Figure 78, the rate sensor, operating between the $\pm 25^\circ/\text{sec}$ lines, would produce a much larger change in amplifier control pressure than $\pm 1\% P_s$. Therefore, the circuit must be altered to prevent this.

9. Make the Operating Ranges Coincide

Effectively, what we require here is to apply some circuit element to reduce the output swing of the rate sensor without affecting the operating bias point. The method for doing this is by means of a restrictor connected between the differential circuit lines (line-to-line). When there is zero input to the rate sensor, both output lines are biased at the same pressure (0.05 psi). Therefore, there is no flow through the restrictor connected between the output lines, and the circuit behaves as if it were not connected. When there is a signal out of the rate sensor, the output lines are unbalanced and there is flow through the restrictor. In this case it appears as a heavier load on the rate sensor, requiring more output flow for the same increase in output pressure. Graphically (as shown in Figure 78), the effect is to rotate the differential load line around the operating bias point.

Now if we want to prevent the pressure swing from exceeding 0.005 psi ($\pm 1\% P_s$) when the rate sensor is driven between the extremes of $\pm 25^\circ/\text{sec}$, it is a simple geometrical exercise to find the line that will pass through the allowable extremes and the operating bias point. The value of the fluid resistance which must be connected across the differential circuit can be calculated from the change in slope from the original differential input line (amplifier input nozzle only) to the final line which fits within the required limits.

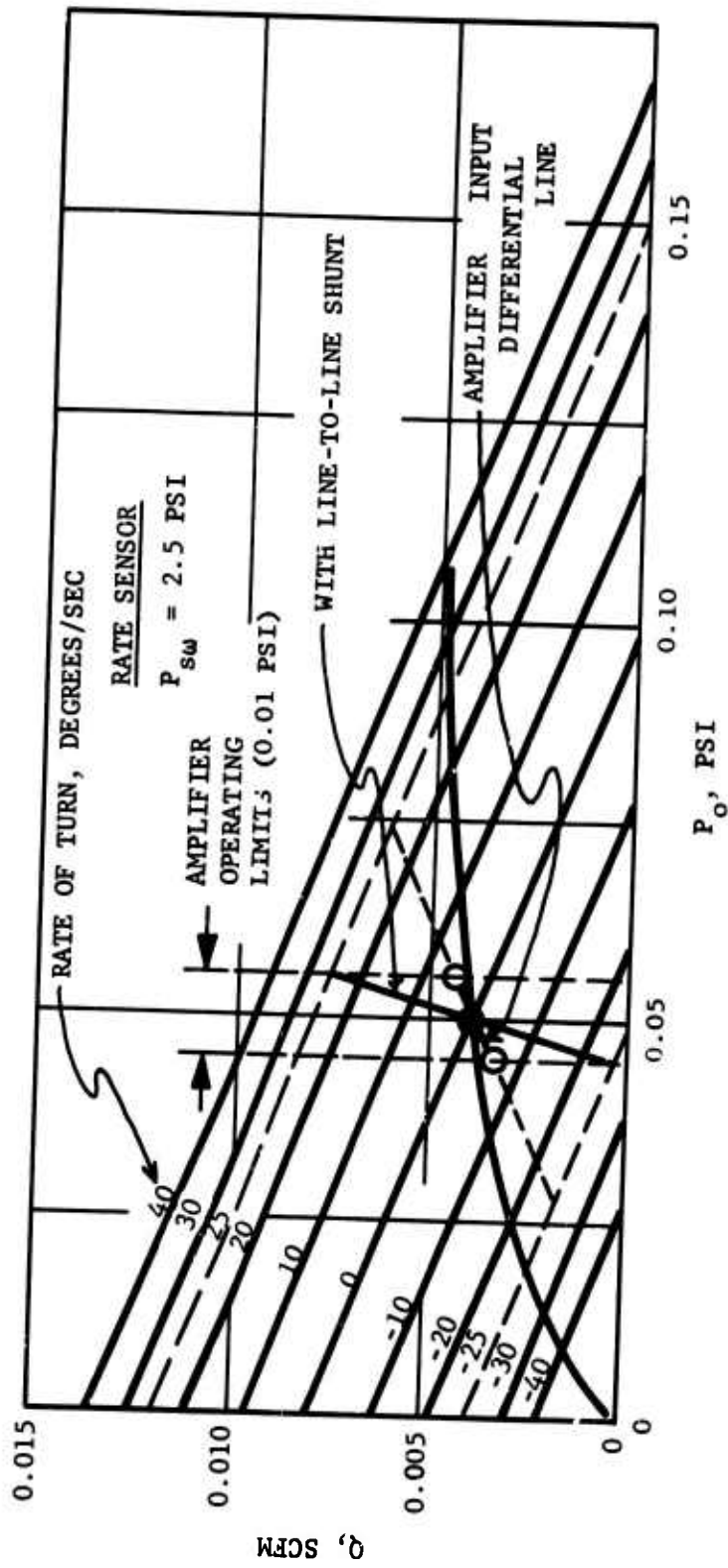


FIGURE 78 - RATE SENSOR OUTPUT CHARACTERISTICS WITH FIRST STAGE INPUT DIFFERENTIAL CHARACTERISTICS SUPERIMPOSED

In summary of the matching problem between the rate sensor and the first stage of amplification, we first explored the matching of operating bias points and found that Amplifier B could be properly matched by using a supply pressure of 0.5 psi. Second, we explored the matching of operating ranges and found that Amplifier B could be properly matched by adding a shunt restrictor between the rate sensor output lines. The value of the resistance required is approximately 0.4 times the value of the input nozzle resistance of Amplifier B (draws 2.5 times the flow of the nozzle for the same pressure).

8.3.2. First and Second Stage Amplifiers

7. Explore the Operating Bias Point Matching Problem

Figure 79 shows the output characteristics of the first stage amplifier. Again, a bias point pressure is assumed, the second stage supply pressure is made 10 times higher, and a corresponding control bias flow is calculated. If the resulting point does not fall on or near the zero signal line for the first stage output, a more realistic bias point pressure is assumed and the process is repeated. Thus we find a second stage amplifier supply pressure which will make it match with the first stage at the point where the second stage input bias is at 10% of the second stage supply pressure. This is illustrated in Figure 79 for a second stage supply pressure of 1.75 psi.

8. Explore the Matching of Preferred Operating Ranges

If we limit the allowable input signal swing of the second stage to $\pm 0.01 F_3$ (± 0.0175 psi), the first stage will overdrive the second stage (see Figure 79). Therefore, it is necessary to reduce the first stage output swing by loading it with a restrictor connected across the differential circuit (line-to-line). Using a linear restrictor, the resulting load will be a line passing through the operating bias point and the intersections of the allowable extremes of first stage output and second stage input. The result is a differential load line, as shown in Figure 79.

Note two important points: First, the extremes of output pressure are not equal with respect to the operating bias point, because the output characteristic curves are not evenly spaced. Second and most important, the situation illustrated is not a practical one because the lower end of the resulting load line passes through the unstable region of the output characteristics. Therefore, we must find a new operating bias point at a higher flow so that the amplifier will not have to operate in the unstable region.

9. Make the Operating Points Coincide and the Operating Ranges Compatible

By inspection of Figure 79, it is clear that we must place the operating bias point at a higher flow level. This means that the slope of the locus of bias points must be raised; in other words, the resistance connected at the output of the first stage must be decreased. The obvious way to do this is by connecting a shunt restrictor to return (atmosphere). With a

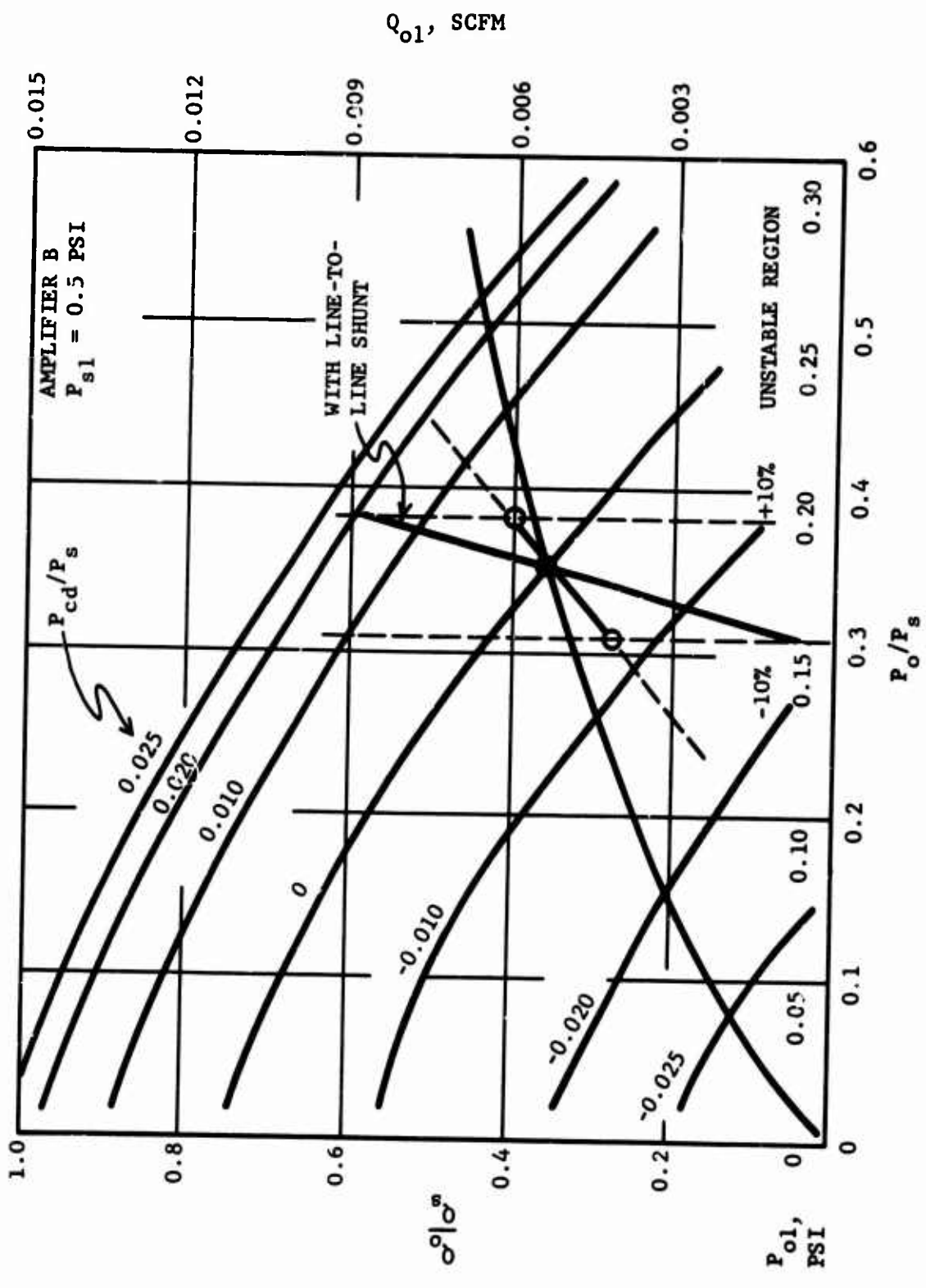


FIGURE 79 - FIRST STAGE AMPLIFIER OUTPUT CHARACTERISTICS WITH SECOND STAGE INPUT CHARACTERISTICS SUPERIMPOSED

linear restrictor, the effect is to add a flow directly proportional to the pressure to the locus of bias points.

With reference to Figure 80, we can estimate that if the output bias were about 0.14 psi, there would be room to get the differential load line in without running into the unstable operating region of the first stage amplifier. Then the second stage amplifier bias would be

$$\begin{aligned}
 P_c &= 0.14 \text{ psi} \\
 \text{Then, if } P_s &= 10 P_c \\
 P_s &= 1.4 \text{ psi} \\
 Q_s &= 0.027 \text{ scfm (see Figure 71)} \\
 \sqrt{Q_s} &= 0.164 \\
 \text{when } P_c/P_s &= 0.1 \\
 Q_c/\sqrt{Q_s} &= 0.03 \text{ (see Figure 70)} \\
 \text{then } Q_c &= 0.03 \times 0.164 \\
 Q_c &= 0.0049 \text{ scfm}
 \end{aligned}$$

Again, with reference to Figure 80, we must add approximately 0.0021 scfm to the flow out of the amplifier at 0.14 psi with the shunt restrictor to return. This places the operating bias point at $P = 0.14$ psi, and $Q = 0.007$ scfm. Now the differential control line with limits can be superimposed to show again that the first stage amplifier will overdrive the second stage amplifier. Then the differential control line must be rotated around the operating bias point by connecting a shunt restrictor line-to-line at the output of the first stage amplifier. The value of this restrictor is approximately 0.2 times the parallel resistance of control nozzle and shunt restrictor to return.

At this point we should stop to check if two stages of amplification will be enough to provide the proper overall gain. The rate sensor sensitivity loaded with the first stage amplifier is (see Figure 78)

$$G_\omega = \frac{P_{od\omega}}{\omega} = \frac{0.010 \text{ psid}}{25^\circ/\text{sec}}$$

The pressure gain of the first stage is

$$G_{p1} = \frac{P_{od1}}{P_{od\omega}} = \frac{0.028}{0.010} = 2.8$$

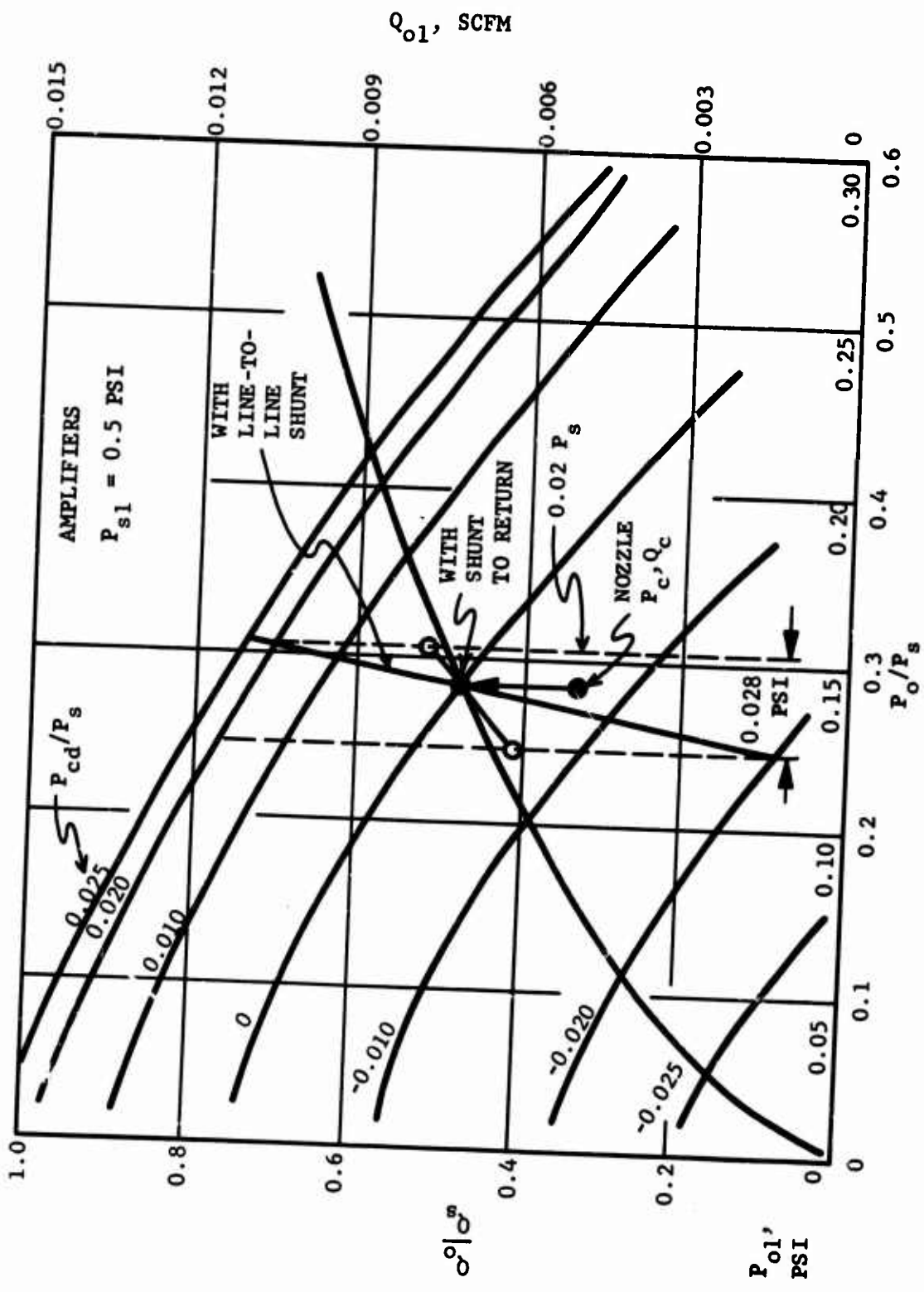


FIGURE 80 - MATCHING THE FIRST STAGE AMPLIFIER WITH THE SECOND STAGE AMPLIFIER

If we assume that the second stage will have the same gain as the first stage,

$$G_{p2} = 2.8$$

Then

$$\frac{P_{od2}}{\omega} = G_{\omega} \times G_{p1} \times G_{p2}$$

$$\frac{P_{od2}}{\omega} = \frac{0.010 \text{ psid}}{25^{\circ}/\text{sec}} \times 2.8 \times 2.8$$

$$\frac{P_{od2}}{\omega} = \frac{0.078 \text{ psid}}{25^{\circ}/\text{sec}}$$

We need (see Figure 64) 2 psid/25°/sec; therefore, at least one more stage of amplification will be necessary.

8.3.3. Second and Third Stage Amplifiers

Since the procedure for the second and third stage amplifiers is the same as that given in paragraph 8.3.2, the exploratory work (7 and 8) will be omitted here.

9. Make the Operating Points Coincide and the Operating Ranges Compatible

With reference to Figure 81, the matching problem, considered on a normalized basis, is almost identical with the situation encountered in the previous stage. Therefore, we can assume that a shunt restrictor to return will be required and that the bias will be at the same normalized point on the characteristics.

The supply pressure to stage 2 is 1.4 psi. Therefore, the actual output bias pressure will be 0.39 psi. Then for stage 3,

$$P_c = 0.39 \text{ psi}$$

$$\text{if } P_s = 10 P_c$$

$$P_s = 3.9 \text{ psi}$$

$$Q_s = 0.043 \text{ scfm (see Figure 71)}$$

$$\sqrt{Q_s} = 0.206$$

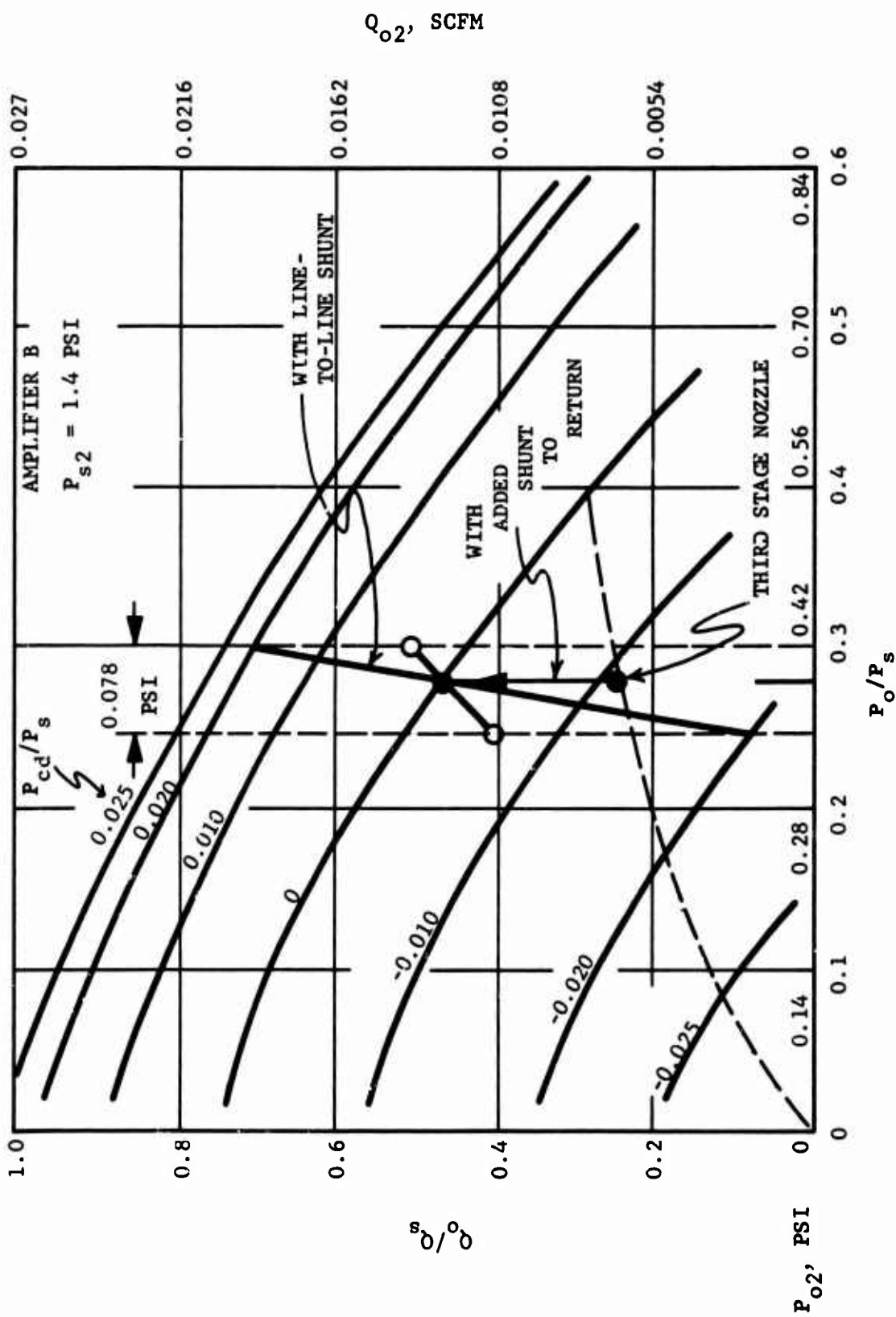


FIGURE 81 - MATCHING THE SECOND STAGE AMPLIFIER WITH THE THIRD STAGE AMPLIFIER

$$\begin{aligned} \text{when } P_c/P_s &= 0.10 \\ Q_c/\sqrt{Q_s} &= 0.03 \text{ (see Figure 70)} \\ \text{then } Q_c &= 0.03 \times 0.206 \\ Q_c &= 0.0062 \end{aligned}$$

To raise the bias flow to the required level of 0.0124 scfm, a restrictor must be shunted from the output of the stage 2 amplifier to return. The value of the restrictor is equal to the resistance of the stage 3 input nozzle at that pressure.

Again, to match the operating ranges it is necessary to connect a shunt restrictor line-to-line at the amplifier output. The value of the restrictor is equal to 0.2 times the resistance of the stage 3 input nozzle differential curve. The gain of the second stage is

$$G_{p2} = \frac{P_{od2}}{P_{od1}} = \frac{0.078 \text{ psi}}{0.028} = 2.8$$

8.3.4. Third and Fourth Stage Amplifiers

With reference to the circuit diagram shown in Figure 76, the third stage must feed two parallel amplifiers in the highpass network. Another feature of this interface is that we prefer to have a restrictor in series with the fourth stage control nozzles. Since the network time constant is a function of the series resistance and an added volume capacitance, the larger we can make this resistance, the smaller will be the volume required.

7. Explore the Operating Bias Point Matching Problem

8. Explore the Matching of Operating Ranges

Referring to Figure 82, the output characteristics of stage 3 are of the same form as stages 2 and 1. Also, we want to maintain the same $\pm 10\%$ P_c signal change around the operating bias point. Therefore, the final matching picture must be similar to Figure 81; that is, the third stage output bias pressure should be about $P_o/P_s = 0.28$ (1.08 psi).

Suppose we want a series resistance of about 1.5 times the stage 4 nozzle resistance at the bias point. This means that only 2/5 of the pressure out of stage 3 appears at the input nozzle of stage 4 ($2/5 \times 1.08 \text{ psi} = 0.43 \text{ psi}$). If we continue the practice of making the supply pressure 10 times the control bias pressure, the supply pressure of stage 4 would then be 4.3 psi. However, to illustrate a different situation (and to get more pressure gain), we will arbitrarily make the supply pressure of stage 4 = 6.0 psi. Then,

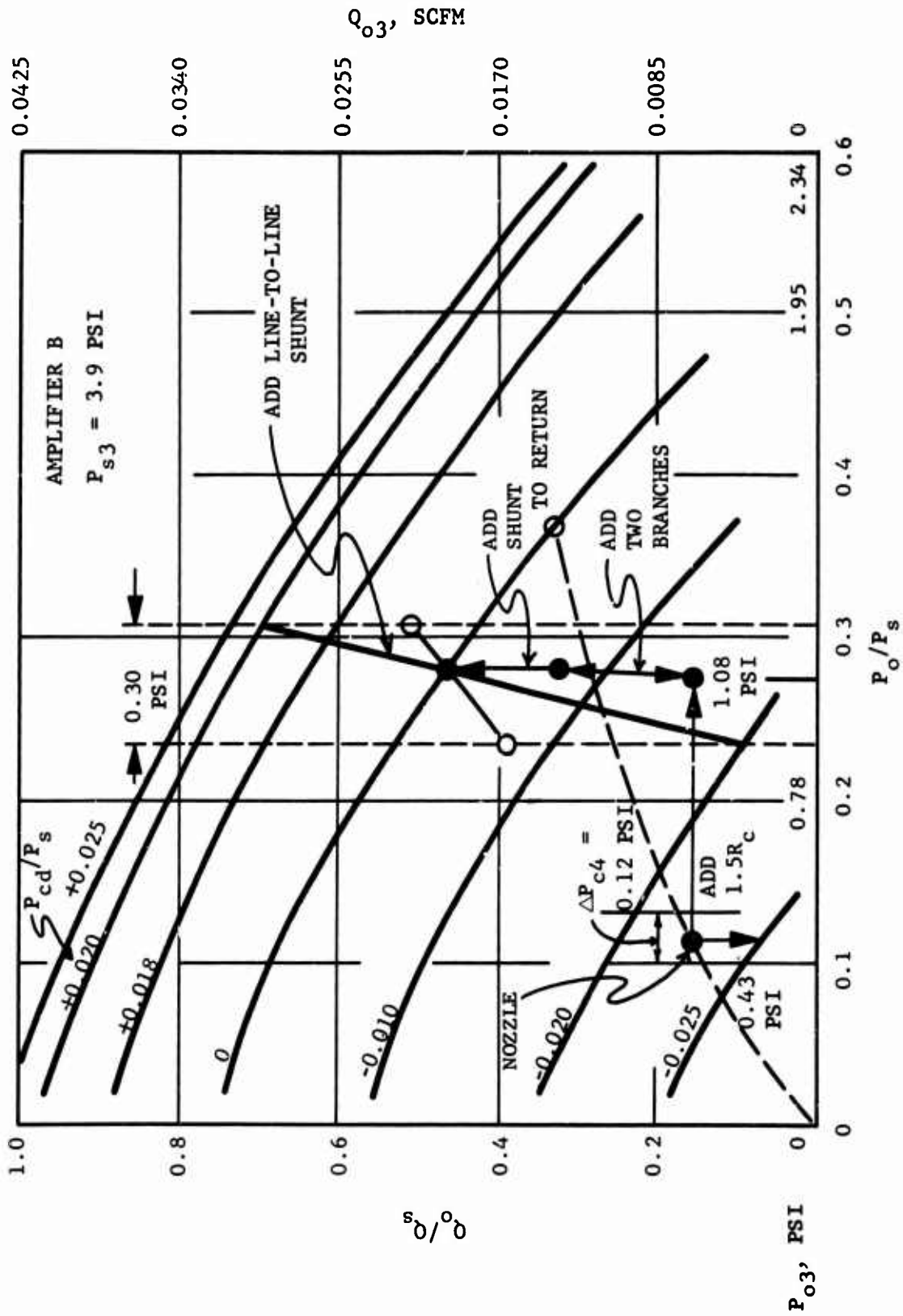


FIGURE 82 - MATCHING THE THIRD STAGE AMPLIFIER WITH PARALLEL FOURTH STAGE AMPLIFIERS

$$\begin{aligned}
 P_s &= 6.0 \text{ psi} & P_c &= 0.43 \text{ psi} \\
 Q_s &= 0.05 \text{ scfm (see Figure 71)} \\
 \sqrt{Q_s} &= 0.223
 \end{aligned}$$

Now $P_c/P_s = 0.43/6.0 = 0.072$

and $Q_c/\sqrt{Q_s} = 0.025$ (see Figure 70)

then $Q_c = 0.025 \times 0.223$

$$Q_c = 0.0056 \text{ scfm}$$

9. Make the Operating Bias Point Coincide and the Operating Ranges Compatible

This point ($P_{c4} = 0.43 \text{ psi}$, $Q_{c4} = 0.0056 \text{ scfm}$) is plotted on Figure 82. When 1.5 times the resistance represented by this point is added in series, the overall pressure is increased 1.5 times for the same flow (as illustrated) to $5/2 \times 0.43 = 1.08 \text{ psi}$. This represents the total resistance seen looking into one branch of the input to one stage 4 amplifier.

As shown in Figure 76, there are two branches to input nozzles of a single stage 4 connected to one output port of the stage 3 amplifier. Therefore, twice the flow calculated for one branch must be supplied by one output, and the point illustrated in Figure 82 is actually at $P_{o3} = 1.08 \text{ psi}$ and $Q_{o3} = 0.0112 \text{ scfm}$. But this is not yet enough flow to satisfy the requirements for the operating bias point ($P_{o3} = 1.08 \text{ psi}$, $Q_{o3} = 0.0198 \text{ scfm}$) we have chosen. Therefore, a shunt restrictor must be connected between each stage 3 output port and the return of a valve which will carry the difference in flow (0.0086 scfm) with a pressure drop of 1.08 psi.

To limit the input swing to stage 4 to $\pm 0.01 P_s$ (0.12 psi), the output from stage 3 must be limited to the same ratio of the bias point, $0.12/0.43 = 0.28$. Then, as shown in Figure 82, the swing must be limited to $0.28 \times 1.08 = 0.30 \text{ psi}$. Again this requires a line-to-line shunt restrictor of a value which will draw an additional flow of 0.0199 scfm at a pressure differential of 0.30 psi.

8.3.5 Fifth Stage Amplifier with Servo Load

Before matching the fourth stage to the fifth stage, we must first define the input requirements of the fifth stage. These are determined by the output required to drive the servo actuator. The process of matching stage 5 to the servo actuator is illustrated in Figure 83.

7. Explore the Operating Bias Point Matching Problem

The servo requires an input bias of 4.0 psi and has an infinite input resistance. By inspection of this situation, as shown in Figure 83, it is

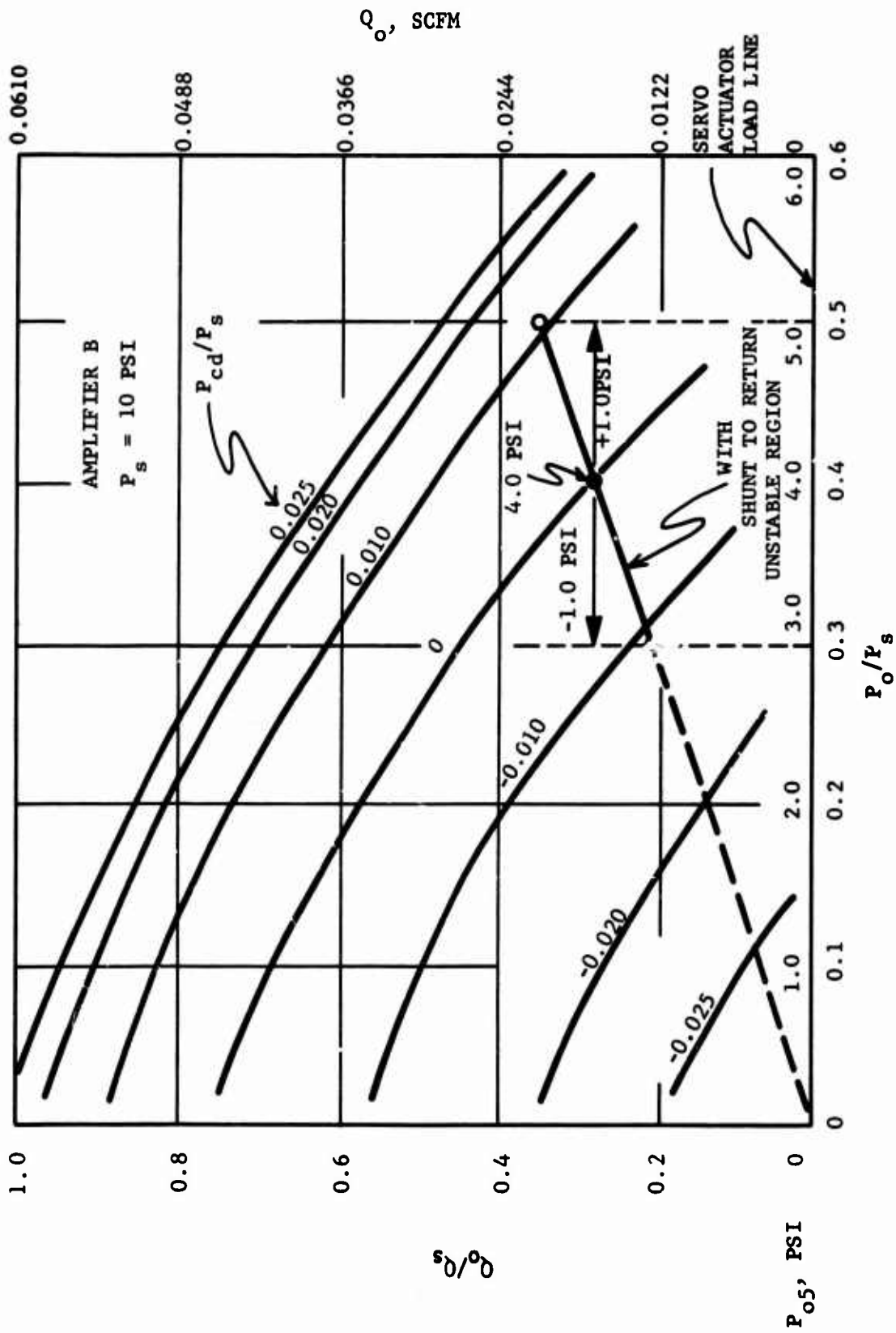


FIGURE 83 - MATCHING THE FIFTH STAGE AMPLIFIER WITH THE SERVO ACTUATOR

clear that some measures must be taken to load the amplifier so that it is not required to operate in the unstable region.

8. Explore the Matching of Preferred Operating Ranges

It is required that the stage 5 amplifier swing from 5.0 psi to 3.0 psi (4.0 ± 1.0 psi). Inspection of Figure 83 makes it clear that, with a high impedance load, the required output swing can be achieved with less than the maximum allowable input swing.

9. Make the Operating Bias Points Coincide and the Operating Ranges Compatible

The first consideration is to get the operating bias point into a stable region of amplifier operation. This can be accomplished (as shown in Figure 83) with a shunt restrictor to return, which raises the slope of the effective load line. A stable point is where the zero signal line crosses the $P_o/P_s = 0.4$ grid line; and since we need an output bias of 4.0 psi, a convenient supply pressure is 10.0 psi. The shunt restrictors to return, connected at each output port, must draw 0.0165 scfm at 4.0 psi.

Drawing a linear load line through the operating bias point shows the range of output swing which can be achieved with a particular input swing. It is clear that the required output swing can be achieved with a control differential pressure of approximately $0.012 P_s$ (0.12 psi). This is well within the linear range of Amplifier B.

8.3.6 Fourth and Fifth Stage Amplifiers

7. Explore the Operating Bias Point Matching Problem

Figure 84 shows the output characteristics of a fourth stage amplifier. To these we must match the input to stage 5, which, because it has a supply pressure of 10 psi, should be between 0.5 psi and 1.0 psi ($5 - 10\% P_s$).

Three other features are important to note; first, two stage 4 amplifiers feed a single stage 5 amplifier; second, we need some series resistance to isolate one fourth stage amplifier from the other and to sum their outputs effectively; and finally, the operating bias point must be raised to a point where the extremes of operation will not be in an unstable region.

8. Explore the Matching of Preferred Operating Ranges

The input of stage 4 is driven ± 0.12 psi (see Figure 82) or to $P_{cd}/P_s = 0.02$. The input to stage 5 cannot be driven more than 0.12 psi. Therefore, with the pressure scale shown in Figure 84, it is clear that a line-to-line shunt restrictor will be required.

9. Make the Operating Bias Points Coincide and the Operating Ranges Compatible

The fifth stage amplifier has the following input bias requirements:

$$\begin{aligned}
 P_s &= 10 \text{ psi} \\
 Q_s &= 0.061 \text{ scfm (see Figure 71)} \\
 \sqrt{Q_s} &= 0.246
 \end{aligned}$$

If we choose

$$\begin{aligned}
 P_c/P_s &= 0.06 \text{ (0.6 psi)} \\
 Q_c/\sqrt{Q_s} &= 0.022 \text{ (see Figure 70)}
 \end{aligned}$$

$$\begin{aligned}
 \text{then } Q_c &= 0.022 \times 0.246 \\
 Q_c &= 0.0054
 \end{aligned}$$

This point ($P_c = 0.6$ psi, $Q_c = 0.0054$ scfm) is shown as point A on Figure 84. Since two stage 4 amplifiers are supplying the stage 5 input requirements, each stage 4 amplifier need only supply half the flow. Therefore, it would see a point represented as point B in Figure 84 which is equivalent to a resistance twice the nozzle resistance of amplifier B ($2R_{c5}$). For isolation, we insert a series restrictor equal to twice the nozzle resistance ($2R_{c5}$), which doubles the pressure required to supply the necessary flow and makes the effective load line on stage 4 pass through point C. This is, of course, in the unstable region, so we must add a shunt restrictor to return, with a value of resistance of about $1/5 R_{c5}$. This matches the operating bias points of stages 4 and 5 (point D).

The operating range at the input of stage 5 must be limited to 0.12 psi. Since twice this pressure is required at the output of stage 4 (because of the series resistance), there it must be limited to 0.24 psi. As shown in Figure 84, the reflected differential control line would not be operated within these limits; therefore, a line-to-line shunt restrictor is required with a resistance of approximately $1/2 R_{c5}$. Then the operating range of stage 4 will be properly matched with the operating range of stage 5.

8.3.7 Complete Fluidic System

The schematic diagram of the complete matched fluidic yaw damper system is shown in Figure 85.

10. Calculate the Transfer Curve of the System

In the process of matching operating ranges, we have automatically generated the proper overall transfer curve. That is, we have deliberately designed the system so that we get a differential pressure to the servo of 2 psid when the rate of turn is $25^\circ/\text{sec}$.

The actual overall transfer curve calculated point-by-point from the curves in Figures 78 through 84 is shown in Figure 86.

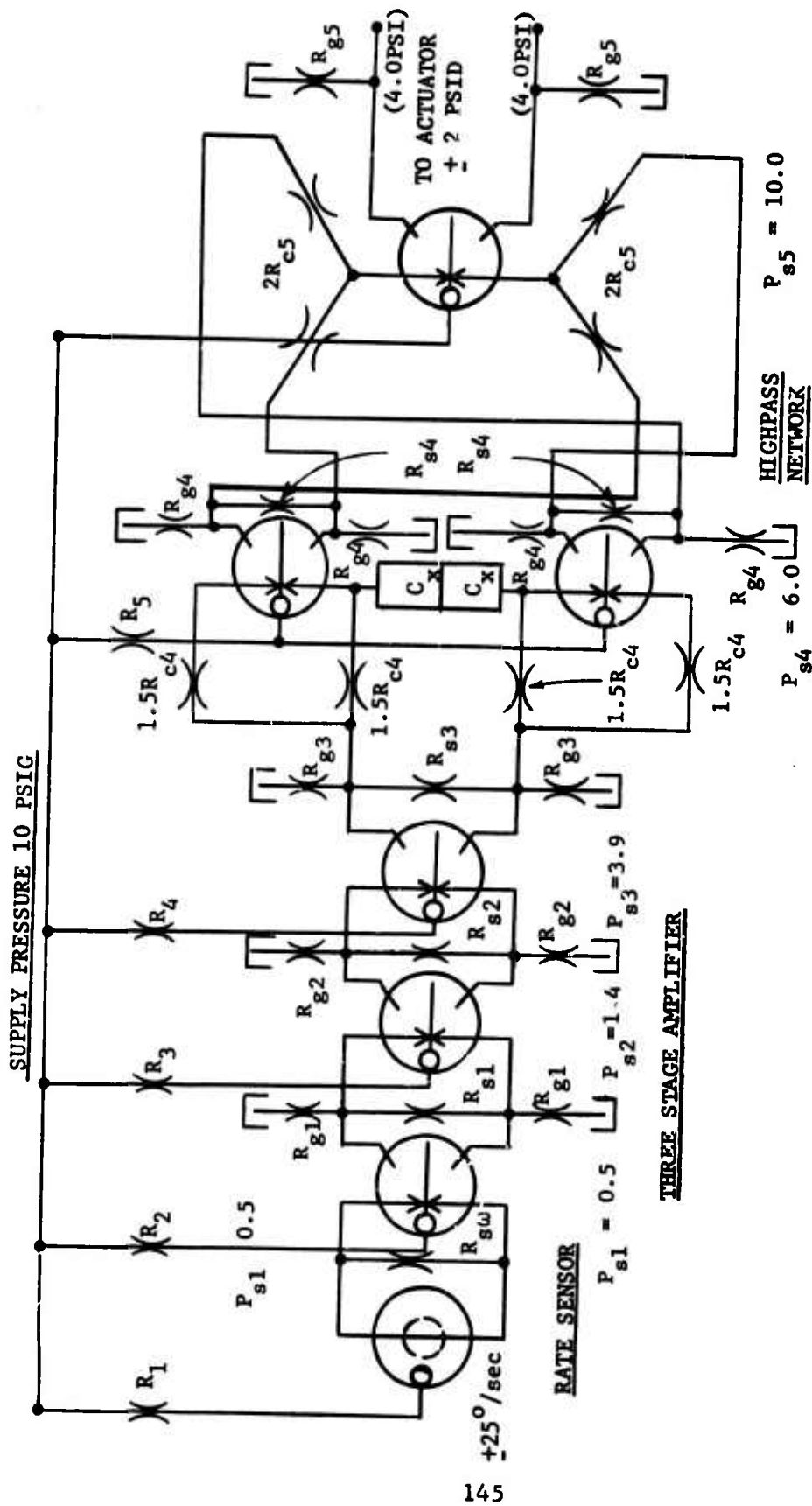


FIGURE 85 - SCHEMATIC DIAGRAM OF COMPLETE MATCHED FLUIDIC YAW DAMPER

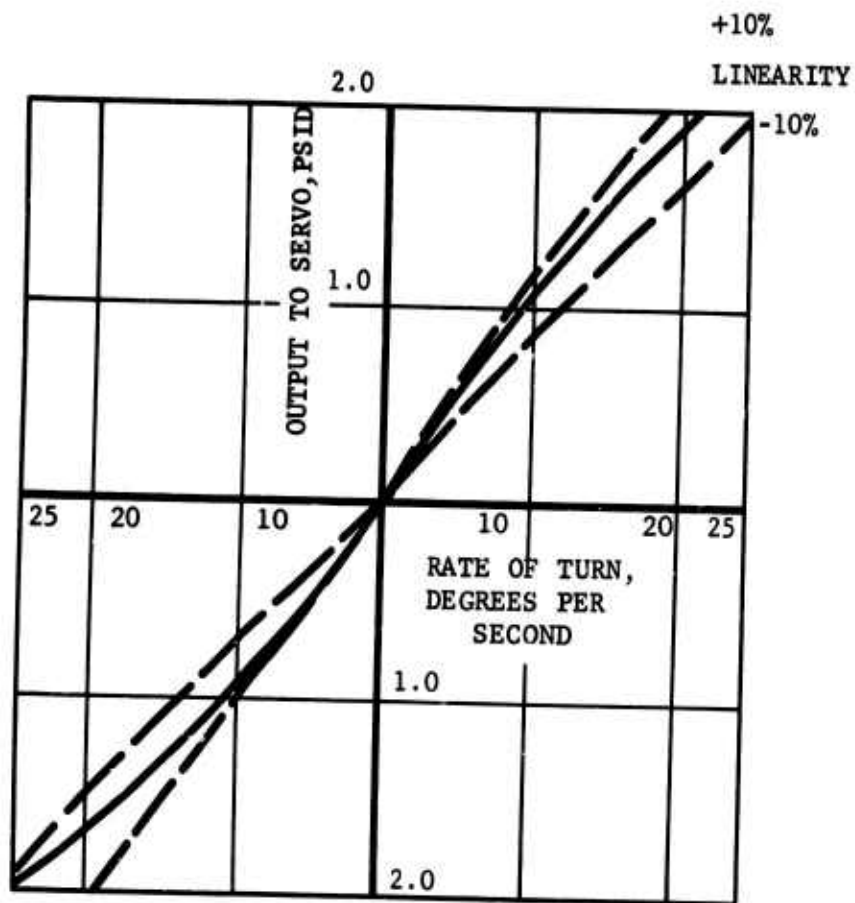


FIGURE 86 - STATIC TRANSFER CURVE OF FLUIDIC YAW
DAMPER WITHOUT HIGHPASS CHARACTERISTIC

11. Investigate Linearity and Inefficient Use of Operating Ranges

With reference to the transfer curve of Figure 86, the requirements for linearity (+ 20%) have been surpassed.

With respect to efficient use of operating ranges, a review of Figures 78 through 84 shows that in every case but one, the maximum allowable operating range has been used. In stage 5 we have limited it to $\pm 0.012 P_s$ rather than $\pm 0.020 P_s$ to avoid overdriving the servo actuator. However, this represents a source of additional linear gain, if it is needed in the final adjustment of performance of the yaw damper system.

12. Select the Appropriate Equivalent Electrical Circuit For Each Component of the System

- a. Rate Sensor —
The equivalent circuit for the rate sensor is identical to that shown in Figure 54, with external resistor added.
- b. Amplifiers —
The equivalent circuit for the amplifier is identical to the circuit for the vented jet-interaction amplifier shown in Figure 51. External resistors and capacitors are added to the appropriate stages.
- c. Actuator —
The equivalent electrical circuit for the actuator is represented simply by a volume capacitance. The input resistance is infinite, and the inductance will be considered negligible.

13. Prepare an Equivalent Electrical Circuit of the Entire Coupled System

The total equivalent circuit, including all matching restrictors and added volume capacitors, is shown in Figure 87. Inductances have been neglected for simplicity; they are later shown to be negligible.

14. Derive the Transfer Function of Each Portion of the Equivalent Circuit

The transfer function of each portion of the circuit between equivalent generators can be developed independently. We will illustrate the process by considering the network between the third stage and the two parallel fourth stages (see Figure 88).

The network can be consolidated as shown in Figure 89. Then by simple circuit analysis,

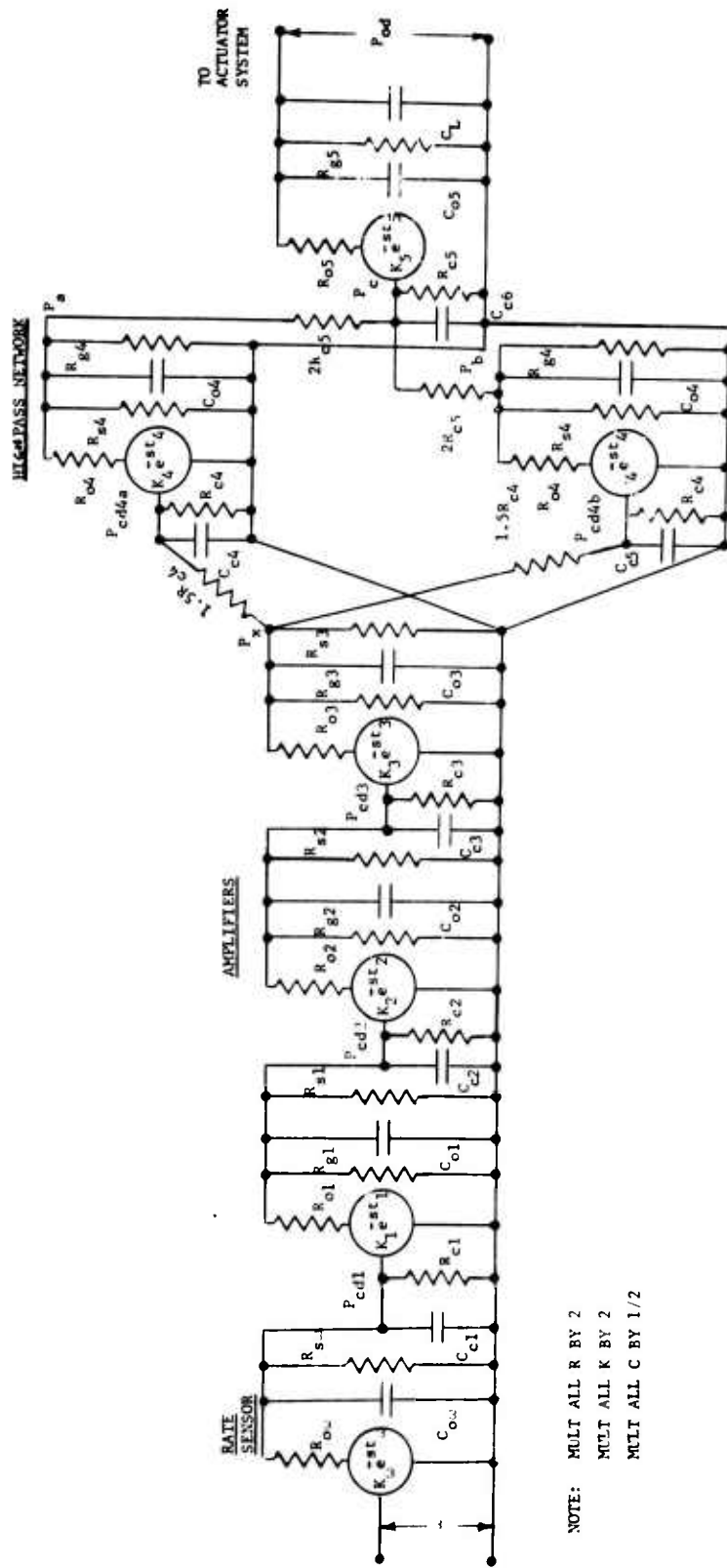


FIGURE 87 - EQUIVALENT ELECTRICAL CIRCUIT FOR THE COMPLETE FLUIDIC YAW DAMPER

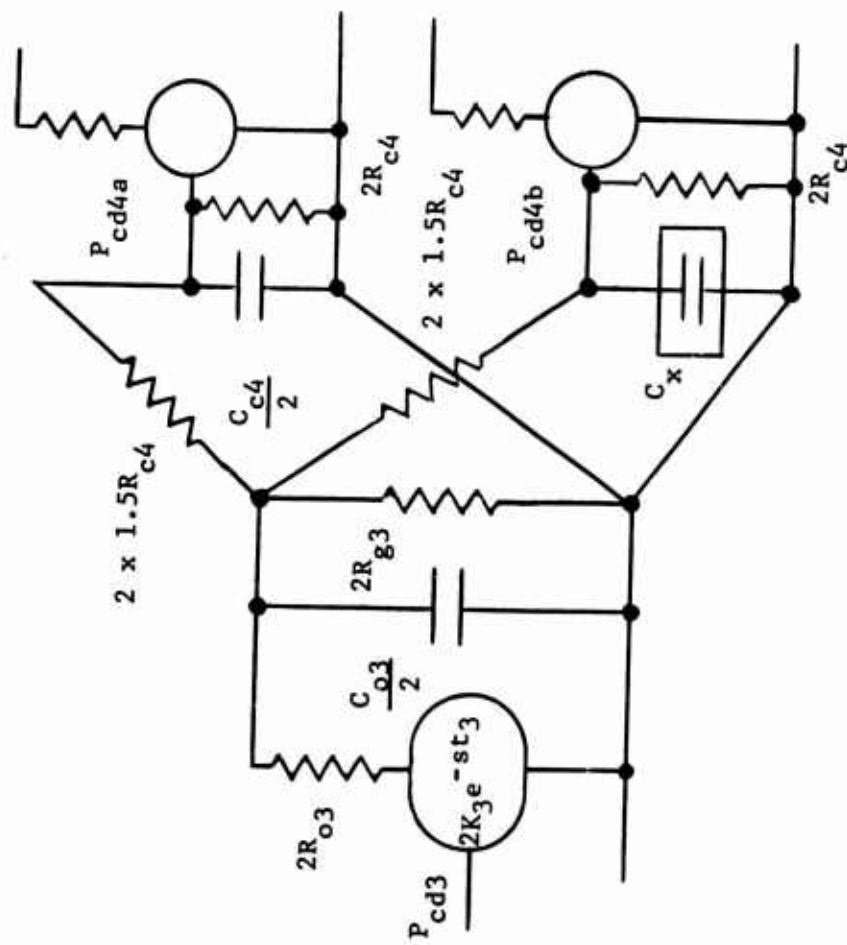
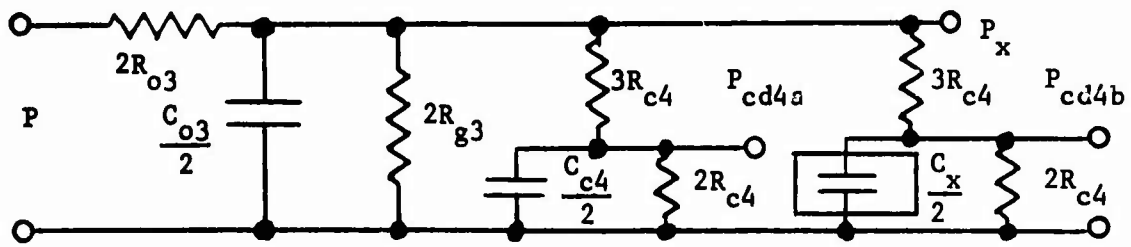
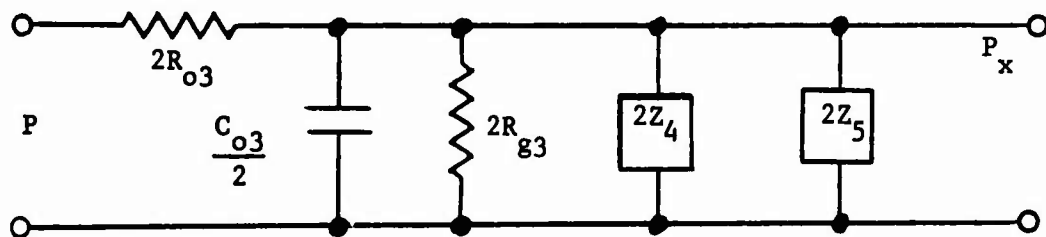


FIGURE 88 - DETAIL OF NETWORK BETWEEN STAGE 3 AND STAGE 4



WHERE $P = 2K_3 P_{cd3} e^{-st_3}$

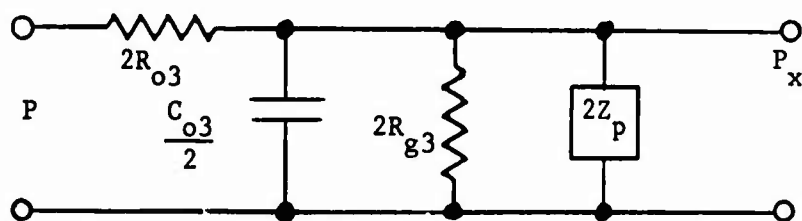
EQUIVALENT TO:



WHERE $2Z_4 = 3R_{c4} + \frac{2R_{c4}/sC_{c4}}{R_{c4} + 1/sC_{c4}}$

$2Z_5 = 3R_{c4} + \frac{2R_{c4}/sC_x}{R_{c4} + 1/sC_x}$

EQUIVALENT TO:



WHERE $2Z_p = \frac{2Z_4 Z_5}{Z_4 + Z_5}$

FIGURE 89 - CONSOLIDATION OF THE NETWORK BETWEEN STAGE 3 AND STAGE 4

$$\frac{P_x}{P} = \frac{\frac{Z_p R_{g3} / sC_{o3}}{Z_p R_{g3} + R_{g3} / sC_{o3} + Z_p / sC_{o3}}}{R_{o3} + \frac{Z_p R_{g3} / sC_{o3}}{Z_p R_{g3} + R_{g3} / sC_{o3} + Z_p / sC_{o3}}}$$

which reduces to

$$\frac{P_x}{P} = \frac{Z_p R_{g3}}{R_{o3} R_{g3} + R_{o3} Z_p + Z_p R_{g3}} \cdot \frac{1}{1 + \frac{sC_{o3} R_{o3} Z_p R_{g3}}{R_{o3} R_{g3} + R_{o3} Z_p + Z_p R_{g3}}}$$

but, $P = 2P_{cd3} K_3 e^{-st_3}$

then

$$\frac{P_x}{P_{cd3}} = \frac{2K_3 Z_p R_{g3} e^{-st_3}}{R_{o3} R_{g3} + R_{o3} Z_p + Z_p R_{g3}} \cdot \frac{1}{1 + sC_{o3} \frac{R_{o3} Z_p R_{g3}}{R_{o3} R_{g3} + R_{o3} Z_p + Z_p R_{g3}}}$$

Referring again to Figure 89, we have

$$\frac{P_{cd4a}}{P_x} = \frac{\frac{R_{c4} / sC_{c4}}{R_{c4} + 1/sC_{c4}}}{1.5R_{c4} + \frac{R_{c4} / sC_{c4}}{R_{c4} + 1/sC_{c4}}}$$

which reduces to

$$\frac{P_{cd4a}}{P_x} = \frac{1}{2.5} \frac{1}{1 + 0.6sC_{c4} R_{c4}}$$

where C_{c4} is the normal circuit volume capacitance.

Similarly, we have the network leading from P_x to P_{cd4b} , which is analyzed in the same fashion to give

$$\frac{P_{cd4b}}{P_x} = \frac{1}{2.5} \frac{1}{1 + 0.6sC_x R_{c4}}$$

where C_x is the total volume capacitance in the circuit, some of which is added volume to generate the highpass filter network time constant (3.0 seconds).

Each isolated portion of the circuit diagram in Figure 87 is analyzed in the same way. The isolated transfer functions are shown in block diagram form in Figure 90. The transfer functions corresponding to the individual blocks are listed in Figure 91.

15. Cascade the Partial System Transfer Functions to Generate the Transfer Function for the Entire System

With reference to the block diagram in Figure 90, the overall transfer function for the fluidic yaw damper system can be developed as follows:

$$\frac{P_{od}}{\omega} = \frac{P_{cd1}}{\omega} \cdot \frac{P_{cd2}}{P_{cd1}} \cdot \frac{P_{cd3}}{P_{cd2}} \cdot \frac{P_x}{P_{cd3}} \left[\frac{P_{cd4a}}{P_x} \cdot \frac{P_a}{P_{cd4a}} \cdot \frac{P_{cd5}}{P_a} \cdot \frac{P_{cd4b}}{P_x} \cdot \frac{P_b}{P_{cd4b}} \cdot \frac{P_{cd5}}{P_b} \right] \frac{P_{od}}{P_{cd5}}$$

Because of the complexity of the result, we will not substitute the individual transfer functions into this expression here, but the process is a straightforward one. It will also be more convenient to evaluate the frequency response of each one separately, then cascade the numerical results.

16. Calculate the Equivalent Circuit Parameters

The values of the elements of the equivalent circuits and the parameters in the transfer functions are calculated according to the procedures described in paragraph 6.4. We will choose a few examples for the yaw damper system to illustrate the approach in detail. Consider first the circuit associated with stages 2 and 3, assuming a physical layout as shown in Figure 92.

a. Pressure Amplification Factor K_2

The pressure amplification factor is defined in paragraph 2.7.4 as

$$K_p = \frac{\Delta P_o}{\Delta P_{cd}} \Bigg|_{Q_o \text{ constant}}$$

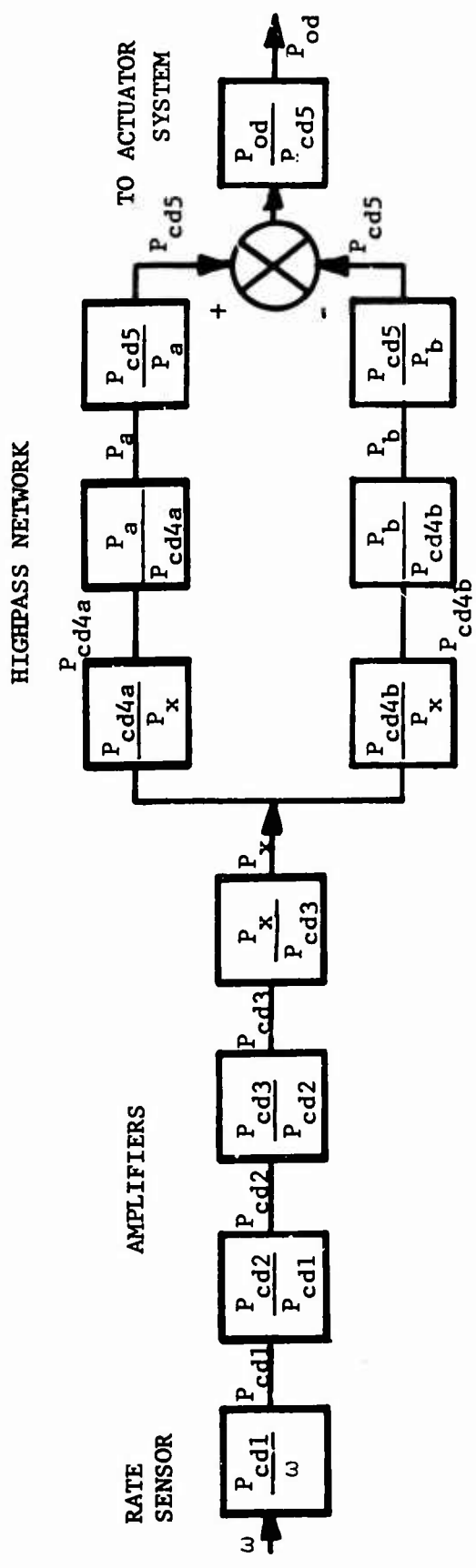


FIGURE 90 - TRANSFER FUNCTION BLOCK DIAGRAM FOR THE COMPLETE FLUIDIC YAW DAMPER

RATE SENSOR:

$$\frac{P_{cd1}}{\omega} = \frac{2K_{\omega} R_{c1} R_{s\omega} e^{-st_{\omega}}}{R_{c1} R_{s\omega} + R_{\omega} R_{c1} + R_{\omega} R_{s\omega}} \frac{1}{1 + s(C_{\omega} + C_{c1})} \frac{R_{c1} R_{\omega} R_{s\omega}}{R_{c1} R_{\omega} + R_{\omega} R_{s\omega} + R_{c1} R_{s\omega}}$$

STAGE 1:

$$\frac{P_{cd2}}{P_{cd1}} = \frac{2K_1 R_{c2} R_{s1} e^{-st_1}}{R_{c2} R_{o1} + R_{o1} R_{s1} + R_{c2} R_{s1}} \frac{1}{1 + s(C_{o1} + C_{c2})} \frac{R_{c2} R_{o1} R_{s1}}{R_{c2} R_{o1} + R_{o1} R_{s1} + R_{c2} R_{s1}}$$

STAGE 2:

$$\frac{P_{cd3}}{P_{cd2}} = \frac{2K_2 R_{c3} R_{s2} e^{-st_2}}{R_{c3} R_{o2} + R_{o2} R_{s2} + R_{c3} R_{s2}} \frac{1}{1 + s(C_{o2} + C_{c3})} \frac{R_{c3} R_{o2} R_{s2}}{R_{c3} R_{o2} + R_{o2} R_{s2} + R_{c3} R_{s2}}$$

STAGE 3:

$$\frac{P_x}{P_{cd3}} = \frac{2K_3 Z_p R_{g3} e^{-st_3}}{R_{o3} R_{g3} + R_{o3} Z_p + Z_p R_{g3}} \frac{1}{1 + sC_{o3}} \frac{R_{o3} Z_p R_{g3}}{R_{o3} R_{g3} + R_{o3} Z_p + Z_p R_{g3}}$$

WHERE

$$Z_p = \frac{Z_4 Z_5}{Z_4 + Z_5}$$

$$Z_4 = 1.5R_{c4} + \frac{R_{c4}/sC_{c4}}{R_{c4} + 1/sC_{c4}}$$

$$Z_5 = 1.5R_{c4} + \frac{R_{c4}/sC_x}{R_{c4} + 1/sC_x}$$

FIGURE 91 - LIST OF TRANSFER FUNCTIONS FOR THE COMPLETE FLUIDIC YAW DAMPER SYSTEM

ALSO

$$\frac{P_{cd4a}}{P_x} = \frac{1}{2.5} \frac{1}{1 + 0.6sC_{c4}R_{c4}}$$

AND

$$\frac{P_{cd4b}}{P_x} = \frac{1}{2.5} \frac{1}{1 + 0.6sC_x R_{c4}}$$

WHERE C_x IS DETERMINED BY EXTERNAL VOLUME ADDED

STAGE 4:

$$\frac{P_a}{P_{cd4a}} = \frac{2K_4 Z_c R_{g4} e^{-st_4}}{R_{o4} R_{g4} + Z_c R_{o4} + Z_c R_{g4}} \frac{1}{1 + sC_{o4} \frac{Z_c R_{g4} R_{o4}}{R_{o4} R_{g4} + Z_c R_{o4} + Z_c R_{g4}}}$$

WHERE

$$Z_c = 2R_{c5} + Z_b$$

$$Z_b = \frac{Z_a R_{c5} / sC_{c5}}{Z_a R_{c5} + R_{c5} / sC_{c5} + Z_a / sC_{c5}}$$

$$Z_a = 2R_{c5} + \frac{R_{o4} / sC_{o4}}{R_{o4} + 1/sC_{o4}}$$

AND

$$\frac{P_{cd5}}{P_a} = \frac{Z_a}{2R_{c5} + 3Z_a} \frac{1}{1 + sC_{c5} \frac{2R_{c5} Z_a}{2R_{c5} + 3Z_a}}$$

FIGURE 91 - CONTINUED

ALSO

$$\frac{P_b}{P_{cd4b}} = \frac{2K_4 Z_c R_{g4} e^{-st_d}}{R_{o4} R_{g4} + Z_c R_{o4} + Z_c R_{g4}} \frac{1}{1 + sC_{o4} \frac{Z_c R_{g4} R_{o4}}{R_{o4} R_{g4} + Z_c R_{o4} + Z_c R_{g4}}}$$

AND

$$\frac{P_{cd5}}{P_b} = \frac{Z_a}{2R_{c5} + 3Z_a} \frac{1}{1 + sC_{c5} \frac{2R_{c5} Z_a}{2R_{c5} + 3Z_a}}$$

STAGE 5:

$$\frac{P_{od}}{P_{cd5}} = \frac{2K_5 R_{L5}}{R_{L5} + R_{o5}} \frac{1}{1 + s(C_{o5} + C_L) \frac{R_{o5} R_{g5}}{R_{g5} + R_{o5}}}$$

FIGURE 91 - CONTINUED

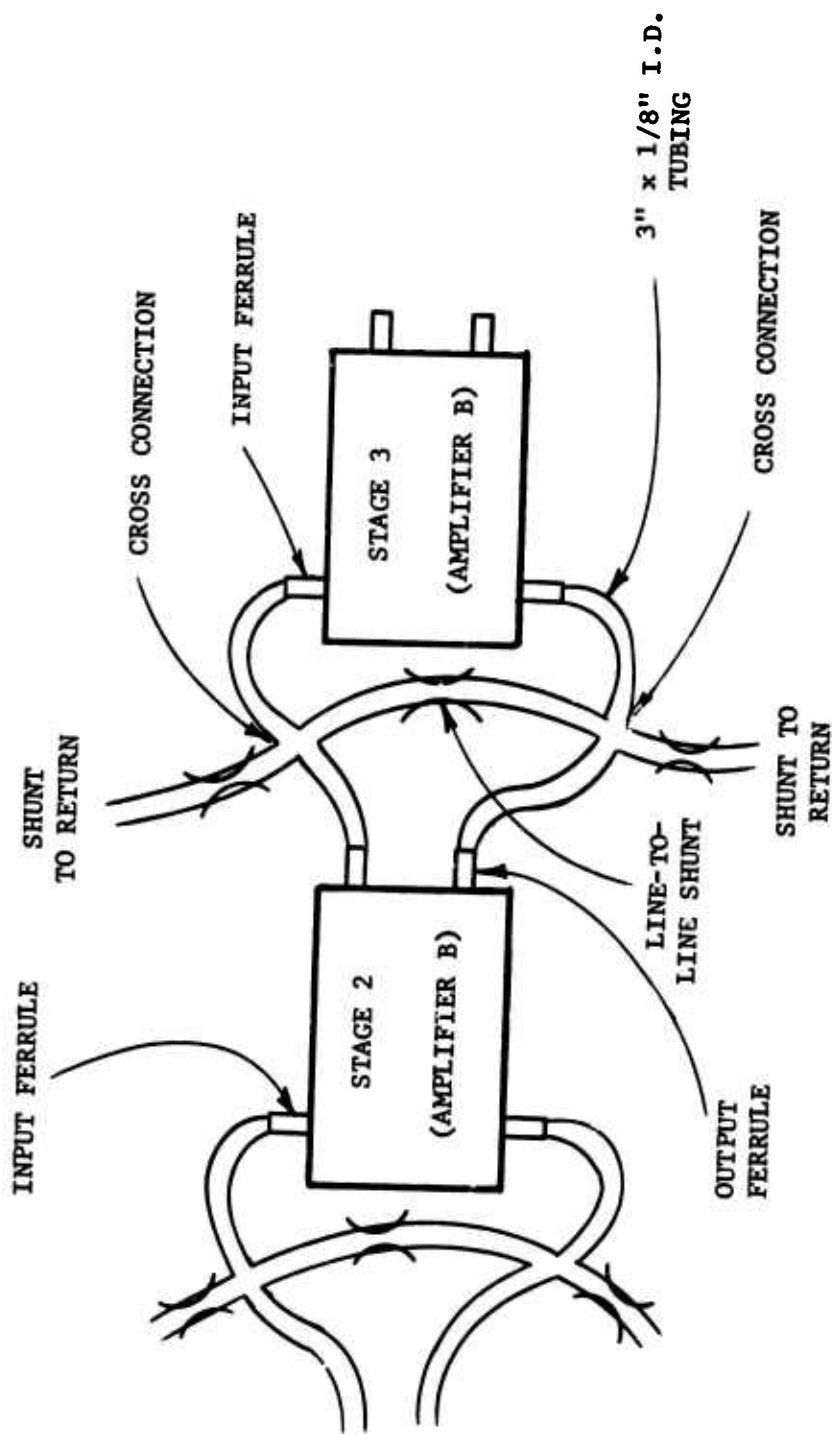


FIGURE 92 - PHYSICAL LAYOUT OF CIRCUIT ASSOCIATED WITH STAGE 2

and is calculated at the operating bias point. With reference to Figure 81, we take the horizontal distance between the $P_{cd}/P_s = \pm 0.01$ lines as the change in output:

$$\Delta P_o = 0.56 - 0.20 \text{ psi}$$

$$\Delta P_o = 0.36 \text{ psi}$$

The corresponding change in control differential is

$$\Delta P_{cd} = 0.02 P_s$$

and the supply pressure for this stage is 1.4 psi

$$\Delta P_{cd} = 0.02 \times 1.4 = 0.028$$

Then

$$\frac{\Delta P_o}{\Delta P_{cd}} = \frac{0.36}{0.028}$$

$$\therefore K_2 = 12.8$$

b. Output Resistance R_{o2}

The output resistance is defined in paragraph 2.7.1 as

$$R_o = \left. \frac{\Delta P_o}{\Delta Q_o} \right|_{P_{cd} \text{ constant}}$$

and is calculated at the operating bias point. With reference to Figure 81, the output resistance is the inverse of the slope of the zero signal line at the operating point, or

$$R_{o2} = \frac{32 \times 0.014 \text{ psi}}{23 \times 0.00054 \text{ scfm}} \times \frac{60}{1728}$$

$$\therefore R_{o2} = 1.26 \frac{\text{lb sec}}{\text{in.}^5}$$

c. Output Capacitance C_{o2}

The output capacitance is defined in paragraph 2.7.7 as

$$C_o = \frac{V}{P_{abs}}$$

calculated at the operating bias point. With reference to Figure 81,

the operating pressure is 0.39 psi gage or 15.09 psi absolute.

The volume V charged to the amplifier output is the volume of the output aperture plus the volume of the connecting ferrule. With reference to Figure 75, the volume of the output aperture is estimated from an integration of the plan area (by counting small dimensional blocks) times the depth of channel. In this case, the volume of the output aperture is 0.00057 in.³. Therefore,

$$C_{O_2} = \frac{0.00057 + 0.0053}{15.09} = \frac{58.7 \times 10^{-4}}{15.09}$$

$$\therefore C_{O_2} = 3.89 \times 10^{-4} \text{ in.}^5/\text{lb}$$

d. Output Inductance (stage 2)

The output inductance is defined in paragraph 2.7.8 as

$$L_o = \frac{\rho l}{A_{\text{eff}}}$$

The effective area of the output aperture and the length of the output aperture can be calculated from dimensions in Figure 75. Directly,

$$l = 0.82 \text{ in.}$$

But

$$A_{\text{eff}} = \frac{A_{\text{in}} - A_{\text{out}}}{\ln \frac{A_{\text{in}}}{A_{\text{out}}}}$$

$$A_{\text{in}} = 4.7 \times 10^{-4} \text{ in.}^2$$

$$A_{\text{out}} = 18.8 \times 10^{-4} \text{ in.}^2$$

$$A_{\text{eff}} = \frac{4.7 \times 10^{-4} - 18.8 \times 10^{-4}}{\ln \frac{4.7 \times 10^{-4}}{18.8 \times 10^{-4}}}$$

$$A_{\text{eff}} = 1.01 \times 10^{-3} \text{ in.}^2$$

Then

$$\frac{l}{A_{\text{eff}}} = 8.09 \times 10^2 \text{ in.}^{-1}$$

Similarly, for the output ferrule,

$$l = 0.44 \text{ in.}$$

$$A = 1.23 \times 10^{-2} \text{ in.}^2$$

$$\frac{l}{A} = 35.6 \text{ in.}^{-1}$$

$$\text{Total } l/A = 809 + 35.6 = 845 \text{ in.}^{-1}$$

The mass density of air at 1 atmosphere is

$$\rho = 2.37 \times 10^{-3} \frac{\text{slugs}}{\text{ft}^3}$$

$$\text{or } \rho = 1.15 \times 10^{-7} \frac{\text{lb sec}^2}{\text{in}^4}$$

At the output bias pressure of stage 2 (15.09 psi absolute), the density is

$$\rho = 1.15 \times 10^{-7} \times \frac{15.09}{14.7}$$

$$\rho = 1.18 \times 10^{-7} \times \frac{\text{lb sec}^2}{\text{in}^4}$$

Then

$$L_{o2} = \frac{\rho l}{A} = (1.18 \times 10^{-7}) (8.45 \times 10^2)$$

$$L_{o2} = 9.93 \times 10^{-5} \frac{\text{lb sec}^2}{\text{in}^5}$$

e. Input Resistance (to stage 3)

Input resistance is defined in paragraph 2.7.6 as

$$R_c = \frac{\Delta P_c}{\Delta Q_c} \quad (P_{c1} + P_{c2}) \text{ constant}$$

With reference to Figure 81,

$$R_{c3} = \frac{7 \times 10^{-2}}{1.08 \times 10^{-3}} \times \frac{60}{1728}$$

$$\therefore R_{c3} = 2.26 \frac{\text{lb sec}}{\text{in}^5}$$

f. Input Capacitance (to stage 3)

Input capacitance is defined in paragraph 2.7.7 as

$$C_c = \frac{V}{P_{abs}}$$

In the case of interconnected amplifiers, we have chosen to charge the line volume to the input of the amplifier. The amplifiers are connected together with 3 inches of 1/8 ID tubing with a cross connection included for attaching shunt restrictors. Therefore, the total volume is made up of tubing, cross connector, ferrule connector, and amplifier input aperture. The volumes can be calculated from dimensions. The total input volume to stage 3 is

$$V = 0.0585 \text{ in.}^3$$

The pressure is the same as stage 2 output pressure; that is,

$$P = 0.39 \text{ psi gage} = 15.09 \text{ psi absolute}$$

Then

$$C_{c3} = \frac{0.0585}{15.09}$$

$$\therefore C_{c3} = 0.00389 \text{ in.}^5/\text{lb}$$

Note that

$$\text{At } 10 \text{ rad/sec } \frac{1}{\omega C_{c3}} = \frac{1}{0.0389} = 25.7 \frac{\text{lb sec}}{\text{in.}^5} \text{ (1.6 cps)}$$

$$\text{At } 100 \text{ rad/sec } \frac{1}{\omega C_{c3}} = \frac{1}{0.389} = 2.57 \frac{\text{lb sec}}{\text{in.}^5} \text{ (16 cps)}$$

g. Input Inductance L_c

Input inductance is defined in paragraph 2.7.8 as

$$L_c = \frac{\rho l}{A_{eff}}$$

In the circuit shown in Figure 92, we are charging all the inductance from the output ferrule of stage 2 into the control apertures of stage 3 as input inductance.

For the 3 in. of 1/8 ID tubing,

$$\frac{l}{A} = 244 \text{ in.}^{-1}$$

For the cross connection,

$$\frac{l}{A} = 118 \text{ in.}^{-1}$$

For the control ferrule,

$$\frac{l}{A} = 35.6 \text{ in.}^{-1}$$

For the control aperture,

$$\frac{l}{A} = 131 \text{ in.}^{-1}$$

$$\text{Total } l/A = 529 \text{ in.}^{-1}$$

Then

$$L_{c3} = 1.18 \times 10^{-7} \times 5.29 \times 10^2$$

$$\therefore L_{c3} = 6.21 \times 10^{-5} \frac{\text{lb sec}^2}{\text{in.}^5}$$

Note that

$$\text{At } 10 \text{ rad/sec } \omega L_{c3} = 6.21 \times 10^{-4} \frac{\text{lb sec}}{\text{in.}^5} \text{ (1.6 cps)}$$

$$\text{At } 100 \text{ rad/sec } \omega L_{c3} = 6.21 \times 10^{-3} \frac{\text{lb sec}}{\text{in.}^5} \text{ (16 cps)}$$

Comparing the inductive reactance of this circuit (which is typical of the yaw damper system) with the capacitive reactance under paragraph f above shows that even up to a frequency of 100 radians per second (16 cps), the relative value of inductive reactance is small compared with the capacitive reactance. Since this circuit is typical of the yaw damper system, we have justified neglecting the inclusion of inductance in the derivation of the transfer functions.

h. Restrictors Shunted to Return

The value of the resistance shunted from the stage 2 output port to return can be calculated from Figure 81. Assuming that it is a linear restrictor, its value can be calculated from the increase in flow that it provides at a given pressure. In Figure 81 we have shown the addition of a shunt restrictor to return, which, at a pressure of 0.39 psi, raises the flow from 0.0062 to 0.0124 scfm.

Then the resistance is

$$R_{g2} = \frac{0.39 \text{ psi}}{(0.0124 - 0.0062)} \times \frac{60}{1728}$$

$$\therefore R_{g2} = 2.16 \frac{\text{lb sec}}{\text{in.}^5}$$

i. Restrictors Shunted Line-to-Line

The value of the resistance shunted across the output lines of the stage 2 amplifier can be calculated from Figure 81. Assuming a linear restrictor, its value can be calculated from the change in flow that it produces. In Figure 81 the pressure swings 0.078 psi around the operating point. Without the line-to-line shunt, the flow swings 0.003 scfm. With the shunt, the flow swings 0.017 scfm. Therefore,

$$R_{s2} = \frac{0.078 \text{ psi}}{(0.017 - 0.003)} \times \frac{60}{1728}$$

$$\therefore R_{s2} = 0.194 \frac{\text{lb sec}}{\text{in.}^5}$$

j. Time Delay

The time delay is defined in paragraph 2.7.9. It is made up of the transport delay in the second stage amplifier interaction chambers, plus wave propagation delays in the second stage output aperture and output ferrule, the tubing, the cross connectors, and the third stage input aperture and input ferrule.

In the stage 2 amplifier interaction chamber, the power jet exit velocity is

$$v_e = \frac{Q}{A} = \frac{0.026}{0.00025} \times \frac{1728}{60}$$

$$v_e = 2990 \text{ in./sec}$$

The receiver impact velocity (0.75 psi recovery) is

$$v_r = \sqrt{\frac{2p}{\rho}}$$

$$v_r = \sqrt{\frac{(6.44 \times 10^{-1})(0.745)(1.44 \times 10^2)}{8.47 \times 10^{-2}}}$$

$$v_r = 3420 \text{ in./sec}$$

Averaging gives

$$v = 3205 \text{ in./sec}$$

The length of the interaction chamber is 0.1 inch (see Figure 75).

Then,

$$t_1 = \frac{0.10}{3205}$$

$$t_1 = 3.1 \times 10^{-5} \text{ sec}$$

In the output aperture,

$$Q_0 = 1.26 \times 10^{-2} \text{ scfm}$$

Taking an average cross-sectional area 8.9×10^{-4} ,

$$v = \frac{1.26 \times 10^{-2}}{8.9 \times 10^{-4}} \times \frac{1728}{60}$$

$$v = 407 \text{ in./sec}$$

The length of the output aperture is approximately 0.82 inch.

Then,

$$t_2 = \frac{0.82}{407 + 13200}$$

where 13200 in./sec is the propagation velocity of sound

$$t_2 = 6.03 \times 10^{-5} \text{ sec}$$

In the output ferrule,

$$v = \frac{1.26 \times 10^{-2}}{1.23 \times 10^{-2}} \times \frac{1728}{60}$$

$$v = 29.5 \text{ in./sec}$$

The length of the ferrule is 0.44 inch. Then,

$$t_3 = \frac{0.44}{29.5 + 13200}$$

$$t_3 = 3.32 \times 10^{-5} \text{ sec}$$

Similarly, we calculate the time delay in the tubing,

$$t_4 = 2.28 \times 10^{-4} \text{ sec}$$

and in the cross connector,

$$t_5 = 6.14 \times 10^{-5} \text{ sec}$$

and in the control ferrule,

$$t_6 = 3.32 \times 10^{-5} \text{ sec}$$

and in the control aperture,

$$t_7 = 2.80 \times 10^{-5} \text{ sec}$$

Adding up the individual time delays, t_1 through t_7 , we have

$$t_{23} = 4.75 \times 10^{-4} \text{ sec}$$

k. Circuit Parameters

A listing of all equivalent circuit parameters for the fluidic yaw damper is given in Figure 93.

17. Substitute the Performance Parameters in the Transfer Functions

With reference to the overall system transfer curve shown in Figure 86, we have shown that the steady-state gain requirements of the fluidic yaw damper have been met. Therefore, in calculating the dynamic behavior, we will consider only the frequency-sensitive portions of the transfer functions.

Referring now to Figure 91,

$$a. \left[\frac{P_{cdl}}{\omega} \right] = \frac{1}{1 + s(C_{ow} + C_{cl}) \frac{R_{cl}R_{ow}R_{sw}}{R_{cl}R_{ow} + R_{ow}R_{sw} + R_{cl}R_{sw}}}$$

$$\left[\frac{P_{cdl}}{\omega} \right] = \frac{1}{1+s(0.0008+0.0033) \frac{0.348 \times 0.435 \times 0.057}{0.348 \times 0.435 + 0.435 \times 0.057 + 0.348 \times 0.057}}$$

$$\left[\frac{P_{cdl}}{\omega} \right] = \frac{1}{1 + 0.00018s}$$

$R_{ow} = 0.435$	$R_{o3} = 2.22$
$R_{c1} = 0.348$	$R_{c4} = 4.00$
$R_{sw} = 0.057$	$R_{s3} = 0.343$
$C_{ow} = 0.0008$	$R_{g3} = 4.49$
$C_{c1} = 0.0033$	$C_{o3} = 0.00038$
$R_{o1} = 0.668$	$C_{c4} = 6.00526/0.0005$
$R_{c2} = 0.652$	$R_{o4} = 3.22$
$R_{s1} = 0.142$	$R_{c5} = 5.00$
$R_{g1} = 2.11$	$R_{s4} = 0.393$
$C_{o1} = 0.0004$	$R_{g4} = 1.50$
$C_{c2} = 0.00394$	$C_{o4} = 0.00038$
$R_{o2} = 1.29$	$C_{c5} = 0.0053/0.0005$
$C_{o2} = 0.00038$	$R_{o5} = 3.34$
$R_{c3} = 2.26$	$R_{g5} = 8.43$
$R_{g2} = 2.16$	$C_{o5} = 0.00032$
$R_{s2} = 0.194$	$C_L = 0.0020/0.0010$
$C_{c3} = 0.00389$	total t = 0.054/0.035

NOTE: UNITS OF R, $\frac{\text{lb sec}^2}{\text{in.}^5}$

UNITS OF C, $\frac{\text{in.}^5}{\text{lb}}$

FIGURE 93 - TABULATION OF EQUIVALENT CIRCUIT PARAMETERS

$$b. \quad \left[\frac{P_{cd2}}{P_{cd1}} \right] = \frac{1}{1 + s(C_{o1} + C_{c2}) \frac{R_{c2}R_{o2}R_{sa}}{R_{c2}R_{o1} + R_{o1}R_{sa} + R_{c2}R_{sa}}}$$

$$\text{where } R_{sa} = \frac{R_{s1}R_{g1}}{R_{s1} + R_{g1}}$$

$$\left[\frac{P_{cd2}}{P_{cd1}} \right] = \frac{1}{1 + 0.0004s}$$

$$c. \quad \left[\frac{P_{cd3}}{P_{cd2}} \right] = \frac{1}{1 + s(C_{o2} + C_{c3}) \frac{R_{c3}R_{o2}R_{sb}}{R_{c3}R_{o2} + R_{o2}R_{sb} + R_{c3}R_{sb}}}$$

$$\text{where } R_{sb} = \frac{R_{s2}R_{g2}}{R_{s2} + R_{g2}}$$

$$\left[\frac{P_{cd3}}{P_{cd2}} \right] = \frac{1}{1 + 0.0006s}$$

$$d. \quad Z_4 = R_{c4} \left(1.5 + \frac{1}{1 + sC_{c4}R_{c4}} \right)$$

$$Z_4 = \frac{10 + 0.126s}{1 + 0.021s}$$

$$e. \quad Z_5 = R_{c4} \left(1.5 + \frac{1}{1 + sC_x R_{c4}} \right)$$

Assuming that we want $P_{cd4b} / P_x = 1/1 + 3s$ to provide the proper highpass network time constant,

$$Z_5 = \frac{10 + 30s}{1 + 5s}$$

$$f. \quad Z_p = \frac{Z_4 Z_5}{Z_4 + Z_5}$$

$$Z_p = \frac{100 + 301s + 3.78s^2}{20 + 80.3s + 1.26s^2}$$

$$g. \quad \left[\frac{P_x}{P_{cd3}} \right] = \frac{1}{1 + sC_{o3} \frac{R_{o3} Z_p R_{g3}}{R_{o3} R_{g3} + R_{o3} Z_p + R_{g3} Z_p}}$$

$$\left[\frac{P_x}{P_{cd3}} \right] = \frac{1}{1 + 0.00043s} \quad (\text{max})$$

$$h. \quad \left[\frac{P_{cd4a}}{P_x} \right] = \frac{1}{1 + 0.6sC_{c4} R_{c4}}$$

$$\left[\frac{P_{cd4a}}{P_x} \right] = \frac{1}{1 + 0.0126s}$$

$$i. \quad Z_a = 2R_{c5} + \frac{R_{o4}}{1 + sC_{o4} R_{o4}}$$

$$Z_a = \frac{13.2 + 0.012s}{1 + 0.0012s}$$

$$j. \quad Z_b = \frac{Z_a R_{c5}}{sC_{cs} Z_a R_{c5} + R_{c5} + Z_a}$$

$$Z_b = \frac{3.52}{1 + 0.019s}$$

$$k. \quad Z_c = 2R_{c5} + Z_b$$

$$Z_c = \frac{13.5 + 0.19s}{1 + 0.019s}$$

$$l. \quad \left[\frac{P_a}{P_{cd4a}} \right] = \frac{1}{1 + sC_{o4} \frac{Z_c R_{g4} R_{o4}}{R_{o4} R_{g4} + Z_c R_{o4} + Z_c R_{g4}}}$$

$$\left[\frac{P_a}{P_{cd4a}} \right] = \frac{1}{1 + 0.00036s} \quad (\text{max})$$

$$m. \quad \left[\frac{P_{cd5}}{P_a} \right] = \frac{1}{1 + sC_{c5} \frac{2R_{c5} Z_a}{2R_{c5} + 3Z_a}}$$

$$\left[\frac{P_{cd5}}{P_a} \right] = \frac{1}{1 + 0.014s} \quad (\text{max})$$

$$n. \quad \left[\frac{P_{od}}{P_{cd5}} \right] = \frac{1}{1 + s(C_{o5} + C_L) \frac{R_{o5} R_{g5}}{R_{g5} + R_{o5}}}$$

$$\left[\frac{P_{od}}{P_{cd5}} \right] = \frac{1}{1 + 0.0055s}$$

$$o. \quad \left[\frac{P_{cd4b}}{P_x} \right] = \frac{1}{1 + 0.6sC_x R_{c4}}$$

$$\left[\frac{P_{cd4b}}{P_x} \right] = \frac{1}{1 + 3.0s}$$

$$p. \quad \left[\frac{P_b}{P_{cd4b}} \right] = \frac{1}{1 + sC_{o4} \frac{Z_c R_{g4} R_{o4}}{R_{o4} R_{g4} + Z_c R_{o4} + Z_c R_{g4}}}$$

$$\left[\frac{P_b}{P_{cd4b}} \right] = \frac{1}{1 + 0.00036s} \quad (\text{max})$$

$$q. \left[\frac{P_{cd5}}{P_b} \right] = \frac{1}{1 + sC_{c5} \frac{2R_{c5}Z_a}{2R_{c5} + 3Z_a}}$$

$$\left[\frac{P_{cd5}}{P_b} \right] = \frac{1}{1 + 0.014s} \quad (\text{max})$$

With reference to Figure 90, the overall frequency-sensitive portion of the transfer function is

$$\frac{P_{od}}{\omega} = \frac{P_{cd1}}{\omega} \cdot \frac{P_{cd2}}{P_{cd1}} \cdot \frac{P_{cd3}}{P_{cd2}} \cdot \frac{P_x}{P_{cd3}} \left[\frac{P_{cd4a}}{P_x} \cdot \frac{P_a}{P_{cd4a}} \cdot \frac{P_{cd5}}{P_a} - \frac{P_{cd4b}}{P_x} \cdot \frac{P_b}{P_{cd4b}} \cdot \frac{P_{cd5}}{P_b} \right] \frac{P_{od}}{P_{cd5}}$$

The frequency response of the individual transfer functions will be evaluated separately and the results analyzed; then they will be combined according to the formula above.

18. Calculate the System Frequency Response

As described in section 6.0, the frequency response is calculated by substituting $j2\pi f$ for s in the transfer function. The phase shift due to time delay is evaluated as a separate factor, and is then added to the total transfer function.

Substituting $j2\pi f$ for s at $f = 10$ cps,

$$(2\pi f = 62.8 \text{ rad/sec})$$

$$\left[\frac{P_{cd1}}{\omega} \right] = \frac{1}{1 + 0.00018s} = \frac{1}{1 + j0.00018 \times 62.8} = \frac{1}{1 + j0.0113}$$

$$\left[\frac{P_{cd1}}{\omega} \right] = 1 / -0.5^\circ$$

$$\left[\frac{P_{cd2}}{P_{cd1}} \right] = \frac{1}{1 + 0.0004s} = \frac{1}{1 + j0.0004 \times 62.8} = \frac{1}{1 + j0.025}$$

$$\left[\frac{P_{cd2}}{P_{cd1}} \right] = 1 / -1.5^\circ$$

$$\left[\frac{P_{cd3}}{P_{cd2}} \right] = \frac{1}{1 + 0.0006s} = \frac{1}{1 + j0.0006 \times 62.8} = \frac{1}{1 + j0.0375}$$

$$\left[\frac{P_{cd3}}{P_{cd2}} \right] = 1 / -2^\circ$$

$$\left[\frac{P_x}{P_{cd3}} \right] = \frac{1}{1 + 0.00043s} = \frac{1}{1 + j0.00043 \times 62.8} = \frac{1}{1 + j0.027}$$

$$\left[\frac{P_x}{P_{cd3}} \right] = 1 / -1.5^\circ$$

$$\left[\frac{P_{cd4a}}{P_x} \right] = \frac{1}{1 + 0.0126s} = \frac{1}{1 + j0.0126 \times 62.8} = \frac{1}{1 + j0.79}$$

$$\left[\frac{P_{cd4a}}{P_x} \right] = 0.78 / -38^\circ$$

$$\left[\frac{P_a}{P_{cd4a}} \right] = \frac{1}{1 + 0.00036s} = \frac{1}{1 + j0.00036 \times 62.8} = \frac{1}{1 + j0.0225}$$

$$\left[\frac{P_a}{P_{cd4a}} \right] = 1 / -1.5^\circ$$

$$\left[\frac{P_{cd5}}{P_a} \right] = \frac{1}{1 + 0.014s} = \frac{1}{1 + j0.014 \times 62.8} = \frac{1}{1 + j0.88}$$

$$\left[\frac{P_{cd5}}{P_a} \right] = 0.76 / -41^\circ$$

$$\left[\frac{P_{od}}{P_{cd5}} \right] = \frac{1}{1 + 0.0055s} = \frac{1}{1 + j0.0055 \times 62.8} = \frac{1}{1 + j0.35}$$

$$\left[\frac{P_{od}}{P_{cd5}} \right] = 0.95 / -19^\circ$$

$$\left[\frac{P_{cd4b}}{P_x} \right] = \frac{1}{1 + 3s} = \frac{1}{1 + j3 \times 62.8} = \frac{1}{1 + j190}$$

$$\left[\frac{P_{cd4b}}{P_x} \right] = 0.0053 \angle -90^\circ$$

$$\left[\frac{P_b}{P_{cd4b}} \right] = 1 \angle -1.5^\circ \text{ (same as } P_a \text{)}$$

$$\left[\frac{P_{cd5}}{P_b} \right] = 0.76 \angle -41^\circ \text{ (same as } P_a \text{)}$$

The phase shift due to time delay is

$$\theta_d = 360 f t_d = 360 \times 10 \times 0.054$$

$$\theta_d = 194^\circ$$

19. Plot the Frequency Response of the System and Compare It with Specified Requirements

The values of the transfer functions at 10 cps are shown in their appropriate places in Figure 94. The lower loop through the highpass network is highly attenuated, so it will be neglected in the evaluation of the yaw damper at high frequencies. Adding up the total phase shift in the system transfer functions through the upper loop, we have

$$\theta_a = 105^\circ$$

Adding

$$\theta_d = 194^\circ$$

gives a total

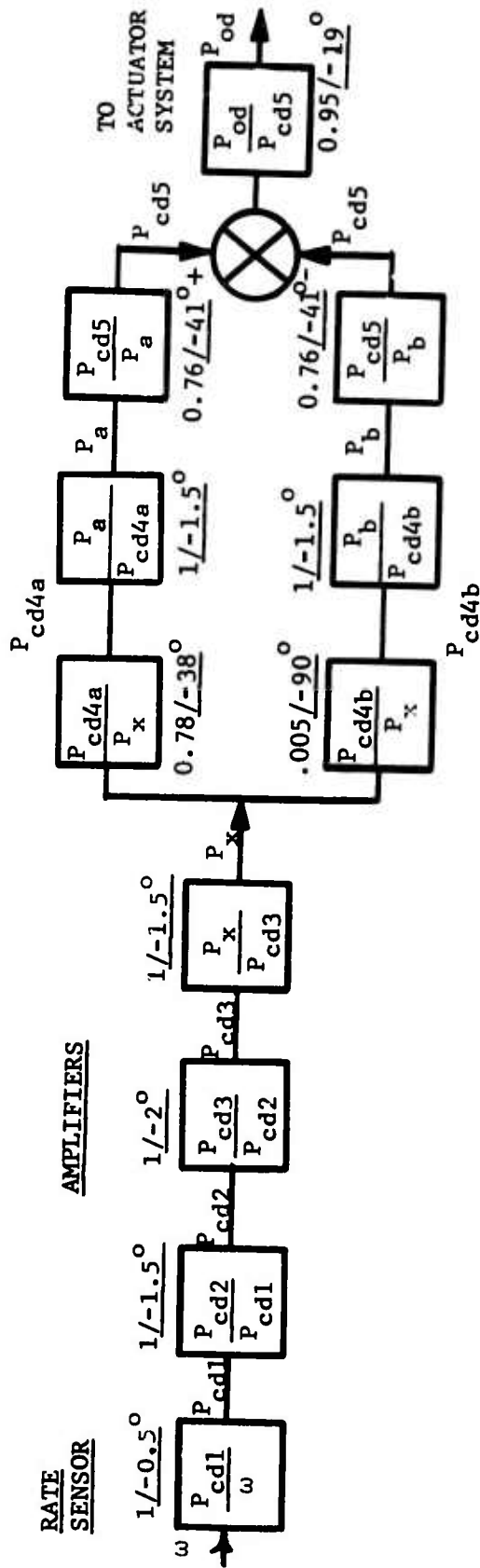
$$\theta = 299^\circ \text{ for the complete system.}$$

Comparing this with the specified allowable phase shift (180°) shows that the requirements at 10 cps have not been met.

20. Investigate Individual Component Transfer Functions and Make Necessary Changes

Examination of the phase shifts shown in Figure 94 reveals that the major contributions come from:

HIGHPASS NETWORK



$$\theta_a = 105^\circ$$

$$\theta_d = 194^\circ$$

$$\text{TOTAL } 299^\circ$$

FIGURE 94 - PRELIMINARY VALUES OF THE TRANSFER FUNCTIONS AT 10 CPS

- a. The input circuit of the highpass network (stage 4)
- b. The input circuit to the summing amplifier (stage 5)
- c. The output circuit of the amplifier driving the actuator (stage 5)

Further review of the transfer functions related to stages 4 and 5 shows that the input capacitance to stage 4 (C_{c4}), the input capacitance to stage 5 (C_{c5}), and the load circuit capacitance on stage 5 (C_L) can be reduced as follows.

The input circuit to stage 4 contains series resistance; therefore, we can reduce the ID of the tubing to a very small value, thereby providing some of the required resistance while reducing the trapped volume of air a great degree. In reexamining the physical circuit layout, we find that it is also possible to reduce the length of tubing. Therefore, it is practical to reduce the value of C_{c4} by a factor of 10.

The input circuit to stage 5 also contains series resistance and excessive lengths of tubing. By the same reasoning applied above, we find it practical to reduce the value of C_{c5} by a factor of 10.

In the load circuit of stage 5, the total capacitance ($0.002 \text{ in.}^5/\text{lb}$) is primarily due to tubing (the actuator is approximately $0.0005 \text{ in.}^5/\text{lb}$). The actuator has infinite input resistance, so the tubing running to it can be very small without introducing a significant amount of loss. Therefore, it appears practical that the total load circuit capacitance can be reduced to less than $0.0008 \text{ in.}^5/\text{lb}$.

Using these new lengths and diameters of tubing also reduces the time delay, because of shorter distances of signal travel and higher flow velocities. Recalculating the total time delay based on new networks of tubing results in a total delay of 0.035 second.

18. Calculate the System Frequency Response

Recalculating the transfer functions affected by these changes, we have

$$\left[\frac{P_{cd4a}}{P_x} \right] = \frac{1}{1 + 0.6sC'_{c4}R_{c4}} = \frac{1}{1 + 0.6s \times 0.0005 \times 4}$$

$$\left[\frac{P_{cd4a}}{P_x} \right] = \frac{1}{1 + 0.00126s}$$

at 10 cps

$$\left[\frac{P_{cd4a}}{P_x} \right] = \frac{1}{1 + j0.00126 \times 62.8} = \frac{1}{1 + j0.079}$$

$$\left[\frac{P_{cd4a}}{P_x} \right] = 1 \angle -4.5^\circ$$

$$\left[\frac{P_{cd5}}{P_a} \right] = \frac{1}{1 + sC'_{c5} \frac{2R_{c5}Z_a}{2R_{c5} + 3Z_a}}$$

$$\left[\frac{P_{cd5}}{P_a} \right] = \frac{1}{1 + 0.0014s}$$

at 10 cps

$$\left[\frac{P_{cd5}}{P_a} \right] = \frac{1}{1 + j0.0014 \times 62.8} = \frac{1}{1 + j0.088}$$

$$\left[\frac{P_{cd5}}{P_a} \right] = 1 \angle -5^\circ$$

$$\left[\frac{P_{od}}{P_{cd5}} \right] = \frac{1}{1 + s(C_{o5} + C'_c) \frac{R_{o5}R_{g5}}{R_{g5} + R_{o5}}}$$

$$\left[\frac{P_{od}}{P_{cd5}} \right] = \frac{1}{1 + 0.0026s}$$

at 10 cps

$$\left[\frac{P_{od}}{P_{cd5}} \right] = \frac{1}{1 + j0.0026 \times 62.8} = \frac{1}{1 + j0.16}$$

$$\left[\frac{P_{od}}{P_{cd5}} \right] = 0.98 \angle -9^\circ$$

The phase shift due to time delay at 10 cps is now

$$\theta_d = 360 ft'_d = 360 \times 10 \times 0.035$$

$$\theta_d = 126^\circ$$

Referring to Figure 95, which contains the final values for the transfer functions of the individual blocks at 10 cps, we see now that the total phase shift is 152°, well within the specified maximum of 180°.

Since we have shown that there is a little phase shift in the individual circuits (except P_{cd4b}/P_x) of the fluidic yaw damper at frequencies below 10 cps, the only circuit we are concerned with at other frequencies is the parallel loop in the highpass network and the difference

$$\left[\frac{P_{od}}{\omega} \right] \approx \left[\frac{P_{cd4a}}{P_x} \right] - \left[\frac{P_{cd4b}}{P_x} \right]$$

The calculated values are tabulated below.

f cps	$\left[\frac{P_{cd4a}}{P_x} \right]$	$\left[\frac{P_{cd4b}}{P_x} \right]$	$\left[\frac{P_{od}}{\omega} \right]$	$\left[\frac{P_{od}}{\omega} \right]$ db
0.001	1 / 0	1 / -1	0.017 / +90	-34db / +90
0.01	1 / 0	0.98 / -11	0.195 / +78	-14db / +78
0.1	1 / 0	0.47 / -62	0.85 / +28	-1.4db / +28
1.0	1 / 0	0.053 / -87	0.997 / +3	0db / +3
10	1 / -4.5	0.0053 / -90	1 / -4	0db / -4

To include the effect of time delay, the following phase shifts must be added:

f cps	θ_d
10.0	126.0
1.0	12.6
0.1	1.26
0.01	0.13
0.001	0.013

19. Plot the Frequency Response of the System and Compare It with Specified Requirements

The results are plotted as a Bode diagram in Figure 96 and compared with the specified frequency response. The fluidic yaw damper has been designed to meet the necessary performance requirements with a reasonable margin of safety.

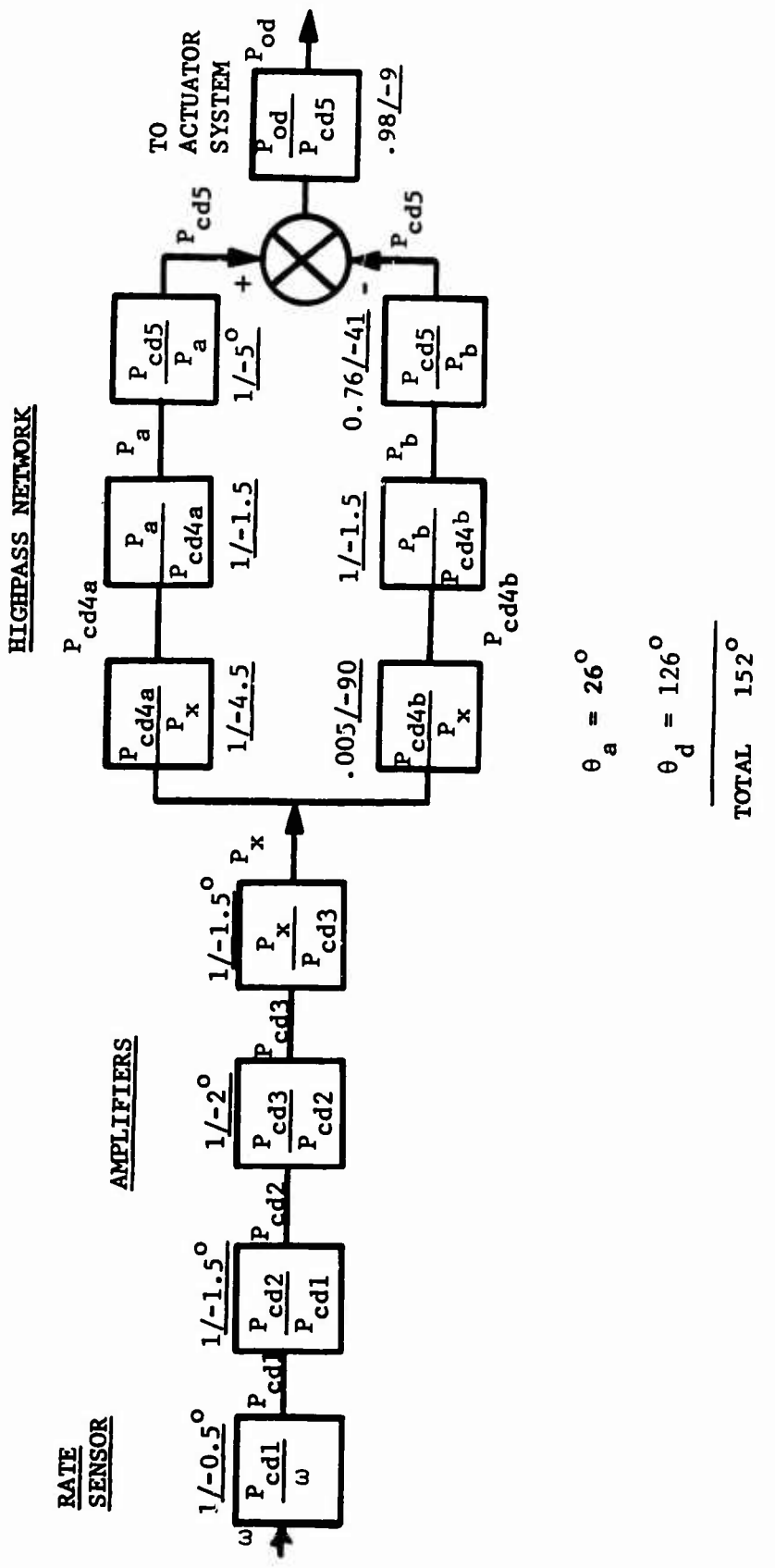


FIGURE 95 - FINAL VALUES OF THE TRANSFER FUNCTIONS AT 10 CPS

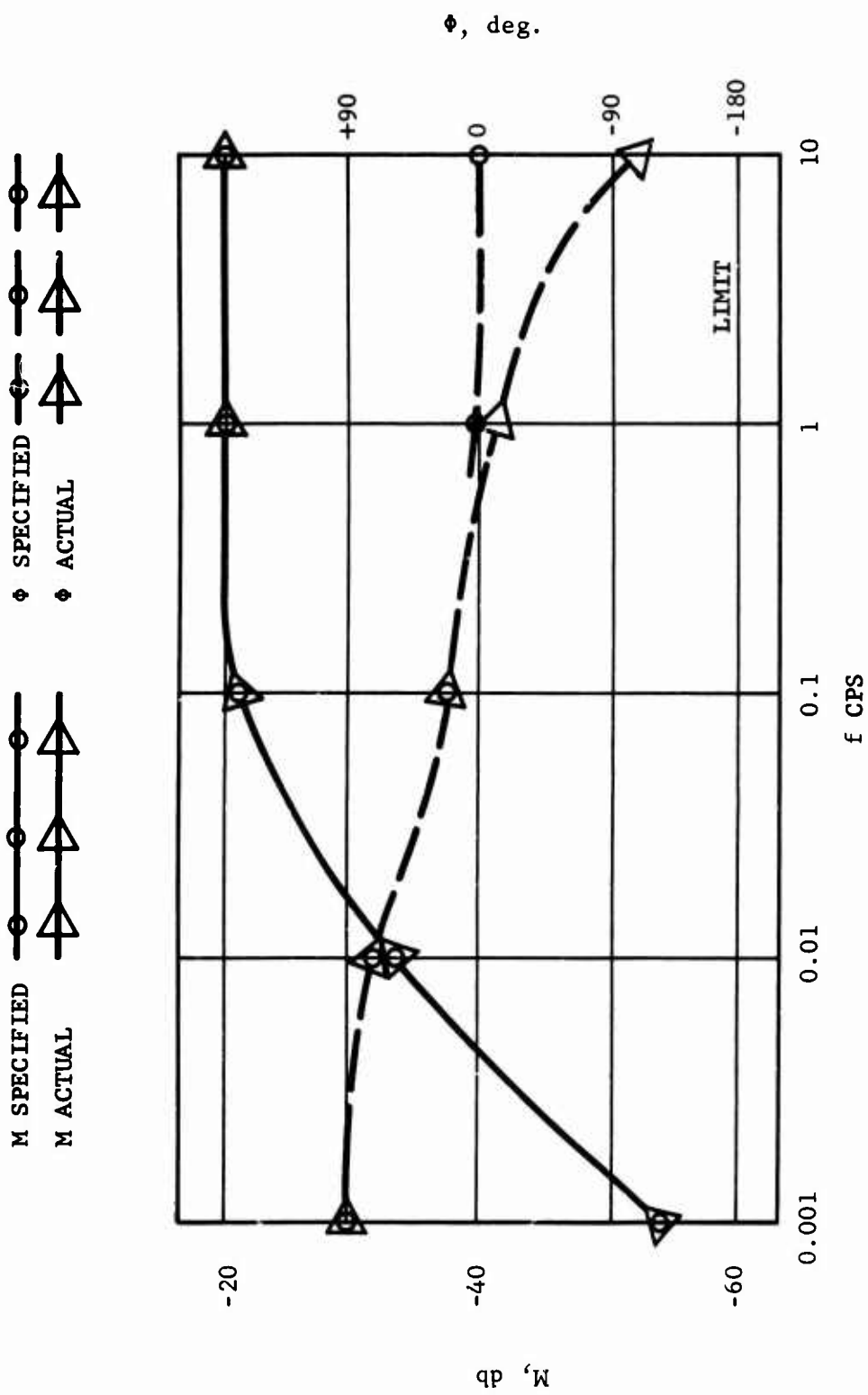


FIGURE 96 - FREQUENCY RESPONSE OF FLUIDIC YAW DAMPER

21. Finalize Preliminary Design

22. List Factors Important to the Performance of the System

The volume required to generate the highpass network time constant of 3.0 seconds can be calculated from the expression P_{cd4a}/P_x (see transfer function listed in Figure 91). In that equation the effective time constant is $0.6C_x R_{c4}$. Then,

$$0.6C_x R_{c4} = 3.0 \text{ seconds}$$

$$C_x = \frac{3.0}{0.6R_{c4}}$$

Substituting the value of $R_{c4} = 4.0$.

$$C_x = \frac{3.0}{0.6 \times 4.0}$$

$$C_x = 1.25 \text{ in.}^5/\text{lb}$$

Then, since

$$C_x = \frac{V_x}{P_{abs}}$$

and P_{abs} in the circuit is 15.13 psia (0.43 psi gage),

$$V_x = C_x P_{ab} = 1.25 \times 15.13$$

$$V_x = 19.2 \text{ in.}^3$$

That is, to obtain the proper highpass network time constant, we must add volume of 19.2 in.^3 to each fourth stage input network in the position (C_x) shown in Figure 85.

For most linear operation at all frequencies of interest, it is important to design the two parallel paths in the highpass network with identical characteristics. Otherwise, there would be more or less phase shift in one path than the other, and the summed output from stage 5 would be seriously distorted.

23. Design Summary

In summary, we have designed a fluidic yaw damper to meet certain performance requirements using available fluidic components. A schematic of the system is shown in Figure 85, and the static transfer characteristics

are illustrated in Figure 86. The equivalent electrical circuit is shown in Figure 87, a transfer function block diagram is shown in Figure 90, and a listing of the corresponding transfer functions is shown in Figure 91. The parameters of the transfer functions are listed in Figure 93, and the final frequency response shown in Figure 96 is compared with the specified requirements.

BIBLIOGRAPHY

1. Aerospace Recommended Practice - Fluidic Technology (Preliminary Draft), Society of Automotive Engineers, Inc., 485 Lexington Avenue, New York, N. Y., October 1966.
2. Belsterling, C. A., Development of the Techniques for the Static and Dynamic Analysis of Fluid State Components and Systems, USAAVLABS Report 66-16, U. A. Army Aviation Materiel Laboratories, Fort Eustis, Virginia, February 1966.
3. Belsterling, C. A., "A Systematic Approach for Designing Fluidic Systems", Control Engineering (Magazine), Volume 13, Number 4, April 1966.
4. Belsterling, C. A. and K. C. Tsui, "Analyzing Proportional Fluid Amplifier Circuits", Control Engineering (Magazine), Volume 12, Number 8, August 1965.
5. Belsterling, C. A. and K. C. Tsui, "Application Techniques for Proportional Pure Fluid Amplifiers", Proceedings of the Second Fluid Amplification Symposium, Harry Diamond Laboratories, Washington, D. C., May 1964.
6. Blackburn, J. F., G. Reethof, and J. L. Shearer, Fluid Power Control, The Technology Press of M. I. T. and John Wiley & Sons, Inc., New York and London, 1960.
7. Boothe, W. A., "A Lumped Parameter Technique for Predicting Analog Fluid Amplifier Dynamics", Joint Automatic Control Conference, Stanford, California, June 1964.
8. Chestnut, H. and R. W. Mayer, Servomechanisms and Regulating System Design, Volume 1, John Wiley & Sons, Inc., New York, 1951.
9. Goldman, S., Transformation Calculus and Electrical Transients, Prentice-Hall, Inc., New York, 1949.
10. Guillemin, E. A., The Mathematics of Circuit Analysis, John Wiley & Sons, Inc., New York, 1949.
11. Katz, S. and R. J. Dockery, "Staging of Proportional and Bistable Fluid Amplifiers", Report TR-1165, Harry Diamond Laboratories, Washington, D. C., August 1963.
12. Ryder, J. D., Electronic Engineering Principles, Prentice-Hall, Inc., New York, 1947.

UNCLASSIFIED

Security Classification

DOCUMENT CONTROL DATA - R & D		
<i>(Security classification of title, body of abstract and indexing annotation must be entered when the overall report is classified)</i>		
1. ORIGINATING ACTIVITY (Corporate author) Astromechanics Research Division Conrac Corporation 179 Lancaster Ave., Malvern, Pa., 19355		2a. REPORT SECURITY CLASSIFICATION UNCLASSIFIED
		2b. GROUP D.N.A.
3. REPORT TITLE FLUIDIC SYSTEMS DESIGN MANUAL		
4. DESCRIPTIVE NOTES (Type of report and inclusive dates) DESIGN MANUAL - 14 FEB 1966 THROUGH MAY 31, 1967		
5. AUTHOR(S) (First name, middle initial, last name) CHARLES A. BELSTERLING		
6. REPORT DATE July 1967	7a. TOTAL NO. OF PAGES 198	7b. NO. OF REFS 12
8a. CONTRACT OR GRANT NO. DA 44-177-AMC-390(T)	9a. ORIGINATOR'S REPORT NUMBER(S) USAAVLABS Technical Report 67-32	
b. PROJECT NO. Task 1F121401A14186	9b. OTHER REPORT NO(S) (Any other numbers that may be assigned this report) ARD-DM-052	
c.		
d.		
10. DISTRIBUTION STATEMENT Distribution of this document is unlimited.		
11. SUPPLEMENTARY NOTES		12. SPONSORING MILITARY ACTIVITY U.S. ARMY AVIATION MATERIEL LABORATORIES FORT EUSTIS, VIRGINIA, 23604
13. ABSTRACT This document is a "how-to-do-it" guide to the design of control systems using analog fluidic devices. It includes reference information on definitions, symbols, and general principles; an integrated set of static and dynamic design methods; and a step-by-step design procedure illustrated with a practical sample problem. The primary purpose of the Design Manual is to provide the control engineer with a unified set of analytical tools for the straightforward design of systems employing fluidic devices. Its secondary purpose is to provide a universally acceptable vocabulary so that the control engineer, the fluidic device manufacturer, and the user's project engineer can communicate in a common language. The Fluidic Systems Design Manual contains the following major sections: <ol style="list-style-type: none">1. Introduction2. Applicable Standards3. Test Methods and Instrumentation4. Graphical Characteristics of Typical Fluidic Devices5. Large Signal Performance Analysis6. Small Signal Performance Analysis7. Detailed System Design Procedure8. Illustrative Example of V/STOL Control System Design		

DD FORM 1473

REPLACES DD FORM 1473, 1 JAN 64, WHICH IS OBSOLETE FOR ARMY USE.

UNCLASSIFIED
Security Classification

UNCLASSIFIED

Security Classification

14. KEY WORDS	LINK A		LINK B		LINK C	
	ROLE	WT	ROLE	WT	ROLE	WT
FLUIDIC SENSORS FLUIDIC AMPLIFIERS FLUIDIC ACTUATORS FLUIDIC SYSTEMS SYSTEMS ANALYSIS						

END

UNCLASSIFIED

Security Classification

5739-67